INDIAN NATIONAL COMMITTEE ON SURFACE WATER (INCSW-CWC)

UID	UP-2006-100
Type (State whether final or draft report)	Final Report
Name of R&D Scheme	Investigation of Local Scour at Bridge Piers under Pressure Flow Conditions
Name of PI & Co-PI	Dr. Ashu Jain
Institute Address	Department of Civil Engineering IIT Kanpur, Kanpur – 208 016, UP
Circulation (State whether Open for public or not)	Open
Month & Year of Report Submission	September 2020

Central Water Commission
E-Mail: incsw-cwc@nic.in

Final Report of Research Scheme On

Investigation of Local Scour at Bridge Piers under Pressure Flow Conditions

Submitted To:

INDIAN NATIONAL COMMITTEE ON SURFACE WATER
Central Water Commission
Ministry of Water Resources
Government of India
712(S) Sewa Bhawan, R.K. Puram
New Delhi – 110 066, INDIA

Submitted By:

Ashu Jain, Former-Professor
Department of Civil Engineering
Indian Institute of Technology Kanpur
Kanpur – 208 016
Uttar Pradesh, INDIA

September 2020

ACKNOWLEDGEMENTS

The author would like to thank the funding agency, Indian National Committee for Hydraulics (INCH), Central Water Commission (CWC), Ministry of Water Resources, Government of India for funding this project.

The author would like to express his gratitude to his colleagues, Prof. Rajesh Srivastava and Prof. Shivam Tripathi, for extending their help during the execution of this project. The author would like to thank all the project staff who helped in carrying out the experiments and developing the mathematical models in this project, particularly Mr. Surendra Pratap Singh and Mr. Vishal Singh.

Thanks are also due to all the staff of the Hydraulics Laboratory of IIT Kanpur, Mr. P. Jagannadham, Mr. Arun Kumar Sharma, Mr. Sunil Nishad and Shri Jagdish Pandey (Panditji) who helped throughout the project duration in conducting the experiments and taking care of the paperwork related to this project.

Ashu Jain
(Principal Investigator)

CONTENTS

LIST OF PICTURES

LIST OF FIGURES

LIST OF TABLES

Chapter 1

Introduction

1.1 General

The development and economic growth of a country needs a well-defined network of transportation system. A transportation system can be either a railways or roadways system. India has one of the largest railways systems in the World. The proper functioning of a transportation system is essential to the economic growth and economic activity of a nation. A transport system, either railway or roadway, routinely comes across natural waterways in the form of rivers or small streams. Hence, bridges form one of the key components of the transportation system in a region. The World Bank has taken up major projects in developing countries including India for the construction of new bridges and restoration of the old bridges. The failure of a bridge can bring the communication between two regions to a standstill, severely affecting the economic activity, and loss of life and property in certain situations.

There are several reasons of the failure of a bridge. One of the important reasons is the inadequate depth of foundation resulting from inaccurate assessment of scour at the bridge piers and abutments. Continuous scour at a structure can lead to its failure, thus an understanding of the scouring process and the ability to predict the scour behaviour is very important (Ali and Karim, 2002). The foundations of piers and abutments at a bridge must extend beyond the maximum scour depths estimated. The researchers have devoted considerable amount of time in studying the scour patterns around bridge piers and abutments, and estimating equilibrium scour depths, for **free-surface flow conditions**, *i.e*. assessment of maximum scour depth at bridge pier when the water surface level during floods is lower than the lowest deck elevation of the bridge. Some notable examples include Subramanya *et al*. (1961); Breusers *et al*. (1977); Melville and Raudkivi (1977); Jain (1981); El-Taher (1984); Raudkivi (1986); Zdravkovich (1977 and 1987); Kothyari *et al.* (1988); Gangadharaiah *et al*. (1989); Garde *et al*. (1989); Yanmaz and Altinbilek

(1991); Kothyari *et al.* (1992a and 1992b); Muzzammil (1992); Gangadharaiah *et al*. (1993); Olsen and Melaaen (1993); Vittal *et al*. (1994); Setia (1997); Rao *et al*. (1998); Kumar *et al*. (1999); Graf and Istiarto (2002); Ali and Karim (2002); Oliverto and Hager (2002); Lyn (2008), and Guo (2011).

Most of the research on scour has been conducted under free-surface flow conditions with the resultant scour prediction equations based on free-surface flows (Lagasse *et al*., 1991; and Richardson *et al*., 1993). No single analytically derived equation is available because of the difficulties of the problem, such as effects of complex turbulent boundary layer, time-dependent flow patterns, combined effects of parameters that affect the scour hole, and the sediment transport mechanism in the scour hole (Yanmaz and Altinbilek, 1991). Further, the efforts of studying the scour depth at bridge piers and abutments during **pressure-flow conditions** have been lacking. It must be recognized that the flow conditions near the streambed during pressure-flow may be different than those during free-surface flow, and the pressure-flow scour may be several times larger than the free-surface flow scour at bridge piers and abutments (Abed, 1991).

1.2 Objectives of the Study

Most of the research on scour has been conducted under free-surface flow conditions with the resultant scour prediction equations based on free-surface flows (Lagasse *et al*., 1991; and Richardson *et al*., 1993). A review of the literature availableshows that there are not many studies that focussed on pressure flow conditions excepta few studies including Abed (1991) and Umbrell *et al*. (1998), Erneson and Abt (1998), and Kumcu (2016). The major risks associated with bridge foundations due to large floods causing pressure-flow conditions makes it prudent for designers to include very large floods in their evaluations of equilibrium scour estimation and depth of foundations to be designed. The efforts of studying the scour depth at bridge piers and abutments during **pressure-flow conditions** have been lacking.Therefore, there is a need to study the effects of pressure-flow conditions on the maximum scour depths at bridge piers and abutments in detail. Such studies may be helpful in the design of foundations of bridge piers and abutments for better safety of the superstructure.

Further, many of the studies reported in the past have relied on conventional modelling techniques, such as curve fitting or regression, in developing mathematical models for prediction of maximum scour depths at bridge piers and abutments. The physical process of scour around bridge piers and abutments and the resulting relationship between the input and output variables is complex, non-linear, and dynamic in nature. The conventional modelling techniques are able to perform reasonably well for linear systems and simple non-linear systems but may not be suitable in capturing the complex and non-linear relationship inherent in the scour process. Recently, Artificial Neural Networks (ANNs) have been proposed as efficient tools for modelling and forecasting.

The objectives of the current research scheme are:

1. Carry out extensive experimentation and develop a comprehensive scour database consisting of data on flow discharge, pier diameter, velocity of flow, flow depth, and equilibrium scour depth for the free-flow and pressure-flow conditions.
2. Analyse the developed scour database for evaluating the impact of various hydraulic parameters on the scour depth.
3. Assess the magnitudes of the scour depth under the free-flow vis-à-vis pressure-flow condition.
4. Capture the shape and size of the scour hole around bridge piers through extensive measurement at several locations within the scour hole.
5. Develop mathematical models (both conventional and ANN) for estimating equilibrium local scour based on hydraulic and geometrical characteristics of the physical system using the calibration or training data set.
6. Test the developed models using testing/validation data set.

This project proposes to study the effects of pressure-flow conditions on the equilibrium scour depths at bridge piers and abutments. Extensive experiments were carried out in the hydraulics laboratory of the Indian Institute of Technology (IIT) Kanpur for both free-flow and the pressure-flow conditions to generate data in terms of maximum scour depths and associated hydraulic parameters such as pier diameter, flow discharge, velocity of flow, and flow-depth. The scour database thus developed will then be employed in mathematical models to develop relationships between the maximum scour depth and the parameters affecting scour using ANNs.

The report is organized as follows: chapter 1 gives an introduction of the problem, a very brief literature and presents the objectives; chapter 2 presents literature review in the area of scour studies around bridge piers and abutments; chapter 3 presents materials and methods including the experimental set up, development of the scour database, modelling techniques employed to develop several mathematical models in this study, and the model performance evaluation measures used to assess the performance of various models developed in this study; chapter 4 provides a detailed description of the models developed including linear and non-linear regression models and the ANN models and the results obtained from the developed models; chapter 5 presents the summary and conclusions along with future scope; and chapter 6 presents the references used in this study. The Appendix-A lists the scour database developed in this study.

Chapter 2

Literature Review

2.1 General

Enormous amount of work has been reported in literature in the area of scour at bridge piers and abutments. The literature cited here includes only the selected advancements in last three decades or so. The validated approaches that can be found in standard texts are not included here. The literature review included in this report is divided into two parts: (a) literature at international level and (b) literature at national level.

2.2 Literature at International Level

Breusers *et al*. (1977) presented the state-of-the report on local scour around cylindrical piers. They presented a description of the scouring process, an analysis of relevant parameters, various formulae available to estimate scour depth, comparison of models and field data, and suggestions for protection against scour and for design relations. They recognized that the basic cause of 'local scour' is the hydrodynamic horse-shoe-vortex that is formed at the leading edge of the pier's junction with the streambed. However, they restricted their focus on non-cohesive granular bed material and one-way-current with no tidal and wave effects. Melville and Raudkivi (1977) summarized the major results of their investigation of flow characteristics in local scour at bridge piers. They reported on flow patterns, turbulence intensity distributions, and boundary shear stress distribution in the scour zone of a circular pier under clear water scour conditions.

Gangadharaiah *et al*. (1985) estimated initial vortex strength by measuring the pressure distribution on the line of symmetry upstream of a circular cylinder. Then they developed a relationship between the equilibrium scour depth and the primary vortex strength. Raudkivi (1986) described the behavioural pattern of scour at cylindrical pier under sub-critical flow conditions through laboratory experiments, and showed that the local scour

depth depends primarily on the ratio of shear or mean velocity to the value at the beginning of sediment movement, grading of the sediment, and flow depth relative to pier width. Yanmaz and Altinbilek (1991) conducted sets of experiments using single cylindrical and square shaped piers in laboratory under clear water conditions with uniform bed materials to investigate time variations in local scour depths around bridge piers. A lot of work has been taken up at the University of Roorkee in the area of scour around bridge piers including the works on maximum scour depth at circular bridge piers in clear water flows by Kothyari *et al*. (1988), live bed scour and temporal variation of scour (Kothyari *et al*., 1992a and 1992b), and clear water scour around cylindrical bridge pier group (Vittal *et al*., 1994) among many others. Kumar *et al*. (1999) examined the use of pier slots and collars for reducing local scour at bridge piers through experiments. Then, using the data collected from their study as well as some earlier studies, they developed an equation for maximum scour depth around circular bridge piers fitted with collars. However, the equation developed by them is applicable to local scour of uniform-sized sediment in clear water flow only.

Graf and Istiarto (2002) experimentally investigated the three-dimensional flow field in an established scour hole using an Acoustic-Doppler-Velocity-Profiler (ADVP) to measure instantaneously the three components of the velocities in the vertical symmetry plane of flow near upstream and downstream ends of the cylinder. The use of the state-of-the-art equipment in this study helped in verifying the earlier works by others that a strong vortex system is established in the upstream end and a rather weaker vortex is formed at the downstream end of the cylindrical pier. Oliverto and Hager (2002) proposed an equation for temporal evolution of scour using similarity arguments and flow resistance. They used a large data set collected at ETH, Zurich, Switzerland on scour around bridge piers and abutments for six different types of sediments of which three were uniform. The results obtained in their study are in agreement with those reported in literature earlier.

Many researchers have studied the effects of interference of piers on the maximum scour depth at bridge piers and abutments for various arrangements and flow conditions (El-Taher, 1984; Zdravkovich, 1977 and 1987; and Gangadharaiah *et al*., 1989).

Most of the studies reported above adopted physical models fabricated at reduced scales in laboratories to study the scour patterns and estimate maximum scour depth around bridge

piers. There are a very few studies employing mathematical models using computers to simulate the physical process of scour around bridge piers. Olsen and Melaaen (1993) attempted to calculate scour depth around cylindrical piers by a numerical solution of three-dimensional non-transient Navier-Stokes equations on a general non-orthogonal grid. The geometry of the scour hole and the flow characteristics given by the numerical model were found to be in agreement with observations from experimental study. Ali and Karim (2002) used FLUENT CFD software to predict three-dimensional field in the form of bed shear stress around a circular cylinder. The numerical model results were obtained for rigid beds and for scour holes of different sizes resulting from different time durations. They reported that the long-term scour at bridge piers depended on three dimensionless numbers: the pile number, the sediment size number, and time duration number. They calibrated the theoretical relationships using various laboratory and field results.

Unfortunately, most of the research on scour has been conducted under free-surface flow conditions with the resultant scour prediction equations based on free-surface flows (Lagasse *et al*., 1991; and Richardson *et al*., 1993). The first studies of localized pressure-flow scour were conducted at Colorado State University by Abed (1991), who tested several pier configurations for both free-surface and pressure-flow conditions. The physical model experiments found pressure-flow scour to be 2.3 to 10 times greater than free-surface pier scour. These findings were shocking and need to be verified. Umbrell *et al*. (1998) reported that under pressure-flow conditions, the flow is directed downward and under the bridge deck, creating an increase in flow velocity and a corresponding increase in bed scour. They conducted a series experiments in laboratory to study scour caused by pressure flow beneath a bridge without the localized effects of piers and abutments under a variety of pressure-flow conditions. They also developed a conceptual relationship between pressure-flow scour and the flow conditions with the use of experimental data.

2.3 Literature at National Level

The majority of the work reported at National level on studying the scour around bridge piers has been taken up either at the University of Roorkee or at IIT Kanpur starting with the early 1980s. The research efforts at National level have focused on characterizing the horse-shoe-vortex, developing empirical formulae to estimate equilibrium scour depth around bridge piers, interference effects on maximum scour of various pier arrangements,

and scour protection devices, for free surface flow conditions.Jain (1981) analysed available data and proposed enveloping equation for maximum clear water scour. Gangadharaiah *et al*. (1985) estimated the initial vortex strength from the pressure distribution measured upstream of a circular cylinder, and the vortex strength at the equilibrium stage of scour from the threshold velocity of the armour coat, which were then related to upstream flow conditions. These vortex strengths were then used to obtain an expression for the equilibrium scour depth. Garde *et al*. (1989) reported on the effects of unsteadiness and stratification on local scour around bridge piers. They showed that both the rate of scour and the equilibrium scour depth decreases as the standard deviation of the particle size distribution increases. This is due to the formation of an armour layer at the base of the scour hole. They also proposed formulae to estimate clear water and live-bed scour depths in terms of certain non-dimensional physical parameters.

Srivastava (1989), in his master's work at IIT Kanpur, investigated the strength characteristics of the horse-shoe-vortex. However, it was the pioneer work by Muzzammil (1992), which gave a detailed insight into the characteristics of a horse-shoe-vortex. Muzzammil (1992) studied the dynamics of scour hole development experimentally in detail. He reported that the whole scour process is governed by hydraulic factors, pier geometry and bed roughness, apart from migration of bed-forms and pier arrangement. This study was able to characterize the horse-shoe-vortex through parameters such as vortex dimensions, rotational frequency, tangential velocity and strength for flows on rigid flat bed, on solidified scoured bed, and on mobile sediment bed for one or more piers.

Gangadharaiah *et al*. (1989) studied the effects of interference of piers on the scour depth around bridge piers. Gangadharaiah *et al*. (1993) and Garde and Kothyari (1995), in their state-of-the-art reports on scour around bridge piers, have summarized the influence of various hydraulic and sediment characteristics on the scour depth around bridge piers. Setia (1997), during his PhD work at IIT Kanpur, studied the mechanism of scour around bridge piers and the characteristics of the scouring horse-shoe-vortex on mobile beds of fine and coarse sediments before and during the development of the scour hole. He also carried out detailed experimental investigation to relatively assess the major scour protection devices, individually and in various combinations. Rao (1997) reported on the interference effects on local scour around bridge piers for three different arrangements of piers, namely, tandem, equilateral triangular, and staggered arrangements. Many

researchers at the University of Roorkee have conducted research in the area of scour patterns around bridge piers and abutments and estimation of equilibrium scour depths in the last couple of decades. Some notable examples include the works on scour around bridge piers by Kothyari *et al*. (1988), Kothyari *et al*. (1989), Kothyari (1993), Garde and Kothyari (1998) among other works.

Rao *et al*. (1998), in an INCH sponsored project at IIT Kanpur, carried out an extensive investigation to study the suitability of different scour protection devices for protection against scour around bridge piers and abutments. In this study, they reported the preliminary results on the effect of submergence on the local scour at an oblong pier. They found that the effect of submergence is to increase the equilibrium scour at bridge piers and abutments. Erneson and Abt (1998) developed a comprehensive program to investigate pressure flow scour in bridge openings. Data were collected and an equation was developed that can be used to estimate the magnitude of vertical contraction scour that could occur at a bridge with water flowing under the pressure-flow conditions.Lyn (2008) examined the scour computation methodology in HEC-18 and reported that the standard equations used in HEC-18 were not suitable for pressure-flow conditions. The regression equation used in HEC-18 suffered from spurious correlation. He proposed an alternative equation based on laboratory and field data, which can be useful in pressure-flow situations.Guo (2011) proposed a power-exponential equation for the time-dependent clear-water scour depth including a nonzero initial condition for submerged bridge flows. The proposed equation resulted in cost cuttings for bridge foundations. The methodology coupled with real-time monitoring system would be able to predict time series of scour depths during flooding conditions, which could be quite helpful for bridge managers in formulating management strategies.

More recently, Kumcu (2016) studied the pressurized flow scour under a bridge deck and downstream deposition that results from eroded sediment material governed by both steady and unsteady clear-water flow conditions. Experimental conditions used in this study involved clear-water scour of a sand bed of given median sediment size d(50) = 0.90 mm and sediment uniformity sigma(g) = 1.29, an approach flow characterized by a flow depth and velocity, a rectangular-shaped bridge deck, and a stepwise flood hydrograph defined by its time to peak and peak discharge. Different flow conditions were considered in confined flow under the bridge deck. Relationship between pressure-flow scour and

flow conditions was presented and discussed under the obtained experimental data. Additionally, effects of single-peaked stepwise flow hydrographs (unsteady flow conditions) on bridge pier scour depth were investigated under clear-water pressure-flow conditions, whereas previous researches mainly focused on the equilibrium pressure scour under steady flow conditions.

It is clear from the literature review presented above that the number of studies focussing on the assessment of the scour around bridge piers under the pressure-flow conditions have been very limited. There is no single study that attempted to capture the size and shape of the scour hole as a function of time that is capable of giving insights into the evolution of the scour hole. Also, most of the mathematical models employed to develop relationships among the scour and other hydraulic parameters have focused on the conventional modelling techniques of linear and/ or non-linear regression. There has not been a single study on the application of ANNs in predicting the scour around bridge piers. This study made an attempt to bridge some of these research gaps.

Chapter 3

Materials and Methods

3.1 General

This chapter describes the details of the experiments conducted, development of the comprehensive scour database,and the modeling techniques employed to develop various mathematical models in this study. The various error statistics used to assess the performance of various regression and artificial neural network models developed in this study are also presented in this chapter.

3.2 Details of the Experiments Conducted

The experiments were carried out in a glass-walled flume in the hydraulics laboratory ofIIT Kanpur. The dimensions of the flume are length 20 m; width 61 cm; and depth 41 cm. The details of the experimental flume are shown in Picture 3.1. First, the flume was filled up to a depth of about 20 cm - 30 cm by Ganga sand (depending on the flow condition). Then, lean flow discharge was allowed in the flume for ten hours to achieve dynamic equilibrium. Then, prescribed flow was allowed for about 10-12 hours, which causes scour around the bridge pier installed in the flume. Measurements of flow depth (h), flow velocity (v), flow discharge (Q), and scour depth (S) were taken at 15 min interval during the first hour and then at 1-hour interval for the remaining time. The velocity was measured using a pitot tube, flow depths were measured using a scale fixed on the glass flume, flow was measured using rectangular-notch and point gauge, and the scour depths were measured using point gauge and scale.

Velocity (v) and flow depth (h) were measured at six locations along the flume; the bed elevations (z) were measured at 13 locations along the flume. Initially, the scour was measured at four different locations around the bridge pier. These locations are designated as Front (F), Back (B), Left Centre (LC), and Right Centre (RC). It was noticed that the

scour in the front and back is higher than that at the locations away from the pier (e.g. LC and RC). Also, the scour in the front of the pier is higher than that at the back. Later, the scour measurements were carried out at 12 different locations around the bridge pier.

Picture 3.1: Glass-walled flume for carrying out experiments

These locations are designated as U1, U2, U3, D1, D2, D3, L1, L2, L3, R1, R2, and R3. Here U stands for upstream of the pier, D is downstream of the pier, L is left of the pier, R is right of the pier, the number 1 is closer to the pier and 3 is away from the pier. The scour measurements were taken at 12 locations around the bridge pier in order to get the accurate assessment of the scour hole around the bridge pier. Once an experiment was completed for specific diameter and discharge for a specific flow condition, then the lean flow was run for ten-hours again to achieve the revised dynamic equilibrium. Then the specified flow was run for 10-12 hours and measurements taken. This procedure was repeated for each experiment.

In all, a total of 48 experiments were carried out including those for free-surface flow and pressure-flow conditions. The details of the experiment conducted are provided in Table 3.1. Out of the 48 experiments, 28 experiments were carried out for free-flow conditions and 20 experiments were carried out for the pressure-flow conditions. A total of four different cylindrical piers were employed to develop scour database having varied bridge pier diameters in the field. The diameters of the cylindrical bridge piers used in the flume experiments were: 5.14 cm, 4.00 cm, 3.20 cm, and 2.10 cm. For each pier diameter,

several discharge values were used in different experiments so as to develop exhaustive database of scour and varying hydraulic conditions under both free-flow and pressure-flow conditions. The discharge in the flume was varied by rotations of the valve controlling the discharge to the flume. As can be seen from Table 3.1, the rotations of 4, 5, 6, 7, 8, 9, and 10 were used to vary the discharge in the flume. The range of discharge for all experiments was from 0.01 m^3/s to 0.1 m^3/s. Please note that several experiments were carried out for free-flow conditions in order to train the staff and standardize the experimental procedures. Once the training and streamlining of the procedure were achieved, the experiments for pressure-flow conditions did not need to be duplicated. Further, the scour during the pressure-flow conditions for larger discharge values (corresponding to 9 & 10 rotations) were so large that unstable conditions were created. Thus, those experiments were discarded and are not included in the data analysis and model development in this report.

Table 3.1: Details of the experiments carried out for free-flow and pressure-flow conditions

Experiment No.	Pier Diameter (cm)	Discharge (Rotations)	No. of Experiments	Type of Flow Condition
1–7, 26	5.14	4, 5, 6, 7x2, 8, 9, 10	8	Free
8-14	3.20	4, 5, 6, 7, 8, 9, 10	7	Free
15-21, 23	4.00	4, 5, 6, 7, 8, 9, 10X2	8	Free
48-52	2.10	4, 5, 6, 7, 8	5	Free
27-30, 32	5.14	4, 5, 6, 7, 8	5	Pressure
33-37	4.00	4, 5, 6, 7, 8	5	Pressure
38-42	3.20	4, 5, 6, 7, 8	5	Pressure
43-47	2.10	4, 5, 6, 7, 8	5	Pressure

The details of some of the experiments carried out are presented in the forms of pictures in the next few pages of this report. Picture 3.2 and Picture 3.3 show the details of experiment for D = 3.2 cm for free-flow conditions. Picture 3.4 and Picture 3.5 show the

details of the scour hole for D = 3.2 cm after the flood flow was run for ten hours under the free-flow conditions.

Picture 3.2: Experiment for D = 3.2 cm under free-flow conditions

Picture 3.3: Experiment for D = 3.2 cm under free-flow conditions

Picture 3.4: Scour details around pier after free-flow (D = 3.2 cm)

Picture 3.5: Scour details around pier after free-flow (D = 3.2 cm)

Picture 3.6 and Picture 3.7 show the details of experiment for D = 5.14 cm under pressure-flow conditions. Picture 3.8 and Picture 3.9 show the details of the scour hole for D = 5.14 cm after the flood flow was run for ten hours under the pressure-flow conditions.

Picture 3.6: Experiment for D = 5.14 cm under pressure-flow conditions

Picture 3.7: Experiment for D = 5.14 cm under pressure-flow conditions

Picture 3.8: Scour details around pier after pressure-flow (D = 5.14 cm)

Picture 3.9: Scour details around pier after pressure-flow (D = 5.14 cm)

3.3 Development of the Scour Database

Once all the experiments were carried out, an effort was made to develop a comprehensive scour data base, which could be used for mathematical model development in this study and by other researchers in the future. The first step in the development of any mathematical model is to graphically examine the relationship among various dependent variables and the independent variable. The maximum scour depth around the bridge pier was first plotted against various hydraulic parameters e.g. flow depth, velocity of low, flow discharge for different diameters of piers. These graphical representations are depicted in Figure 3.1 through Figure 3.8 for free-flow and pressure-flow conditions.

Figure 3.1(a) presents the relationship between scour at different locations upstream and downstream of the pier and the depth of flow the under free-flow conditions. The scour depth at all the 12 locations appears to increase with an increase in the depth of flow as expected. Figure 3.1(b) presents the relationship between scour at different locations left and right of the pier and the depth of flow under free-flow conditions. It can be noted from Figure 3.1(a) and Figure 3.1(b) that the scour tens to increase with the increase in the depth of flow.

Figure 3.2(a) presents the relationship between scour at different locations upstream and downstream of the pier and the velocity of flow the under free-flow conditions. Figure 3.2(b) presents the relationship between scour at different locations left and right of the pier and the velocity of flow the under free-flow conditions. Although it appears to decrease, there does not appear to be a definite pattern of increase or decrease in the scour depth at all the 12 locations with an increase in the velocity of flow.

Figure 3.3(a) presents the relationship between scour at different locations upstream and downstream of the pier and the flow discharge under free-flow conditions. Figure 3.3(b) presents the relationship between scour at different locations left and right of the pier and the flow discharge under free-flow conditions. The scour depth at all the 12 locations appears to increase with an increase in the flow discharge, as expected.

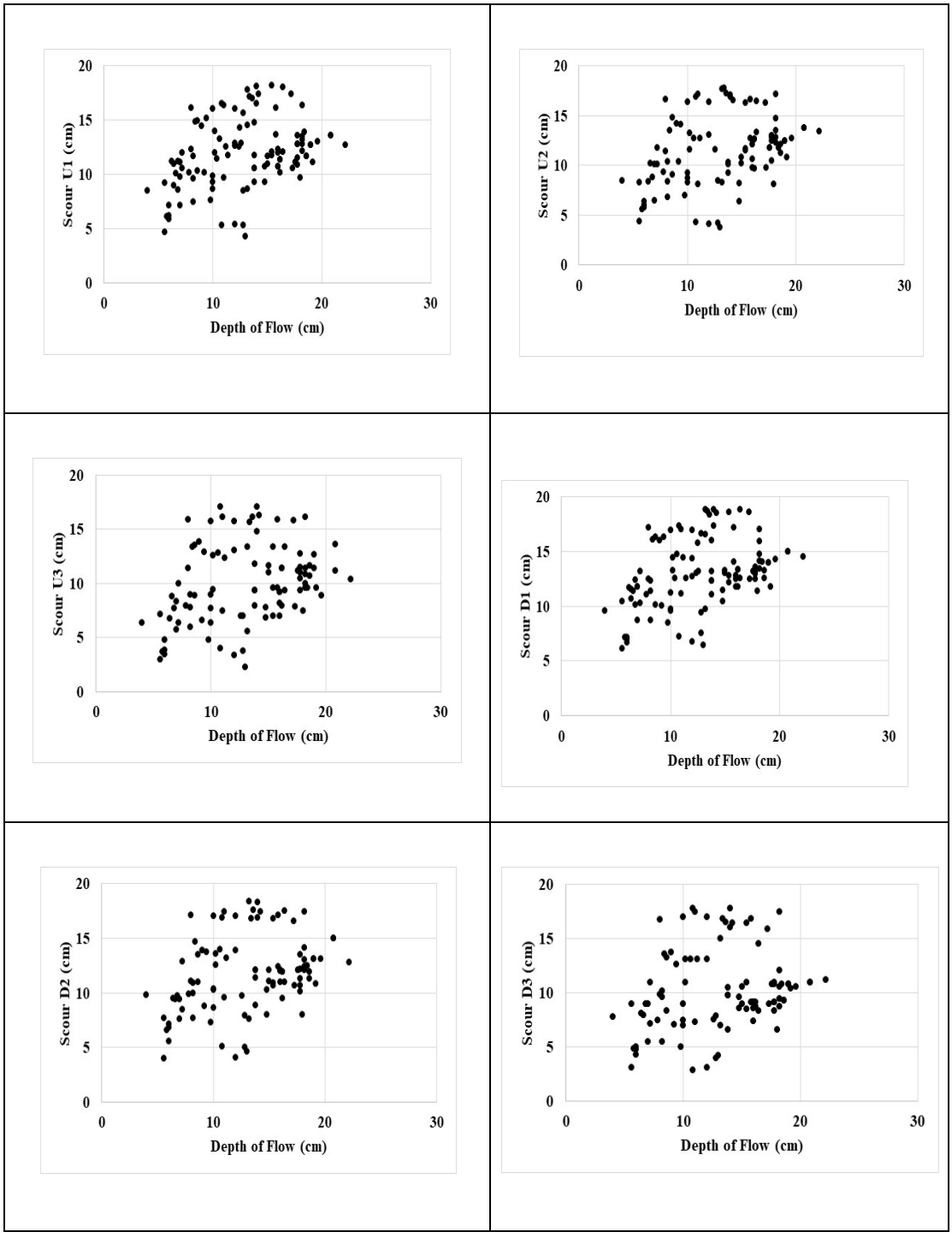

Figure 3.1(a): Scour depth at various locations (upstream & downstream of pier) versus flow depth under free-flow conditions

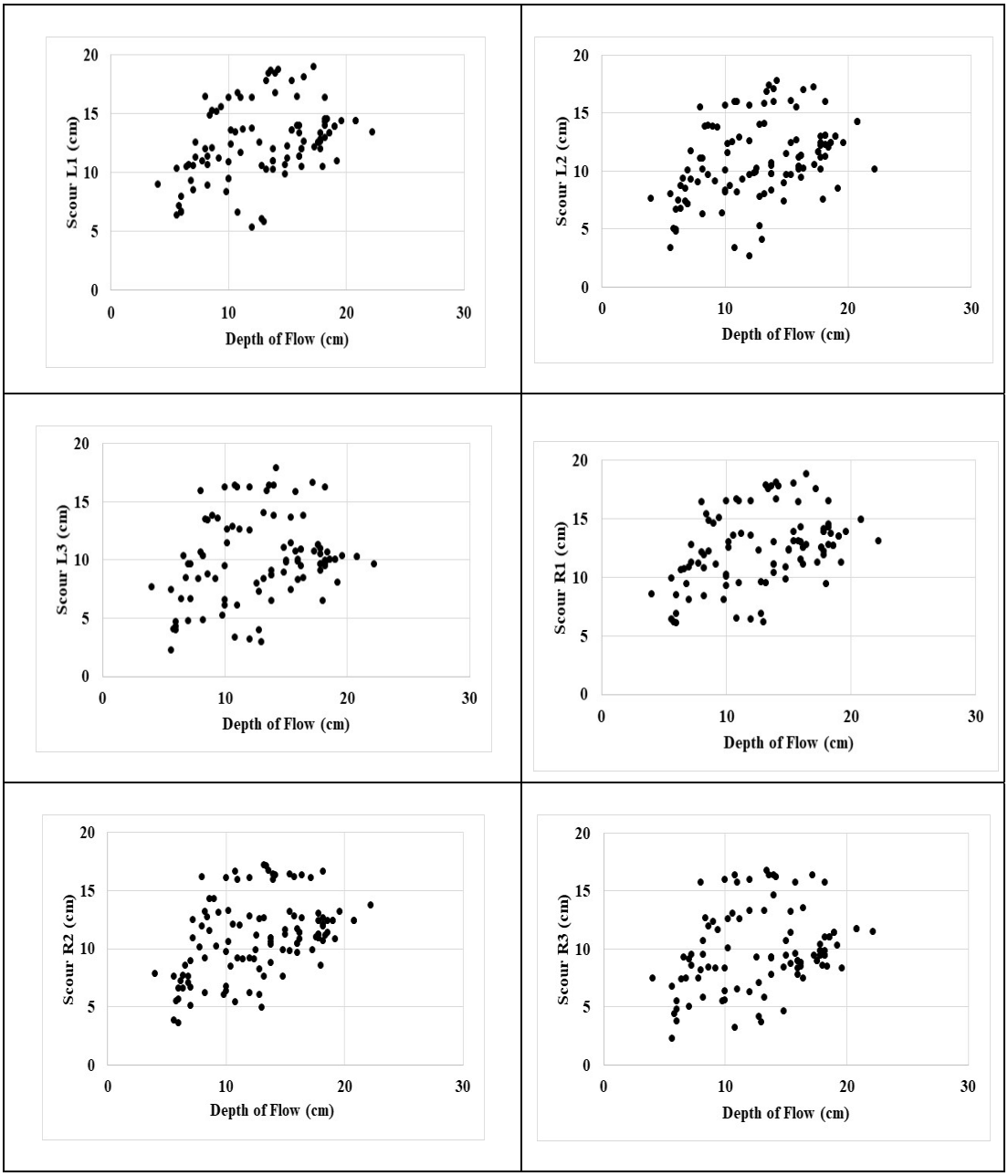

Figure 3.1(b): Scour depth at various locations (left and right of pier) versus flow depth under free-flow conditions

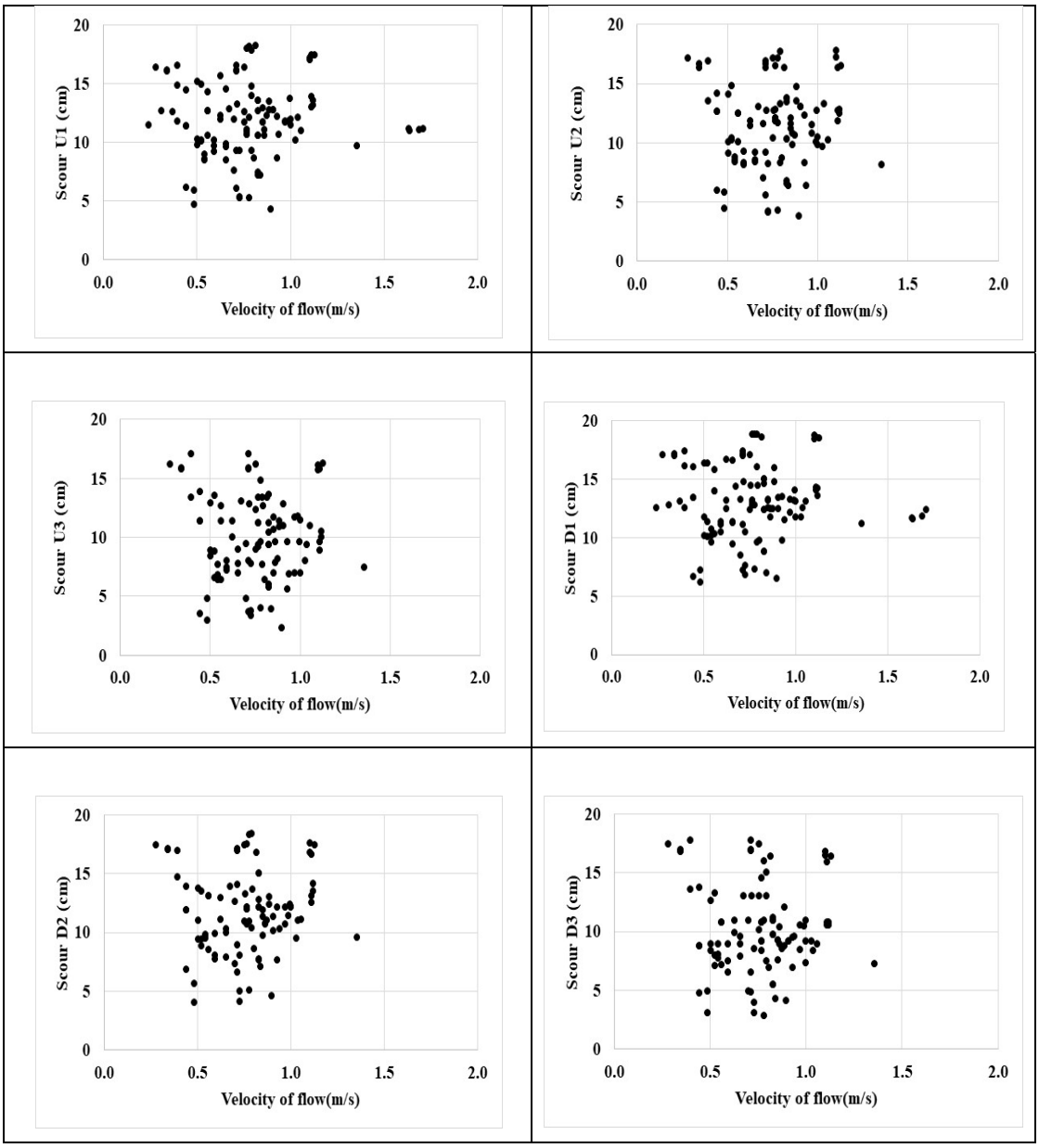

Figure 3.2(a): Scour depth at various locations (upstream & downstream of pier) versus velocity of flow under free-flow conditions

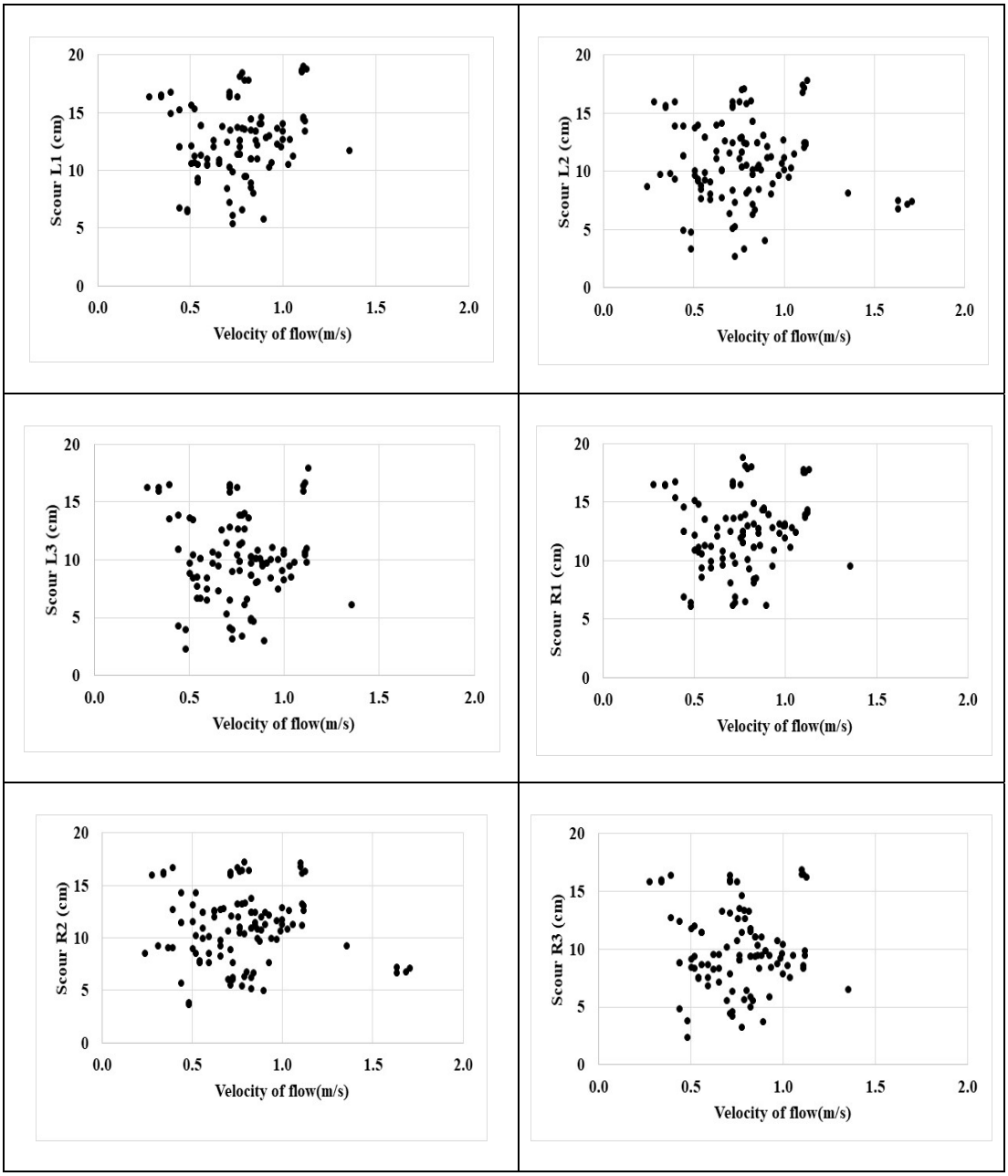

Figure 3.2(b): Scour depth at various locations (left and right of pier) versus velocity of flow under free-flow conditions

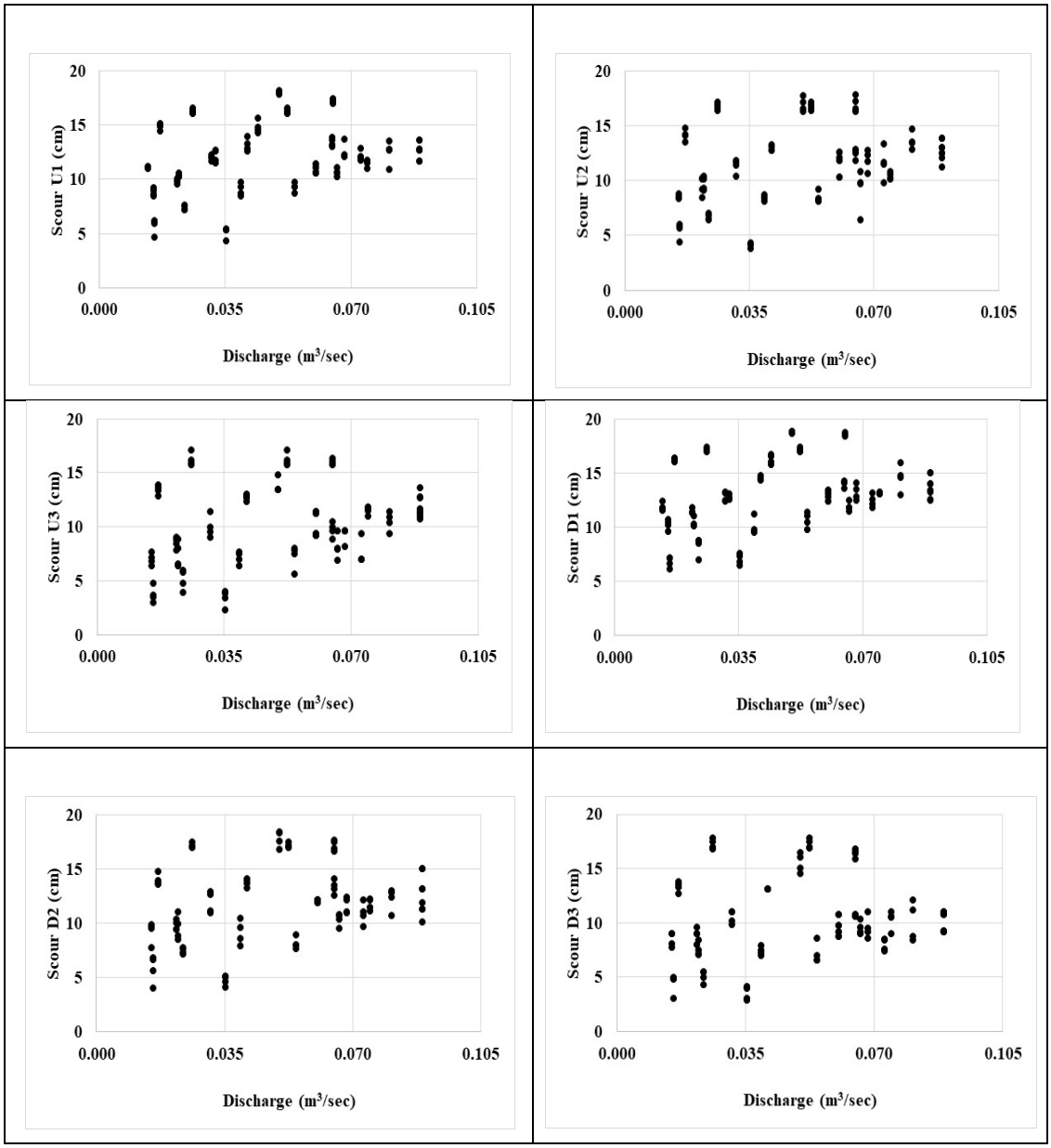

Figure 3.3(a): Scour depth at various locations (upstream & downstream of pier) versus the flow discharge under free-flow conditions

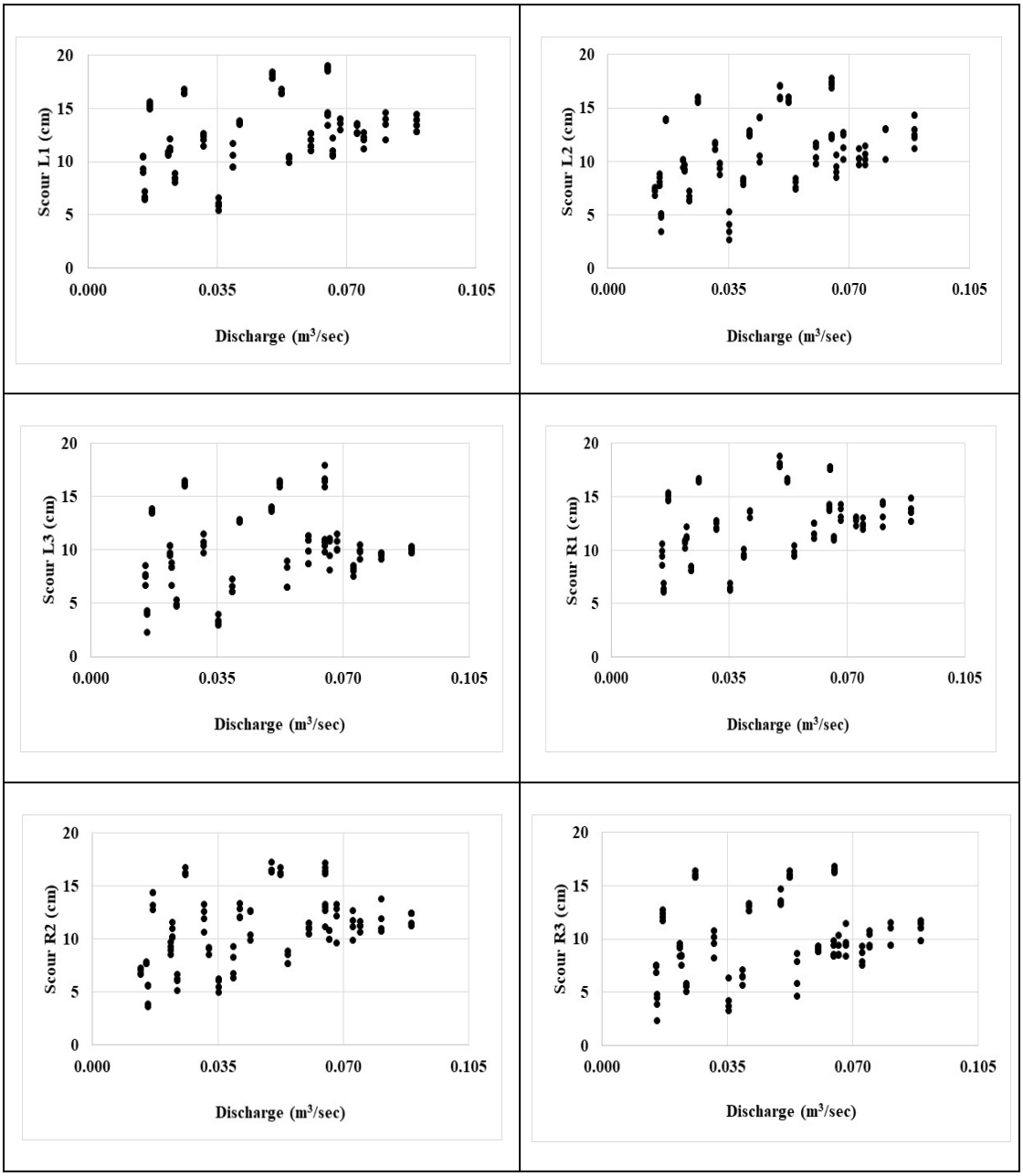

Figure 3.3(b): Scour depth at various locations (left and right of pier) versus the flow discharge under free-flow conditions

Figure 3.4(a) presents the relationship between scour at different locations upstream and downstream of the pier and the pier diameter under free-flow conditions. The scour depth at all the 12 locations appears to increase with an increase in the pier diameter, as expected. However, the scour depths at all locations for D = 2.10 cm appears to be higher than expected for all the experiments.

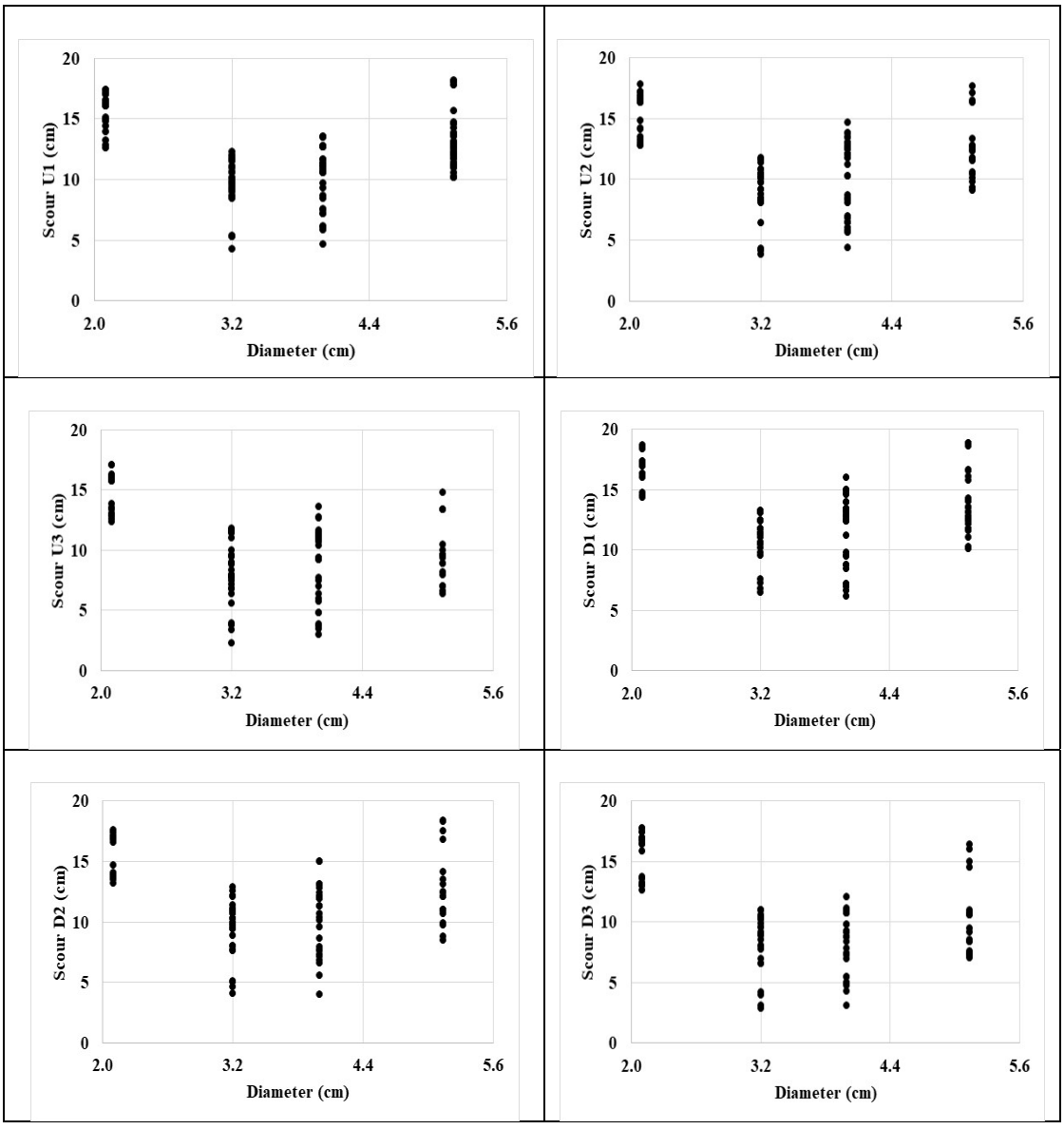

Figure 3.4(a): Scour depth at various locations (upstream & downstream of pier) versus the pier diameter under free-flow conditions

Figure 3.4(b) presents the relationship between scour at different locations left and right of the pier and the pier diameter under free-flow conditions. The trend is similar to upstream and downstream as the scour depth at all the 12 locations appears to increase with an increase in the pier diameter, as expected, with D = 2.10 being the exception.

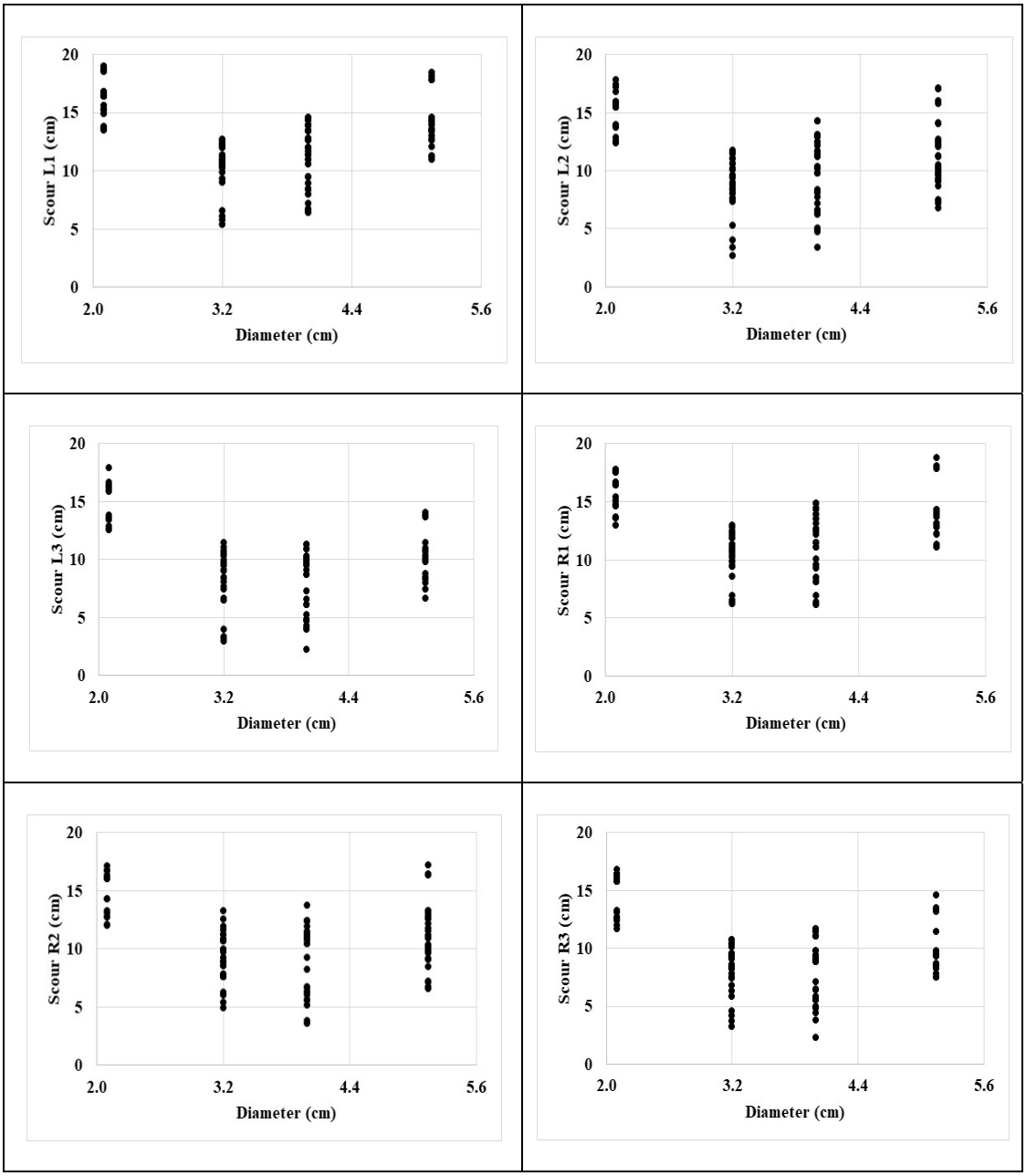

Figure 3.4(b): Scour depth at various locations (left and right of pier) versus the pier diameter under free-flow conditions

Figure 3.5(a) presents the relationship between scour at different locations upstream and downstream of the pier and the depth of flow under pressure-flow conditions. The scour depth at all the 12 locations appears to increase with an increase in the depth of flow, as expected.

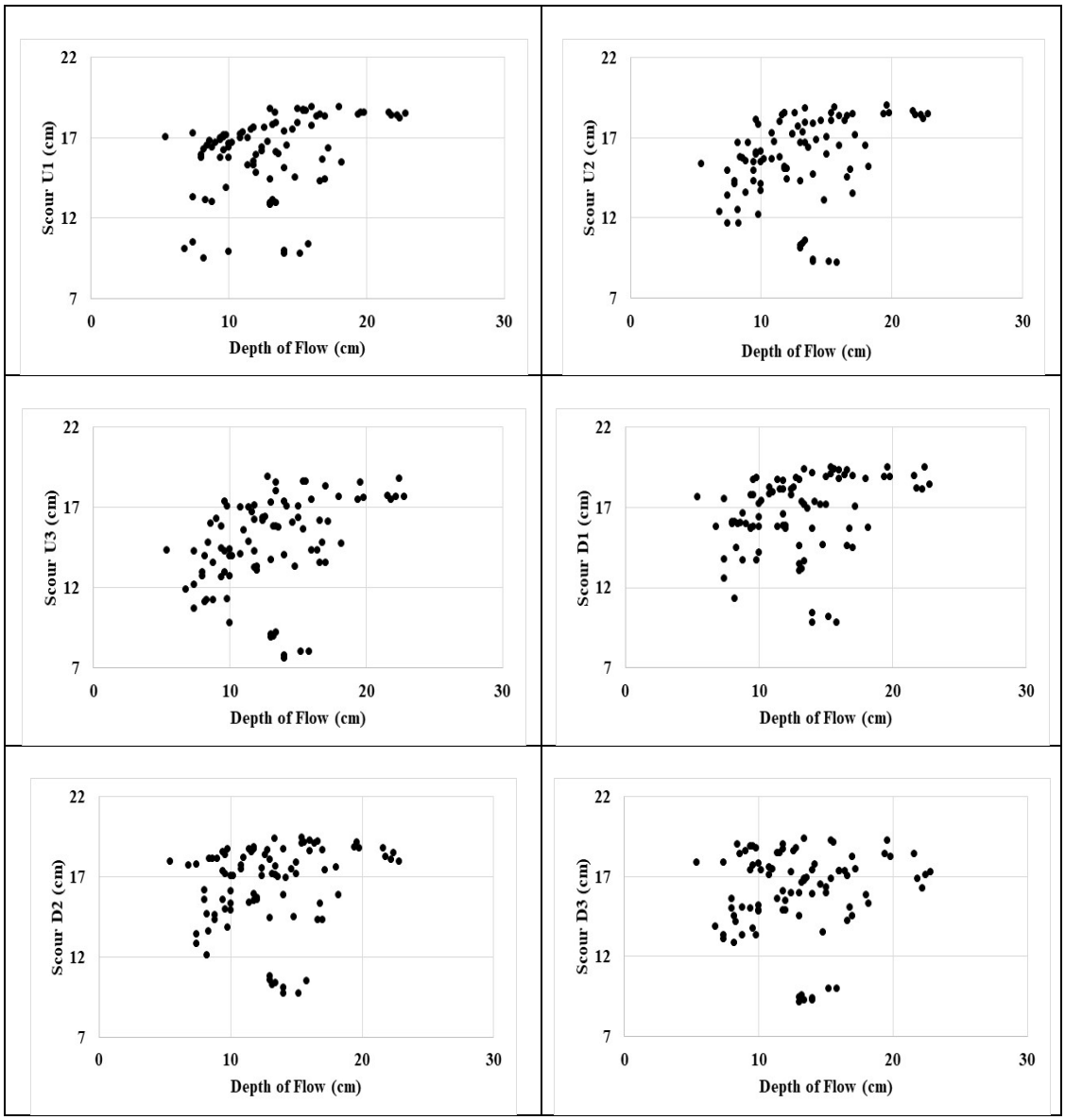

Figure 3.5(a): Scour depth at various locations (upstream & downstream of pier) versus the depth of flow under pressure-flow conditions

Figure 3.5(b) presents the relationship between scour at different locations left and right of the pier and the depth of flow under pressure-flow conditions. The pattern is similar to that for Figure 3.5(a).

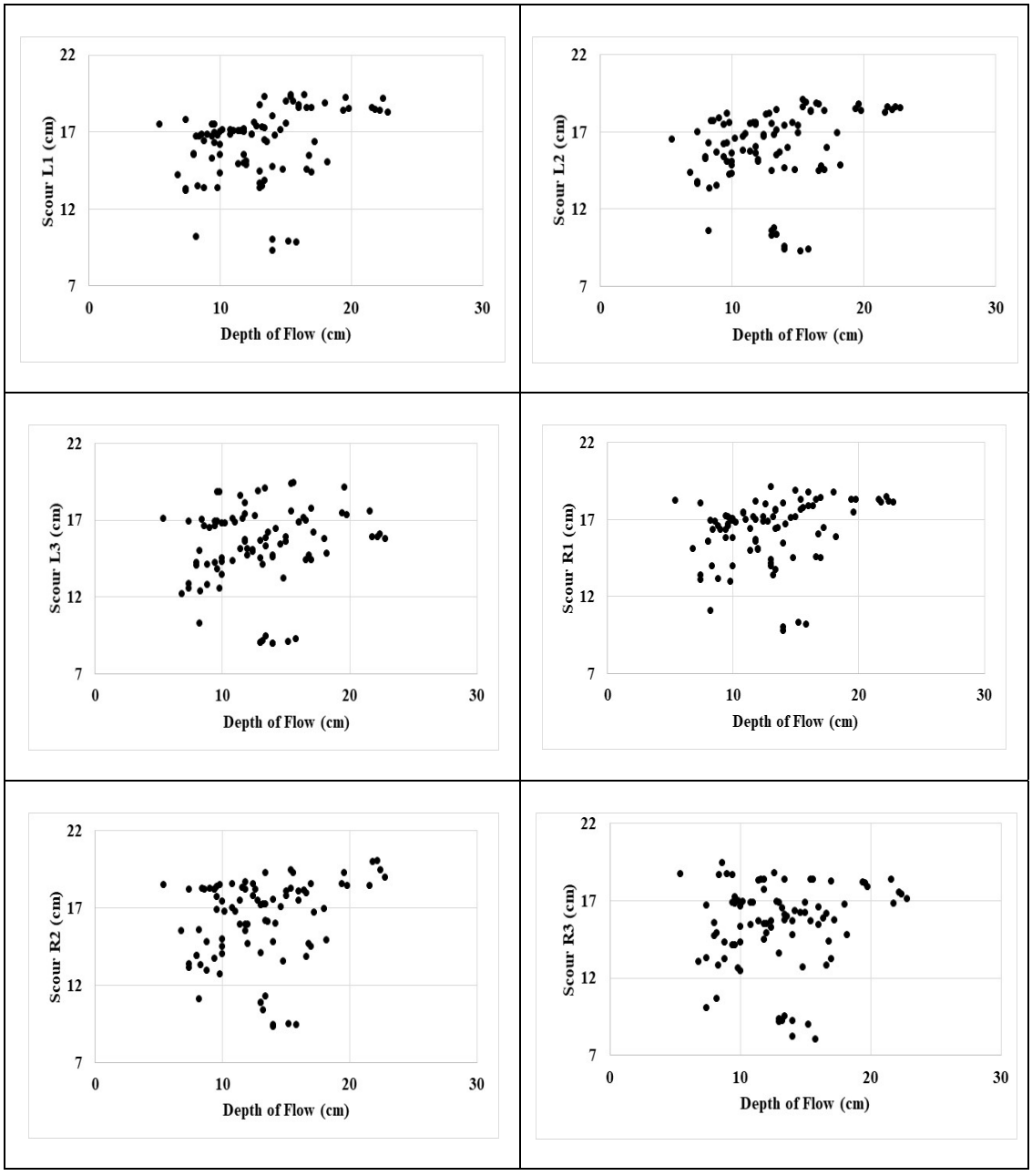

Figure 3.5(b): Scour depth at various locations (left and right of pier) versus the depth of flow under pressure-flow conditions

Figure 3.6(a) presents the relationship between scour at different locations upstream and downstream of the pier and the velocity of flow under pressure-flow conditions. Similar to the free-flow conditions, there does not appear to be a definite trend in depth of scour with an increase in velocity of flow for pressure-flow conditions also.

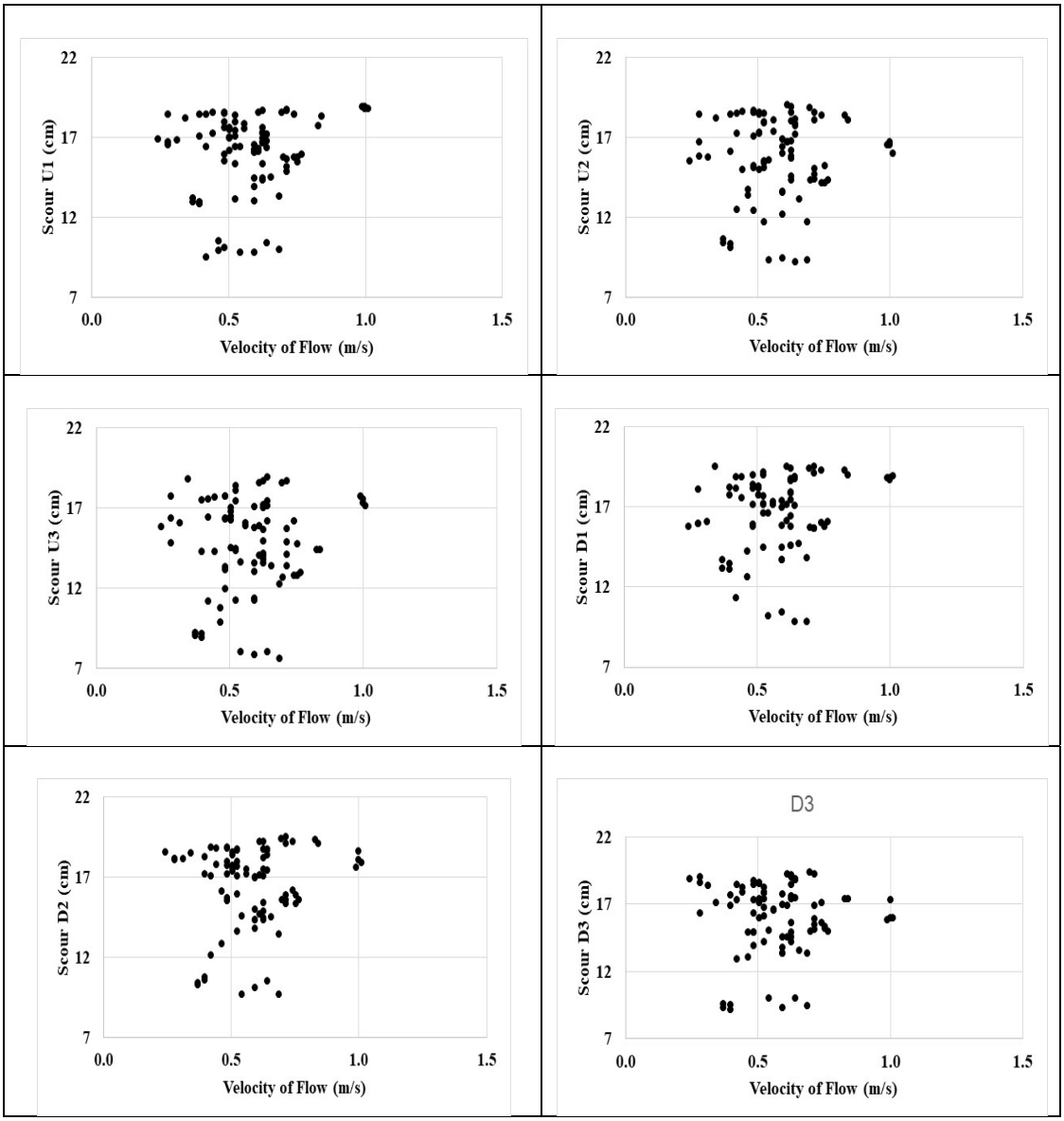

Figure 3.6(a): Scour depth at various locations (upstream & downstream of pier) versus the velocity of flow under pressure-flow conditions

Figure 3.6(b) presents the relationship between scour at different locations left and right of the pier and the velocity of flow under pressure-flow conditions. The pattern is similar to that for Figure 3.6(a).

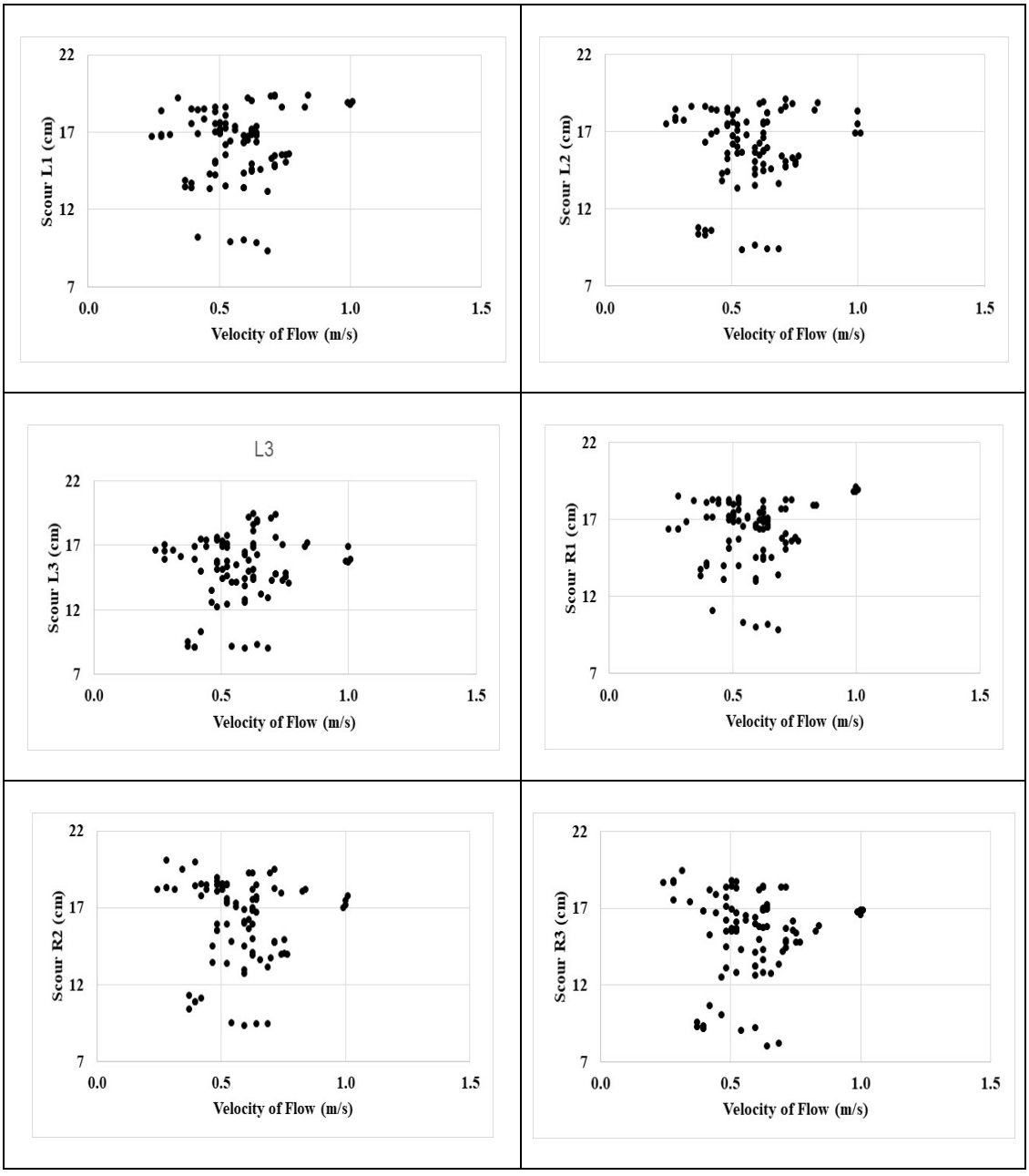

Figure 3.6(b): Scour depth at various locations (left and right of pier) versus the velocity of flow under pressure-flow conditions

Figure 3.7(a) presents the relationship between scour at different locations upstream and downstream of the pier and the flow discharge under pressure-flow conditions. The scour depth at all the 12 locations appears to increase with an increase in the flow discharge, as expected, except for a few outliers. The outliers may be attributed to manual, experimental, and/ or measurement errors.

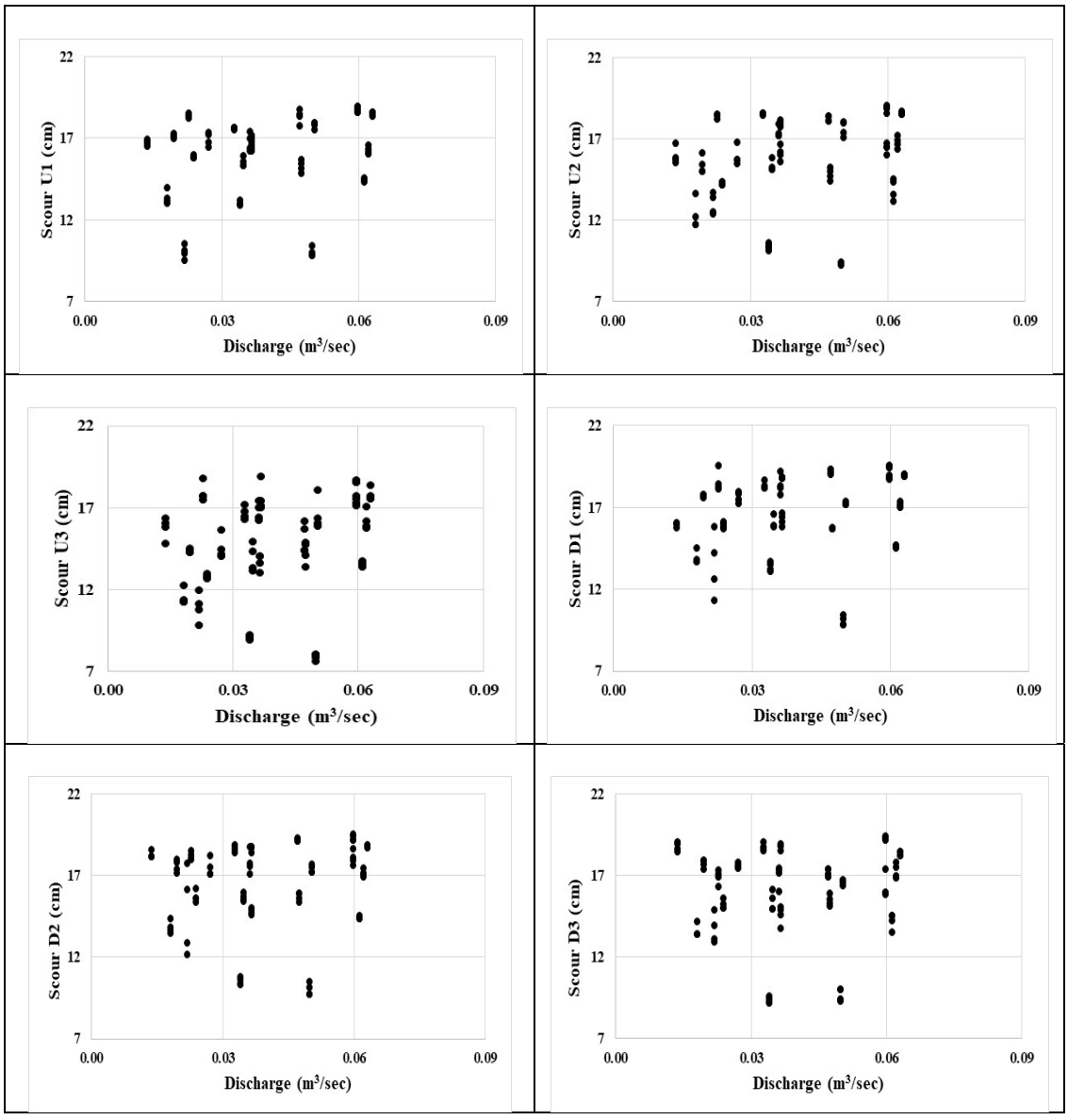

Figure 3.7(a): Scour depth at various locations (upstream & downstream of pier) versus the flow discharge under pressure-flow conditions

Figure 3.7(b) presents the relationship between scour at different locations left and right of the pier and the flow discharge under pressure-flow conditions. The pattern is similar to that for Figure 3.7(a).

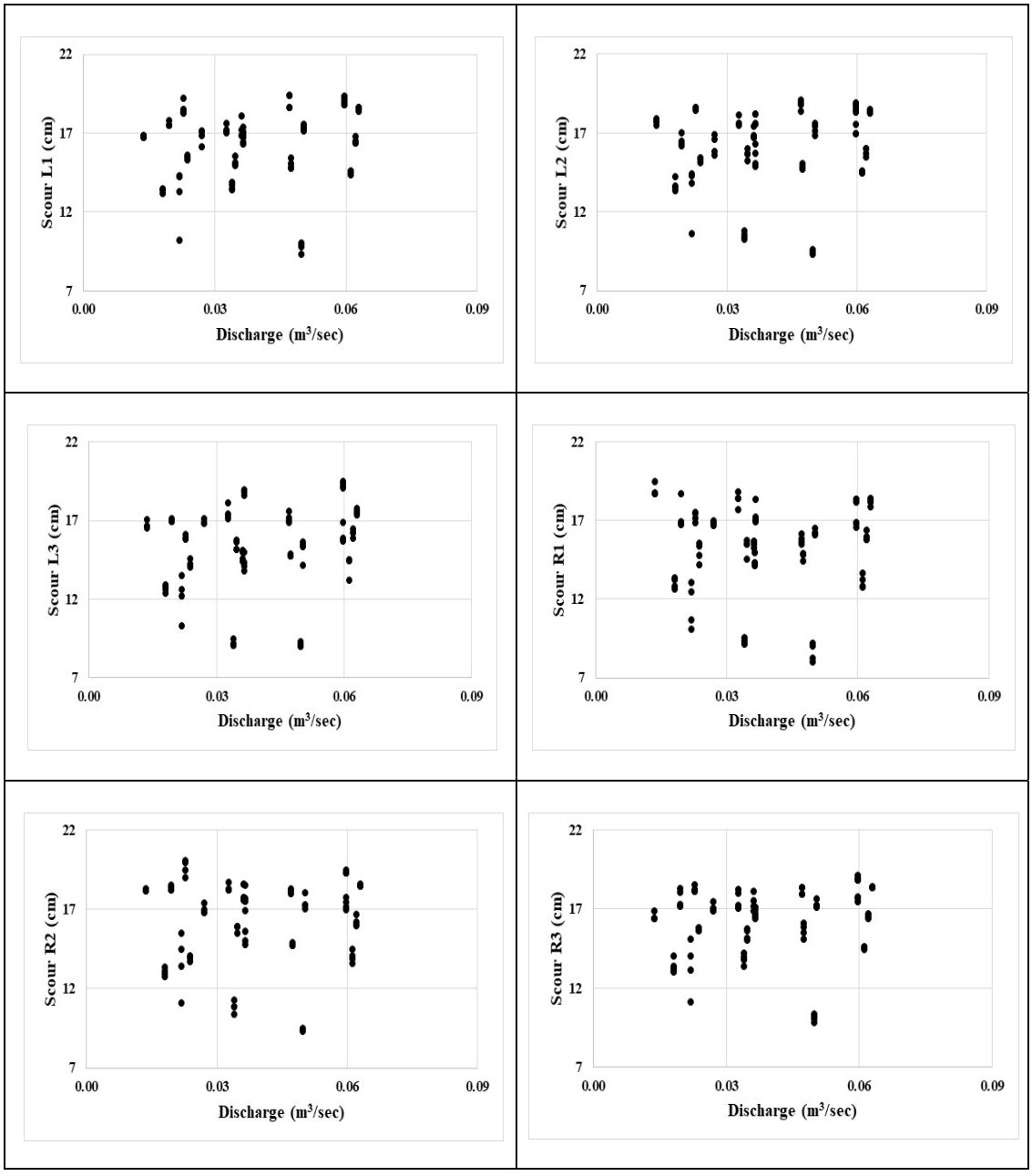

Figure 3.7(b): Scour depth at various locations (left and right of pier) versus the flow discharge under pressure-flow conditions

Figure 3.8(a) presents the relationship between scour at different locations upstream and downstream of the pier and the pier diameterunder pressure-flow conditions. The scour depth at all the 12 locations appears to increase with an increase in the pier diameter, as expected. However, the scour depth for D = 5.14 cm appears to be on the lower side than expected at-least in some of the experiments carried out in this study. This may be attributed to to manual, experimental, and/ or measurement errors.

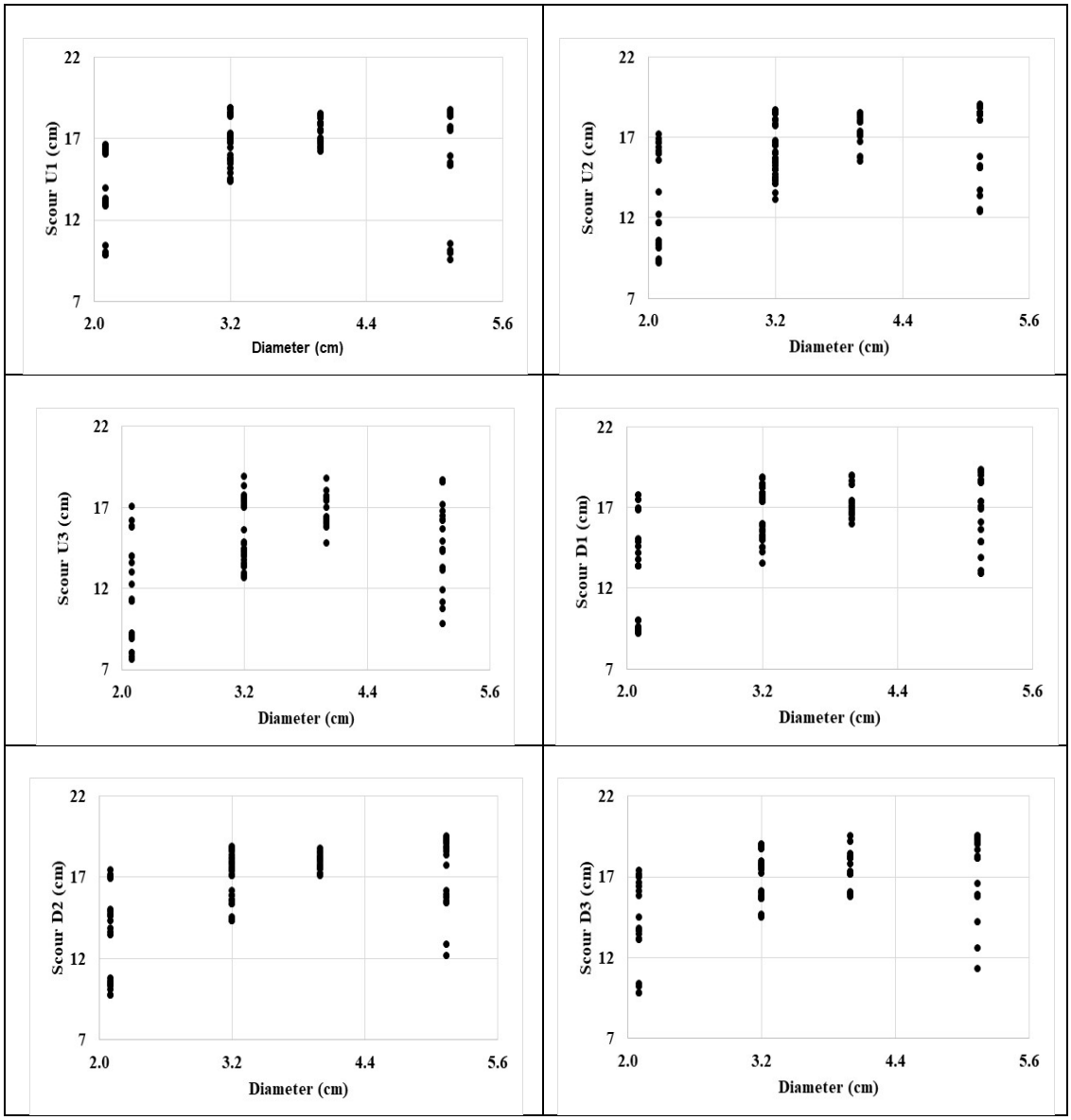

Figure 3.8(a): Scour depth at various locations (upstream & downstream of pier) versus the pier diameter under pressure-flow conditions

Figure 3.8(b) presents the relationship between scour at different locations left and right of the pier and the pier diameterunder pressure-flow conditions. The pattern is similar to that for Figure 3.8(a).

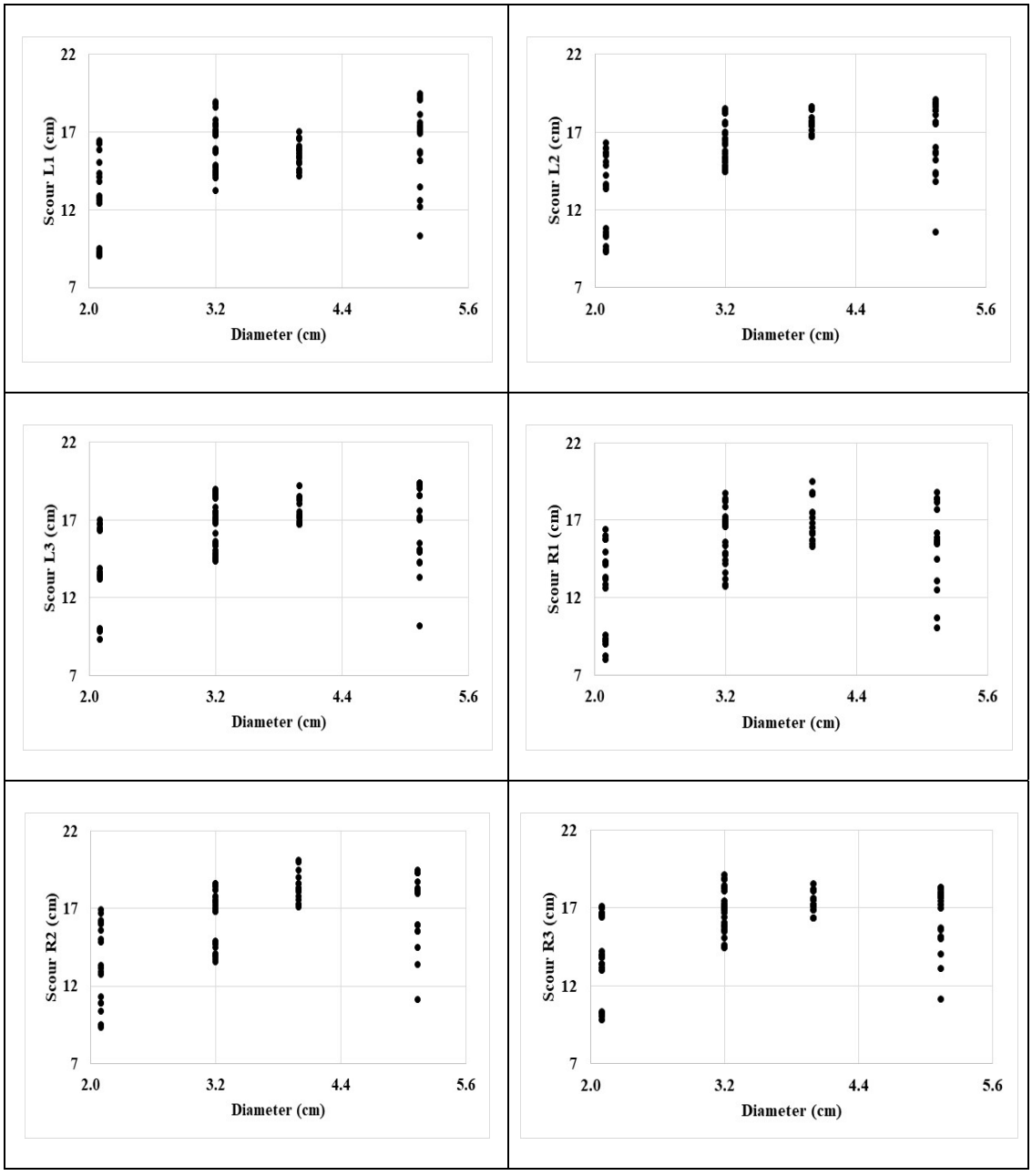

Figure 3.8(b): Scour depth at various locations (left and right of pier) versus the pier diameter under pressure-flow conditions

The graphical evaluation of the scour against the hydraulic parameters presented above gives an idea of the maximum scour but how the depth of scour evolves with time needs to be examined also. A graphical representation of the time distribution of the scour at 12 different locations around a bridge pier was prepared for each experiment conducted.

A few sample figures of such time-distribution of scour are presented in Figure 3.9 and Figure 3.10 for free-flow and pressure-flow conditions, respectively.

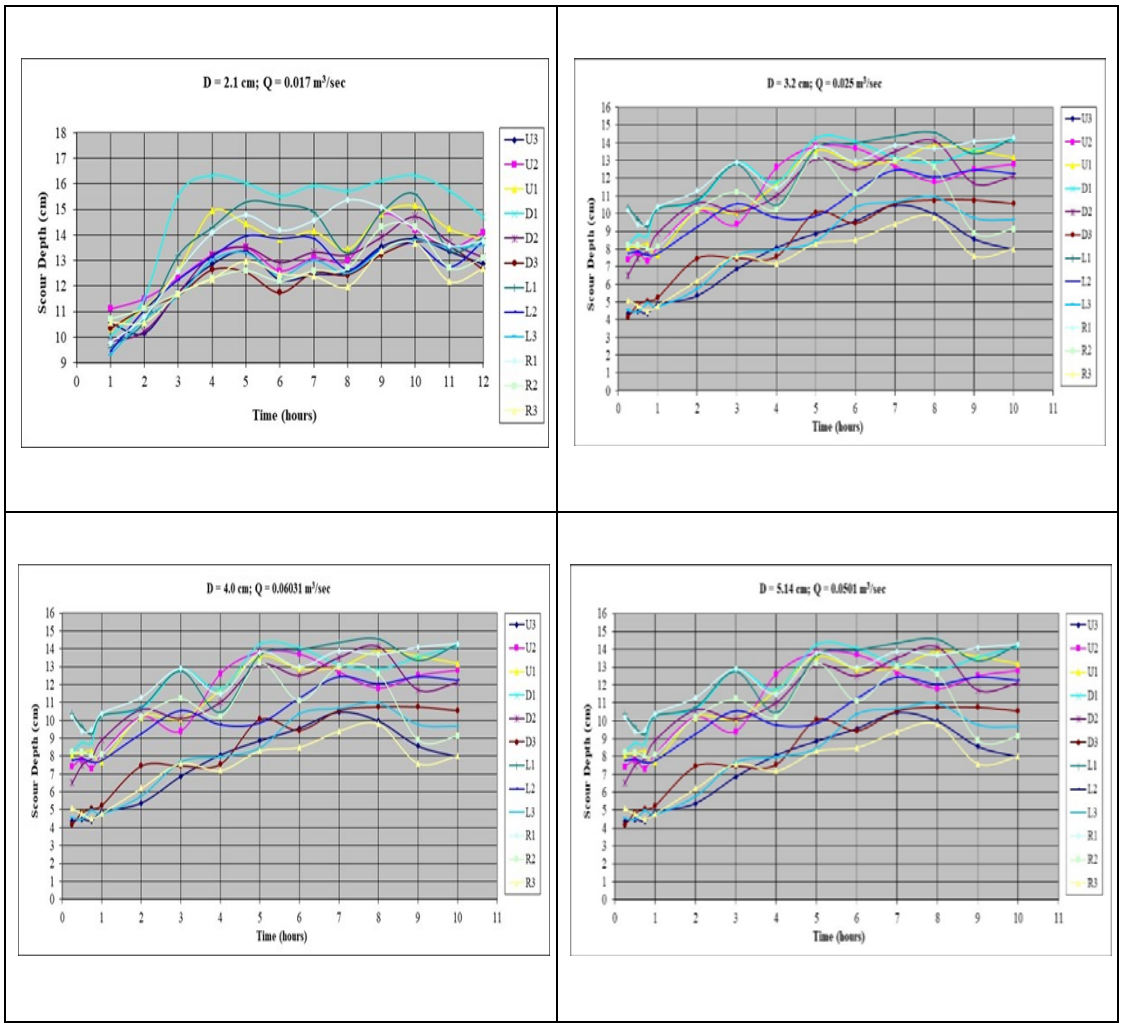

Figure 3.9: Time-distribution of scour under free-flow conditions for different pier diameters for all twelve scour locations

It is clear from these graphs that the scour at each of the 12 locations around the bridge pier initially increases slowly with time and then attains the maximum value (known as the equilibrium scour) after about 5-6 hours for the free-flow conditions. However, the scour reaches its equilibrium value much faster in case of the pressure-flow conditions. It shows that the pressure-flow conditions are very important in the design of bridge pier foundations.

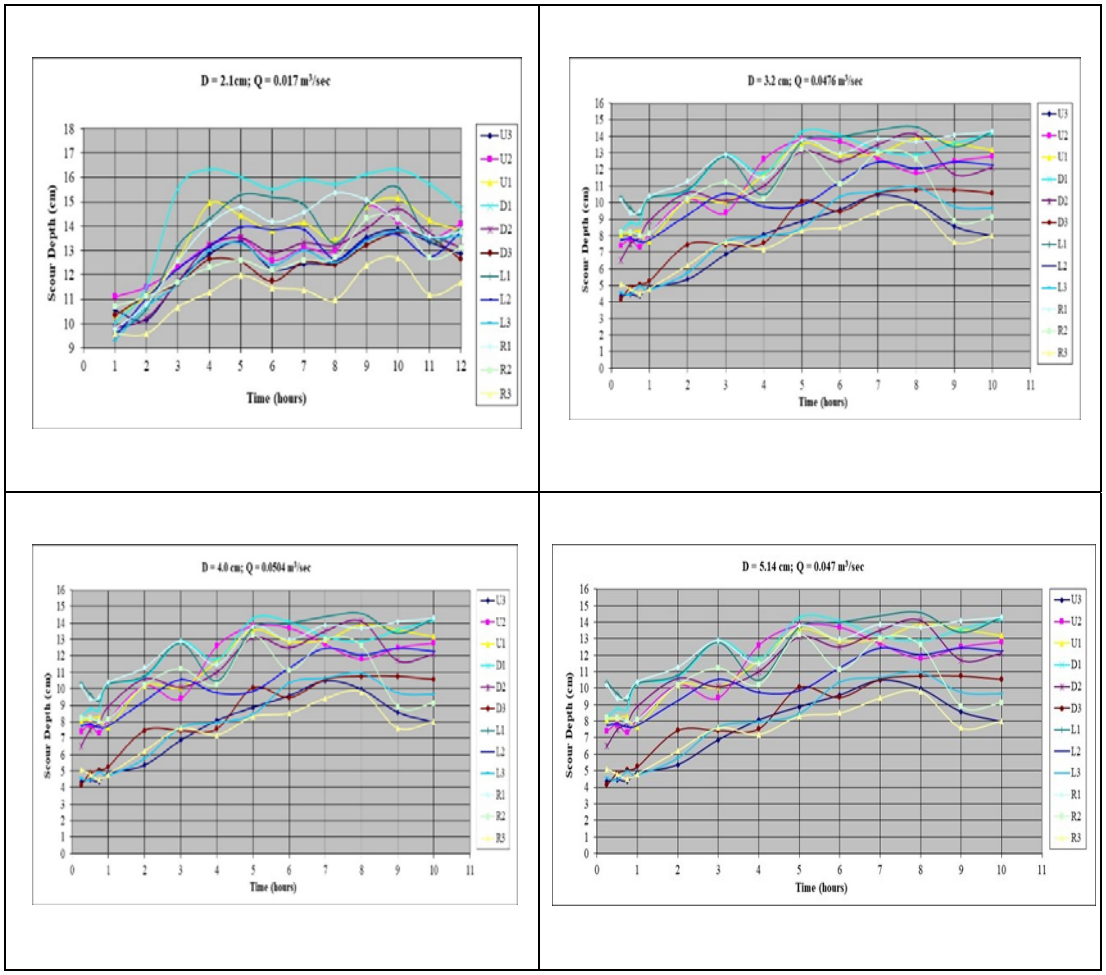

Figure 3.10: Time-distribution of scour under pressure-flow conditions for different pier diameters for all twelve scour locations

It has been found that the value of scour around bridge pier oscillates around the mean equilibrium scour value after about five hours into the experiment. Therefore, the values of four maximum scour depths after five hours were recorded and transferred into the scour database for each of the 12 scour locations. It is to be noted that the corresponding

hydraulic variables e.g. pier diameter, flow depth, flow velocity, and flow discharge values were also recorded and transferred into the scour database. The values of the hydraulic parameters were recorded at the same time at which scour depth is recorded to maintain consistency. Out of the four maximum scour depth values for each of the 12 locations around the bridge pier, the lowest and the highest values were kept in the training/calibration dataset and the middle two values were kept in the validation/testing data set for the development of all the mathematical models investigated in this study. The databases for both free-flow and pressure-flow conditions are presented in different tables Appendix-A.

A comparison of the maximum scour depths at locations closest to the pier (i.e. at U1, D1, R1, and L1) under free-flow and pressure-flow conditions for each pier diameter was carried out next. This was done by plotting average of maximum scour at each of the four locations (U1, D1, L1, and R1) for each pier diameter under free-flow and pressure-flow conditions versus the discharge values as a bar chart. These bar charts are sown in Figure 3.11 through Figure 3.14 for different diameter piers. These figures show that the pressure-flow scour significantly increases as compared to the free-flow scour for a particular pier diameter, discharge, and location except for D = 2.1 cm.

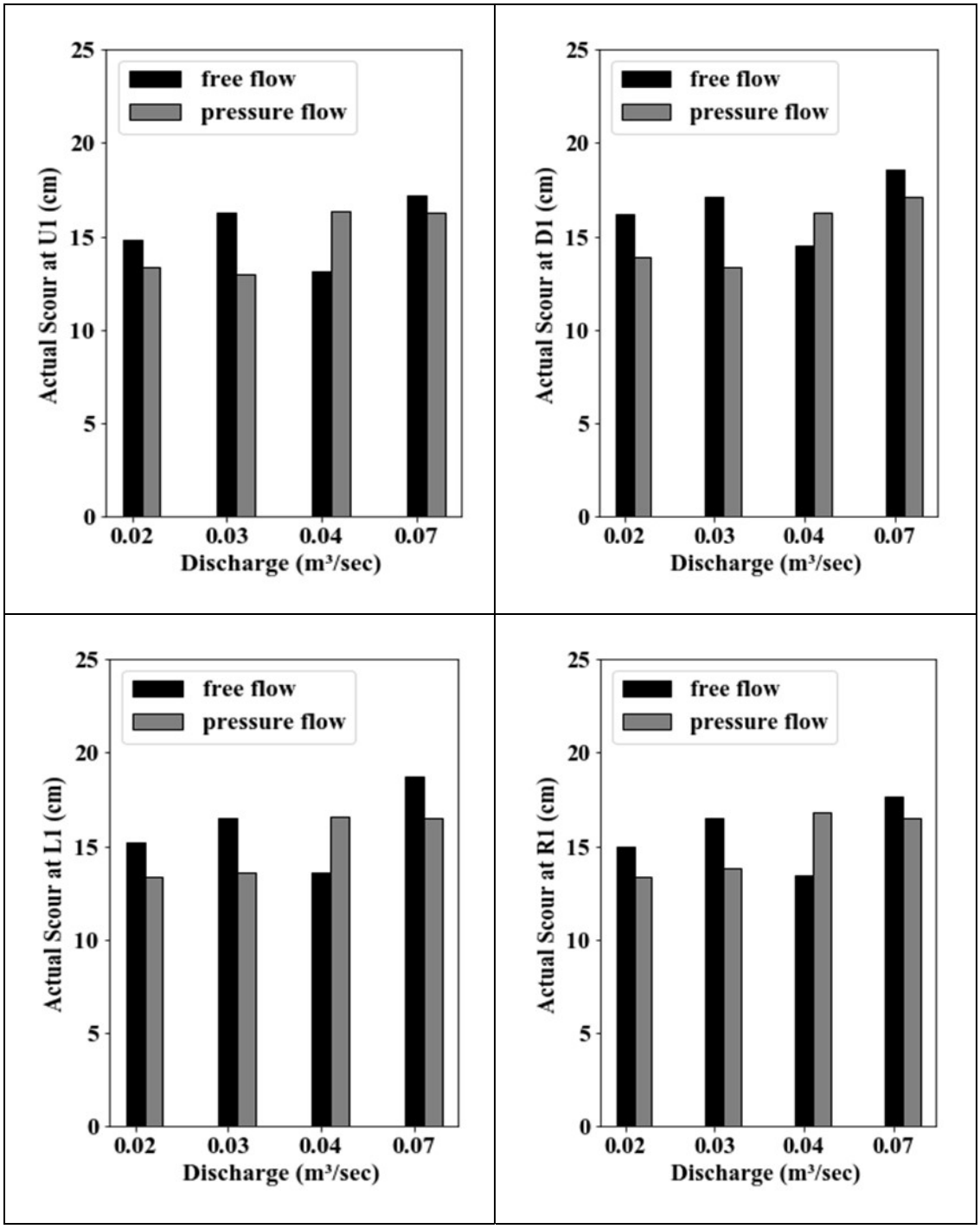

Figure 3.11: Comparison of maximum scour around bride piers under free-flow and pressure-flow conditions for pier diameter D = 2.1 cm

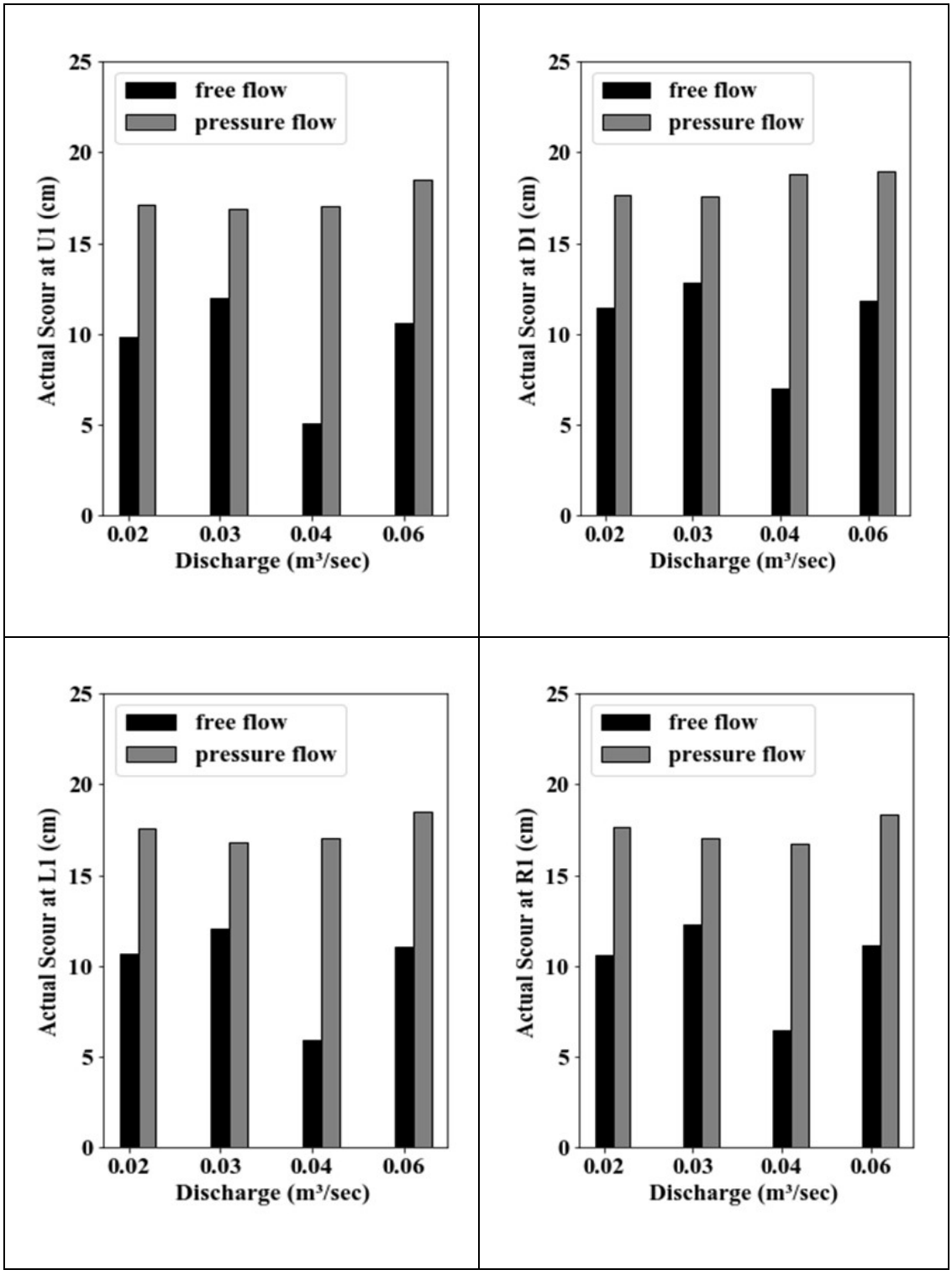

Figure 3.12: Comparison of maximum scour around bride piers under free-flow and pressure-flow conditions for pier diameter D = 3.2 cm

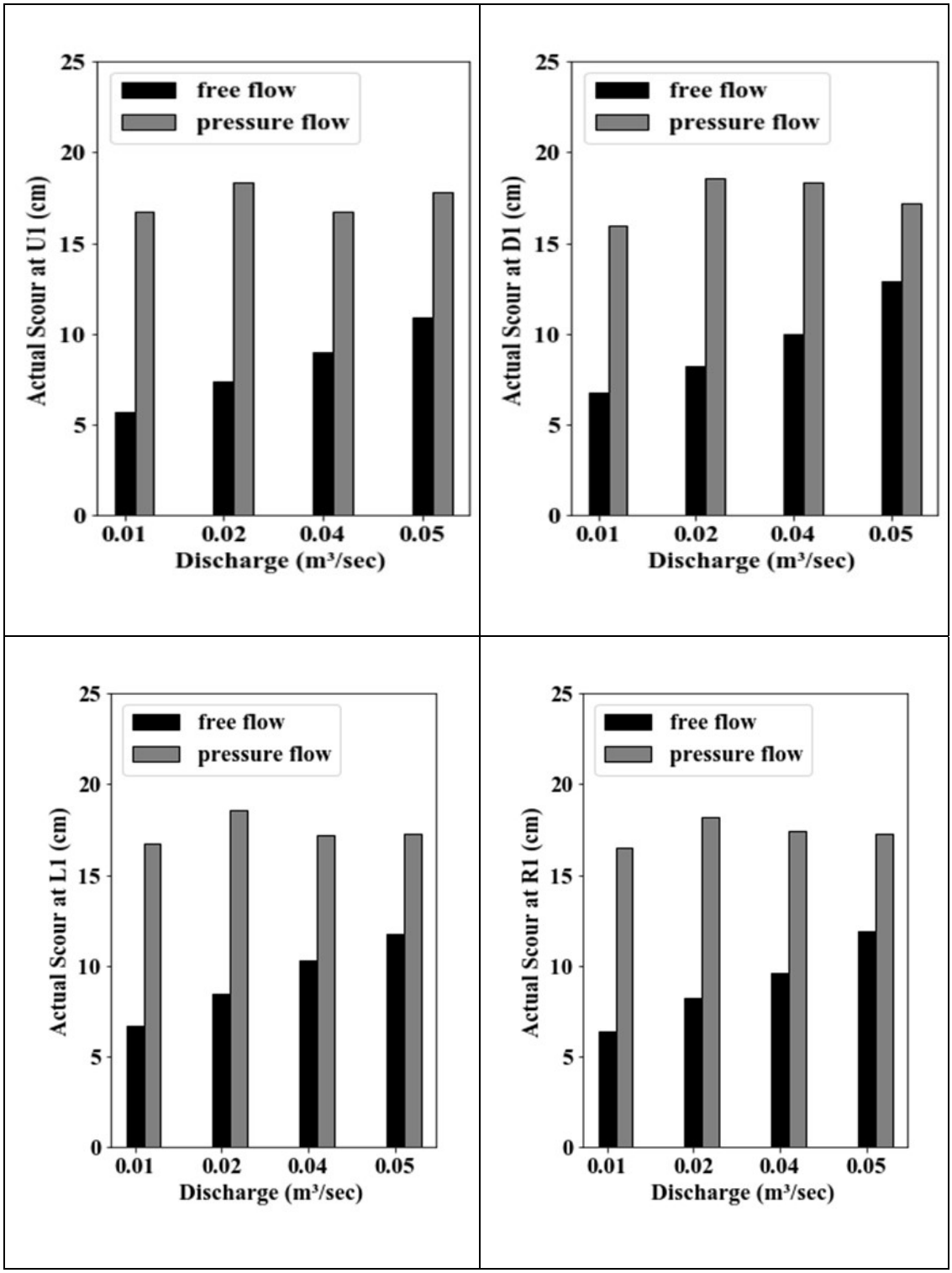

Figure 3.13: Comparison of maximum scour around bride piers under free-flow and pressure-flow conditions for pier diameter D = 4.0 cm

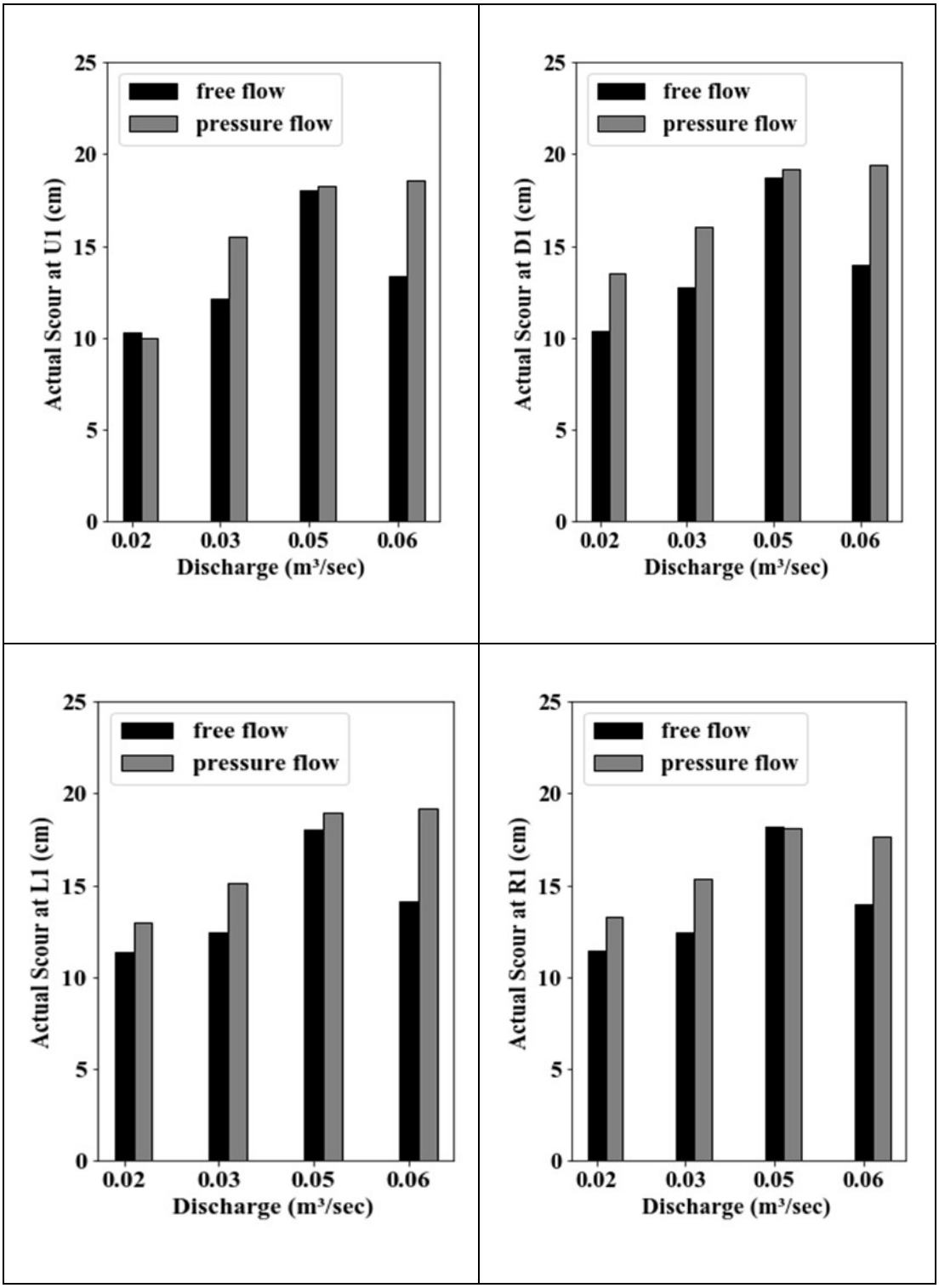

Figure 3.14: Comparison of maximum scour around bride piers under free-flow and pressure-flow conditions for pier diameter D = 5.14 cm

In order to quantify the increase in the pressure-flow scour in comparison to the free-flow scour, the ratios are calculated and presented in Table 3.2. Table 3.2 shows the ratio of pressure-flow scour and the free-flow scour for different diameters and discharge values. The far-right column shows the average ratio of pressure-flow and free-flow scours taken over all the four scour locations (U1, D1, L1, and R1) for a particular discharge. The average maximum scour at a location taken over all the experiments for a particular pier diameter and various discharge values are shown at every fifth row in the table in bold font.

Table 3.2: Ratios of pressure-flow scour and free-flow scour at different pier diameters locations, and discharges

Diameter (cm)	Discharge (m^3/s)	Ratio-U1	Ratio-D1	Ratio-L1	Ratio-R1	Avg.
5.14	0.02	0.97	1.30	1.14	1.16	**1.14**
5.14	0.03	1.28	1.26	1.21	1.23	**1.25**
5.14	0.05	1.01	1.02	1.05	1.00	**1.02**
5.14	0.06	1.39	1.39	1.36	1.26	**1.35**
Avg.	**0.04**	**1.16**	**1.24**	**1.19**	**1.16**	**1.19**
4.00	0.01	2.94	2.35	2.50	2.58	2.59
4.00	0.02	2.50	2.26	2.21	2.21	2.29
4.00	0.04	1.86	1.84	1.67	1.81	1.79
4.00	0.05	1.63	1.33	1.48	1.45	1.47
Avg.	**0.03**	**2.23**	**1.94**	**1.96**	**2.01**	**2.04**
3.20	0.02	1.74	1.55	1.64	1.66	1.65
3.20	0.04	3.37	2.68	2.87	2.59	2.88
3.20	0.03	1.41	1.37	1.39	1.39	1.39
3.20	0.06	1.74	1.60	1.67	1.65	1.66
3.20	0.06	2.04	1.76	1.84	1.94	1.90
Avg.	**0.05**	**2.14**	**1.85**	**1.94**	**1.89**	**1.96**
2.10	0.02	0.90	0.86	0.88	0.89	0.88
2.10	0.03	0.80	0.78	0.82	0.84	0.81
2.10	0.04	1.25	1.12	1.22	1.25	1.21
2.10	0.07	0.94	0.92	0.88	0.94	0.92
Avg.	**0.04**	**0.97**	**0.92**	**0.95**	**0.98**	**0.96**

It is clear from the Table 3.2 that the scour around a bridge pier increases significantly for all diameters and discharges except for D = 2.1 cm. There appears to be some experimental or systematic error in the experiments corresponding to D = 2.1 cm. For D =

5.14 cm, the overall increase in scour for pressure-flow is about 19%; the same is 104% for D = 4.0 cm; and the increase is 96% for D = 3.2 cm. Increase in pressure scour at location U1 is 16% for D=5.14 cm; 123% for D = 4.0 cm; 114% for D = 3.2 cm; and no increase for D = 2.1 cm. Similarly, for increase in pressure-flow scour for location D1 are as follows: 24% for D = 5.14 cm; 94% for D = 4.0 cm; 85% for D = 3.2 cm; and reduction of 8% for D = 2.1 cm. The increased numbers at scour location L1 are: 19% for D = 5.14 cm, 96% for D = 4.0 cm, and 94% for D = 3.2 cm. The increases in pressure-flow scour at location R1 are: 16% for D = 5.14 cm, 101% for D = 4.0 am, 89% for D = 3.2 cm, and a reduction of 2% for D = 2.1 cm. Therefore, it may be concluded that the pressure-flow scour increases by about 20% to 100% depending upon the pier diameter and discharge in the channel/river.

3.4 Modeling Techniques

Two types of mathematical models have been employed in this study, regression models and Artificial Neural Network (ANN) models. Among the regression models, one linear model, one non-linear model of order two, and a power regression model are developed. In recent times, ANNs have evolved as extremely useful tools for the modeling and forecasting of complex engineering systems. The ANNs are useful in systems where intrinsic non-linearities are involved in the dynamics of the physical process being modeled e.g. scour mechanisms. It is claimed that with the use of ANNs, highly accurate predictions can be made even if the physical mechanism is not understood clearly, thus ANNs are very appropriate for scour predictions. In this study, both regression and ANN models were developed for the prediction of scour at all 12 locations around a bridge pier. The details of regression modeling technique are provided in Section 3.4.1 and the details of the ANN models are described in Section 3.4.2. A wide variety of standard error statistics was utilized in this study to evaluate the performance of various models. A description of the model performance evaluation statistics is provided in Section 3.4.3.

3.4.1 Regression Models

The regression models essentially employ the conventional technique of regression analysis. In regression analysis, we develop a relationship among input and output variables by first assuming the functional form of the relationship, and then calibrating the

model parameters through the use of the experimental data. Regression analysisinvolves one dependent variable and one or more independent variables. The regression models help us understand the behaviour of the dependent variable when any one of the independent variables is varied. Let ***X***be the independent variables, ***Y***be the dependent variable, and the unknown parameters generally be denoted as **β**. Then the relationship among them may be written as:

$$\boldsymbol{Y} \sim f(\boldsymbol{X}, \boldsymbol{\beta}) \tag{3.1}$$

Regression models can be either linear or non-linear in nature. In a linear regression model, we regress the output variable *Y*linearly with one or more input variables *X*. In linear regression, data are modelled using linear functions, and unknown model parameters are estimated from the data. Linear regression is the most common type of regression models probably because it can be used as a bench mark model. Once a regression model has been calibrated, an additional value of input(s) *X*can begivento the fitted model to make a prediction of the value of the output *Y*. Least squares method is the most commonly used method for calculating (or fitting) the model parameters of the linear regression models. The functional form of a linear regression model may be written as follows:

$$y_i = \beta_0 + \beta_1 x_{i1} + \beta_2 x_{i2} + \beta_3 x_{i3} + \cdots + \beta_p x_{ip} \tag{3.2}$$

Where, x_{ij} is the i^{th}observation (i= 1 to n) on the j^{th}independent variable (j=1 to p); y_i is the i^{th} observation of the dependent variable; and β's are the regression coefficients to be determined through least squares or some other method.

A special form of linear regression is called polynomial regression where the relationship between the dependent and the independent variables is modelled as an n^{th} order polynomial. Polynomial regression generally fits a non-linear relationship between the values of independent and dependent variables. The multiple polynomial (quadratic) regression models can be expressed as the following equation:

$$y_i = \beta_0 + \beta_1 x_{i1} + \beta_2 x_{i1}^2 + \beta_3 x_{i2} + \beta_3 x_{i2}^2 + \cdots \tag{3.3}$$

Statistically, the two regression models represented in equations (3.2) and (3.3) are linear and considered as a special case of multiple linear regression model. Therefore, the least squares estimator is used for the determination of the model parameters.

In non-linear regression analysis, the observational data or predictor variables are modelled as a nonlinear combination of model parameters. A typical non-linear regression model (also known as power regression model) can be written as follows:

$$y = \beta_0 x_1^{\beta_1} x_2^{\beta_2} \ldots \tag{3.4}$$

Some non-linear problems can be made linear and solved by suitable transformation of the model formulation. For example, for equation (3.4), taking logarithm on both sides, it becomes a problem of linear regression, as follows:

$$\ln(y) = \ln(\beta_0) + \beta_1 \ln(x_1) + \beta_2 \ln(x_2) + \cdots \tag{3.5}$$

This can then be solved by ordinary least squares estimation as discussed earlier. In the present study, both linear and non-linear regression models were developed for the prediction of scour around bridge piers under both free-flow and pressure-flow conditions.

3.4.2 Artificial Neural Networks

An ANN is a mathematical model that attempts to simulate the structural and functional aspects of a biological neural network. The biological neural networks are made up of the basic building block in human nervous system known as the 'biological neuron'. Figure 3.15 shows the basic structure of a biological neuron.

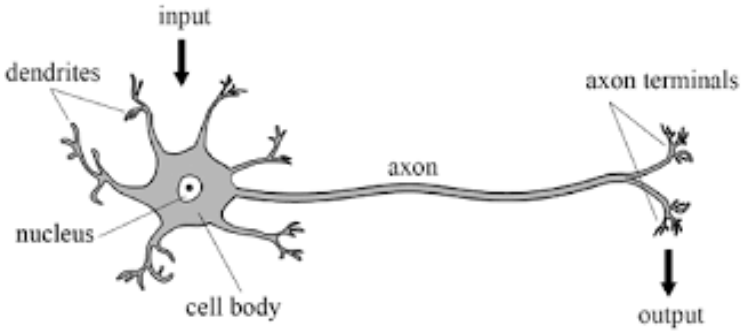

Figure 3.15: Structure of a Biological Neuron
(Source Google Images)

A biological neuron basically consists of three parts, the cell body (soma), the dendrites and the axon. The biological neurons receive information through the dendrites of other neurons and pass on the same to a neuron through the long structure called axon. The cell body (or soma) is capable of releasing many different types of electro-chemical signals and pass on such information to other biological neurons through axons and dendrites. When one of the neurons fires, a positive or negative charge is received by one of the dendrites, the strengths of all the received charges are added. The aggregate input is then passed into the axon, if this is greater than the axon hillocks threshold value, then the neuron fires. The terminal button of a neuron is connected to other neurons across a small gap called the synapse. Neurotransmitter chemicals trigger other neurons in the vicinity and their stimulation can be excitatory or inhibitory.

McCulloch and Pitts (1943) first proposed a mathematical model based on the structure and functions of a biological neuron. The structure of an artificial neuron proposed by McCulloch and Pitts (1943) is shown in Figure 3.16. An artificial neuron consists of two main parts (a)an aggregation function, which receives various inputs from an external source, multiplies them by the respective weights and computes the weighted sum, and (b) an activation function, which squashes the aggregated input through the use of some non-linear function. An artificial neuron resembles the human brain in two respects: (a) the knowledge is acquired from the environment through learning process, and (b) inter-neuron connection strengths, known as synaptic weights, are used to store the required knowledge. Thus, an ANN may be defined as a massively parallel distributed processor made up of simple processing units, which has a natural propensity for storing knowledge and making it available for use.

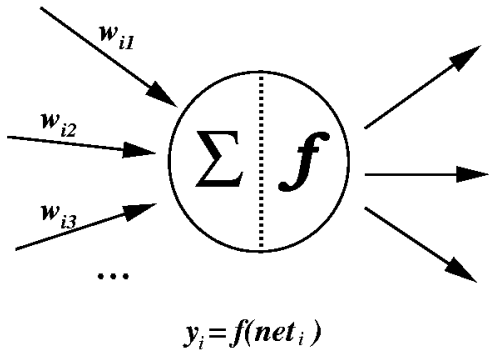

Figure 3.16: Artificial Neuron Model Proposed by McCulloch and Pitts (1943) (Source Google Images)

The ANNs are non-linear statistical data modelling tools, which are usually used to model the complex and non-linear relationships among inputs and outputs. The advantage of ANNs is that they are very appropriate for problems where the underlying physical phenomenon is not very well understood e.g. scour mechanisms.

An ANN's architecture can be classified either as a feed-forward network or a feed-back network depending upon how the information presented at the input layer neurons flows through the ANN. Most of the ANN applications reported in engineering and sciences have employed the feed-forward neural network (FFNN) architecture. In this study, FFNNs have been developed for prediction of scour around bridge piers. Therefore, a brief description of the FFNN only is included here. In an FFNN, the neurons are arranged in layers, the first layer where the input is received is termed as the input layer, the output from the input layer goes as input to the next layer generally known as hidden layer through a series of connections or weights (there may be more than one hidden layer in a network). The weighted sum of the inputs composes the activation signal of the neuron. The activation signal is then passed through an activation function to produce the output from the neuron. The layer from which the output is obtained is called the output layer. The data flow in an FFNN is strictly from the input units to the output units. The data flow can extend to multiple units but there are no feedback connections present, that is, connections extending from outputs of units to inputs of units in the same layer or previous layers.

Multilayer feed forward networks are a class of networks which consists of multiple layers of computational units interconnected in a feed forward way. Feed forward networks are used in pattern recognition and find many engineering applications including civil engineering and are also widely used in hydrology. In FFNNs, the input to the ith neuron in a layer (hidden or output) is calculated as:

$$Net_i = \sum_{j=1}^{n1} w_{ij} x_j + b \tag{3.6}$$

Where,

w_{ij} = the weight of the connection joining the i^{th} neuron in a layer with the j^{th} neuron in a previous layer,

x_j = the value of input (for input layer) or the output from the j^{th} neuron from the previous layer,

Net_i = the net input received by the neuron i,

$n1$ = the number of neurons in the previous layer than the one in which neuron i is located, and

b = the bias to the neuron i.

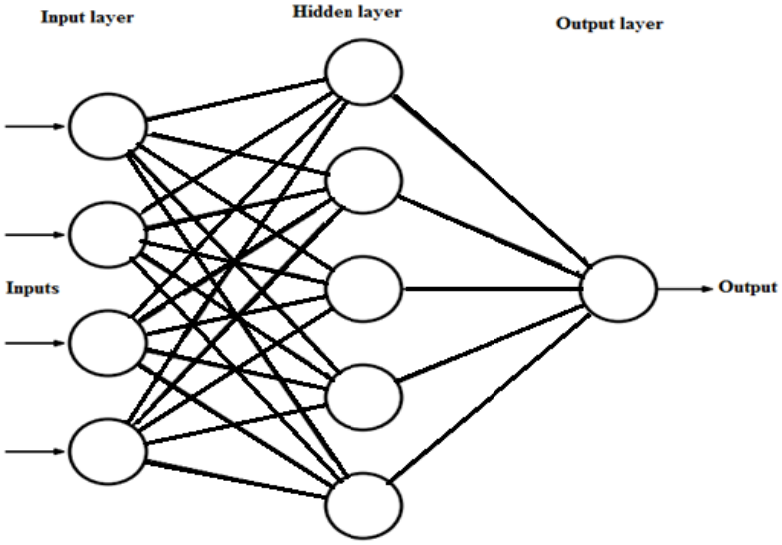

Figure 3.17: A Three Layer Feed Forward Neural Network

(Source Google Images)

Like any other mathematical model, ANNs also need to be calibrated or 'trained'. 'Training' an ANN means presenting training examples and letting it change its weights according to some learning rule. This allows the ANN weights to be adjusted in a way that the set of inputs produces the desired set of outputs. The ANN training can be either supervised or unsupervised. In supervised training, an external teacher is used to train an ANN while in unsupervised training, an ANN self-organizes itself to learn the patterns inherent in the input domain. Most ANN applications including this study use supervised learning methods to train FFNNs. Supervised training is a training methodology in which both the inputs and the matching output patterns are provided to the network. The network processes the inputs and then compares the outputs with the desired outputs. The resulting errors are propagated back through the network and the weights are adjusted. The same set of training patterns are presented to an ANN and the training process is repeated till the desired level of accuracy based on some statistics is achieved. The training of an ANN is an optimization problem and it may happen that the desired accuracy may never be reached then we have to terminate the training after a fixed number of iterations. The most commonly used training algorithm is the error back-propagation training algorithm popularly known as back propagation (Rumelhart et al., 1986).

The back-propagation training method is notorious because it gets stuck in local minima and is slow in convergence. Alternatively, several new training algorithms have been proposed recently. In this study, we have employed Adam training algorithm to train all the ANN models developed. Adam is a deep-learning training algorithm employed in neural network learning. It is a first-order gradient-based optimization algorithm with an ability of having a stochastic objective function. The Adam method adaptively revises the lower-order moments during the learning algorithm.The Adam method is easy to implement, is computationally efficient, has little memory requirements, is invariant to diagonal rescaling of the gradients, and is well suited for problems that are large in terms of data and/or parameters such as ANNs. The method is also appropriate for non-stationary objectives and problems with very noisy and/or sparse gradients. The training parameters of the Adam method (called hyper-parameters) can be fixed using trial and error and need very little tuning. More details of the Adam method can be found in Kingma and Ba (2015).

3.4.3 Model Performance Evaluation Statistics

A number of standard statistical parameters have been used for evaluating the performance of various models developed in this study. Most error statistics employed use square of the deviations between the observed and calculated values of the variable being modelled. For proper evaluation of the model performance, error statistics based on the square of residuals are not enough as they provide a general measure of the model performance and do not provide specific regions where the model is deficient. It is therefore better to consider certain other statistical measures that are unbiased and have a different form in order to test the effectiveness of the developed models in terms of their prediction ability.

The error statistics that are employed in this study include coefficient of correlation (R), Nash Sutcliffe efficiency (E), root mean square error (RMSE),average absolute relative error (AARE), and threshold statistics (TS). These error statistics have been employed extensively in literature for the assessment of ANN model performance (Jain et al., 2001; Jain and Indurthy, 2003; Jain and Ormsbee, 2002; Jain and Srinivasulu, 2004, 2006; and Jain and Kumar, 2007). Scatter plots of predicted versus observed values were used as graphical aides in assessing the model performance. A description of the error statistics employed in this study is presented next.

3.4.3.1 Correlation Coefficient (*R*)

The correlation coefficient measures the correlation between the modelled and the observed output values. Its value ranges between +1 and -1, values close to 1.0 indicates good model performance and values close to 0 indicate poor model performance. The correlation coefficient is calculated as follows:

$$R = \frac{\sum_{i=1}^{N}(RO(t) - \overline{RO})(RF(t) - \overline{RF})}{\sqrt{\sum_{i=1}^{N}(RO(t) - \overline{RO})^2(RF(t) - \overline{RF})^2}} \tag{3.7}$$

Where, $RO(t)$is the observed output variable at time *t*, $RF(t)$ is the forecasted output variable at time *t*, $\overline{RO}$ and $\overline{RF}$ is the mean of the observed and predicted values and *N* is the total number of data points forecasted.

3.4.3.2 Nash-Sutcliffe Coefficient of Efficiency (*E*)

The Nash-Sutcliffe coefficient of efficiency (*E*) compares the modelled and observed values and evaluates how far the total variance of data is explained by the model. The value of *E* ranges between -∞ and 1.0, the values close to 1.0 indicates good model performance. *E* is calculated by the following equations:

$$E = \frac{E_1 - E_2}{E_1} \tag{3.8}$$

$$E_1 = \sum_{i=1}^{N} (RO(t) - \overline{RO})^2 \tag{3.9}$$

$$E_1 = \sum_{i=1}^{N} (RO(t) - RF(t))^2 \tag{3.10}$$

A higher value of *E* indicates better model performance, value of *E*=0 indicates that the model is a naïve model with predicted value as the mean of observed value. Value of *E* above 0.8 indicates very good model performance.

3.4.3.3 Average Absolute Relative Error (*AARE*)

The Average Absolute Relative Error (*AARE*) is the average of the absolute values of the relative errors in predicting certain number of data points. Mathematically *AARE* is expressed as:

$$RE(t) = \frac{RO(t) - RF(t)}{RO(t)} \times 100\% \tag{3.11}$$

$$AARE = \frac{1}{N} \sum_{t=1}^{N} |RE(t)| \tag{3.12}$$

RE(*t*) is the relative error in prediction of the output variable at time *t*. The lower values of *AARE* indicate better model performance and vice-versa.

3.4.3.4 Root Mean Square Error (RMSE)

The root mean square error is an important error statistic which can be used to compare the performances from different models, it is given by the following equation:

$$RMSE = \sqrt{\frac{1}{N}\left[\sum_{i=1}^{N}(RO(t) - RF(t))^2\right]} \tag{3.13}$$

The lower values of *RMSE* indicate better model performance, but *RMSE* can be biased towards high magnitude as the numerator involves the square of the deviation.

3.4.3.5 Threshold Statistics (TS_x)

The threshold statistics give us a picture of the distribution of errors; the average error may not be enough to ascertain the model performance in most cases. The threshold statistic is defined for a certain level of absolute relative error (*ARE*), say *x%*. The threshold statistic for *ARE* level of *x%* may be defined as the percentage of data points forecasted for which *ARE* is less than *x%*. It can be calculated as follows:

$$TS_x = \frac{n_x}{N} \times 100\% \tag{3.14}$$

Where, n_x is the number of data points forecasted with *ARE* less than *x%*. In this study, threshold statistics were calculated for ARE levels of 5%, 10%, and 25%. The higher the *TS* value the better is model performance.

Chapter 4

Model development

4.1 General

This chapter describes the details of the various models developed in this study for the prediction of scour around a bridge pier under free-flow and pressure-flow conditions. Two types of mathematical models have been developed: regression models and Artificial Neural Network (ANN) models. This chapter describes the development of both regression and ANN models for the prediction of scour around a bridge pier.

4.2 Regression Model Development

Three different regression models were developed in this study: a linear regression model, a polynomial model of order-2, and a power regression models. The output variable in all the regression models was the scour at a particular location around a bridge pier. The explanatory variables were diameter of the pier (*D*), flow discharge upstream of the bridge (*Q*), flow depth just upstream of the bridge (*d*), and flow velocity just upstream of the bridge (*v*). The structure of the three regression models is presented in the following equations:

$$h_s = \beta_0 + \beta_1 D + \beta_2 Q + \beta_3 d + \beta_4 v \tag{4.1}$$

$$h_s = \beta_0 + \beta_1 D + \beta_2 Q + \beta_3 d + \beta_4 v + \beta_5 D^2 + \beta_6 Q^2 + \beta_7 d^2 + \beta_8 v^2 \tag{4.2}$$

$$h_s = \beta_0 D^{\beta_1} Q^{\beta_2} d^{\beta_2} v^{\beta_4} \tag{4.3}$$

where h_s is the depth of scour around bridge pier at a particular location(cm), D is the pier diameter (cm), Q is the flow discharge (m^3/s), d is the flow depth (cm) just upstream of the

bridge, v is the velocity of flow just upstream of the bridge (m/s), and β's are the regression coefficients to be determined.

Please note that the scour depth was measured at 12 different locations around a bridge pier. Therefore, twelve different regression models were developed for predicting scour around a bridge pier at each of the 12-locations for a given combination of input variables. Thus, there were 12 linear regression models represented by eq. 4.1, 12 regression models represented by eq. 4.2, and 12 regression models represented by eq. 4.3 for the free-flow conditions. Similarly, there were 36 regression models developed (12 each of linear, second order polynomial, and power regression type) for the pressure flow conditions. The regression coefficients were determined using the method of least squares in Excel software using the calibration/training data set. The regression coefficients from various models are presented in Table 4.1through Table 4.6 for the free-flow and pressure-flow conditions.

Table 4.1: Regression coefficients for linear regression model for free-flow conditions

	β_0	β_1	β_2	β_3	β_4
	Intercept	***D***	***Q***	***d***	***v***
U1	0.4496	-0.2273	0.0889	0.3971	-0.2413
U2	0.5200	-0.2273	0.0889	0.3971	-0.2413
U3	0.5362	-0.3902	0.0489	0.5568	-0.2657
D1	0.4335	-0.1681	0.0150	0.3799	-0.0266
D2	0.4206	-0.2077	-0.1843	0.6954	-0.1297
D3	0.5081	-0.3687	-0.1700	0.6157	-0.1485
L1	0.3795	-0.1530	-0.1202	0.5754	-0.0663
L2	0.5007	-0.1854	0.1774	0.2015	-0.1172
L3	0.5588	-0.3596	0.1287	0.2010	-0.0750
R1	0.4254	-0.1861	0.2128	0.2349	-0.1050
R2	0.4162	-0.1861	0.2128	0.2349	-0.1050
R3	0.5323	-0.3622	0.0490	0.3571	-0.0438

Table 4.2: Regression coefficients for quadratic polynomial regression model for free-flow conditions

	β_0	β_1	β_2	β_3	β_4	β_5	β_6	β_7	β_8
	Intercept	D	Q	d	v	D^2	Q^2	d^2	v^2
U1	43.84	-17.88	107.11	-0.3894	-5.356	2.341	-360.46	0.0157	2.36
U2	50.27	-17.84	232.54	-1.1676	-15.940	2.321	-1017.74	0.0394	6.75
U3	42.18	-16.13	110.95	-0.1333	-10.996	1.968	-253.35	0.0094	3.04
D1	40.10	-15.44	65.73	0.0234	-7.011	1.981	-67.09	0.0035	3.30
D2	46.16	-17.22	157.16	-0.9400	-8.167	2.215	-1047.52	0.0453	2.66
D3	48.65	-19.77	209.97	-1.0377	-2.195	2.468	-1378.32	0.0440	-2.23
L1	42.21	-15.53	24.26	-0.1488	-10.830	2.033	202.26	0.0113	6.35
L2	45.25	-18.29	116.93	-0.7811	-1.345	2.347	-24.58	0.0241	-0.68
L3	42.41	-16.75	158.92	-0.0271	-13.147	2.069	-769.13	0.0025	5.19
R1	42.79	-16.38	130.05	-0.5354	-5.697	2.150	-366.07	0.0188	1.44
R2	38.89	-16.57	44.73	-0.1807	0.896	2.108	35.53	0.0131	-1.35
R3	40.31	-17.57	23.60	-0.0108	0.967	2.175	309.67	0.0055	-2.33

Table 4.3: Regression coefficients for power regression model for free-flow conditions

	β_0	β_1	β_2	β_3	β_4
	Intercept	D	Q	d	v
U1	2.3785	-0.1859	0.0830	0.2191	-0.0513
U2	3.0758	-0.3382	0.3028	0.2179	-0.3901
U3	2.6868	-0.6195	0.2992	0.4211	-0.5998
D1	1.8171	-0.2310	-0.0223	0.3757	-0.0385
D2	2.4040	-0.3571	0.1546	0.3376	-0.2700
D3	2.4570	-0.6339	0.1778	0.3999	-0.4128
L1	1.9624	-0.2141	0.0535	0.3657	-0.1763
L2	3.1395	-0.3296	0.2424	0.1340	-0.1416
L3	3.4185	-0.6532	0.3735	0.2513	-0.5001
R1	3.3721	-0.2631	0.2825	0.0978	-0.2723
R2	1.3702	-0.3467	-0.0196	0.5320	-0.0957
R3	0.4302	0.2671	-0.0865	0.1767	0.0381

Table 4.4: Regression coefficients for linear regression model for pressure-flow conditions

	β_0	β_1	β_2	β_3	β_4
	Intercept	D	Q	d	v
U1	0.3157	0.1977	-0.0705	0.3716	0.2972
U2	0.2990	0.3620	0.0530	0.2607	0.0555
U3	0.2821	0.2655	0.0936	0.3545	-0.0009
D1	0.3494	0.2796	-0.0226	0.2454	0.1966
D2	0.3532	0.4097	0.0250	0.1116	0.0911
D3	0.3925	0.3670	0.0382	-0.0375	0.1463
L1	0.3631	0.2252	-0.0774	0.3687	0.1634
L2	0.2544	0.3433	-0.1526	0.4018	0.2996
L3	0.3179	0.3343	0.1145	-0.0252	0.1142
R1	0.3784	0.1827	-0.0901	0.2860	0.2504
R2	0.3401	0.3546	-0.0460	0.2148	0.0622
R3	0.4302	0.2671	-0.0865	0.1767	0.0381

Table 4.5: Regression coefficients for quadratic polynomial regression model for pressure-flow conditions

	β_0	β_1	β_2	β_3	β_4	β_5	β_6	β_7	β_8
	Intercept	D	Q	d	v	D^2	Q^2	d^2	v^2
U1	-0.632	7.00	-80.0	0.468	0.462	-0.869	920.2	-0.0099	2.016
U2	2.656	7.03	73.4	-0.736	4.294	-0.790	-239.6	0.0270	-3.882
U3	-4.133	9.53	-95.7	-0.252	7.152	-1.155	1742.8	0.0147	-5.490
D1	5.889	6.41	86.4	-0.592	-2.639	-0.747	-607.7	0.0212	3.595
D2	4.571	8.15	-111.2	-0.639	2.154	-0.920	1891.2	0.0210	-0.558
D3	2.103	8.25	-214.6	-0.653	15.991	-0.937	3107.5	0.0198	-11.385
L1	8.778	5.72	69.2	-0.555	-10.090	-0.666	-446.1	0.0224	9.188
L2	1.663	7.12	-172.9	-0.196	8.727	-0.810	2069.6	0.0121	-4.054
L3	0.613	7.64	-161.6	-0.579	16.208	-0.870	2553.1	0.0178	-11.026
R1	8.575	5.72	87.9	-0.640	-5.550	-0.705	-776.7	0.0235	6.252
R2	5.632	8.13	3.5	-1.009	0.085	-0.929	540.7	0.0348	-0.019
R3	3.481	8.56	-186.2	-0.415	2.142	-1.020	2322.8	0.0165	-0.764

Table 4.6: Regression coefficients for power regression model for pressure-flow conditions

	β_0	β_1	β_2	β_3	β_4
	Intercept	***D***	***Q***	***d***	***v***
U1	1.8606	0.1596	-0.0671	0.2220	0.1347
U2	2.1665	0.3129	0.0151	0.1053	0.0394
U3	1.8208	0.3139	0.0166	0.2108	0.0227
D1	2.2724	0.2271	-0.0103	0.1017	0.0668
D2	2.2983	0.3359	-0.0105	0.0316	0.0592
D3	2.4395	0.3384	-0.0177	-0.0322	0.1282
L1	1.8647	0.1887	-0.0592	0.2052	0.0668
L2	1.5459	0.2909	-0.1162	0.2234	0.1644
L3	2.5876	0.3242	0.0369	-0.0397	0.0970
R1	2.2727	0.1618	-0.0359	0.0969	0.0922
R2	2.1136	0.3289	-0.0312	0.0713	0.0534
R3	1.8528	0.3040	-0.0842	0.0968	0.0613

As per Table 4.1 for free-flow conditions, depth of flow was the most significant variable followed by diameter of pier and velocity of flow with discharge being the least significant variable in predicting the scour at most of the locations based on the linear regression model. As per Table 4.2 for free-flow conditions, flow discharge was the most significant variable followed by diameter of pier and velocity of flow with flow depth being the least significant variable in calculating the scour at most of the locations based on the non-linear regression model of order-2. As per Table 4.3 for free-flow conditions, pier diameter was the most significant variable followed by depth of flow and velocity of flow with flow discharge being the least significant variable in estimating the scour at most of the locations based on the power regression model. Therefore, by looking at the magnitude of the regression coefficients of the various regression models for free-flow conditions, there is no apparent trend of significance of various hydraulic variables.

Analysing the significance of various hydraulic variables for pressure-flow conditions from Table 4.4 for linear regression model, pier diameter was the most significant variable followed by flow depth and flow velocity with flow discharge being the least significant of the variables. As per the non-linear regression model of order-2 for the pressure-flow

conditions, flow discharge is the most significant variable followed by pier diameter and velocity of flow with flow depth being the least-significant of the hydraulic variables. As per the power regression model for the pressure-flow conditions, pier diameter is the most significant variable followed by depth of flow and velocity of flow with discharge being the least-significant of the hydraulic variables. Therefore, by looking at the magnitude of the regression coefficients of the various regression models for pressure-flow conditions, there is no apparent trend of significance of various hydraulic variables. Thus, it appears that the significance depends upon the structure of the regression model being considered.

4.3 Results from Regression Models

The performance of various regression models developed in this study was evaluated in terms of various model performance evaluation statistics and graphical scatter plots between observed and estimated scour depths at all the 12 locations around a bridge pier. Once the regression models have been calibrated, they were tested by calculating various model performance evaluation measures considered in this study under free-flow and pressure-flow conditions. The performance of various regression models for free-flow conditions is first presented in section 4.3.1 and that for the pressure-flow conditions is presented later in section 4.3.2.

4.3.1 Results from Regression Models for Free-Flow Conditions

The values of various error statistics from the three regression models under free-flow conditions are presented in Table 4.7 through Table 4.9. The Table 4.7 shows the performance of the 12 linear regression models (one each for each of the 12 locations around a bridge pier) in terms of various error statistics both during calibration and validation data sets. The last row presents the average error statistics over the 12 scour locations. The best and the worst error statistic in each column is highlighted in bold font. The values of average correlation coefficient (R) and average Nash-Sutcliffe efficiency (E) over the 12 scour locations during calibration were found to be 0.5248 and 0.2810, respectively, which is not good. The average RMSE is 2.91 and the average AARE is 26.2%, which is not adequate. The value of average TS5 of 15.6% during calibration means that in only 15.6% of the cases predicted in calibration had absolute relative error (ARE) of less than 5%. Similarly, analysing the error statistics during testing data set, the

average values of R & E over the 12 scour locations of 0.5085 and 0.2395 represented less than adequate performance. The average RMSE and AARE of 2.89 and 24.8%, respectively, are similar to those during calibration dataset.

Table 4.7: Statistical results from linearregression model under free-flow conditions

Scour	R	E	RMSE	AARE	TS5	TS10	TS25
Location	During Calibration / Training Data Set						
U1	**0.3578**	**0.1280**	3.02	24.9	14.8	27.8	72.2
U2	0.5119	0.2620	**3.10**	27.2	12.5	31.3	75.0
U3	**0.6533**	**0.4268**	2.82	30.8	16.7	29.2	66.7
D1	0.4389	0.1926	2.84	19.6	20.4	**40.7**	77.8
D2	0.5455	0.2976	3.00	25.3	14.6	31.3	72.9
D3	0.5754	0.3311	**3.10**	30.7	10.4	25.0	62.5
L1	0.5191	0.2695	**2.71**	**19.3**	**20.8**	33.3	79.2
L2	0.5001	0.2501	3.01	29.6	13.0	33.3	68.5
L3	0.5498	0.3022	3.04	**34.6**	**8.3**	**18.8**	**60.4**
R1	0.4662	0.2174	2.76	19.7	20.8	29.2	**81.3**
R2	0.5843	0.3414	2.74	22.8	20.4	38.9	70.4
R3	0.5947	0.3537	2.83	30.0	14.6	27.1	62.5
Min	0.3578	0.1280	2.71	19.3	8.3	18.8	60.4
Max	0.6533	0.4268	3.10	34.6	20.8	40.7	81.3
Avg	0.5248	0.2810	2.91	26.2	15.6	30.5	70.8
Scour	R	E	RMSE	AARE	TS5	TS10	TS25
Location	During Validation / Testing Data Set						
U1	0.4307	0.1854	2.82	22.1	14.8	32.1	71.6
U2	0.5026	0.2516	2.96	25.2	14.6	27.1	68.8
U3	**0.6026**	0.3214	2.92	29.1	10.4	22.9	64.6
D1	0.4892	0.2378	2.69	**17.8**	**25.9**	**42.6**	74.1
D2	**0.3894**	**0.0815**	**3.24**	23.1	25.0	41.7	70.8
D3	0.5393	0.2738	3.12	29.6	10.4	25.0	64.6
L1	0.4168	0.1369	2.93	19.9	14.6	41.7	75.0
L2	0.5393	0.2867	2.80	25.0	18.5	40.7	72.2
L3	0.5869	**0.3350**	2.86	**32.2**	12.5	20.8	68.8
R1	0.5234	0.2730	**2.64**	19.0	18.8	35.4	**81.3**
R2	0.4918	0.1893	2.87	24.9	**8.9**	**19.6**	69.6
R3	0.5903	0.3010	2.80	29.5	14.6	31.3	**60.4**
Min	0.3894	0.0815	2.64	17.8	8.9	19.6	60.4
Max	0.6026	0.3350	3.24	32.2	25.9	42.6	81.3
Avg	0.5085	0.2395	2.89	24.8	15.7	31.7	70.1

For linear regression model (see Table 4.7), R ranged between 0.3578 for (U1) and 0.6533 (for U3); E ranged between 0.1280 for (U1) and 0.4268 (for U3); RMSE ranged between 3.10 (for U2 & D3) and 2.71 (for L1); AARE ranged between 34.6 (for L3) and 19.3% (for L1); TS5 ranged between 8.3 (for L3) and 20.8 (for L1); TS10 ranged between 18.8 (for L1) and 40.7 (for D1); and TS25 ranged between 60.4 (for L3) and 81.3 (R1) during calibration. Similarly, the ranges of various error statistics from linear regression model during testing were as follows: R (0.3894-D2, 0.6026-U3); E (0.0815-D2, 0.3350-L3); RMSE (2.64-R1, 3.24-D2); AARE (17.8-D1, 32.2-L3); TS5 (8.8-R2, 25.9-D1); TS10 (19.6-R2, 42.6-D1); and TS25 (60.4-R3, 81.3-R1). These results indicate that the linear regression model is not adequate in capturing the non-linear dynamics inherent in the input and output data of the scour mechanism under free-flow conditions.

Analysing the statistical results from the non-linear regression models of order-2 (NLRM-2) for free-flow conditions from Table 4.8, it can be noted that the values of average R, E, RMSE, and AARE during calibration data set were 0.8317, 0.6920, 1.91, 16.7%, respectively; while those during testing were found as 0.8297, 0.6816, 1.87, 15.5%, respectively. The values of average TS5, TS10, and TS25 during calibration were 26.7, 49.5, and 81.9; and those during testing were 29.0, 48.7, 82.5, respectively.

For NLRM-2 (see Table 4.8), R ranged between 0.8055 for (L2) and 0.8526 (for R3); E ranged between 0.6488 for (L2) and 0.7269 (for R3); RMSE ranged between 1.71 (for R1) and 2.06 (for L2); AARE ranged between 11.7 (for R1) and 22.6% (for U3); TS5 ranged between 10.4 (for U3) and 38.9 (for U1); TS10 ranged between 37.5 (for U3) and 58.3 (for R1); and TS25 ranged between 72.9 (for L3) and 91.7 (L1) during calibration. Similarly, the ranges of various error statistics from non-linear regression model of order-2 during testing were as follows: R (0.7722-D2, 0.8646-R3); E (0.5781-D2, 0.7443-R3); RMSE (1.66-R1, 2.22-D3); AARE (11.5-D1, 21.2-D3); TS5 (18.8-U2, 39.6-L1); TS10 (35.4-D3, 60.4-L1); and TS25 (72.9-U3, 90.7-D1). The TS25 of 91.7% during calibration (for L1) means that more than 91% of the data predicted during calibration had ARE of less than 25%, which is very good. Similarly, the performance of the non-linear regression model in terms of TS statistics was also good during testing data set. The value of TS25 of 90.7% during testing (for D1) shows that in more than 90% of the testing data, the ARE was less than 25%. These results for the NLRM-2 for free-flow conditions indicate that the performance of the NLRM-2 is very good in capturing the non-linear

dynamics inherent in the input and output data of the scour mechanism under free-flow conditions. Also, its performance is significantly better as compared to the linear regression model performance for free-flow conditions.

Now, analysing the statistical results from the power regression models under free-flow conditions from Table 4.9, it can be noted that the values of average R, E, RMSE, and AARE during calibration data set were 0.6067, 0.3608, 2.74, 23.4, respectively; while those during testing were found as 0.6028, 0.3485, 2.67, 21.7, respectively. For power regression model (see Table 4.9), R ranged between 0.4445 for (U1) and 0.7269 (for U3); E ranged between 0.1813 for (U1) and 0.5159 (for U3); RMSE ranged between 2.55 (for R3) and 2.96 (for U2); AARE ranged between 17.8 (for L1) and 29.0 (for L3); TS5 ranged between 8.3 (for L3) and 25.9 (for R2); TS10 ranged between 20.8 (for L3) and 44.4 (for D1); and TS25 ranged between 66.7 (for D3) and 83.3 (R1) during calibration. Similarly, the ranges of various error statistics from power regression model during testing were as follows: R (0.5001-U1, 0.6988-U3); E (0.2384-U1, 0.4641-R3); RMSE (2.45-R3, 2.86-D2); AARE (16.3-D1, 26.6-L3); TS5 (12.5-U3, 29.6-D1); TS10 (25.0-U3, 51.9-D1); and TS25 (64.6-U3, 85.4-D2).

The TS25 of 83.3% during calibration (for R1) means that in more than 83% of the data predicted during calibration had ARE of less than 25%, which is good. Similarly, the performance of the power regression model in terms of TS statistics was also good during testing data set. The value of TS25 of 85.4% during testing (for D2) shows that in more than 85% of the testing data, the ARE was less than 25%.

Examining the statistical results from Table 4.7 through Table 4.9 for regression models under free-flow conditions together, it is clear that the performance of the linear regression models in terms of all the error statistics at all the scour locations during both calibration and testing datasets is poor and not acceptable. The performance of the power regression model (Table 4.9) is slightly better than that of the linear regression models at all of the 12 scour locations in terms of the various error statistics and is less than satisfactory. The performance of the NLRM-2 was the best among the three regression models investigated in this study for free-flow conditions and can be characterized as good. Thus, we can say that the non-linear regression model of order-2 is the best followed by the power regression model while linear model is the worst for free-flow case.

Table 4.8: Statistical results from non-linear regression model of order-2 under free-flow conditions

Scour	R	E	RMSE	AARE	TS5	TS10	TS25
Location	During Calibration / Training Data Set						
U1	0.8278	0.6853	1.81	13.8	**38.9**	55.6	88.9
U2	0.8250	0.6807	2.04	17.7	25.0	45.8	79.2
U3	0.8479	0.7189	1.98	**22.6**	**10.4**	**37.5**	77.1
D1	0.8079	0.6527	1.86	12.4	25.9	53.7	88.9
D2	0.8188	0.6705	2.05	16.9	22.9	54.2	81.3
D3	0.8462	0.7161	2.02	20.1	18.8	37.5	79.2
L1	0.8403	0.7061	1.72	12.0	25.0	56.3	**91.7**
L2	**0.8055**	**0.6488**	**2.06**	19.6	27.8	38.9	77.8
L3	0.8488	0.7205	1.92	20.3	35.4	56.3	**72.9**
R1	0.8364	0.6995	**1.71**	**11.7**	37.5	**58.3**	87.5
R2	0.8230	0.6774	1.91	15.1	29.6	48.1	79.6
R3	**0.8526**	**0.7269**	1.83	18.6	22.9	52.1	79.2
Min	0.8055	0.6488	1.71	11.7	10.4	37.5	72.9
Max	0.8526	0.7269	2.06	22.6	38.9	58.3	91.7
Avg	0.8317	0.6920	1.91	16.7	26.7	49.5	81.9
Scour	R	E	RMSE	AARE	TS5	TS10	TS25
Location	During Validation / Testing Data Set						
U1	0.8345	0.6932	1.72	12.2	33.3	57.4	88.9
U2	0.8331	0.6876	1.91	16.0	**18.8**	39.6	85.4
U3	0.8328	0.6858	1.99	20.4	29.2	41.7	**72.9**
D1	0.8149	0.6620	1.79	**11.5**	33.3	51.9	**90.7**
D2	**0.7722**	**0.5781**	2.20	17.4	20.8	39.6	83.3
D3	0.8108	0.6332	**2.22**	**21.2**	20.8	**35.4**	72.9
L1	0.8464	0.7160	1.68	11.5	**39.6**	**60.4**	89.6
L2	0.8012	0.6311	2.02	17.0	25.9	42.6	75.9
L3	0.8556	0.7249	1.84	17.5	37.5	58.3	77.1
R1	0.8443	0.7102	**1.66**	11.8	27.1	58.3	87.5
R2	0.8457	0.7131	1.71	12.9	39.3	55.4	83.9
R3	**0.8646**	**0.7443**	1.69	16.7	22.9	43.8	81.3
Min	0.7722	0.5781	1.66	11.5	18.8	35.4	72.9
Max	0.8646	0.7443	2.22	21.2	39.6	60.4	90.7
Avg	0.8297	0.6816	1.87	15.5	29.0	48.7	82.5

Table 4.9: Statistical results from power regression model under free-flow conditions

Scour	R	E	RMSE	AARE	TS5	TS10	TS25
Location	During Calibration / Training Data Set						
U1	**0.4445**	**0.1813**	2.93	23.2	16.7	27.8	68.5
U2	0.5872	0.3296	**2.96**	24.5	12.5	31.3	77.1
U3	**0.7269**	**0.5159**	2.60	27.2	10.4	25.0	68.8
D1	0.5270	0.2685	2.70	18.0	20.4	**44.4**	79.6
D2	0.6068	0.3552	2.87	23.1	18.8	33.3	70.8
D3	0.6723	0.4371	2.85	27.0	14.6	22.9	**66.7**
L1	0.5835	0.3322	2.60	**17.8**	16.7	43.8	81.3
L2	0.5737	0.3096	2.89	27.4	14.8	27.8	68.5
L3	0.6673	0.4297	2.74	**29.0**	**8.3**	**20.8**	68.8
R1	0.5496	0.2920	2.63	17.9	20.8	33.3	**83.3**
R2	0.6451	0.4061	2.60	20.6	**25.9**	40.7	70.4
R3	0.6967	0.4725	**2.55**	24.9	18.8	33.3	70.8
Min	0.4445	0.1813	2.55	17.8	8.3	20.8	66.7
Max	0.7269	0.5159	2.96	29.0	25.9	44.4	83.3
Avg	0.6067	0.3608	2.74	23.4	16.5	32.0	72.9
Scour	R	E	RMSE	AARE	TS5	TS10	TS25
Location	During Validation / Testing Data Set						
U1	**0.5001**	**0.2384**	2.72	20.2	18.5	38.9	74.1
U2	0.5953	0.3309	2.80	22.5	16.7	27.1	79.2
U3	**0.6988**	0.4608	2.60	26.2	**12.5**	**25.0**	**64.6**
D1	0.5720	0.3239	2.53	**16.3**	**29.6**	**51.9**	79.6
D2	0.5489	0.2831	**2.86**	20.6	22.9	37.5	**85.4**
D3	0.6721	0.4383	2.74	24.8	12.5	33.3	77.1
L1	0.5243	0.2707	2.69	19.1	12.5	37.5	77.1
L2	0.5994	0.3305	2.72	22.5	22.2	33.3	74.1
L3	0.6638	0.3944	2.73	**26.6**	12.5	29.2	64.6
R1	0.5845	0.3290	2.53	17.3	18.8	39.6	83.3
R2	0.5768	0.3173	2.64	21.0	17.9	32.1	71.4
R3	0.6977	**0.4641**	**2.45**	23.1	12.5	29.2	70.8
Min	0.5001	0.2384	2.45	16.3	12.5	25.0	64.6
Max	0.6988	0.4641	2.86	26.6	29.6	51.9	85.4
Avg	0.6028	0.3485	2.67	21.7	17.4	34.5	75.1

The graphical results from the various regression models under free-flow conditions in terms of scatter plots are examined next. The scatter plots from linear regression model under free-flow conditions are presented in Figure 4.1 and Figure 4.2, respectively, during calibration and testing data sets; Figure 4.3 and Figure 4.4 depict the performance of the NLRM-2 in terms of scatter plots during calibration and testing data sets; and Figure 4.5 and Figure 4.6 show the performance of the power regression model in terms of scatter plots during calibration and testing data sets, respectively. On all the scatter plots, an ideal line at 45-degrees is drawn to assess the performance. It is to be noted that all the predicted points should fall on the ideal line from an ideal model and from a good model the scatter around the ideal line should be as narrow as possible.

From Figure 4.1, it is clear that the performance of linear regression model under free-flow conditions during calibration is not good due to large scatter around the ideal line. It is noted that the linear model is unable to capture the scour dynamics particularly just around the bridge pier (see scatter plots for U1, D1, L1, and R1). As we move away from the pier, the performance of the linear regression model becomes slightly better. The pattern of scatter plots from the linear regression models under free-flow during testing data sets (see Figure 4.2) is similar.

Looking at the results from the NLRM-2 for the free-flow conditions from Figure 4.3 and Figure 4.4, it can be seen that its performance is very good during both calibration and testing data sets. Also, the performance of the NLRM-2 is good at all the 12 locations irrespective of the distance from the pier. It shows that the NLRM-2 model was able to adequately capture the non-linear dynamics inherent in the scour mechanism around a bridge pier.

Analysing the graphical results in terms of the scatter plots from Figure 4.5 and Figure 4.6 from the power regression model under free-flow conditions, it can be seen that its performance is better than the linear regression model but worse than the NLRM-2 model. Also, the performance of the power regression model was consistent regardless of the distance from the pier.

Thus, the graphical results strengthen the conclusions drawn from the statistical results about the suitability of the various regression models in predicting the scour around bridge

piers under free-flow conditions that the NLRM-2 model is the best followed by power regression model while the linear regression model is not suitable at all.

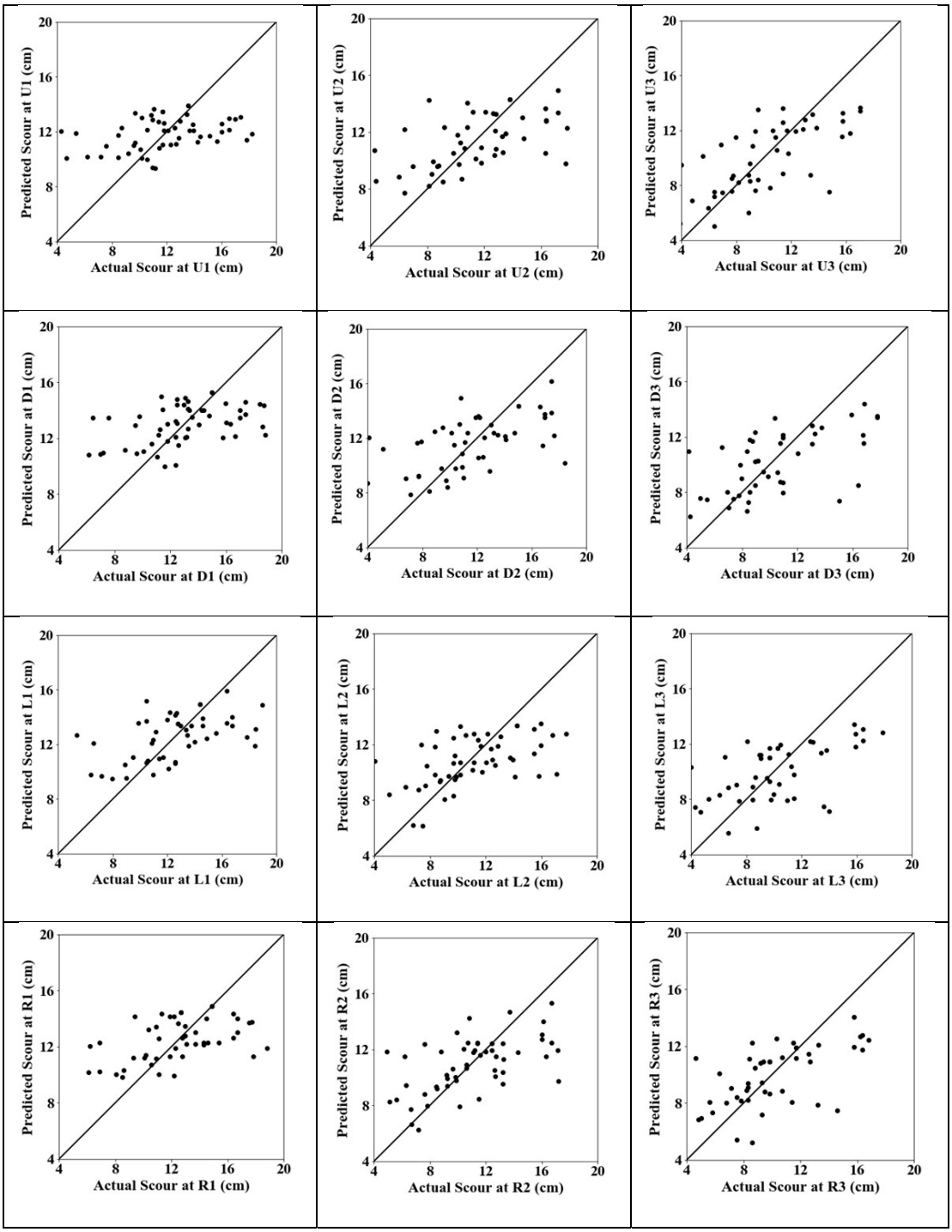

Figure 4.1: Scatter plots from linear regression models under free-flow conditions during calibration

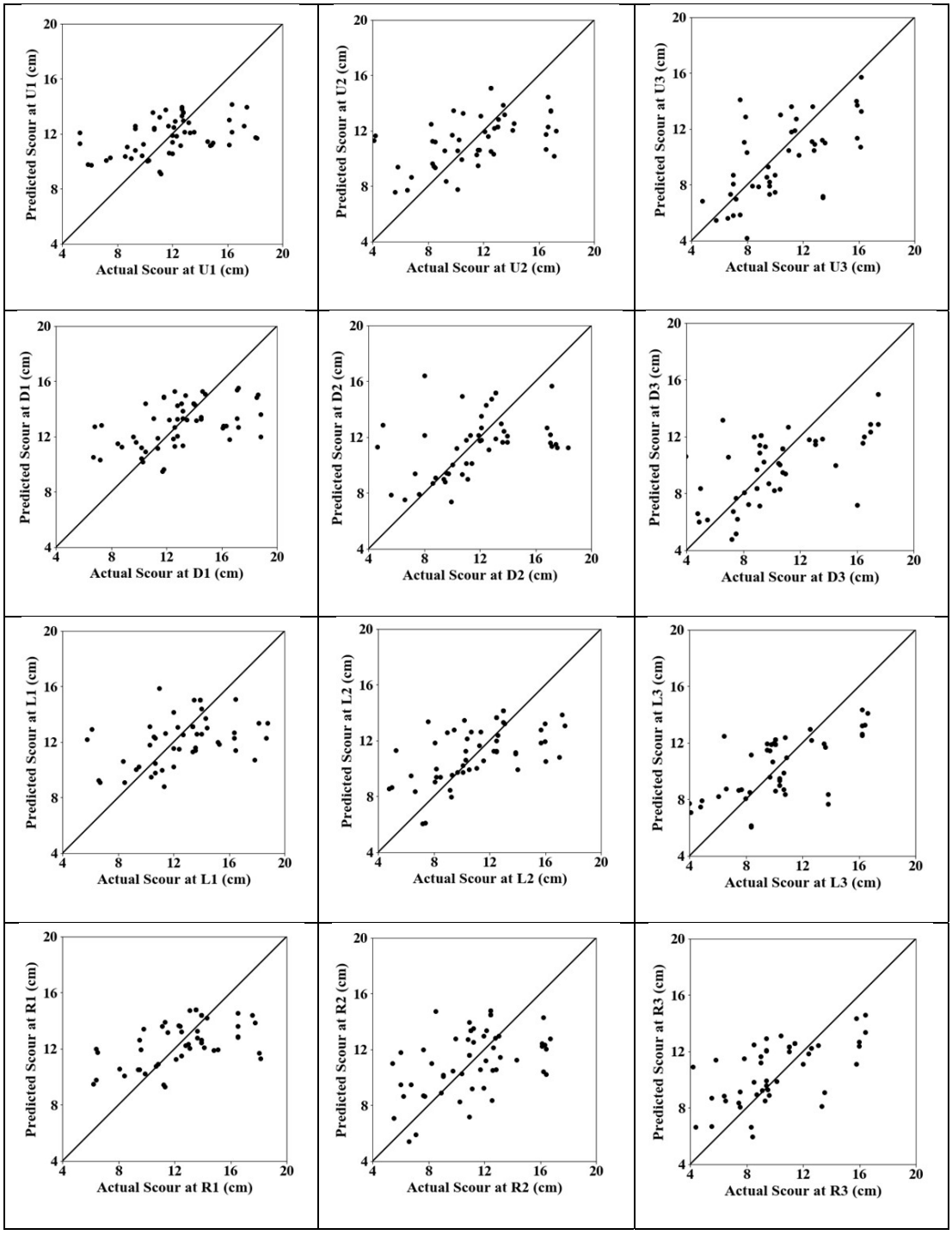

Figure 4.2: Scatter plots from linear regression models under free-flow conditions during testing

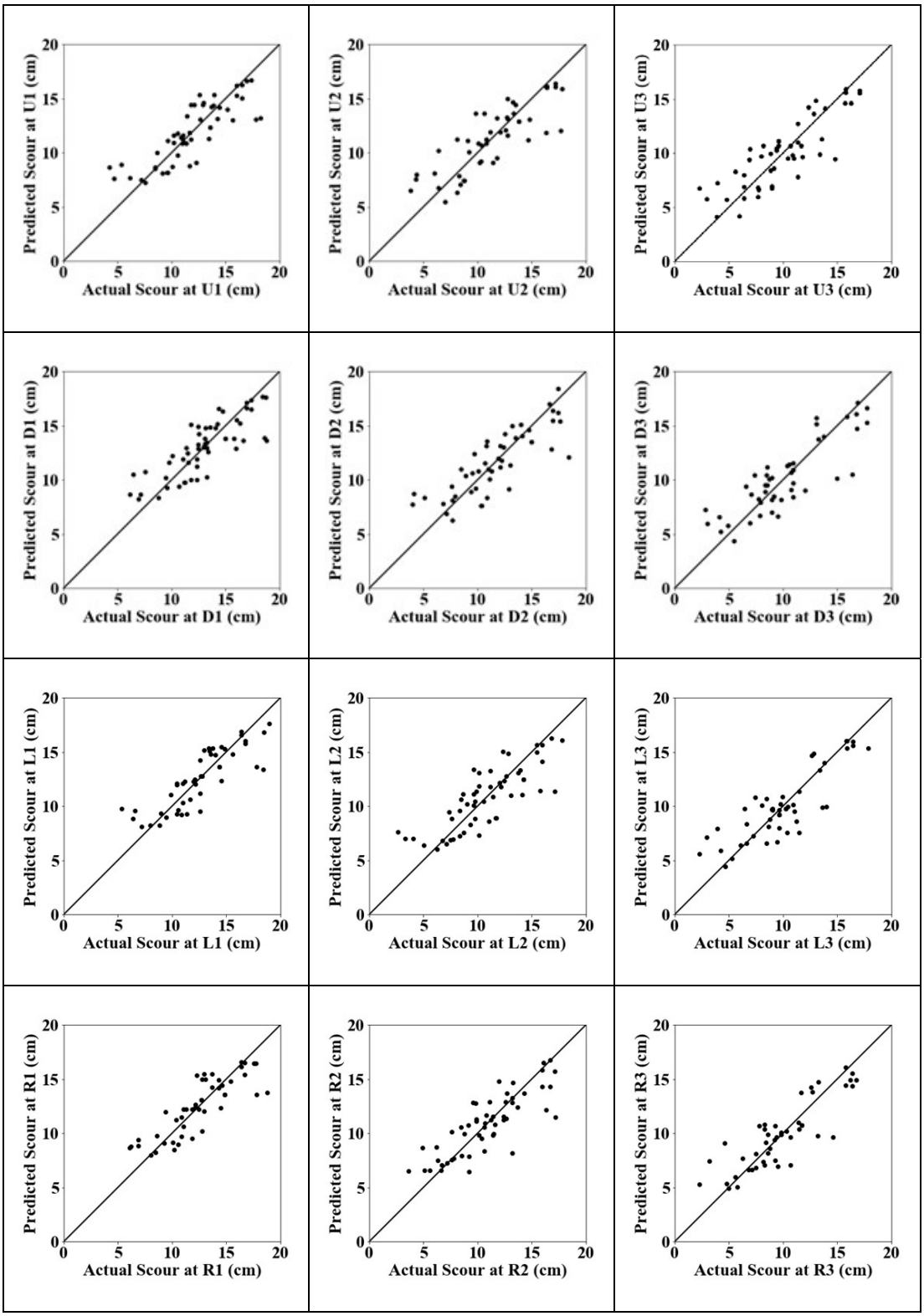

Figure 4.3: Scatter plots from non-linear regression models of order-2 under free-flow conditions during calibration

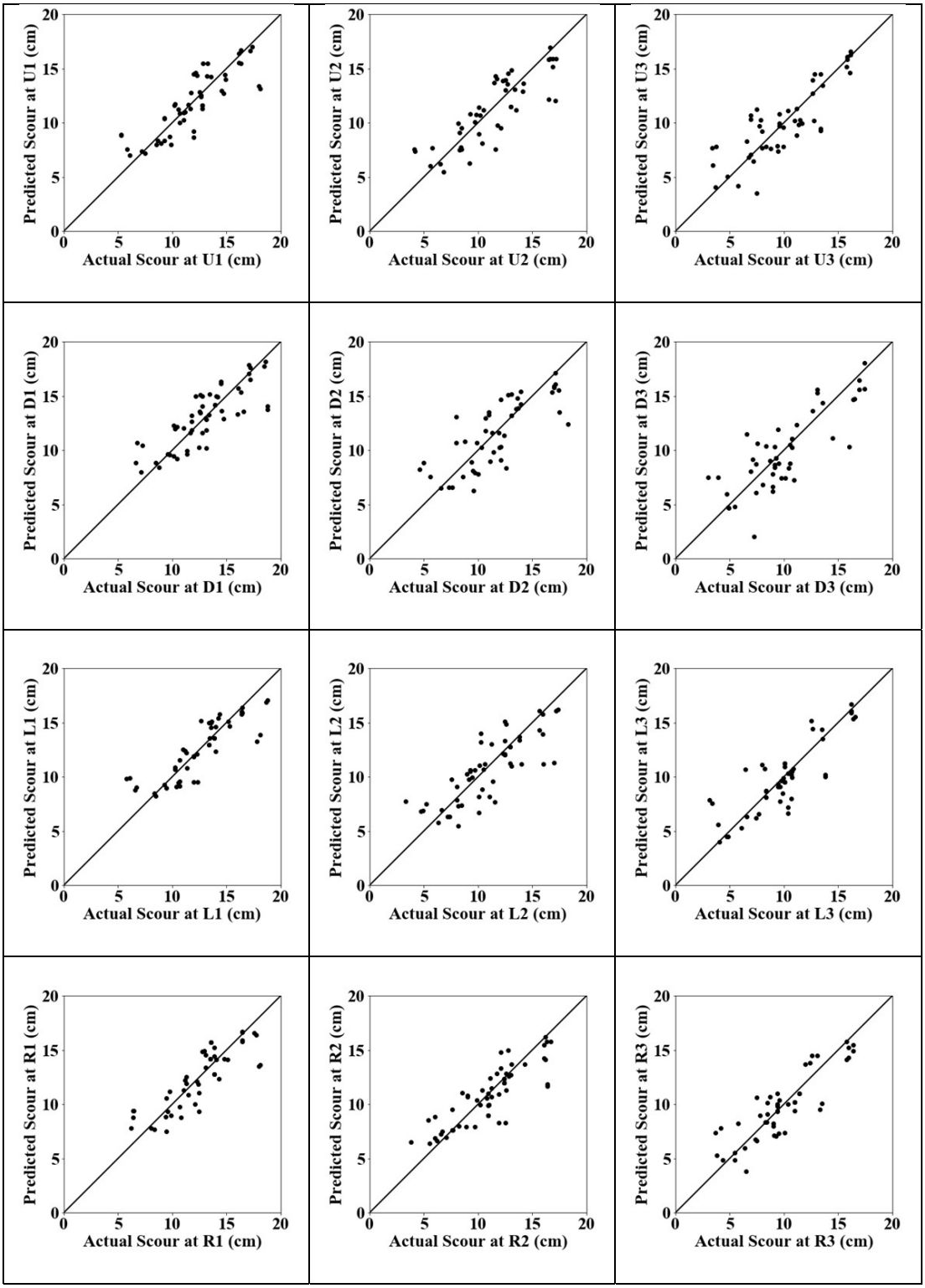

Figure 4.4: Scatter plots from non-linear regression models of order-2 under free-flow conditions during testing

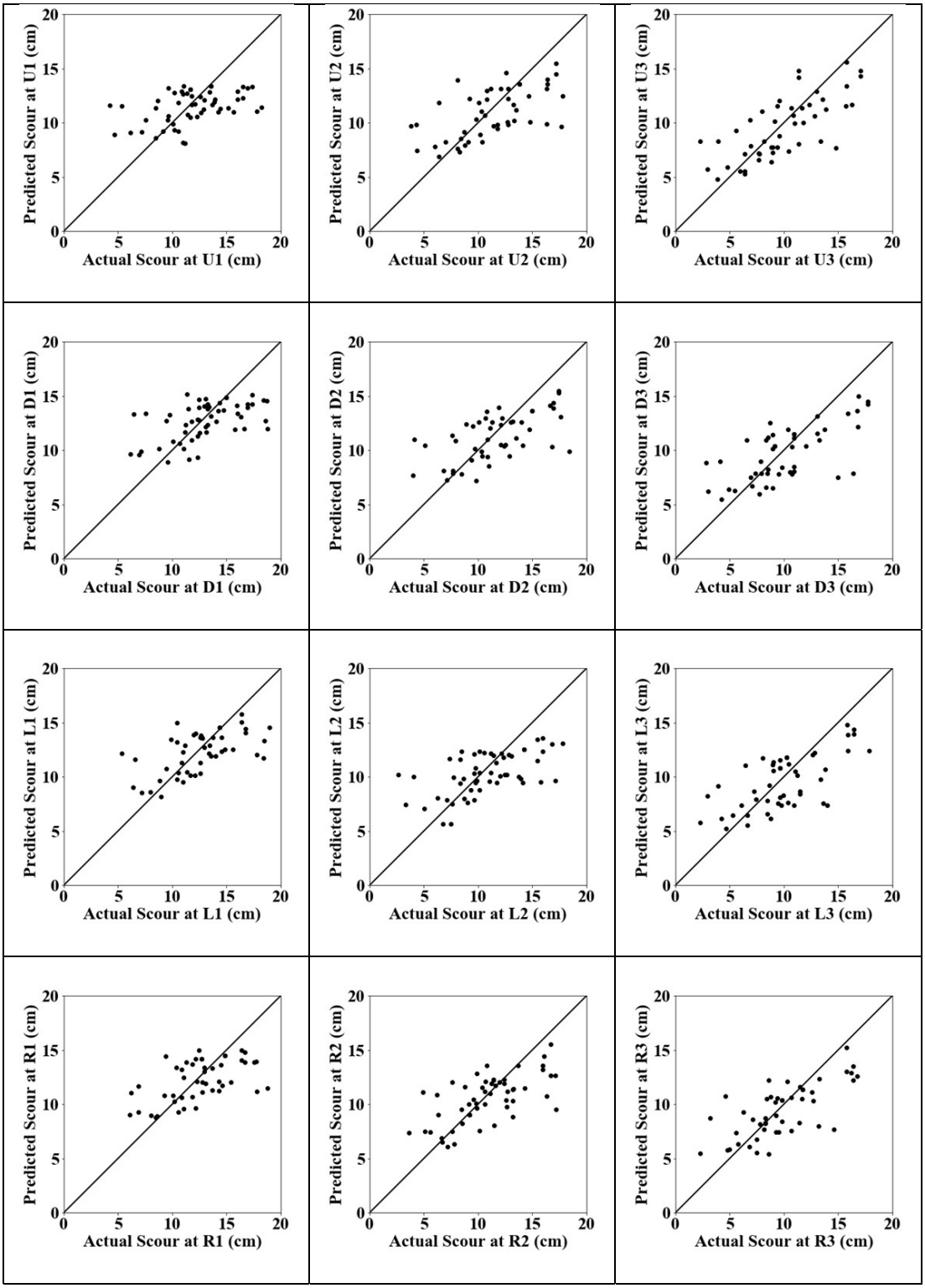

Figure 4.5: Scatter plots from power regression models under free-flow conditions during calibration

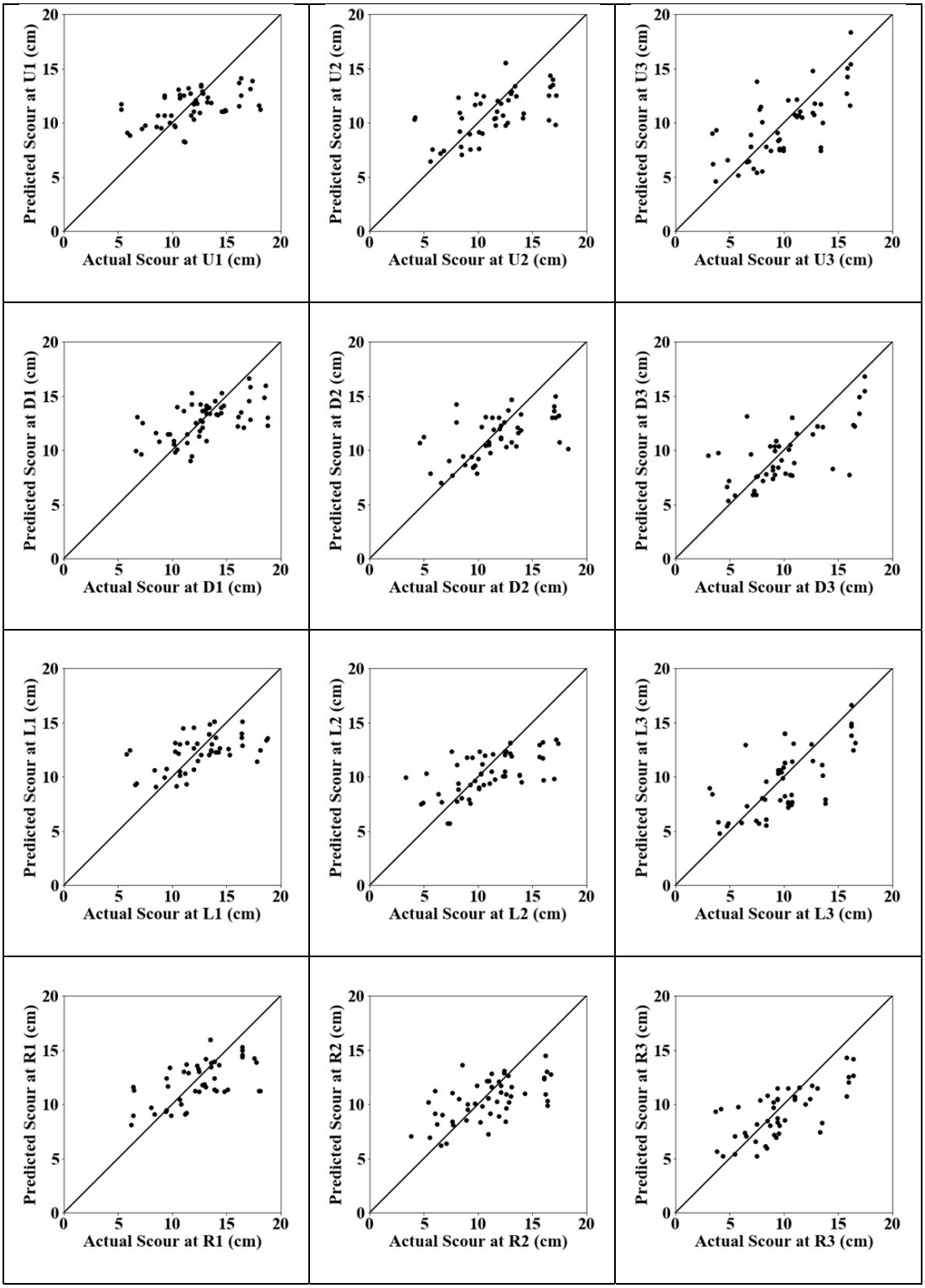

Figure 4.6: Scatter plots from power regression models under free-flow conditions during testing

4.3.2 Results from Regression Models for Pressure-Flow Conditions

The values of various error statistics from the three regression models under the pressure-flow conditions are presented in Table 4.10 through Table 4.12, respectively. The various error statistics are presented during both calibration and testing data sets; the minimum and maximum value of an error statistic in a column is highlighted in bold font; and the minimum, maximum, average error statistic over all the 12 scour locations are presented in the bottom three rows, respectively.

Table 4.10 presents the statistical results from the linear regression model under pressure-flow conditions. Looking at Table 4.10, it can be noted that the average values of R, E, RMSE, and AARE over the 12 scour locations during calibration data set are 0.5107, 0.2634, 2.21, 12.6%, respectively; and those during testing data set are 0.5065, 0.2556, 2.16, and 12.3%, respectively. These results are not very good but are slightly better than those for the free-flow conditions presented in the previous section. Analysing the performance of the linear regression model under pressure-flow conditions during calibration in terms of various TS statistics considered in this study, it can be observed that the average values of TS5, TS10, and TS25 are 27.8, 55.5, 89.8, respectively and those during testing data set are 29.5, 56.1, 89.8, respectively. These results show that the performance of the linear regression model on an average during calibration and testing data sets is comparable. Looking at the min and max values of various error statistics over all the 12 scour locations during calibration data set, it may be noted that R ranges between 0.4207 for R3 and 0.5836 for L2; E ranges between 0.1770 for R3 and 0.3406 for L2 (which is not good at all); RMSE ranges between 1.95 for R1 and 2.56 for R3; AARE ranges between 10.5 for R1 and 15.5 for R3; TS5 ranges between 22.7 for U3 and 40.9 for D2; TS10 ranges between 34.1 for R2 and 68.2 for R1; and TS25 ranges between 86.4 for R3 and 93.2 for D1, L1, and R1. The ranges of various performance statistics from the linear regression model under pressure-flow conditions during testing were as follows: R[0.4224,0.5982], E [0.1734, 0.3540], RMSE, [1.85, 2.47], AARE [10.1, 15.5]. TS5 [18.2, 43.2], TS10 [50.0, 65.9], and TS25 [86.4, 95.5]. These results show that the performance of the linear regression model under pressure-flow conditions during calibration and testing data sets is comparable.

Table 4.11 presents the statistical results from the NLRM-2 under pressure-flow conditions. Looking at Table 12, it can be noted that the average values of R, E, RMSE, and AARE over the 12 scour locations during calibration data set are 0.6658, 0.4452, 1.91, 10.6 and those during testing data set are 0.6777, 0.4581, 1.84, 10.2, respectively. These results are better than those for the linear regression model discussed in the previous section. Analysing the performance of the NLRM-2 under the pressure-flow conditions during calibration in terms of various TS statistics considered in this study, it can be observed that the average values of TS5, TS10, and TS25 are 38.1, 63.6, 91.7, respectively and those during testing data set are 36.7, 63.6, 92.0, respectively. These results show that the performance of the NLRM-2 model on an average during calibration and testing data sets is comparable. Also, the performance of the NLRM-2 is much better than that of the linear regression model. Looking at the min and max values of various error statistics over all the 12 scour locations during calibration data set from NLRM-2 model, it may be noted that ranges of various error statistics are as follows: R [0.5961, 0.7272]; E [0.3553, 0.5289]; RMSE [1.73, 2.16]; AARE [8.8, 13.0]; TS5 [27.3, 50.0]; TS10 [54.5, 75.0]; and TS25 [84.1, 95.5]. The ranges of various performance statistics from the NLRM-2 model under pressure-flow conditions during testing were as follows: R[0.5959, 0.7325], E [0.3540, 0.5357], RMSE, [1.55, 2.03], AARE [7.9, 12.6]. TS5 [25.0, 45.5], TS10 [50.0, 75.0], and TS25 [86.4, 95.5].

These results show that the performance of the NLRM-2 model under pressure-flow conditions during calibration and testing data sets is comparable. A comparison of the results from linear regression model and NLRM-2 model under the pressure-flow conditions in terms of various error statistics, it can be concluded that the performance of the NLRM-2 was significantly better than that of the linear regression model under pressure-flow conditions also.

Table 4.10: Statistical results from linear regression model under pressure-flow conditions

Scour	R	E	RMSE	AARE	TS5	TS10	TS25
Location	During Calibration / Training Data Set						
U1	0.4822	0.2325	2.14	12.0	25.0	59.1	90.9
U2	0.5800	0.3365	2.12	12.2	27.3	56.8	88.6
U3	0.5542	0.3072	2.45	**15.5**	**22.7**	54.5	88.6
D1	0.5102	0.2603	2.05	10.6	31.8	63.6	**93.2**
D2	0.5577	0.3110	2.16	11.4	**40.9**	56.8	88.6
D3	0.5012	0.2512	2.28	13.0	27.3	52.3	88.6
L1	0.5059	0.2560	2.08	11.4	22.7	63.6	**93.2**
L2	**0.5836**	**0.3406**	2.06	11.5	36.4	61.4	88.6
L3	0.4828	0.2331	2.32	13.6	27.3	52.3	88.6
R1	0.4288	0.1838	**1.95**	**10.5**	25.0	**68.2**	**93.2**
R2	0.5213	0.2718	2.36	13.8	22.7	**34.1**	88.6
R3	**0.4207**	**0.1770**	**2.56**	**15.5**	25.0	43.2	**86.4**
Min	0.4207	0.1770	1.95	10.5	22.7	34.1	86.4
Max	0.5836	0.3406	2.56	15.5	40.9	68.2	93.2
Avg	0.5107	0.2634	2.21	12.6	27.8	55.5	89.8
Scour	R	E	RMSE	AARE	TS5	TS10	TS25
Location	During Validation / Testing Data Set						
U1	0.4254	0.1757	2.26	12.7	27.3	52.3	90.9
U2	**0.5982**	**0.3540**	2.10	12.4	25.0	56.8	88.6
U3	0.5182	0.2598	2.40	**15.5**	22.7	**50.0**	**86.4**
D1	0.5331	0.2826	1.98	10.4	34.1	**65.9**	93.2
D2	0.5815	0.3380	2.09	11.2	**43.2**	54.5	88.6
D3	0.4521	0.2018	2.35	13.4	29.5	52.3	**86.4**
L1	0.4869	0.2292	1.94	10.6	29.5	63.6	**95.5**
L2	0.5405	0.2767	2.06	11.5	36.4	52.3	90.9
L3	0.5130	0.2629	2.20	12.7	38.6	56.8	86.4
R1	**0.4224**	0.1757	**1.85**	**10.1**	25.0	**65.9**	**95.5**
R2	0.5820	0.3370	2.16	12.7	**18.2**	52.3	88.6
R3	0.4247	**0.1734**	**2.47**	15.0	25.0	50.0	**86.4**
Min	0.4224	0.1734	1.85	10.1	18.2	50.0	86.4
Max	0.5982	0.3540	2.47	15.5	43.2	65.9	95.5
Avg	0.5065	0.2556	2.16	12.3	29.5	56.1	89.8

Table 4.11: Statistical results from non-linear regression model of order-2 under pressure-flow conditions

Scour	R	E	RMSE	AARE	TS5	TS10	TS25
Location	During Calibration / Training Data Set						
U1	0.6204	0.3849	1.92	10.1	**50.0**	65.9	90.9
U2	0.6750	0.4556	1.92	11.0	34.1	56.8	90.9
U3	0.7108	0.5052	2.07	**13.0**	31.8	**54.5**	90.9
D1	0.6206	0.3851	1.87	9.9	34.1	**75.0**	93.2
D2	**0.7272**	**0.5289**	1.78	9.5	38.6	65.9	**95.5**
D3	0.7212	0.5201	1.82	10.0	40.9	61.4	93.2
L1	0.6226	0.3876	1.89	9.6	47.7	68.2	93.2
L2	0.7062	0.4988	1.80	9.8	38.6	65.9	93.2
L3	0.6573	0.4320	1.99	11.6	**27.3**	59.1	90.9
R1	**0.5961**	**0.3553**	**1.73**	**8.8**	43.2	72.7	93.2
R2	0.6884	0.4739	2.00	11.3	29.5	63.6	90.9
R3	0.6437	0.4144	**2.16**	12.4	40.9	**54.5**	**84.1**
Min	0.5961	0.3553	1.73	8.8	27.3	54.5	84.1
Max	0.7272	0.5289	2.16	13.0	50.0	75.0	95.5
Avg	0.6658	0.4452	1.91	10.6	38.1	63.6	91.7
Scour	R	E	RMSE	AARE	TS5	TS10	TS25
Location	During Validation / Testing Data Set						
U1	**0.5959**	**0.3540**	2.00	10.6	**45.5**	68.2	90.9
U2	0.6871	0.4712	1.90	10.6	36.4	63.6	90.9
U3	0.6996	0.4808	2.01	**12.6**	29.5	**50.0**	**86.4**
D1	0.6543	0.4252	1.77	9.4	36.4	72.7	93.2
D2	**0.7325**	**0.5357**	1.75	9.2	43.2	70.5	93.2
D3	0.6715	0.4493	1.95	10.9	34.1	59.1	90.9
L1	0.6548	0.4274	1.68	8.8	43.2	68.2	**95.5**
L2	0.7230	0.5196	1.67	9.4	36.4	65.9	**95.5**
L3	0.6781	0.4581	1.88	11.0	**25.0**	54.5	90.9
R1	0.6547	0.4216	**1.55**	**7.9**	45.5	**75.0**	**95.5**
R2	0.7175	0.5141	1.85	10.5	31.8	59.1	93.2
R3	0.6636	0.4400	**2.03**	11.8	34.1	56.8	88.6
Min	0.5959	0.3540	1.55	7.9	25.0	50.0	86.4
Max	0.7325	0.5357	2.03	12.6	45.5	75.0	95.5
Avg	0.6777	0.4581	1.84	10.2	36.7	63.6	92.0

Table 4.12 presents the statistical results from the power model under pressure-flow conditions. Looking at Table 4.12, it can be noted that the average values of R, E, RMSE,

and AARE over the 12 scour locations during calibration data set are 0.5322, 0.2765, 2.17, 12.3and those during testing data set are 0.5282, 0.2706, 2.13, 12.1, respectively.

Table 4.12: Statistical results from power regression model under pressure-flow conditions

Scour	R	E	RMSE	AARE	TS5	TS10	TS25
Location	During Calibration / Training Data Set						
U1	0.5085	0.2536	2.11	12.0	25.0	59.1	90.9
U2	0.5986	0.3529	2.09	12.1	22.7	59.1	90.9
U3	0.5708	0.3186	2.43	**15.2**	**18.2**	47.7	88.6
D1	0.5345	0.2816	2.02	10.5	34.1	61.4	93.2
D2	0.5841	0.3326	2.12	11.2	34.1	56.8	88.6
D3	0.5321	0.2680	2.25	12.7	27.3	52.3	86.4
L1	0.5019	0.2251	**1.95**	10.6	22.7	59.1	**95.5**
L2	**0.6112**	**0.3682**	2.02	11.2	34.1	59.1	90.9
L3	0.5044	0.2439	2.30	13.4	27.3	45.5	88.6
R1	**0.4340**	**0.1836**	1.95	**10.4**	**36.4**	**63.6**	93.2
R2	0.5442	0.2883	2.33	13.5	22.7	45.5	90.9
R3	0.4616	0.2016	**2.52**	15.1	20.5	**45.5**	**86.4**
Min	0.4340	0.1836	1.95	10.4	18.2	45.5	86.4
Max	0.6112	0.3682	2.52	15.2	36.4	63.6	95.5
Avg	0.5322	0.2765	2.17	12.3	27.1	54.5	90.3
Scour	R	E	RMSE	AARE	TS5	TS10	TS25
Location	During Validation / Testing Data Set						
U1	**0.4510**	0.1900	2.24	12.7	**15.9**	63.6	90.9
U2	**0.6147**	**0.3766**	2.06	12.0	31.8	59.1	88.6
U3	0.5497	0.2914	2.35	**15.2**	22.7	**40.9**	86.4
D1	0.5472	0.2985	1.96	10.2	34.1	59.1	93.2
D2	0.6022	0.3576	2.05	10.8	**36.4**	61.4	88.6
D3	0.4595	**0.1745**	**2.39**	13.3	27.3	56.8	**86.4**
L1	0.4869	0.2292	1.94	10.6	29.5	63.6	**95.5**
L2	0.5756	0.2968	2.03	11.3	31.8	52.3	93.2
L3	0.5214	0.2567	2.21	12.6	34.1	54.5	86.4
R1	0.4548	0.2056	**1.82**	**9.9**	29.5	**65.9**	93.2
R2	0.5929	0.3470	2.14	12.5	18.2	40.9	93.2
R3	0.4830	0.2230	2.39	14.3	27.3	43.2	86.4
Min	0.4510	0.1745	1.82	9.9	15.9	40.9	86.4
Max	0.6147	0.3766	2.39	15.2	36.4	65.9	95.5
Avg	0.5282	0.2706	2.13	12.1	28.2	55.1	90.1

These results are slightly better than those from the linear regression model but are worse than those from the NLRM-2 model under the pressure-flow conditions.

Analysing the performance of the power regression model under the pressure-flow conditions during calibration in terms of various TS statistics considered in this study, it can be observed that the average values of TS5, TS10, and TS25 are 27.1, 54.5, 90.3, respectively and those during testing data set are 28.2, 55.1, 90.1, respectively. It shows that the results during testing are comparable to those during calibration. Further, it can be inferred that the performance of the power regression model is worse than that of the NLRM-2 and slightly better in comparison to the linear regression model in terms of various TS statistics for pressure-flow conditions also. Looking at the min and max values of various error statistics over all the 12 scour locations during calibration data set from power regression model, it may be noted that ranges of various error statistics are as follows: R [0.4340, 0.6112]; E [0.1836, 0.3682]; RMSE [1.95, 2.52]; AARE [10.4, 15.2]; TS5 [18.2, 36.4]; TS10 [45.5, 63.6]; and TS25 [86.4, 95.5]. The ranges of various performance statistics from the power regression model under pressure-flow conditions during testing were as follows: R [0.4510, 0.6147], E [0.1745, 0.3766], RMSE, [1.82, 2.39], AARE [9.9, 15.2]. TS5 [15.9, 36.4], TS10 [40.9, 65.9], and TS25 [86.4, 95.5].

Next, the graphical results from the various regression models under pressure-flow conditions in terms of scatter plots are examined. The scatter plots from linear regression model under pressure-flow conditions are presented in Figure 4.7 and Figure 4.8 during calibration and testing data sets, respectively; Figure 4.9 and Figure 4.10 depict the performance of the NLRM-2 in terms of scatter plots during calibration and testing data sets, respectively; and Figure 4.11 and Figure 4.12 show the performance of the power regression model in terms of scatter plots during calibration and testing data sets, respectively. On all the scatter plots, an ideal line at 45-degrees is drawn to assess the performance. It is to be noted that all the predicted points should fall on the ideal line from an ideal model and from a good model the scatter around the ideal line should be as narrow as possible.

From Figure 4.7 and Figure 4.8, it is clear that the performance of linear regression model under pressure-flow conditions is not good due to large scatter around the ideal line. The

linear regression model appears to significantly over-predict the scour particularly that of the low magnitude as evident from these figures.

Looking at the results from the NLRM-2 for the pressure-flow conditions from Figure 4.9 and Figure 4.10, it can be seen that its performance is very good during both calibration and testing data sets. It shows that the NLRM-2 model was able to adequately capture the non-linear dynamics inherent in the scour mechanism around a bridge pier for pressure-flow.

Analysing the graphical results in terms of the scatter plots from Figure 4.11 and Figure 4.12 from the power regression model under pressure-flow conditions, it can be seen that its performance is better than the linear regression model but worse than the NLRM-2 model.

Thus, the graphical results strengthen the conclusions drawn from the statistical results about the suitability of the various regression models in predicting the scour around bridge piers under pressure-flow conditions that the NLRM-2 model is the best followed by power regression model while the linear regression model is not suitable at all.

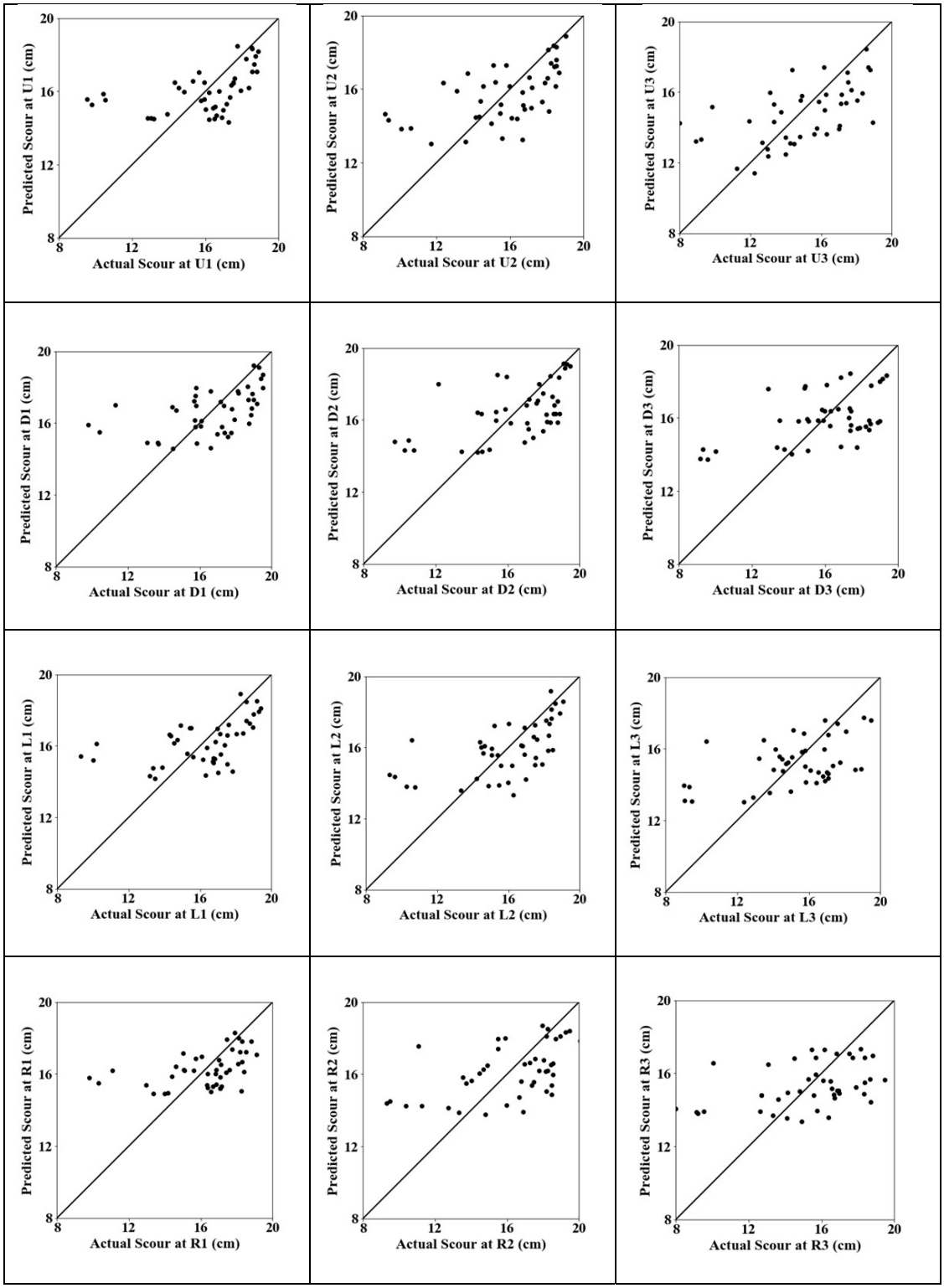

Figure 4.7: Scatter plots from linear regression models under pressure-flow conditions during calibration

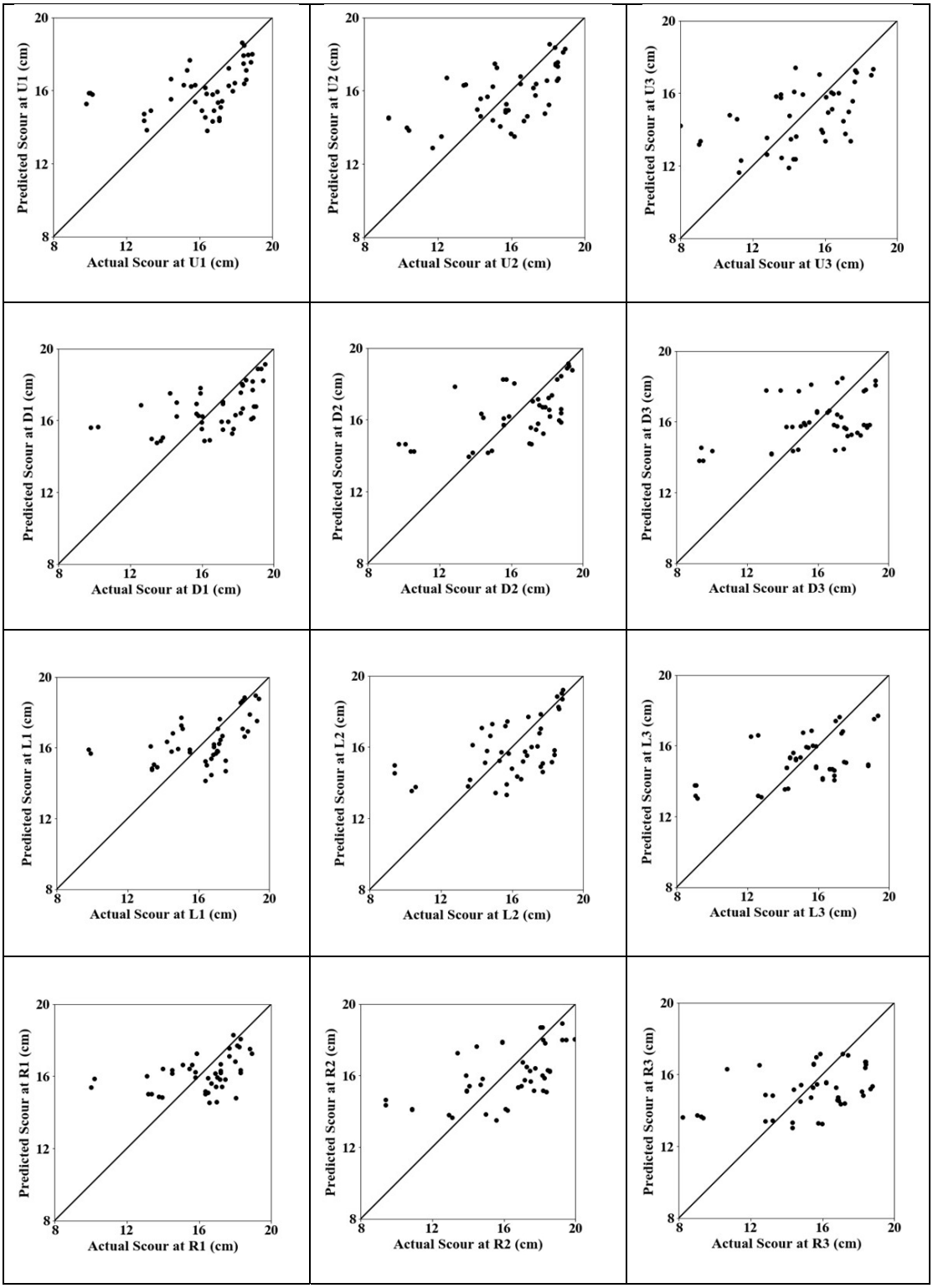

Figure 4.8: Scatter plots from linear regression models under pressure-flow conditions during testing

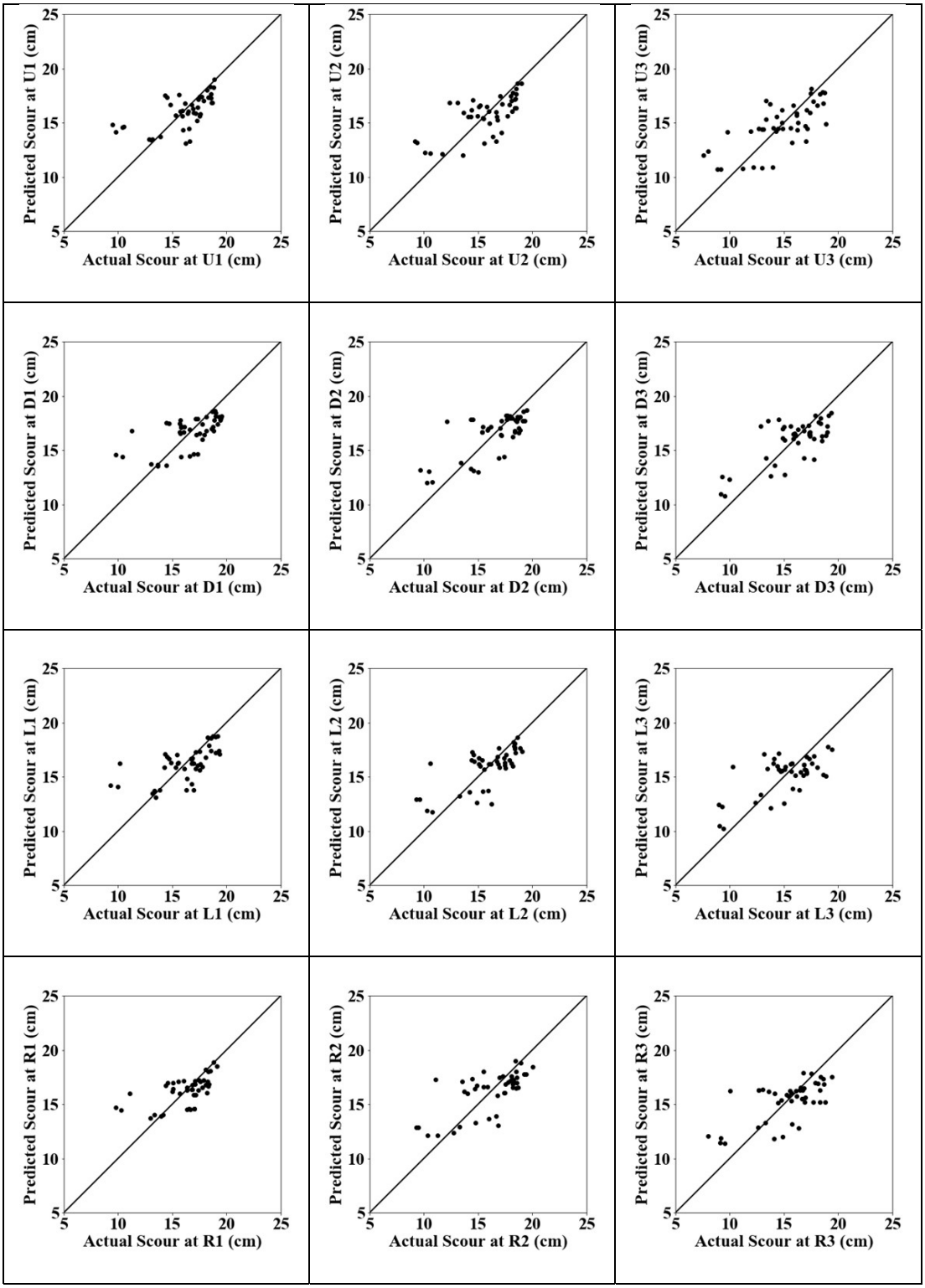

Figure 4.9: Scatter plots from NLRM-2 models under pressure-flow conditions during calibration

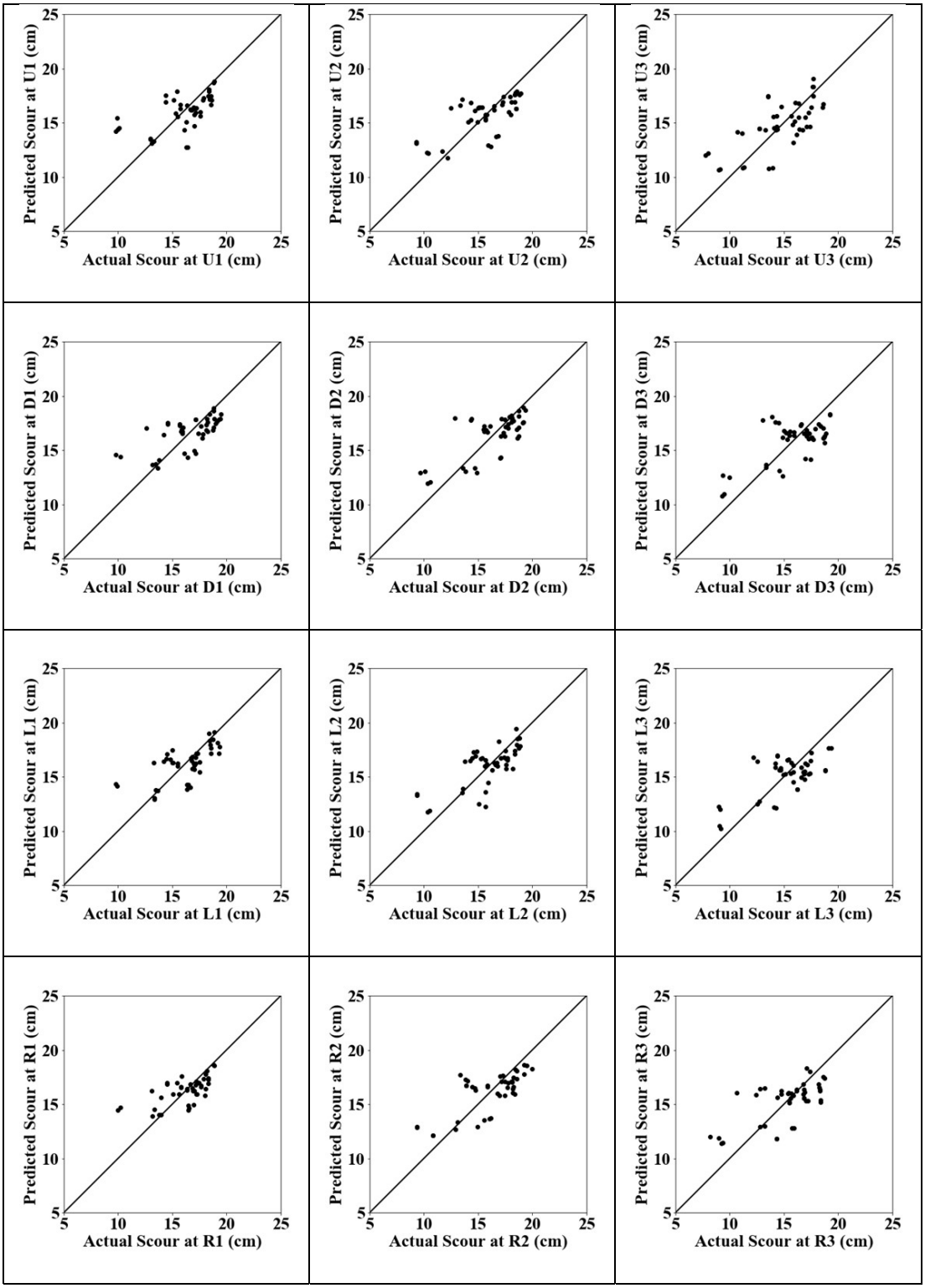

Figure 4.10: Scatter plots from NLRM-2 models under pressure-flow conditions during testing

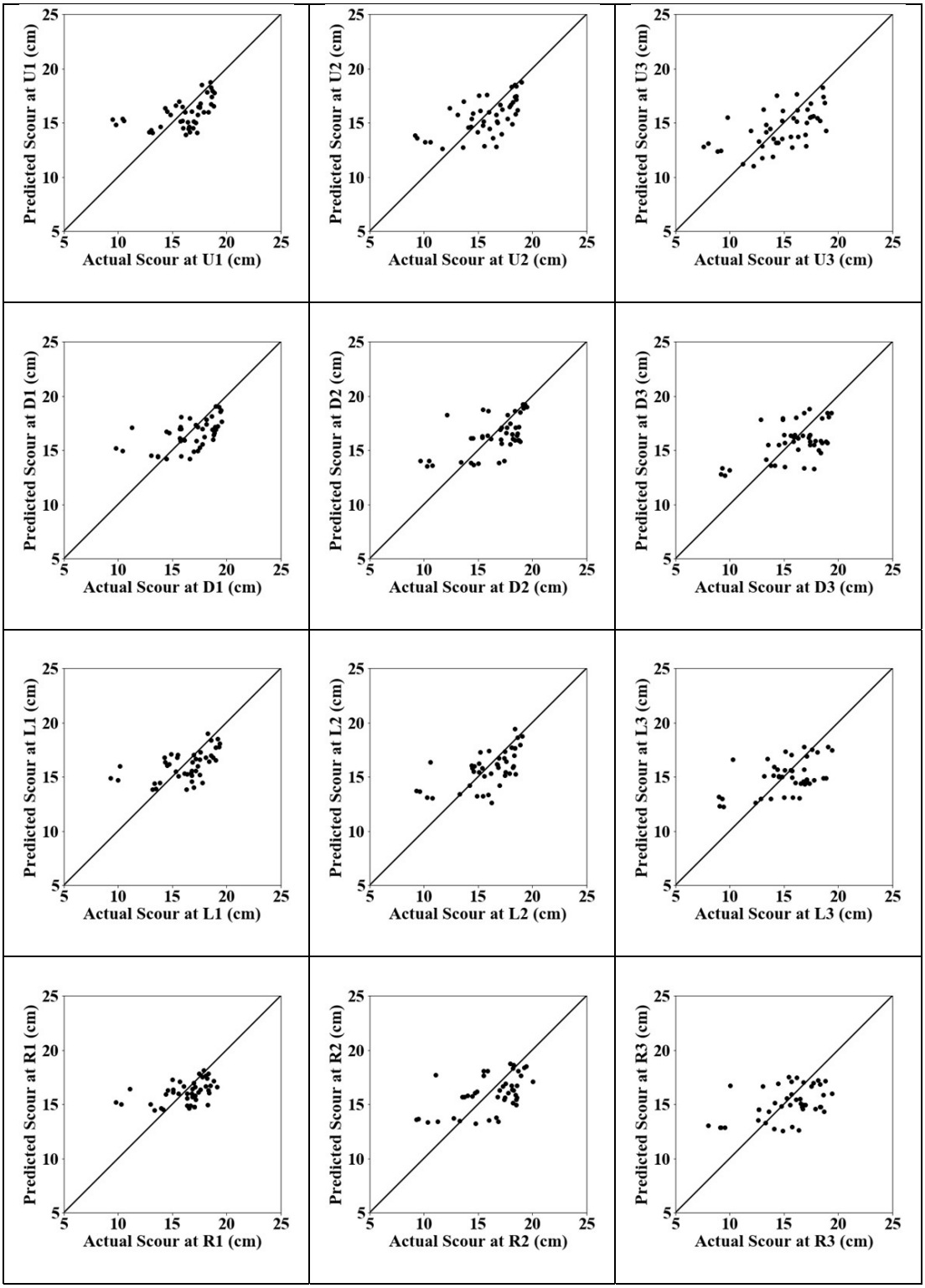

Figure 4.11: Scatter plots from power regression models under pressure-flow conditions during calibration

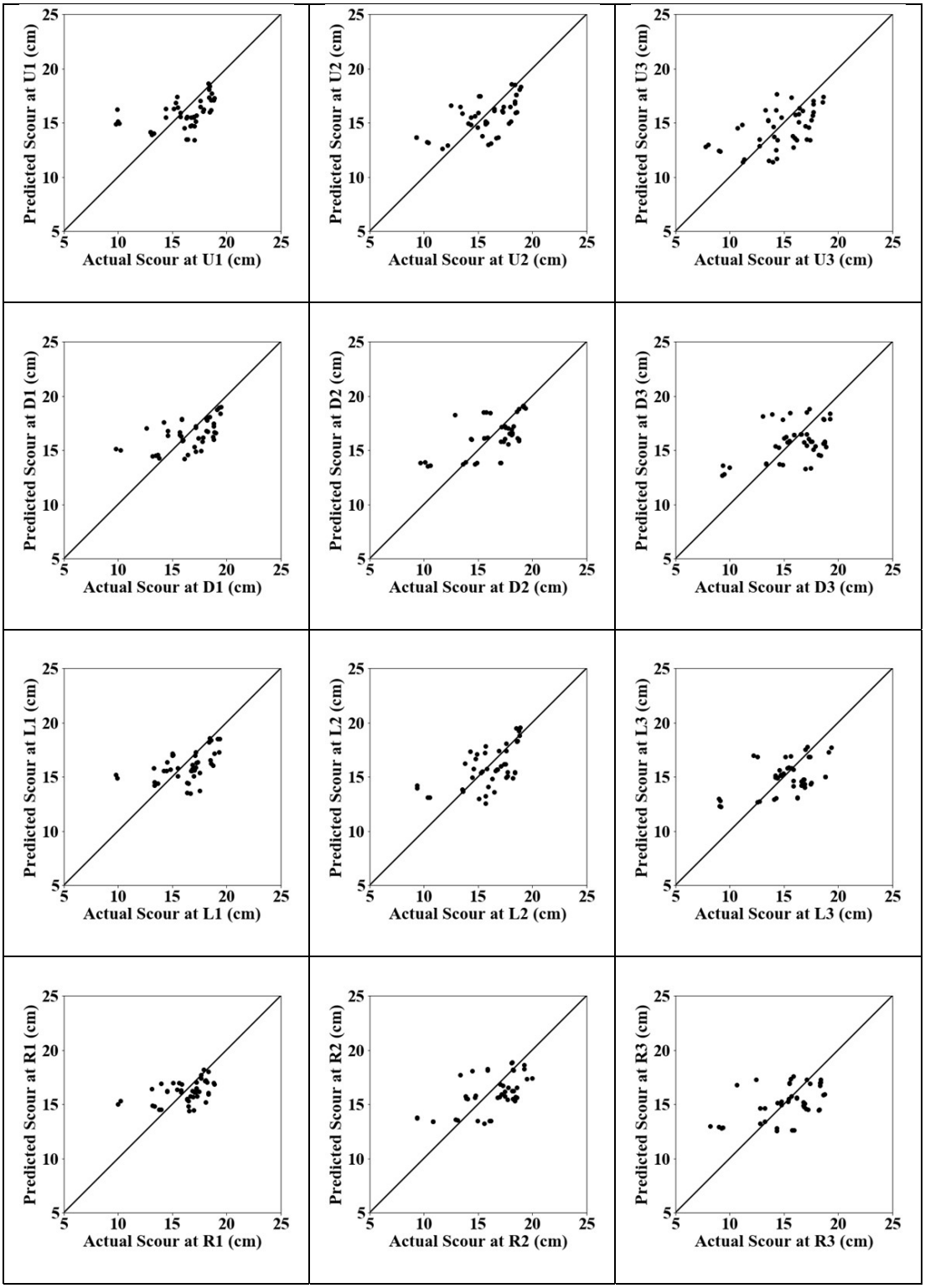

Figure 4.12: Scatter plots from power regression models under pressure-flow conditions during testing

4.4 ANN Model Development

In this study, a total of 24 ANN models have been developed. The first 12 ANN models are for predicting the scour around a bridge pier at 12 different locations under free-flow conditions. The next 12 ANN models are developed for predicting the scour around a bridge pier at 12 different locations under pressure-flow conditions. A feedforward ANN architecture trained using the new Adam training algorithm was employed to develop all the ANN models in this study. Each of the ANN models consisted of three layers: an input layer, a hidden layer, and an output layer. The number of neurons in the input layer of each of the ANN model was four representing pier diameter, flow discharge, flow depth, and velocity of flow. These inputs are same as those employed in developing the regression models described earlier. There was only one output in all the ANN models representing scour depth to be modelled. For each of the scour locations (U1, U2, U3, etc.), a separate ANN model was developed. The ANN models were trained using the training data set and their model performance was evaluated using both training and testing data sets. The training and testing data were scaled in the range (0.1, 0.9).

The ANN development was carried out using Python and the ANNs were trained using Anaconda Development Environment (ADE) and Spyder application which supports python language. Training algorithm used was Adam and activation function used was Rectified Linear Unit (ReLu). The more popular Sigmoid function was also tried but it was not found to give encouraging results in this study. The objective function to be minimized in the ANN model development was kept same as in the regression models (i.e. Mean Square Error). Early stopping criteria was used to stop model from over-training. Maximum number of epochs was set to 1,000 and validation MSE was used to monitor over training. Minimum delta was set to be 0.000001 and patience of 10 epochs was given to check further training. The Adam training algorithm involves two hyper parameters ($\beta 1$ and $\beta 2$), which are used to calculate running average of gradients from last calculated moments and latest moments. The starting values of the two hyper-parameters is set equal to 0.9 and 0.999, respectively, and their values are automatically reduced internally as the training progresses

In developing an ANN model in this study, an ANN architecture of 4-N-1 was explored where N is the number of neurons in the hidden layer. The value of N was determined

using a trial and error procedure in which the value of N was varied from 1 to 20 during training phase and different error statistics were assessed to see which architecture provides the best performance. The two error statistics used to determine the optimal ANN architectures were R and AARE. The two error statistics were plotted against the number of hidden neurons (N) and the value of N giving minimum AARE and maximum R value during training was selected as the optimal ANN architecture. The error plots to determine optimal ANN architectures to predict scour around bridge piers at all the 12 locations are shown in Figure 4.13 and Figure 4.14 for the free-flow and pressure-flow conditions, respectively. The optimal ANN architectures were then determined by physically examining these plots and finding the hidden neuron that best fits the data for a particular location scour in terms of R and AARE statistics. The optimal ANN architecture thus determined are presented in Table 4.13.

Table 4.13: Optimal ANN architecture for ANN models

ANN for Scour Location	Optimal No. of Hidden Neurons Free-Flow	Optimal No. of Hidden Neurons Pressure-Flow
U1	15	17
U2	14	19
U3	19	16
D1	18	12
D2	12	20
D3	12	16
L1	18	14
L2	13	14
L3	15	15
R1	16	17
R2	20	19
R3	15	11

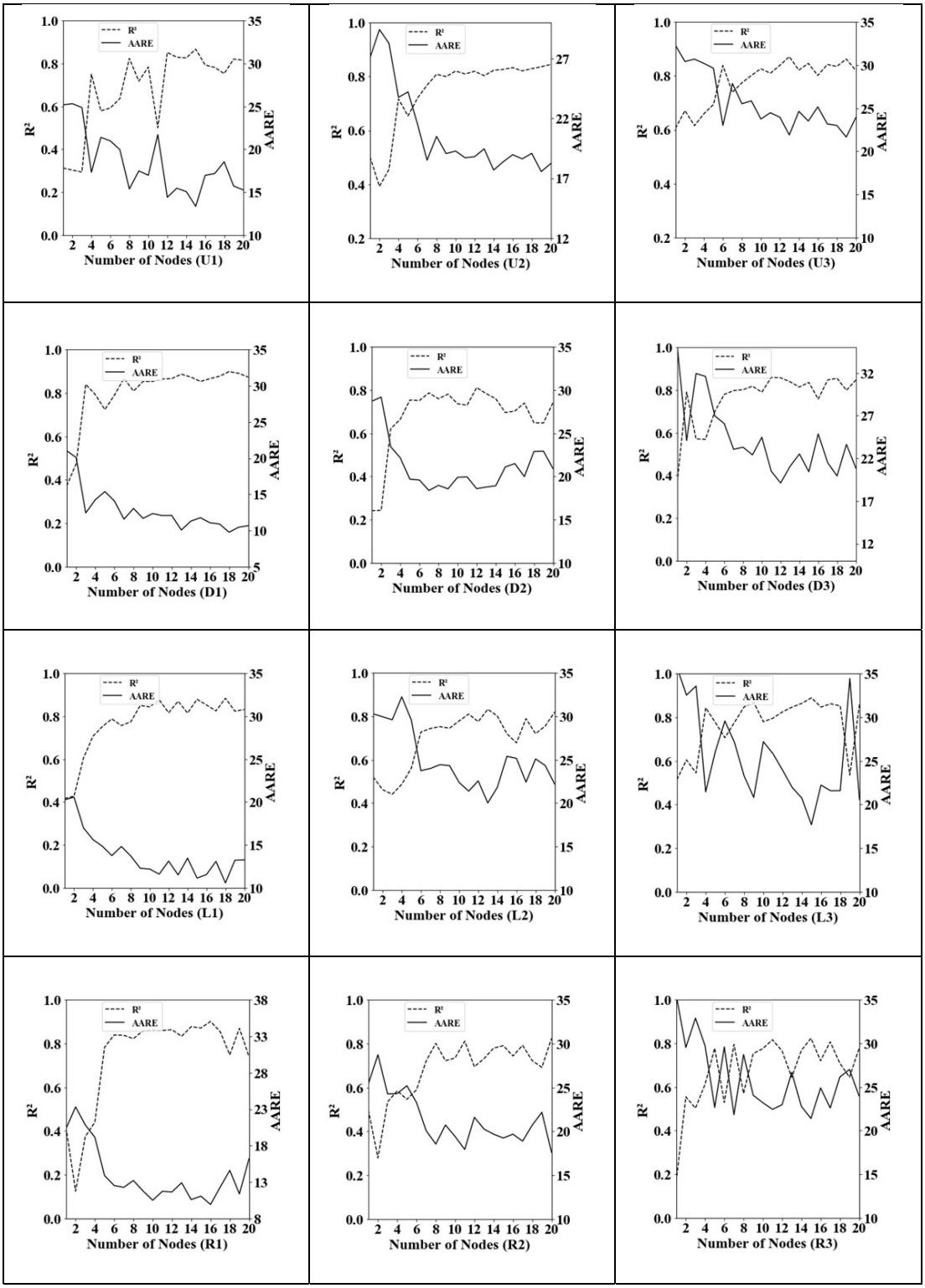

Figure 4.13: Error plots to determine optimal ANN architectures under free-flow conditions

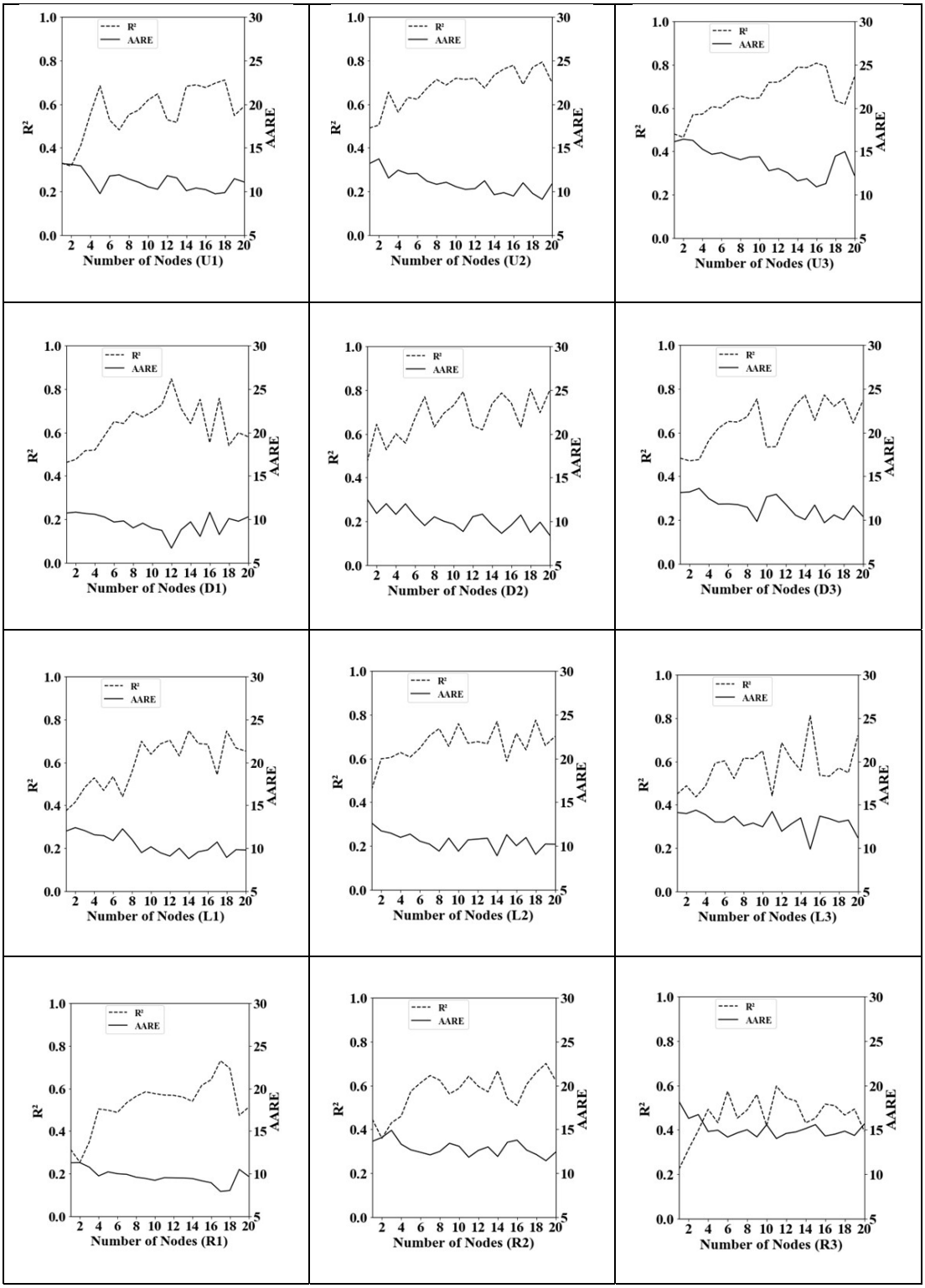

Figure 4.14: Error plots to determine optimal ANN architectures under pressure-flow conditions

4.5 Results from the ANN Models

Once the ANN models were trained, they were tested by calculating various model performance evaluation measures considered in this study under the free-flow and the pressure-flow conditions. The performance of various ANN models for free-flow and pressure-flow conditions is presented in Table 4.14 and Table 4.15, respectively. The best and worst error statistic in a column is highlighted in bold font. The last three rows in these tables present the minimum, maximum, and average error statistic over the 12 scour locations. Looking at the results from Table 4.14 for the free-flow conditions, it is observed that the average R, E, RMSE, and AARE during training data set were 0.8585, 0.7241, 1.80, and 16.7 and those during testing data set were 0.8276, 0.6805, 1.86, and 16.4, respectively, which is excellent. The average values TS5, TS10, and TS25 statistics during training were 27.0, 50.9, 85.5 and those during testing were 24.6, 51.3, 85.6, respectively.

The range of R during training for free-flow is (0.8118, 0.9011) which is excellent; range of E is (0.6317, 0.8015), which is very good; range of RMSE is (1.39, 2.17); range of AARE is (9.9, 21.9); range of TS5 is (16.7, 39.6); range of TS10 is (35.4, 66.7); and range of TS25 is (75.0, 93.8), which are all very good results. The ranges of various model performance evaluation statistics obtained from the ANN models under free-flow conditions during testing were as follows: R (0.7206, 0.8915), E (0.5092, 0.7840), RMSE (1.45, 2.35), AARE (10.5, 23.7), TS5 (16.7, 31.3), TS10 (37.5, 70.8), and TS25 (72.9, 96.3), which are also very good results.

The TS25 value of 93.8 for L1 under free-flow conditions indicate that in more than 93% of the predicted cases during training, the ARE was less than 25%. Similarly, a TS25 value of 96.3% during training for ANN model under free-flow condition for U1 shows that more than 96% of the testing cases had ARE of less than 25%. It is to be noted that U1 is the prime location just upstream of the pier where the scour value is maximum. These are excellent results. The AARE of 9.9% during training from the ANN model demonstrates excellent result which basically means that average error was less than 10% during training from the ANN model for R1. Apparently, the values of R, E, and RMSE were also the best from the ANN model for R1 during training. The ANN results in

testing are also very good with R & E values of 0.8915 and 0.7840 from the ANN model for L3.

Table 4.14: Statistical results from ANN models under free-flow conditions

Model	R	E	RMSE	AARE	TS5	TS10	TS25
During Calibration / Training Data Set							
U1	0.8671	0.7286	1.68	13.3	37.0	59.3	90.7
U2	0.8452	0.6942	2.00	18.2	22.9	54.2	83.3
U3	0.8714	0.7484	1.87	**21.9**	**16.7**	37.5	81.3
D1	0.8912	0.7838	1.44	10.4	35.4	**66.7**	91.7
D2	**0.8118**	**0.6317**	**2.17**	18.5	25.0	45.8	85.4
D3	0.8595	0.7304	1.97	20.5	20.8	**35.4**	77.1
L1	0.8843	0.7719	1.51	10.6	**39.6**	64.6	**93.8**
L2	0.8327	0.6837	1.91	20.0	22.9	45.8	89.6
L3	0.8894	0.7880	1.67	17.7	20.8	50.0	83.3
R1	**0.9011**	**0.8015**	**1.39**	**9.9**	35.4	62.5	93.8
R2	0.8244	0.6667	1.92	17.6	25.0	41.7	81.3
R3	0.8239	0.6601	2.05	21.4	22.9	47.9	**75.0**
Min	0.8118	0.6317	1.39	9.9	16.7	35.4	75.0
Max	0.9011	0.8015	2.17	21.9	39.6	66.7	93.8
Avg	0.8585	0.7241	1.80	16.7	27.0	50.9	85.5
During Validation / Testing Data Set							
Model	**R**	**E**	**RMSE**	**AARE**	**TS5**	**TS10**	**TS25**
U1	0.8578	0.7303	1.61	12.3	24.1	57.4	**96.3**
U2	0.8426	0.7040	1.86	16.3	25.0	56.3	91.7
U3	0.8341	0.6926	1.96	20.8	20.8	**37.5**	75.0
D1	0.8788	0.7677	**1.45**	**10.5**	27.1	**70.8**	95.8
D2	0.7953	0.6248	2.07	16.0	20.8	54.2	87.5
D3	0.8233	0.6757	2.08	21.5	**16.7**	43.8	**72.9**
L1	0.8348	0.6846	1.77	12.4	31.3	54.2	93.8
L2	0.8263	0.6692	1.88	16.8	25.0	47.9	83.3
L3	**0.8915**	**0.7840**	1.63	17.5	29.2	56.3	85.4
R1	0.8867	0.7806	**1.45**	10.8	**31.3**	56.3	93.8
R2	0.7397	0.5438	2.17	18.8	18.8	41.7	79.2
R3	**0.7206**	**0.5092**	**2.35**	**23.7**	25.0	39.6	**72.9**
Min	0.7206	0.5092	1.45	10.5	16.7	37.5	72.9
Max	0.8915	0.7840	2.35	23.7	31.3	70.8	96.3
Avg	0.8276	0.6805	1.86	16.4	24.6	51.3	85.6

Table 4.15: Statistical results from ANN models under pressure-flow conditions

Model	R	E	RMSE	AARE	TS5	TS10	TS25
During Calibration / Training Data Set							
U1	0.7111	0.4909	1.74	9.9	38.6	65.9	90.9
U2	0.7935	0.6107	1.62	9.1	38.6	63.6	**95.5**
U3	0.8078	0.6455	1.75	10.9	34.1	61.4	93.2
D1	**0.8468**	**0.6952**	**1.31**	**6.7**	**52.3**	**84.1**	93.2
D2	0.8053	0.6170	1.61	8.7	40.9	72.7	93.2
D3	0.7722	0.5870	1.69	9.7	29.5	59.1	**95.5**
L1	0.7488	0.5429	1.63	8.8	43.2	68.2	93.2
L2	0.7756	0.5914	1.62	9.0	43.2	68.2	93.2
L3	0.8114	0.6184	1.63	9.9	25.0	63.6	93.2
R1	0.7304	0.4980	1.53	7.9	50.0	81.8	93.2
R2	0.7006	0.4787	1.99	11.4	27.3	52.3	90.9
R3	**0.5976**	**0.3562**	**2.26**	**14.0**	**22.7**	**52.3**	**84.1**
Min	0.5976	0.3562	1.31	6.7	22.7	52.3	84.1
Max	0.8468	0.6952	2.26	14.0	52.3	84.1	95.5
Avg	0.7584	0.5610	1.70	9.7	37.1	66.1	92.4
During Validation / Testing Data Set							
Model	**R**	**E**	**RMSE**	**AARE**	**TS5**	**TS10**	**TS25**
U1	0.6885	0.4595	1.83	10.3	31.8	65.9	90.9
U2	0.7959	**0.6133**	1.62	9.4	43.2	65.9	95.5
U3	0.7837	0.6111	1.96	11.4	22.7	52.3	95.5
D1	0.7752	0.5879	1.50	8.0	43.2	72.7	95.5
D2	**0.8165**	0.6083	1.60	8.8	38.6	**79.5**	95.5
D3	0.7527	0.5521	1.76	10.1	29.5	61.4	**97.7**
L1	0.7226	0.5210	1.53	8.1	43.2	72.7	95.5
L2	0.7232	0.5215	1.67	9.3	38.6	59.1	95.5
L3	0.8075	0.6118	1.59	9.7	31.8	61.4	90.9
R1	0.7160	0.4971	**1.44**	**7.4**	**47.7**	75.0	95.5
R2	0.6954	0.4669	1.93	11.1	31.8	50.0	93.2
R3	**0.5917**	**0.3432**	**2.20**	**13.5**	**22.7**	**50.0**	**86.4**
Min	0.5917	0.3432	1.44	7.4	22.7	50.0	86.4
Max	0.8165	0.6133	2.20	13.5	47.7	79.5	97.7
Avg	0.7391	0.5328	1.72	9.8	35.4	63.8	93.9

The superiority of the ANNs in modelling pressure flow conditions is demonstrated by the single digit AARE values during training (see Table 4.15) for most of the scour locations. The R & E values of 0.8468 and 0.6952 from the best ANN model under pressure-flow conditions for D1 show promising results. The values of AARE for many of the ANN models at several scour locations are in single digits demonstrating its efficacy in efficiently predicting the local scour around bridge piers under pressure-flow conditions.

The graphical results from the various ANN models under free-flow and pressure-flow conditions in terms of scatter plots are examined next. The scatter plots from ANN models under free-flow conditions are presented in Figure 4.15 and Figure 4.16, respectively, during training and testing data sets; while Figure 4.17 and Figure 4.18 depict the performance of the ANN models under pressure-flow conditions in terms of scatter plots during calibration and testing data sets. On all the scatter plots, an ideal line at 45-degrees is drawn to assess the performance. It is to be noted that all the predicted points should fall on the ideal line from an ideal model and from a good model the scatter around the ideal line should be as narrow as possible. It is very pleasing to note that the performance of all the ANN models for all 12 scour locations during both training and testing for the free-flow conditions is excellent as the scatter around the ideal line is narrow and consistent. It is important to note that the ANN models for free-flow were able to capture in inherent complex and non-linear dynamics in the scour mechanism for all the magnitudes e.g. low, medium, and high as the scatter around the ideal line is consistent throughout. The performance of the ANN models for pressure flow conditions was also very good except for some low magnitude values. The scatter around the ideal line is narrow but not consistent for the ANN models under pressure-flow conditions due to its moderate performance for the low magnitude scour values. Overall, the performance of all the ANN models for predicting the scour around bridge piers under pressure-flow can be characterized as very good.

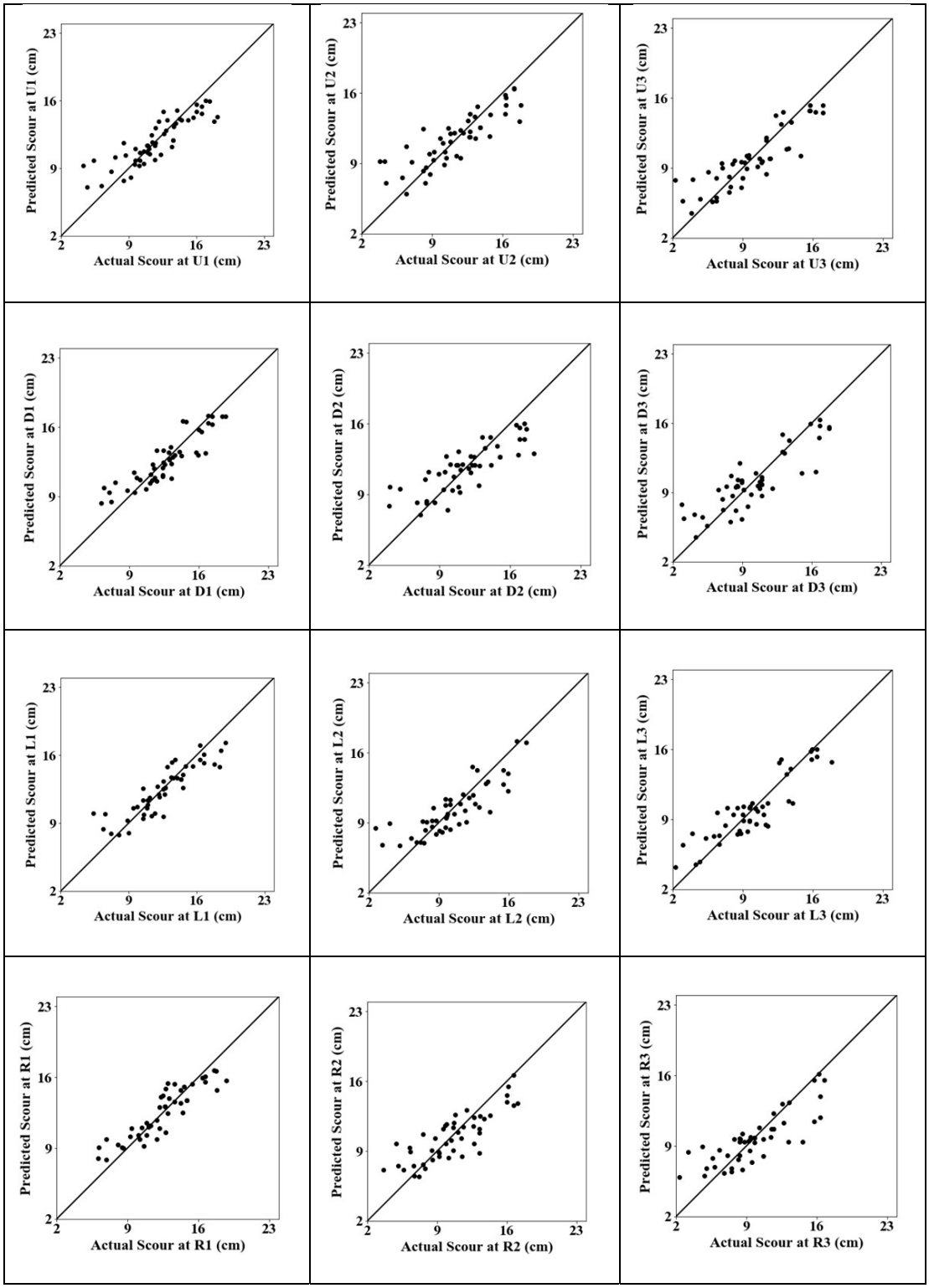

Figure 4.15: Scatter plots from ANN models under free-flow conditions during training

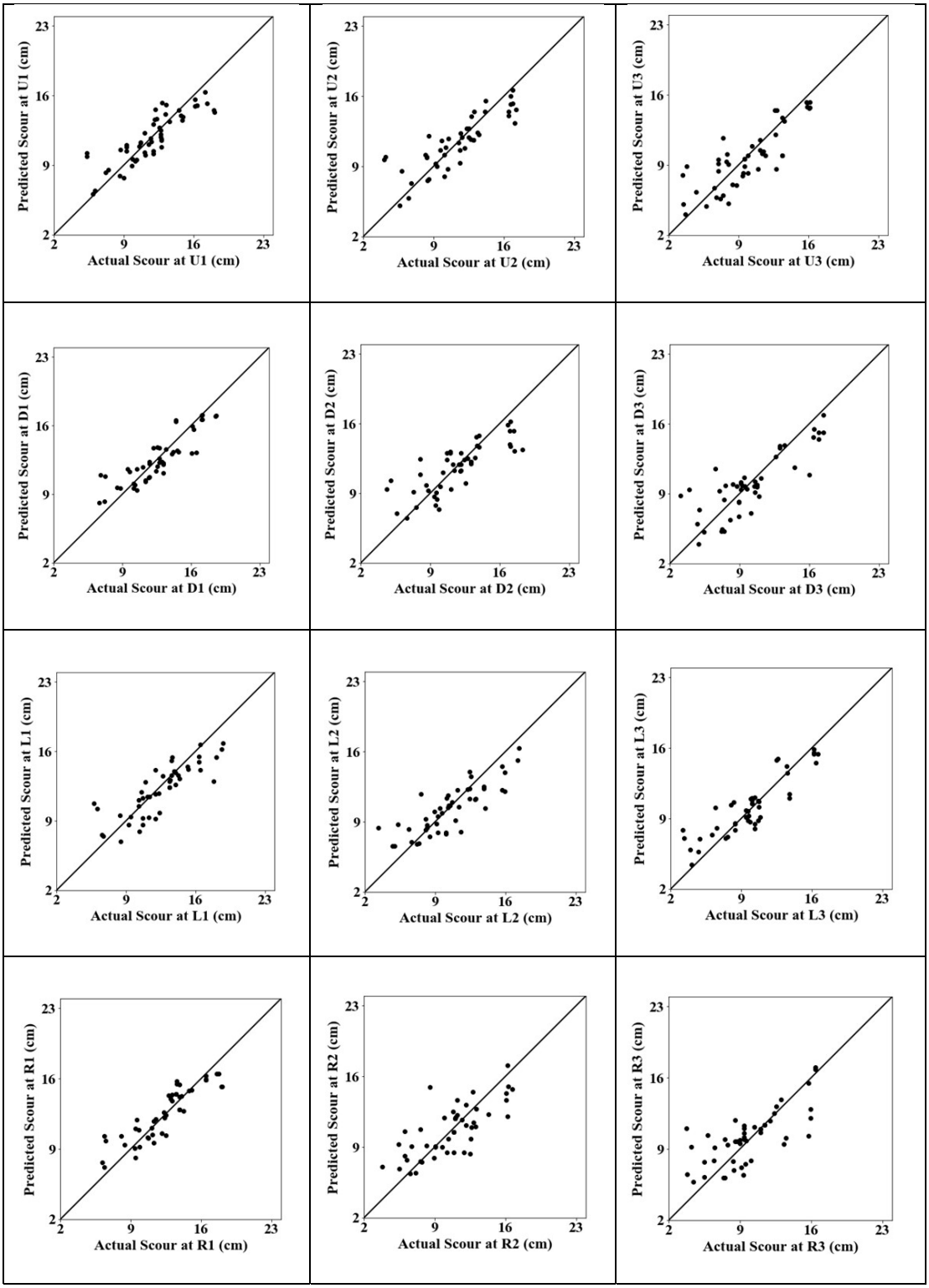

Figure 4.16: Scatter plots from ANN models under free-flow conditions during testing

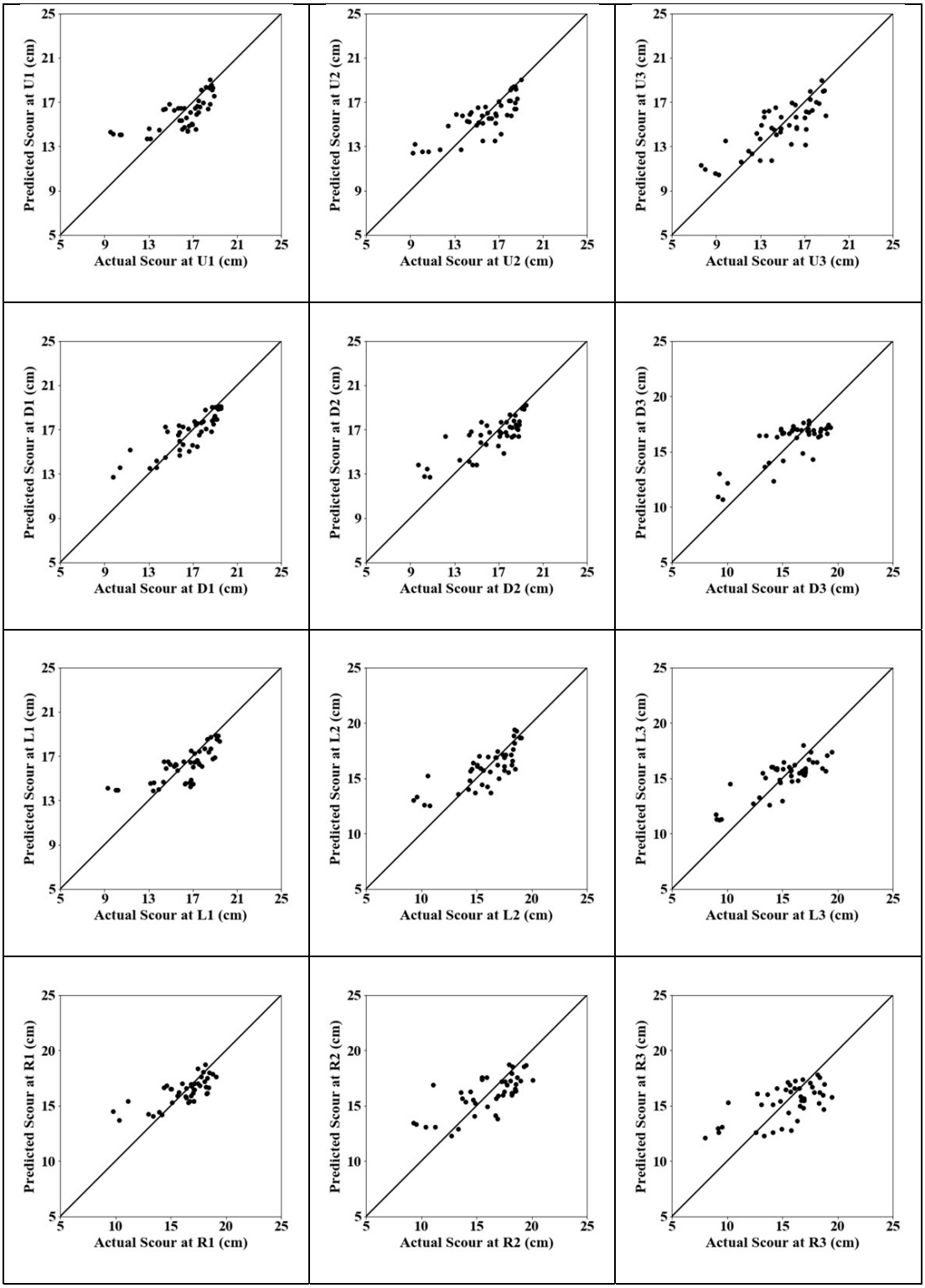

Figure 4.17: Scatter plots from ANN models under pressure-flow conditions during training

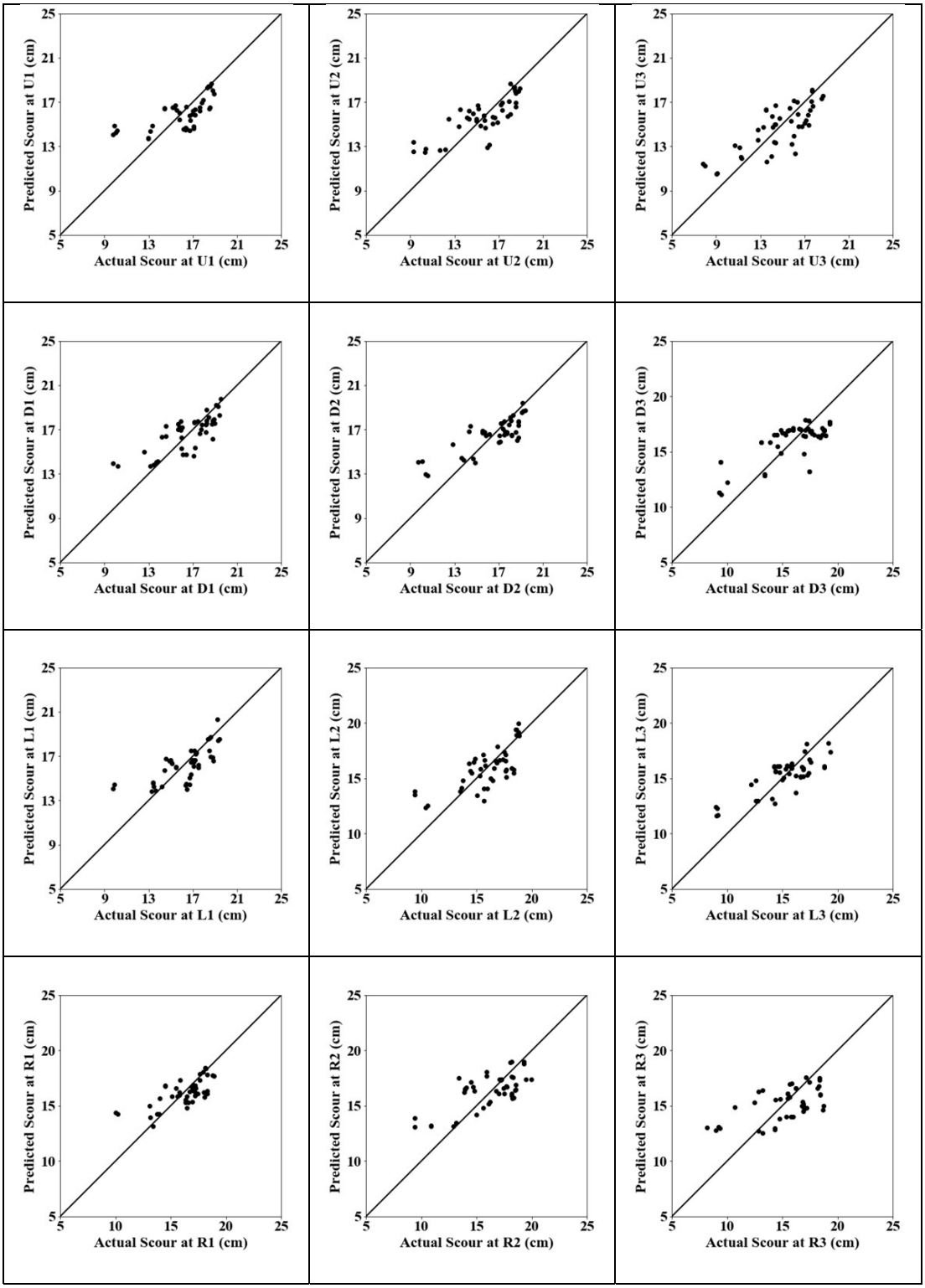

Figure 4.18: Scatter plots from ANN models under pressure-flow conditions during testing

4.6 Comparison of Best Regression and ANN Models

In this section, a comparison of the best regression model (NLRM-2) with the ANN model is carried out. For this, only four scour locations that are closest to the pier (U1, D1, L1, and R1) are selected as the scour is expected to be the maximum at these locations, which will be critical in bridge foundation design. In addition, the minimum, maximum, and average error statistics are also considered. The comparative statistical results from the NLRM-2 and ANN models under free-flow conditions are presented in Table 4.16. The first part of the statistical results is for training data set and at the bottom of the table, statistical results from testing data set are presented.

Analysing the average statistical results during training, it is observed that the average values of R from the NLRM-2 and ANN models are 0.8317 and 0.8585, respectively; average of values of E from the two models are (0.6920, 0.7241); that of RMSE are (1.91, 1.81); that of AARE are (16.7, 16.7); TS5 are (26.7, 27.0); TS10 are (49.5, 50.9); and TS25 are (81.9, 85.5). The average statistics over all the 12 scour locations show that the ANN model performed better than the NLRM-2 model in terms of most of the error statistics except AARE which was same from both the models. The results in terms of average error statistics during testing data from the two models are: R (0.8297, 0.8276); E (0.6816, 0.6805); RMSE (1.87, 1.86); AARE (15.5, 16.4); TS5 (29.0, 24.6); TS10 (48.7, 51.3); TS25 (82.5, 85.6). These results in indicate that the NLRM-2 performs slightly better during testing except for the RMSE, AARE, TS10, and TS25 statistics for which the ANN model performed better. Overall, we can say that the ANN model performed better in terms of average error statistics.

Looking at the minimum error statistics over the 12 scour locations during training from Table 4.16, it may be observed that the ANN model obtained better minimum error statistics except for E and TS10; and the ANN model performed better than the NLMR-2 model in terms of all minimum error statistics during testing except E, R and TS5. Similarly, examining the maximum error statistics during training from Table 4.16, it can be observed that the ANN model performed better than the NLRM-2 model except for RMSE; and the ANN model was better than the NLRM-2 model during testing in terms of all maximum error statistics except R, AARE, and TS5. Therefore, based on statistical

results in terms of minimum and maximum error statistics, we can say that the ANN model performed better than the NLRM-2 model.

Analysing the error statistics in predicting scour at location U1, we see that the ANN model outperformed the NLRM-2 model except TS5 during training data set; and it performed better than the NLRM-2 model in terms of all error statistics except TS5 during testing data set. Further, when ANN was not the better model then it was only slightly. Similarly, the statistical results for scour location D1 show that the ANN model was much better than the NLRM-2 model in terms of all the error statistics during training and much better than NLRM-2 model in terms of all error statistics during testing except TS5. For L1, ANN performed much better than the NLRM-2 model in terms of all the error statistics during training except TS5 and the NLRM-2 model performed better than the ANN model in terms of all error statistics during testing except TS25. Lastly, analysing the results for the scour location R1, it is noted that the ANN model performed better than the NLRM-2 model in terms of all the error statistics during training except TS5 and in terms of all the error statistics during testing except TS10. Thus, based on results for predicting scour close to pier, we can say that the ANN model performed better than the NLRM-2 model.

The comparative statistical results from the NLRM-2 and ANN models under pressure-flow conditions are presented in Table 4.17. Analysing the statistical results in terms of average error statistics over the 12 scour locations during training, it is noted that the ANN model performed significantly better than the NLRM-2 model in terms of all the error statistics except TS10 and TS25 where is slightly under-performed.

Looking at the average error statistics over all 12 scour locations during testing data set, it is observed that the ANN model was better than the NLRM-2 model in terms of the average error statistics except TS5. Therefore, we can say that on an average the ANN model performed better than the NLRM-2 model under pressure-flow conditions also.

Table 4.16: Comparative analysis of statistical results from NLRM-2 and ANN models under free-flow conditions

	R	E	RMSE	AARE	TS5	TS10	TS25
During Calibration / Training Data Set							
NLMR-2 Model							
Min	0.8055	0.6488	1.71	11.7	10.4	37.5	72.9
Max	0.8526	0.7269	2.06	22.6	38.9	58.3	91.7
Avg	0.8317	0.6920	1.91	16.7	26.7	49.5	81.9
U1	0.8278	0.6853	1.81	13.8	38.9	55.6	88.9
D1	0.8079	0.6527	1.86	12.4	25.9	53.7	88.9
L1	0.8403	0.7061	1.72	12.0	25.0	56.3	91.7
R1	0.8364	0.6995	1.71	11.7	37.5	58.3	87.5
ANN Model							
Min	0.8118	0.6317	1.39	9.9	16.7	35.4	75.0
Max	0.9011	0.8015	2.17	21.9	39.6	66.7	93.8
Avg	0.8585	0.7241	1.80	16.7	27.0	50.9	85.5
U1	0.8671	0.7286	1.68	13.3	37.0	59.3	90.7
D1	0.8912	0.7838	1.44	10.4	35.4	66.7	91.7
L1	0.8843	0.7719	1.51	10.6	39.6	64.6	93.8
R1	0.9011	0.8015	1.39	9.9	35.4	62.5	93.8
During Validation / Testing Data Set							
NLMR-2 Model							
Min	0.7722	0.5781	1.66	11.5	18.8	35.4	72.9
Max	0.8646	0.7443	2.22	21.2	39.6	60.4	90.7
Avg	0.8297	0.6816	1.87	15.5	29.0	48.7	82.5
U1	0.8345	0.6932	1.72	12.2	33.3	57.4	88.9
D1	0.8149	0.6620	1.79	11.5	33.3	51.9	90.7
L1	0.8464	0.7160	1.68	11.5	39.6	60.4	89.6
R1	0.8443	0.7102	1.66	11.8	27.1	58.3	87.5
ANN Model							
Min	0.7206	0.5092	1.45	10.5	16.7	37.5	72.9
Max	0.8915	0.7840	2.35	23.7	31.3	70.8	96.3
Avg	0.8276	0.6805	1.86	16.4	24.6	51.3	85.6
U1	0.8578	0.7303	1.61	12.3	24.1	57.4	96.3
D1	0.8788	0.7677	1.45	10.5	27.1	70.8	95.8
L1	0.8348	0.6846	1.77	12.4	31.3	54.2	93.8
R1	0.8867	0.7806	1.45	10.8	31.3	56.3	93.8

Examining the minimum error statistics taken over all the 12 scour locations during training, it can be observed that the minimum error statistics obtained from the ANN model were better than those obtained from the NLRM-2 model in terms of all the error statistics except TS5 and TS10; and the NLRM-2 model performed slightly better than the ANN model during training. Looking at the maximum error statistics across the 12 scour locations during training, we see that the ANN model was better than the NLRM-2 model in terms of all the error statistics except RMSE and AARE, and in terms of all error statistics during testing except E and the TS statistics. It is again interesting to note that when the ANN model performs better than the NLRM-2 model then it performs significantly better but when the NLRM-2 model performs better than the ANN model it only performs marginally better. Thus, we can say that the performance of the ANN model in capturing the non-linear and complex scour dynamics under the pressure-flow conditions is comparable to the NLRM-2 model when it is not performing better. Therefore, overall, the ANN model is chosen as the best model in predicting the scour values across all the 12 locations.

As we analysed the comparative performance of the two models for free-flow conditions at the scour locations very close to the pier, we do the same under the pressure-flow conditions as well. Analysing the comparative statistical results during training for U1, it can be noted that the ANN model significantly outperformed the NLRM-2 model in terms of all the error statistics and the ANN model performed significantly better than the NLRM-2 model during testing except for TS5 and TS10 statistics when it performed marginally worse. Analysing results for D1, we see that the NLRM-2 model performed very poorly as compared to the ANN model during both testing and training data sets. Examining results for L1, ANN was better than NLRM-2 model except for TS5 and ANN model performed much better than the NLRM-2 model during testing. Lastly, analysing the results for modelling scour at location R1, we notice that the performance of ANN was much better than that of the NLRM-2 model in terms of all the error statistics during both training and testing data sets. Therefore, we can clearly conclude that the ANN was a better model in terms of predicting the scour around bridge pier under pressure-flow conditions also.

Comparative performance of the NLRM-2 and the ANN models in terms of scatter plots under free-flow and pressure-flow conditions is shown in Figure 4.19 through Figure 4.22. It is noted that the ANN model performs significantly better than the NLRM-2 model both for training and testing data sets under the free-flow conditions and better than the NLRM-2 model both for training and testing data sets under the pressure-flow conditions.

Table 4.17: Comparative analysis of statistical results from NLRM-2 and ANN models under pressure-flow conditions

	R	E	RMSE	AARE	TS5	TS10	TS25
During Calibration / Training Data Set							
NLMR-2 Model							
Min	0.5961	0.3553	1.73	8.8	27.3	54.5	84.1
Max	0.7272	0.5289	2.16	13.0	50.0	75.0	95.5
Avg	0.6658	0.4452	1.91	10.6	38.1	63.6	91.7
U1	0.6204	0.3849	1.92	10.1	50.0	65.9	90.9
D1	0.6206	0.3851	1.87	9.9	34.1	75.0	93.2
L1	0.6226	0.3876	1.89	9.6	47.7	68.2	93.2
R1	0.5961	0.3553	1.73	8.8	43.2	72.7	93.2
ANN Model							
Min	0.5976	0.3562	1.31	6.7	22.7	52.3	84.1
Max	0.8468	0.6952	2.26	14.0	52.3	84.1	95.5
Avg	0.7584	0.5610	1.70	9.7	37.1	66.1	92.4
U1	0.7111	0.4909	1.74	9.9	38.6	65.9	90.9
D1	0.8468	0.6952	1.31	6.7	52.3	84.1	93.2
L1	0.7488	0.5429	1.63	8.8	43.2	68.2	93.2
R1	0.7304	0.4980	1.53	7.9	50.0	81.8	93.2
During Validation / Testing Data Set							
NLMR-2 Model							
Min	0.5959	0.3540	1.55	7.9	25.0	50.0	86.4
Max	0.7325	0.5357	2.03	12.6	45.5	75.0	95.5
Avg	0.6777	0.4581	1.84	10.2	36.7	63.6	92.0
U1	0.5959	0.3540	2.00	10.6	45.5	68.2	90.9
D1	0.6543	0.4252	1.77	9.4	36.4	72.7	93.2
L1	0.6548	0.4274	1.68	8.8	43.2	68.2	95.5
R1	0.6547	0.4216	1.55	7.9	45.5	75.0	95.5
ANN Model							
Min	0.5917	0.3432	1.44	7.4	22.7	50.0	86.4
Max	0.8165	0.6133	2.20	13.5	47.7	79.5	97.7
Avg	0.7391	0.5328	1.72	9.8	35.4	63.8	93.9
U1	0.6885	0.4595	1.83	10.3	31.8	65.9	90.9
D1	0.7752	0.5879	1.50	8.0	43.2	72.7	95.5
L1	0.7226	0.5210	1.53	8.1	43.2	72.7	95.5
R1	0.7160	0.4971	1.44	7.4	47.7	75.0	95.5

Thus, the conclusions drawn about the superiority of the ANN models based on the statistical results are strengthened by the graphical results.

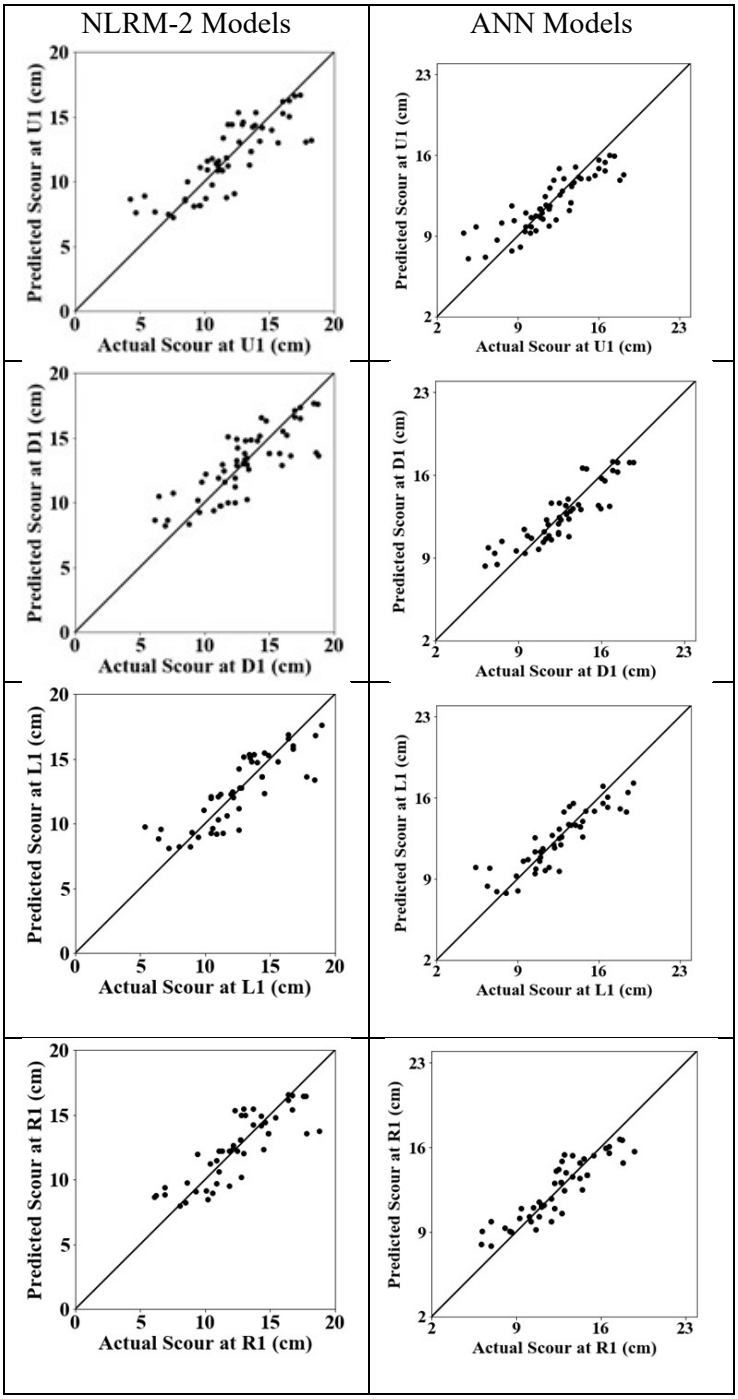

Figure 4.19: Comparison of NLRM-2 and ANN models during calibration/training data set under free-flow conditions

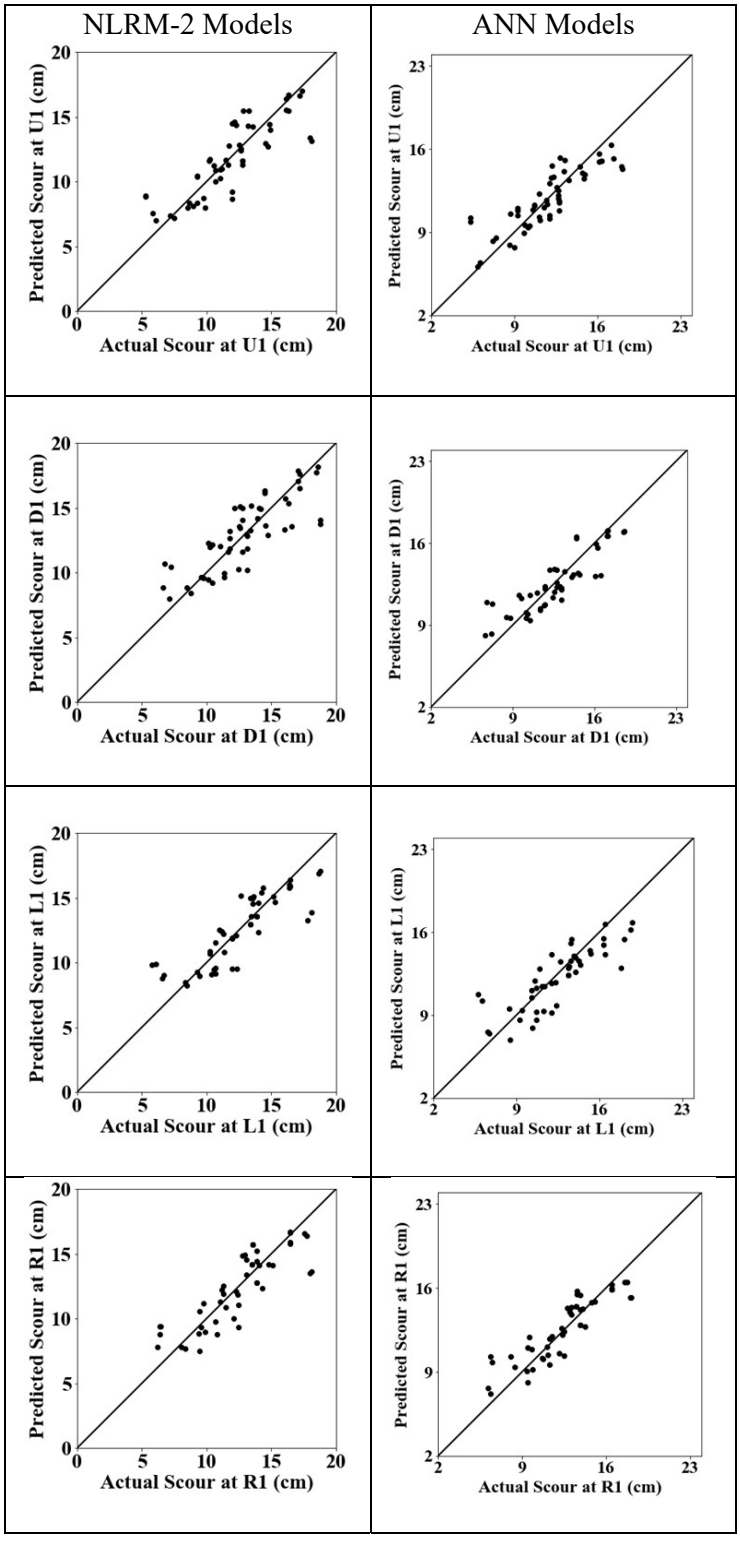

Figure 4.20: Comparison of NLRM-2 and ANN models during validation/testing data set under free-flow conditions

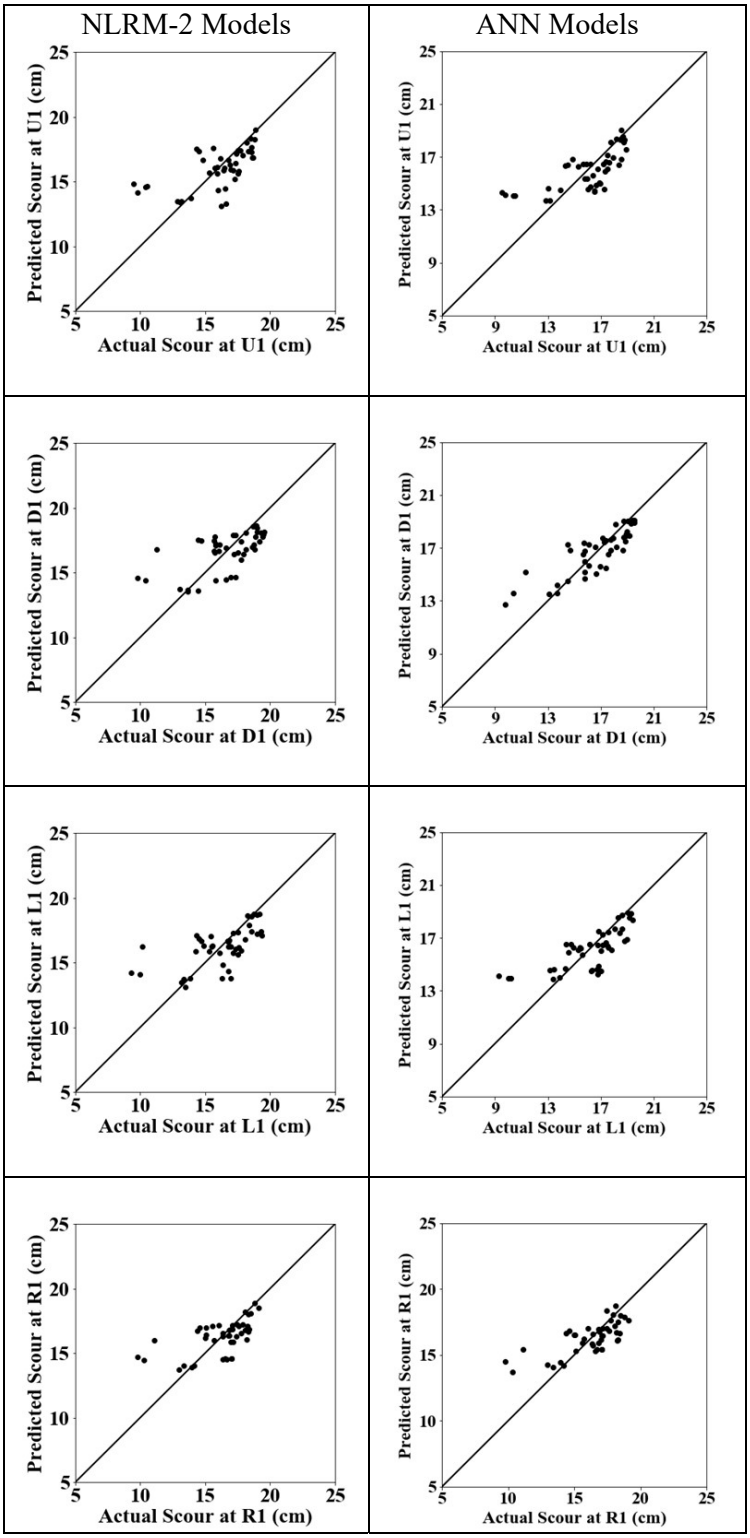

Figure 4.21: Comparison of NLRM-2 and ANN models during calibration/training data set under pressure-flow conditions

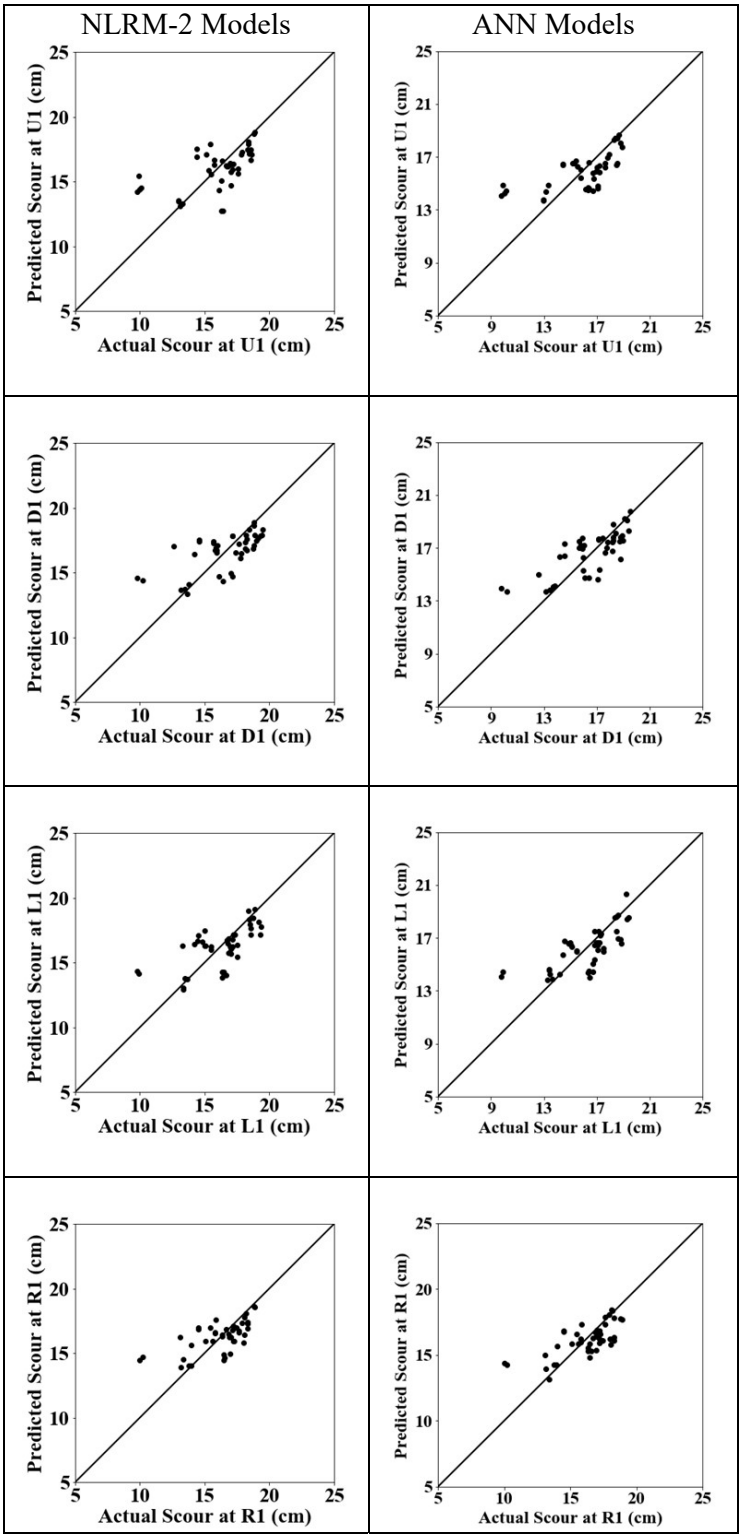

Figure 4.22: Comparison of NLRM-2 and ANN models during validation/testing data set under pressure-flow conditions

4.7 Analysis of the Results for Scour Hole

In this section, we examine the statistical results from the best model (the ANN model) in predicting the scour depths as we move away from the pier in all the four directions. Therefore, the statistical results are analysed as we move away from the pier in the upstream direction (U1, U2, and U3); in the downstream direction (D1, D2, and D3); in the left direction (L1, L2, and L3); and in the right direction (R1, R2, and R3). These results are analysed during testing data set only.

Figure 4.23 shows the comparison of various error statistics as we move upstream (U1, U2, U3) and downstream (D1, D2, D3) from the pier from ANN model during testing data set under the free-flow conditions. It can be noted from Figure 4.23 that the values of error statistics R & E decrease as we move away from the pier in an upstream direction meaning the performance of the ANN model decreases as we move away from the pier upstream. The values of RMSE and AARE increase from U1 to U2 to U3 indicating that the performance of the ANN model in terms of RMSE and AARE statistics decreases as we move away from the pier in an upstream direction. The values of TS10 and TS25 decrease as we move away from the pier in an upstream direction meaning the performance of the ANN model worsens as we move away from the pier upstream. Therefore, in terms of all the error statistics investigated in this study, it is found that the performance of the best model decreases as we move away from the pier in an upstream direction.

Analysing the performance of the ANN model downstream in terms of R & E statistics, it is noted that the general trend is that the performs gets bad moving downstream from the pier except for the performance of ANN model at D2 which is slightly better. Looking at the performance of the ANN models as we moving away from the pier in the downstream direction, we observe that the error statistics RMSE and AARE increase and that the TS10 and TS25 decrease meaning that the performs becomes worse. Therefore, we can say that the performance of the ANN models becomes worse as we move away from the pier in a downstream direction also.

Figure 4.24 shows the comparison of various error statistics as we move left (L1, L2, L3) and right(R1, R2, R3) from the pier from ANN model during testing data set under the

free-flow conditions. It can be noted from Figure 4.24 that the values of error statistics R, E, and RMSE become worse as we move away to the left side of the pier except for L3, which becomes better. The values of AARE increase from L1 to L2 to L3 indicating that the performance of the ANN model in terms of AARE statistics decreases as we move away from the pier towards left direction. The values of TS5 and TS25 decrease as we move away from the pier in left direction (except for L3 which becomes better) meaning the performance of the ANN model worsens as we move away from the pier to the left. Therefore, in terms of all the error statistics investigated in this study, it can be said that the performance of the best model decreases as we move away from the pier in the left direction.

Analysing the performance of the ANN model to the right of the pier in terms of R, E, and RMSE statistics, it is noted that the performance gets bad moving to the right from the pier. Looking at the performance of the ANN models as we move away from the pier in the left direction, we observe that the error statistics AARE increase and that the TS10 and TS25 decrease meaning that the performs becomes worse. Therefore, we can say that the performance of the ANN models becomes worse as we move away from the pier in a downstream direction also.

The comparative results were also analysed for the pressure-flow conditions when we move away from the pier in all the four directions. The results were found to be similar in the downstream and right directions i.e. the ANN model performance becomes worse as we move away from the pier in the downstream and right directions but there was no definite trend in the upstream and left direction. However, the best performance was close to the pier i.e. at U1 and L1.

Thus, overall we can conclude that the performance of the best performing model (ANN model) becomes worse moving away from the pier in all four directions in modelling the scour around bridge pier under free-flow and pressure-flow conditions. This is an interesting finding that needs further investigation for finding the reasons for the same.

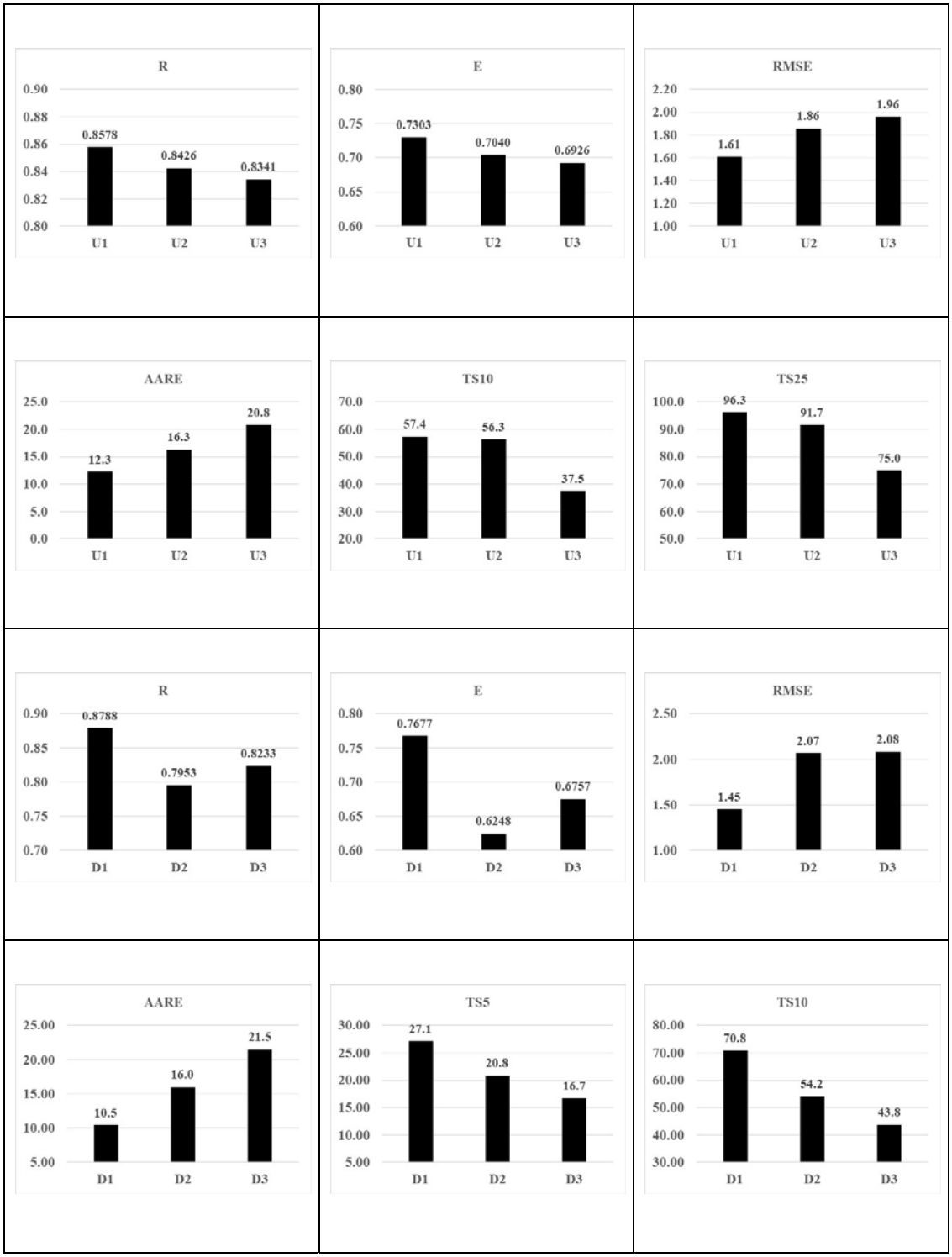

Figure 4.23: Evaluation of ANN models moving away from pier in upstream and downstream directions during testing data set under free-flow conditions

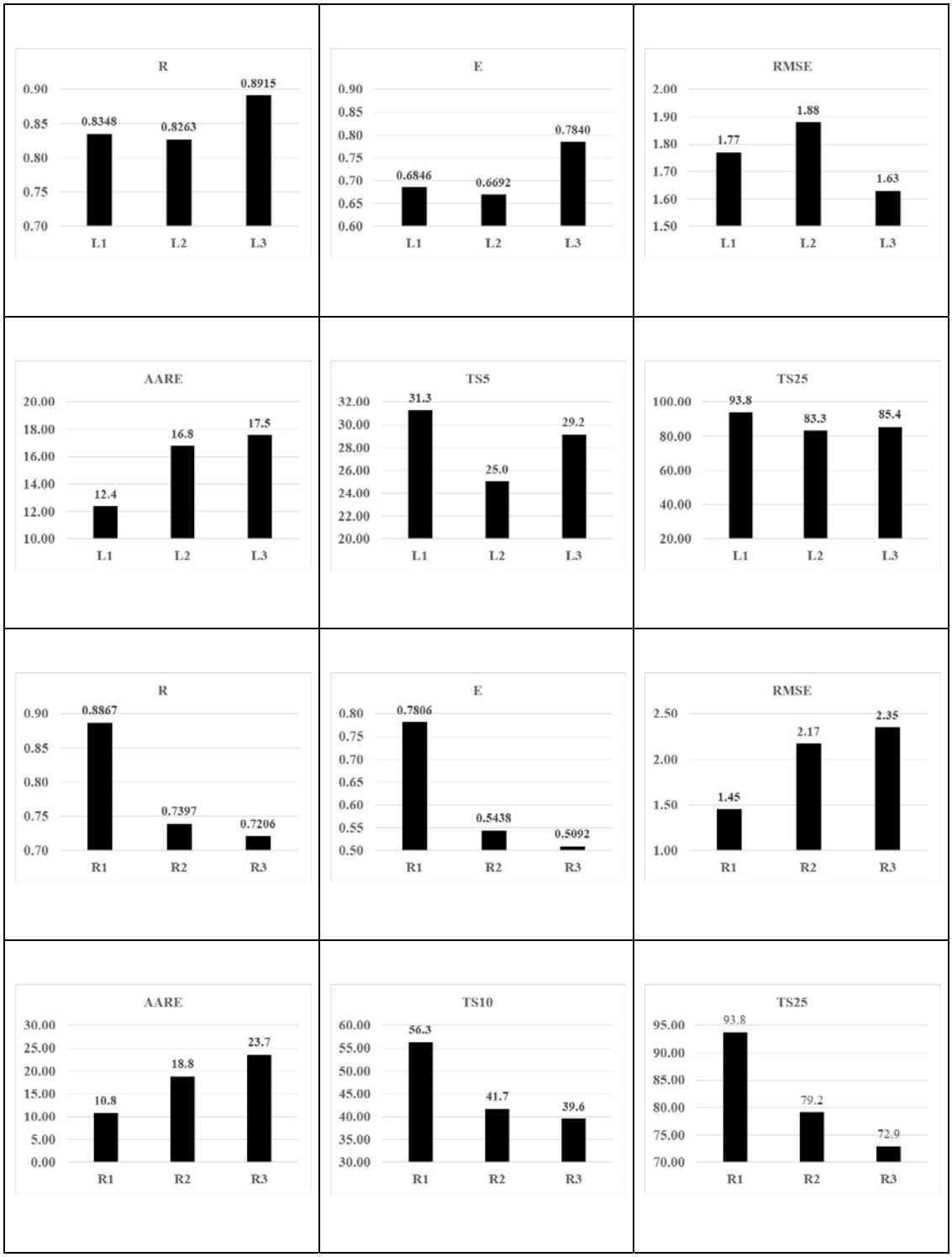

Figure 4.24: Evaluation of ANN models moving away from pier in left and right directions during testing data set under free-flow conditions

Chapter 5

Summary, Conclusions, and Future Scope

5.1 Summary

This report describes the findings of a study aimed at carrying out extensive experimentation to develop a scour data base for determining scour depth around a bridge pier under both free-flow and pressure-flow conditions, analyze the developed scour database, and develop mathematical models to predict the scour around a bridge pier given the various hydraulic parameters under both free-flow and pressure-flow conditions. A total of 48 experiments were conducted in the hydraulics laboratory of the Indian Institute of Technology (IIT) Kanpur in a flume of size length 20 m; width 61 cm; and depth 41 cm including both free-flow and pressure-flow conditions. Four different cylindrical bridge piers of diameters 5.14 cm, 4.00 cm, 3.20 cm, and 2.10 cm were used and for each diameter several flood-flow values were employed to develop an extensive scour database for both free-flow and pressure-flow conditions. Each experiment was conducted for 10-hours and the measurements of flow depth, velocity, discharge, and scour depth were taken at 15 min interval during the first hour and then at 1-hour interval for theremaining time in order to capture the time distribution of the scour around a bridge pier. In order to quantify the dimensions of the scour hole created around a bridge pier during a flood flow, the scour depths were measured at 12 different locations around a bridge pier in all the four directions i.e. upstream, downstream, left, and right of the bridge pier. The scour database developed in this study is presented in Appendix-I, which will be a very important data resource for the researchers working in the experimental hydraulics.

Two types of mathematical models were developed using the developed scour database to predict the scour at each of the 12 scour locations around a bridge pier as a function of the hydraulic parameters e.g. flow depth, velocity, discharge, and pier diameter. The techniques investigated include regression models and the Artificial Neural Network (ANN) models. Three regression models were developed: linear regression models,

polynomial regression models of order-2 and a power regression model. There were a total of 36 regression models developed to predict the scour around bridge piers under free-flow conditions: 12 linear models, 12 polynomial models of order-2, and 12 power regression models. Similarly, 36 regression models were also developed for predicting the scour around the bridge piers at all the 12 locations using the linear, polynomial, and power regression models under the pressure-flow conditions. For the ANN, a feed-forward neural network of Multilayer Perceptron (MLP) type of architecture trained using the more recent Adam optimization algorithm was employed. A total of 24 ANN models were developed, 12 each for the free-flow and pressure-flow conditions to predict the scour depth around a bridge pier at each of the 12 locations considered in this study. The entire database was divided into two parts: a training or calibration data set on which the models were trained/ calibrated and a testing/ validation data set on which the performance of the developed models was tested. The performance of each mathematical model developed in this study was evaluated by using a wide variety of standard model performance evaluation statistics and in terms of scatter plots to graphically evaluate the model performance.

5.2 Conclusions

The scatter plots between the scour at all the 12 locations plotted against the various hydraulic parameters show that the relationship between flow depth and scour around the bridge pier is very well defined with the scour increasing with an increase in the flow depth for the free-flow conditions. The pattern of relationships among the scour depth and the velocity of flow and the discharge is not very apparentwhile that between scour and pier diameter is very clear with scour increasing with pier diameter, as expected. The patterns were found to be similar under pressure-flow conditions as well.

It has been found that the scour at a location in the scour hole increases with time and then attains the equilibrium scour and oscillates around the equilibrium scour. The pattern for scour around bridge piers at all of the 12 locations is similar; however, the scour reaches its equilibrium scour much faster in case of the pressure-flow conditions. The results obtained here indicate that the magnitude of scour is maximum just downstream of the pier as compared to all other locations in most of the cases barring a few exceptions both for the free-flow and the pressure-flow conditions. A comparison of the free-flow and

pressure-flow scours keeping all other parameters same revealed that the pressure-flow scour is almost twice that of the free-flow scour in most cases and increased in the other cases to great extent. The fact that the pressure scour is much more than the free-flow scour and the pressure-flow scour mechanics is much more dynamic as it reaches the maximum value faster show that the assessment of the pressure-flow scour values is extremely important in the design of bridge piers. Therefore, the pier foundations should be designed for pressure-flow conditions and also a factor safety and suitable free-board must be provided to avoid the pressure-flow conditions for the safety of the bridges.

A close examination of the magnitudes of the regression coefficients of the three different regression models did not show any fixed pattern with linear model indicating depth of flow as the most significant variable, polynomial regression model of order-2 showing discharge as the most significant variable, and the power regression model indicating the pier diameter as the most significant variable in predicting the scour under the free-flow conditions. Further, by looking at the magnitude of the regression coefficients of the various regression models for pressure-flow conditions, there is no apparent trend of significance of various hydraulic variables. Thus, it appears that the significance of the hydraulic parameters depends upon the structure of the regression model being considered. However, considering the fact that the polynomial regression model performed the best, it can be said that the discharge was the most significant variable from both free-flow and pressure-flow conditions.

The results in terms of various standard performance evaluation measures considered in this study indicate that the polynomial regression model of order-2 was the best regression model followed by the power regression model and the linear regression model performed the worst for both free-flow and the pressure-flow conditions. In fact, the performance of the linear regression models was poor. The power regression model is not recommended and the polynomial regression model of order-2 is recommended for predicting the scour around bridge piers under both free-flow and pressure-flow conditions. The results obtained in this study in terms of graphical evaluation of all the regression models corroborated the conclusions obtained based on the various error statistics for both free-flow and the pressure-flow conditions. It has been found that all the ANN models at all the 12 locations under both free-flow and pressure-flow conditions outperformed the corresponding regression models. Therefore, the ANN models are recommended for

predicting the scour around bridge piers based on the results obtained in this study. A comparison of the best regression models and the ANN models for predicting the maximum scour around bridge pier in all the four directions (upstream, downstream, left, and right) also revealed that the ANN model was superior to the polynomial regression model of order-2. Therefore, ANN model is recommended for estimating the maximum or equilibrium scour around bridge piers. However, the performance of the polynomial regression model of order-2 was also good and it may also be employed in predicting scour around bridge pier due to its compact structure and when ANN model development is difficult or is not available.

A separate analysis of the results was carried out to examine the impact of distance on ANN modeling as we move away from the bridge pier in all the four directions (upstream, downstream, left, and right). The results of this examination revealed that the performance of the ANN models was the best closest to the pier (i.e. at U1, D1, L1, and R1) and deteriorates as we move away from the pier. This is an interesting finding of this study. On one hand, it is good to note that the performance of the ANN models is good just close to the pier where the magnitude of the scour is expected to be the maximum. Therefore, we can rely on the ANN model results in designing the depths of foundations at bridge piers. On the other hand, it is intriguing to note that the performance of the best performing model investigated in this study deteriorates as we move away from the bridge pier in the four directions. More research is needed to find out the reasons for this phenomenon. Some of the possible reasons may be: (a) the scour hole develops fully very close to the piers where the scour depths are maximum and the impact of the hydraulic characteristics at these locations is well defined and thus captured by the ANN models very well, (b) as we move away from the pier, the bed roughness starts to become more predominant and starts adding to the complexity of the hydro-dynamic phenomenon and the scour mechanism making it difficult for any mathematical model to capture such dynamics. However, these phenomena need to be further explored and researched.

A unique and novel aspect of the study carried out here has been the prediction of the entire scour hole around bridge piers rather than the maximum/ equilibrium scour only as found in other studies reported in literature in the past. The knowledge of the size, shape, and characteristics of the scour hole gives us some idea of the horse-shoe vortex characteristics and the hydro-dynamic forces responsible for producing the scour hole.

The availability of mathematical models having the capability of predicting the size and shape of the scour hole can be extremely important not only in the visualization of the evolving scour hole around bridge piers but also in designing the suitable protection measures against the scour around bridge piers.

5.3 Future Scope

No study is complete and there are always scopes for improvements. In light of the study presented in this report, a few limitations and / or scope for future research works have been identified. First and fore-most, we would like to stress that all the experiments conducted in this study were for 'clear-water scour' process. In the field, there is sediment inflowing into the bridge opening which may affect the hydro-dynamic conditions around bridge pier and hence the scour values. The results may be different for sediment scour conditions; thus more studies/ research is needed to be carried out to understand the behavior of scour patterns around bridge piers under sediment scour conditions under both free-flow and pressure-flow conditions. The scour around bridge piers is also a function of the gradation of soil-sediment and bed-material in the rivers/ channels. The experiments conducted in this study considered only one type of sand and more experiments are needed to evaluate the impact of sediment size and other sediment characteristics on the scour around bridge piers under both free-flow and pressure-flow conditions. The experiments were conducted more than ten years ago and the equipment used in the study may be obsolete now and new and more precise measurements of the scour and other hydraulic characteristics may be needed to have more confidence in the conclusions drawn here.

Various mathematical models developed in this study are for the prediction of the maximum scour or the equilibrium scour around bridge piers at 12 different locations; however, time-varying mathematical models are needed to study how the scour hole around a bridge pier evolves with time. Research is needed in developing mathematical models predicting scour as a function of time in addition to the hydraulic characteristics. A limited number of mathematical models were investigated in this study. There are host of other complex and non-linear models available that may be tried among both conventional and data-driven type of approaches. Only one type of ANN architecture (feedforward) was considered in this study; whereas, there are many other types of ANN

architectures available e.g. feedback networks, generalized regression neural networks, radial-basis function neural networks and so on. The data generated in this study are provided at the end of this report (Appendix-I) with an objective to motivate other researchers to take-up the research in the area of the development of more sophisticated and complex models for estimating the scour around bridge piers under both free-flow and pressure-flow conditions. Further, it would be interesting to develop mathematical models by employing a hybrid data set by integrating the scour database developed here with other scour data sets available in literature to assess the validity of the results obtained here and to have more confidence in them.

It is hoped that future research efforts will focus in some of these directions to improve the understanding and assessment of the scour process around bridge piers that would be helpful in design of bridge piers with more confidence.

Chapter 6

References

1. Abed, L.M. (1991), “Local scour around bridge piers in pressure flow”, PhD dissertation, Colorado State Univ., Fort Collins, Colorado, USA.

2. Ali, K.H.M. and Karim, O. (2002), “Simulation of flow around piers”, J Hydraul. Res., 40(2), 161-174.

3. Breusers, H.N.C., Nicollet, G., and Shen, H.W. (1977), “Local scour around cylindrical piers”, J. Hydr. Res., 15(3), 211-252.

4. Brownlee, J. (2020), A Gentle Introduction To The Rectified Linear Unit (Relu), Machine Learning MasteryAvailable at: <https://machinelearningmastery.com/rectified-linear-activation-function-for-deep-learning-neural-networks/> [Accessed 31 May 2020].

5. El-Taher, R.M. (1984), “Experimental study on the interaction between a pair of circular cylinders normal to a uniform shear flow”, J. Wind Engg. Aerodyn., 17, 117-132.

6. Gangadharaiah, T., Muzzammil, M., and Subramanya, K. (1985), “Vortex strength approach for bridge pier scour predictions”, Proc. of 2nd Intl. Workshop on Alluvial River Problems, University of Roorkee, Roorkee, India, pp. 151-158.

7. Gangadharaiah, T., Shah, B.P., and Muzzammil, M. (1989), “Interference effects on scour depth around on bridge piers”, Water 30, pp. 281-290, Division of Water Resources Engg., Asian Inst. of Tech., Bangkok, Thailand.

8. Gangadharaiah, T., Subramanya, K., and Muzzammil, M. (1993), “Scour around bridge piers – An overview of current status”, River Scour Proceedings, pp. 22-29, CBIP, Varanasi, India.

9. Garde, R.J., Ranga Raju, K.G., and Kothyari, U.C. (1989), “Research report on effect of unsteadiness and stratification on local scour”, CBIP sponsored project, Civil Engg. Dept., Univ. of Roorkee, Roorkee, India.

10. Garde, R.J. and Kothyari, U.C. (1995), “State of art report on scour around bridge piers”, submitted to IIBE, New Delhi, India.

11. Garde, R.J. and Kothyari, U.C. (1998), “Scour around bridge piers”, J. Indian National Sci. Acad. 64, (64), New Delhi, India.

12. Jain, S.C. (1981), “Maximum clear-water scour around circular piers”, J. Hydraul. Divn., ASCE, 107(HY5).

13. Kingma, D.P. and Ba, J.L. (2015), Adam: A method for stochastic optimization, Proceedings: 3rd International Conference on Learning Representations, ICLR 2015, San Diego, CA, USA, May 7-9, 2015.

14. Kothyari, U.C., Garde, R.J., and Ranga Raju, K.G. (1988), “Maximum scour depth at circular bridge piers in clear water flows”, Proc. 6th APD IAHR Congress, Kyoto, Japan, pp. 261-268.

15. Kothyari, U.C., Garde, R.J., and Ranga Raju, K.G. (1989), “Estimation of equilibrium scour depth around circular bridge piers”, Proc. 3rd Intl workshop on alluvial river problems, Roorkee, India, pp. 39-45.

16. Kothyari, U.C., Garde, R.J., and Ranga Raju, K.G. (1992a), “Live bed scour around cylindrical bridge piers”, J. Hydraul. Res., IAHR, 30(5), 701-715.

17. Kothyari, U.C., Garde, R.J., and Ranga Raju, K.G. (1992b), “Temporal variation of scour around cylindrical bridge piers”, J. Hydraul. Engg., ASCE, 118(8), 1091-1106.

18. Kothyari, U.C. (1993), “A theme paper on scour around bridge piers”, Proc. workshop on river scour, CBIP, India, Varanasi, pp. 1-10.

19. Kumar, V., Ranga Raju, K.G., and Vittal, N. (1999), “Reduction of local scour around bridge piers using slots and collars”, J. Hydraul. Engg., ASCE, 125(12), 1302-1305.

20. Lagasse, P.F., Schall, J.D., Johnson, F., Richardson, E.V., Richardson, J.R., and Chang, F. (1991), “Stream stability of highway structures”, Hydr. Engg. Circular No. 20, Rep. No. FHWA-IP-90-014, US Dept. of Transp., Fed. Hwy. Admin., Washington, D.C., USA, pp. 1-57.

21. Medium (2020), Everything You Need To Know About Adam OptimizerAvailable at: <https://medium.com/@nishantnikhil/adam-optimizer-notes-ddac4fd7218> [Accessed 31 May 2020].

22. Melville, B.W. and Raudkivi, A.J. (1977), “Flow characteristics in local scour at bridge piers”, J. Hydraul. Res., 15(4), 373-380.

23. Melville, B.W. (1988), “Scour at bridge sites”, Ch 15, Civil Engg. Practice, Cheremisioff (ed), Technology Publishing Company, USA.

24. Muzzammil, M. (1992), “Characteristics of Horse Shoe vortex at cylindrical bridge pier models”, PhD Thesis, IIT Kanpur, India.

25. Oliverto, G. and Hager, W.H. (2002), “Temporal evolution of clear water pier and abutment scour”, J. Hydraul. Engg., ASCE, 128(9), 811-820.

26. Olsen, N.R.B. and Melaaen, M.C. (1993), “Three-dimensional calculation of scour around cylinders”, J. Hydraul. Engg., ASCE, 119(9), 1048-1054.

27. Rao, G.P. (1997), “Interference effects on local scour around bridge piers”, M. Tech. Thesis, Dept. of Civil Engg. IIT Kanpur, India.

28. Rao, R.S., Setia, B., Gangadharaiah, T., and Gupta, A.K. (1998), "Scour protection around bridge piers and abutments", Research Report submitted to INCH by Dept. of Civil Engg., IIT Kanpur, India.

29. Raudkivi, A.J. (1986), "Functional Trends of scour at bridge piers", J. Hydraul. Engg., ASCE, 112(1), 1-13.

30. Richardson, E.V., Harrison, L.J., Richardson, J.R., and Davis, S.R. (1993), "Evaluating scour at bridges", Hydr. Engg. Circular No. 18, Rep. No. FHWA-IP-90-017, US Dept. of Transp., Fed. Hwy. Adimn., Washington, D.C., USA, pp. 5-53.

31. Setia, B. (1997), "Scour around bridge piers: Mechanism and protection", PhD Thesis, Dept. of Civil Engg., IIT Kanpur, India.

32. Srivastava, P. (1989), "Strength characteristics of the horse-shoe-vortex", M. Tech Thesis, Dept. of Civil Engg., IIT Kanpur, India.

33. Subramanya, K., Garde, R.J., and Namboodripad, K.D. (1961), "Study of scour around obstructions", J. Irrg. & Power, CBIP (India), 18, 651-660.

34. Umbrell, E.R., Young, G.K., Stein, S,M,, and Jones, J.S. (1998), "Clear water contraction scour under bridges in pressure flow", J. Hydraul. Engg., ASCE, 124(2), 236-240.

35. Vittal, N., Kothyari, U.C., and Haghighat, M. (1994), "Clear water scour around bridge-pier group", J. Hydraul. Engg., ASCE, 120(11), 1309-1318.

36. Yanmaz, A.M., Altinbilek, H.D. (1991), "Study of time-dependent local scour around bridge piers", J. Hydraul. Engg., ASCE, 117(10), 1247-1268.

37. Zdravkovich, M.M. (1977), "Review of flow interference between two cylinders in various arrangements", J. Fluids Engg., 99, 618-633.

38. Zdravkovich, M.M. (1987), “The effects of interference between circular cylinders in cross flow”, J. Fluids Str., 1, 235-261.

APPENDIX-A

Scour Database

Table A.1: Scour database for free-flow conditions at U1

Calibration/Training

D (cm)	*Q* (m^3/s)	*d* (cm)	*v* (m/s)	U1 (cm)
2.10	0.01697	9.0	0.443	14.44
2.10	0.01697	9.4	0.505	15.14
2.10	0.02610	10.0	0.343	16.02
2.10	0.02610	10.8	0.396	16.52
2.10	0.04123	10.2	0.794	13.96
2.10	0.04123	11.2	0.757	12.56
2.10	0.05249	12.0	0.714	16.02
2.10	0.05249	14.0	0.714	16.52
2.10	0.06501	13.6	1.102	16.97
2.10	0.06501	14.2	1.129	17.37
5.14	0.01363	6.2	1.633	11.17
5.14	0.01363	6.4	1.635	10.97
5.14	0.03249	12.0	0.313	12.65
5.14	0.03249	10.4	0.242	11.45
5.14	0.04413	12.8	0.626	15.65
5.14	0.04413	12.5	0.560	14.25
5.14	0.02233	7.2	0.560	10.57
5.14	0.02233	7.8	0.594	10.17
5.14	0.06494	19.6	1.111	12.97
5.14	0.06494	18.4	1.111	13.87
5.14	0.07286	12.6	0.852	12.87
5.14	0.07286	15.4	0.970	11.77
5.14	0.06831	15.4	0.779	12.07
5.14	0.06831	15.8	0.998	13.67
3.20	0.07475	13.8	0.990	11.77
3.20	0.07475	15.0	1.057	10.97
3.20	0.06627	16.2	1.029	10.17
3.20	0.06627	19.2	0.863	11.07
3.20	0.05450	13.2	0.929	8.67
3.20	0.05450	18.0	0.594	9.67
3.20	0.03538	13.0	0.896	4.27
3.20	0.03538	12.0	0.727	5.37
3.20	0.03129	8.0	0.626	12.27
3.20	0.03129	8.2	0.754	11.67
3.20	0.02188	8.2	0.657	9.57
3.20	0.02188	6.6	0.524	10.07
3.20	0.01514	4.0	0.542	8.47
3.20	0.01514	5.6	0.594	9.17
4.00	0.01553	5.6	0.485	4.67
4.00	0.01553	6.0	0.443	6.17
4.00	0.02374	9.8	0.700	7.57
4.00	0.02374	6.0	0.840	7.17
4.00	0.03937	12.8	0.657	8.47
4.00	0.03937	11.0	1.357	9.67
4.00	0.06039	13.8	0.828	10.57
4.00	0.06039	16.2	0.443	11.37
4.00	0.08071	18.2	0.885	13.47
4.00	0.08071	17.8	0.767	10.87
4.00	0.08912	18.6	0.852	11.67
4.00	0.08912	20.8	0.828	13.57
4.00	0.08912	18.6	0.852	11.67
4.00	0.08912	20.8	0.828	13.57
5.14	0.05007	13.2	0.792	17.80
5.14	0.05007	15.4	0.816	18.20

Validation/Testing

D (cm)	*Q* (m^3/s)	*d* (cm)	*v* (m/s)	U1 (cm)
2.10	0.01697	8.4	0.396	14.84
2.10	0.02610	8.0	0.343	16.12
2.10	0.04123	12.0	0.674	12.86
2.10	0.05249	15.8	0.714	16.12
2.10	0.06501	13.4	1.102	17.17
5.14	0.01363	6.8	1.709	11.17
5.14	0.03249	11.4	0.396	11.75
5.14	0.04413	13.8	0.792	14.75
5.14	0.02233	9.2	0.524	10.17
5.14	0.06494	17.8	1.120	13.57
5.14	0.07286	16.0	1.000	11.97
5.14	0.06831	16.0	0.874	12.27
3.20	0.07475	15.0	0.970	11.67
3.20	0.06627	14.8	0.939	10.67
3.20	0.05450	14.8	0.727	9.27
3.20	0.03538	10.8	0.779	5.27
3.20	0.03129	7.2	0.626	11.97
3.20	0.02188	7.0	0.505	9.77
3.20	0.01514	6.4	0.542	8.97
4.00	0.01553	6.0	0.485	5.87
4.00	0.02374	8.2	0.828	7.47
4.00	0.03937	10.0	0.792	9.27
4.00	0.06039	16.0	0.767	10.67
4.00	0.08071	22.2	0.828	12.67
4.00	0.08912	19.0	0.560	12.67
4.00	0.08912	17.8	0.907	12.77
5.14	0.05007	16.4	0.767	18.00
2.10	0.01697	8.6	0.524	14.94
2.10	0.02610	11.0	0.280	16.32
2.10	0.04123	10.6	0.717	13.26
2.10	0.05249	18.2	0.754	16.32
2.10	0.06501	17.2	1.111	17.37
5.14	0.01363	7.0	1.686	11.07
5.14	0.03249	12.4	0.370	12.55
5.14	0.04413	13.2	0.657	14.55
5.14	0.02233	8.6	0.505	10.27
5.14	0.06494	18.2	1.120	13.17
5.14	0.07286	16.4	1.038	12.07
5.14	0.06831	18.2	0.929	12.17
3.20	0.07475	17.8	1.000	11.47
3.20	0.06627	17.3	0.863	10.57
3.20	0.05450	13.8	0.714	9.27
3.20	0.03538	12.8	0.727	5.27
3.20	0.03129	10.2	0.700	11.97
3.20	0.02188	10.0	0.657	9.87
3.20	0.01514	6.8	0.542	8.57
4.00	0.01553	5.8	0.714	6.07
4.00	0.02374	7.0	0.828	7.17
4.00	0.03937	10.0	0.804	8.67
4.00	0.06039	17.6	0.767	11.07
4.00	0.08071	18.2	0.885	12.77
4.00	0.08912	17.8	0.907	12.77
4.00	0.08912	19.0	0.560	12.67
5.14	0.05007	14.0	0.779	18.10

Table A.2: Scour database for free-flow conditions at U2

Calibration/Training					Validation/Testing				
D	***Q***	***d***	***v***	**U2**	***D***	***Q***	***d***	***v***	**U2**
(cm)	**(m^3/s)**	**(cm)**	**(m/s)**	**(cm)**	**(cm)**	**(m^3/s)**	**(cm)**	**(m/s)**	**(cm)**
2.10	0.01697	8.4	0.396	13.50	2.10	0.01697	9.0	0.443	14.20
2.10	0.01697	8.6	0.524	14.80	2.10	0.02610	10.8	0.396	16.86
2.10	0.02610	10.0	0.343	16.36	2.10	0.04123	11.2	0.757	12.75
2.10	0.02610	11.0	0.280	17.16	2.10	0.05249	14.0	0.714	16.86
2.10	0.04123	10.2	0.794	13.25	2.10	0.06501	14.2	1.129	16.51
2.10	0.04123	10.6	0.717	12.75	5.14	0.02233	7.8	0.594	9.30
2.10	0.05249	12.0	0.714	16.36	5.14	0.06494	19.6	1.111	12.70
2.10	0.05249	18.2	0.754	17.16	5.14	0.07286	12.6	0.852	11.60
2.10	0.06501	13.4	1.102	17.81	5.14	0.06831	15.4	0.779	11.70
2.10	0.06501	17.2	1.111	16.31	3.20	0.07475	15.0	1.057	10.20
5.14	0.02233	9.2	0.524	10.40	3.20	0.06627	16.2	1.029	9.70
5.14	0.02233	8.6	0.505	9.10	3.20	0.05450	14.8	0.727	8.20
5.14	0.06494	18.4	1.111	11.80	3.20	0.03538	12.0	0.727	4.10
5.14	0.06494	18.2	1.120	12.80	3.20	0.03129	8.2	0.754	10.40
5.14	0.07286	16.0	1.000	9.80	3.20	0.02188	7.0	0.505	10.10
5.14	0.07286	16.4	1.038	13.30	3.20	0.01514	4.0	0.542	8.50
5.14	0.06831	16.0	0.874	10.60	4.00	0.01553	6.0	0.485	5.80
5.14	0.06831	15.8	0.998	12.70	4.00	0.02374	8.2	0.828	6.80
3.20	0.07475	13.8	0.990	10.10	4.00	0.03937	10.0	0.792	8.30
3.20	0.07475	15.0	0.970	10.80	4.00	0.06039	16.0	0.767	12.10
3.20	0.06627	14.8	0.939	6.40	4.00	0.08071	22.2	0.828	13.40
3.20	0.06627	19.2	0.863	10.80	4.00	0.08912	17.8	0.907	13.00
3.20	0.05450	13.8	0.714	9.20	4.00	0.08912	17.8	0.907	13.00
3.20	0.05450	18.0	0.594	8.10	5.14	0.05007	16.4	0.767	16.50
3.20	0.03538	13.0	0.896	3.80	2.10	0.01697	9.4	0.505	14.10
3.20	0.03538	10.8	0.779	4.30	2.10	0.02610	8.0	0.343	16.66
3.20	0.03129	7.2	0.626	11.80	2.10	0.04123	12.0	0.674	13.05
3.20	0.03129	8.0	0.626	11.40	2.10	0.05249	15.8	0.714	16.66
3.20	0.02188	8.2	0.657	8.40	2.10	0.06501	13.6	1.102	17.21
3.20	0.02188	6.6	0.524	10.20	5.14	0.02233	7.2	0.560	10.10
3.20	0.01514	5.6	0.594	8.30	5.14	0.06494	17.8	1.120	12.50
3.20	0.01514	6.8	0.542	8.80	5.14	0.07286	15.4	0.970	11.50
4.00	0.01553	5.6	0.485	4.40	5.14	0.06831	18.2	0.929	12.30
4.00	0.01553	6.0	0.443	6.00	3.20	0.07475	17.8	1.000	10.50
4.00	0.02374	9.8	0.700	7.00	3.20	0.06627	17.3	0.863	9.80
4.00	0.02374	6.0	0.840	6.40	3.20	0.05450	13.2	0.929	8.30
4.00	0.03937	10.0	0.804	8.70	3.20	0.03538	12.8	0.727	4.20
4.00	0.03937	11.0	1.357	8.10	3.20	0.03129	10.2	0.700	11.60
4.00	0.06039	13.8	0.828	10.30	3.20	0.02188	10.0	0.657	9.20
4.00	0.06039	16.2	0.443	12.60	3.20	0.01514	6.4	0.542	8.40
4.00	0.08071	18.2	0.885	14.70	4.00	0.01553	5.8	0.714	5.60
4.00	0.08071	17.8	0.767	12.80	4.00	0.02374	7.0	0.828	6.50
4.00	0.08912	18.6	0.852	11.20	4.00	0.03937	12.8	0.657	8.50
4.00	0.08912	20.8	0.828	13.80	4.00	0.06039	17.6	0.767	11.80
4.00	0.08912	18.6	0.852	12.10	4.00	0.08071	18.2	0.885	13.50
4.00	0.08912	20.8	0.828	13.80	4.00	0.08912	19.0	0.560	12.50
5.14	0.05007	13.2	0.792	17.70	4.00	0.08912	19.0	0.560	12.50
5.14	0.05007	15.4	0.816	16.30	5.14	0.05007	14.0	0.779	17.10

Table A.3: Scour database for free-flow conditions at U3

Calibration/Training				
D	***Q***	***d***	***v***	**U3**
(cm)	**(m^3/s)**	**(cm)**	**(m/s)**	**(cm)**
2.10	0.01697	9.0	0.443	13.86
2.10	0.01697	9.4	0.505	12.86
2.10	0.02610	10.0	0.343	15.75
2.10	0.02610	10.8	0.396	17.05
2.10	0.04123	12.0	0.674	13.02
2.10	0.04123	11.2	0.757	12.32
2.10	0.05249	12.0	0.714	15.75
2.10	0.05249	14.0	0.714	17.05
2.10	0.06501	13.4	1.102	15.69
2.10	0.06501	14.2	1.129	16.29
5.14	0.02233	7.2	0.560	6.37
5.14	0.02233	8.6	0.505	8.87
5.14	0.06494	19.6	1.111	8.87
5.14	0.06494	17.8	1.120	10.47
5.14	0.07286	15.4	0.970	6.97
5.14	0.07286	16.4	1.038	9.37
5.14	0.06831	16.0	0.874	8.17
5.14	0.06831	15.4	0.779	9.57
3.20	0.07475	13.8	0.990	11.77
3.20	0.07475	15.0	1.057	10.97
3.20	0.06627	14.8	0.939	6.87
3.20	0.06627	19.2	0.863	9.57
3.20	0.05450	13.2	0.929	5.57
3.20	0.05450	13.8	0.714	7.97
3.20	0.03538	13.0	0.896	2.27
3.20	0.03538	10.8	0.779	3.97
3.20	0.03129	8.0	0.626	11.37
3.20	0.03129	8.2	0.754	8.97
3.20	0.02188	8.2	0.657	7.77
3.20	0.02188	10.0	0.657	8.97
3.20	0.01514	4.0	0.542	6.37
3.20	0.01514	6.8	0.542	7.67
4.00	0.01553	5.6	0.485	2.97
4.00	0.01553	6.0	0.485	4.77
4.00	0.02374	8.2	0.828	5.97
4.00	0.02374	6.0	0.840	3.87
4.00	0.03937	10.0	0.804	6.37
4.00	0.03937	10.0	0.792	7.67
4.00	0.06039	16.0	0.767	9.17
4.00	0.06039	16.2	0.443	11.37
4.00	0.08071	18.2	0.885	10.87
4.00	0.08071	17.8	0.767	9.37
4.00	0.08912	18.6	0.852	10.67
4.00	0.08912	19.0	0.560	11.37
4.00	0.08912	18.6	0.852	11.67
4.00	0.08912	20.8	0.828	13.57
5.14	0.05007	16.4	0.767	13.40
5.14	0.05007	14.0	0.779	14.80

Validation/Testing				
D	***Q***	***d***	***v***	**U3**
(cm)	**(m^3/s)**	**(cm)**	**(m/s)**	**(cm)**
2.10	0.01697	8.4	0.396	13.36
2.10	0.02610	8.0	0.343	15.85
2.10	0.04123	10.6	0.717	12.82
2.10	0.05249	15.8	0.714	15.85
2.10	0.06501	13.6	1.102	16.09
5.14	0.02233	7.8	0.594	7.97
5.14	0.06494	18.4	1.111	9.57
5.14	0.07286	12.6	0.852	6.97
5.14	0.06831	18.2	0.929	9.57
3.20	0.07475	15.0	0.970	11.67
3.20	0.06627	16.2	1.029	7.97
3.20	0.05450	14.8	0.727	7.77
3.20	0.03538	12.0	0.727	3.37
3.20	0.03129	7.2	0.626	9.97
3.20	0.02188	7.0	0.505	8.37
3.20	0.01514	6.4	0.542	6.77
4.00	0.01553	6.0	0.443	3.47
4.00	0.02374	9.8	0.700	4.77
4.00	0.03937	12.8	0.657	6.97
4.00	0.06039	13.8	0.828	9.37
4.00	0.08071	22.2	0.828	10.37
4.00	0.08912	17.8	0.907	10.97
4.00	0.08912	17.8	0.907	12.77
5.14	0.05007	15.4	0.816	13.40
2.10	0.01697	8.6	0.524	13.56
2.10	0.02610	11.0	0.280	16.15
2.10	0.04123	10.2	0.794	12.62
2.10	0.05249	18.2	0.754	16.15
2.10	0.06501	17.2	1.111	15.79
5.14	0.02233	9.2	0.524	6.57
5.14	0.06494	18.2	1.120	9.97
5.14	0.07286	16.0	1.000	6.97
5.14	0.06831	15.8	0.998	9.57
3.20	0.07475	17.8	1.000	11.47
3.20	0.06627	17.3	0.863	7.87
3.20	0.05450	18.0	0.594	7.47
3.20	0.03538	12.8	0.727	3.77
3.20	0.03129	10.2	0.700	9.47
3.20	0.02188	6.6	0.524	8.77
3.20	0.01514	5.6	0.594	7.17
4.00	0.01553	5.8	0.714	3.67
4.00	0.02374	7.0	0.828	5.77
4.00	0.03937	11.0	1.357	7.47
4.00	0.06039	17.6	0.767	11.17
4.00	0.08071	18.2	0.885	11.37
4.00	0.08912	20.8	0.828	11.17
4.00	0.08912	19.0	0.560	12.67
5.14	0.05007	13.2	0.792	13.40

Table A.4: Scour database for free-flow conditions at D1

Calibration/Training

D (cm)	*Q* (m^3/s)	*d* (cm)	*v* (m/s)	D1 (cm)
2.10	0.01697	8.6	0.524	16.31
2.10	0.01697	9.0	0.443	16.01
2.10	0.02610	10.0	0.343	16.96
2.10	0.02610	10.8	0.396	17.36
2.10	0.04123	12.0	0.674	14.36
2.10	0.04123	10.6	0.717	14.76
2.10	0.05249	12.0	0.714	16.96
2.10	0.05249	14.0	0.714	17.36
2.10	0.06501	13.4	1.102	18.69
2.10	0.06501	13.6	1.102	18.39
5.14	0.01363	6.8	1.709	12.37
5.14	0.01363	6.4	1.635	11.57
5.14	0.03249	12.4	0.370	13.05
5.14	0.03249	10.4	0.242	12.55
5.14	0.04413	12.8	0.626	16.65
5.14	0.04413	12.5	0.560	15.75
5.14	0.02233	7.8	0.594	11.06
5.14	0.02233	9.2	0.524	10.06
5.14	0.06494	19.6	1.111	14.26
5.14	0.06494	17.8	1.120	13.56
5.14	0.07286	16.0	1.000	11.76
5.14	0.07286	12.6	0.852	13.16
5.14	0.06831	16.0	0.874	12.46
5.14	0.06831	15.8	0.998	14.06
3.20	0.07475	15.0	0.970	13.26
3.20	0.07475	17.8	1.000	13.06
3.20	0.06627	14.8	0.939	11.46
3.20	0.06627	17.3	0.863	12.46
3.20	0.05450	13.2	0.929	9.76
3.20	0.05450	18.0	0.594	11.36
3.20	0.03538	13.0	0.896	6.46
3.20	0.03538	12.8	0.727	7.56
3.20	0.03129	8.2	0.754	12.36
3.20	0.03129	10.2	0.700	13.26
3.20	0.02188	7.0	0.505	11.76
3.20	0.02188	10.0	0.657	11.26
3.20	0.01514	6.4	0.542	10.66
3.20	0.01514	4.0	0.542	9.56
4.00	0.01553	5.6	0.485	6.16
4.00	0.01553	6.0	0.485	7.16
4.00	0.02374	6.0	0.840	6.96
4.00	0.02374	7.0	0.828	8.76
4.00	0.03937	12.8	0.657	9.46
4.00	0.03937	11.0	1.357	11.16
4.00	0.06039	13.8	0.828	12.36
4.00	0.06039	16.2	0.443	13.36
4.00	0.08071	17.8	0.767	12.96
4.00	0.08071	18.2	0.885	15.96
4.00	0.08912	17.8	0.907	12.46
4.00	0.08912	20.8	0.828	14.96
4.00	0.08912	18.6	0.852	13.26
4.00	0.08912	20.8	0.828	14.96
5.14	0.05007	13.2	0.792	18.80
5.14	0.05007	15.4	0.816	18.60

Validation/Testing

D (cm)	*Q* (m^3/s)	*d* (cm)	*v* (m/s)	D1 (cm)
2.10	0.01697	8.4	0.396	16.11
2.10	0.02610	8.0	0.343	17.16
2.10	0.04123	10.2	0.794	14.46
2.10	0.05249	15.8	0.714	17.16
2.10	0.06501	14.2	1.129	18.49
5.14	0.01363	6.2	1.633	11.67
5.14	0.03249	12.0	0.313	12.75
5.14	0.04413	13.8	0.792	16.05
5.14	0.02233	7.2	0.560	10.26
5.14	0.06494	18.4	1.111	14.06
5.14	0.07286	15.4	0.970	12.16
5.14	0.06831	15.4	0.779	12.76
3.20	0.07475	15.0	1.057	13.06
3.20	0.06627	16.2	1.029	11.76
3.20	0.05450	14.8	0.727	10.46
3.20	0.03538	10.8	0.779	7.26
3.20	0.03129	8.0	0.626	12.46
3.20	0.02188	8.2	0.657	11.36
3.20	0.01514	5.6	0.594	10.46
4.00	0.01553	6.0	0.443	6.66
4.00	0.02374	8.2	0.828	8.76
4.00	0.03937	10.0	0.792	9.56
4.00	0.06039	16.0	0.767	12.76
4.00	0.08071	18.2	0.885	14.76
4.00	0.08912	18.6	0.852	12.56
4.00	0.08912	17.8	0.907	13.36
5.14	0.05007	16.4	0.767	18.80
2.10	0.01697	9.4	0.505	16.31
2.10	0.02610	11.0	0.280	17.06
2.10	0.04123	11.2	0.757	14.46
2.10	0.05249	18.2	0.754	17.06
2.10	0.06501	17.2	1.111	18.59
5.14	0.01363	7.0	1.686	11.77
5.14	0.03249	11.4	0.396	12.55
5.14	0.04413	13.2	0.657	16.55
5.14	0.02233	8.6	0.505	10.16
5.14	0.06494	18.2	1.120	14.16
5.14	0.07286	16.4	1.038	12.56
5.14	0.06831	18.2	0.929	13.46
3.20	0.07475	13.8	0.990	13.16
3.20	0.06627	19.2	0.863	11.76
3.20	0.05450	13.8	0.714	11.06
3.20	0.03538	12.0	0.727	6.76
3.20	0.03129	7.2	0.626	13.16
3.20	0.02188	6.6	0.524	11.36
3.20	0.01514	6.8	0.542	10.16
4.00	0.01553	5.8	0.714	7.16
4.00	0.02374	9.8	0.700	8.46
4.00	0.03937	10.0	0.804	9.76
4.00	0.06039	17.6	0.767	13.16
4.00	0.08071	22.2	0.828	14.56
4.00	0.08912	19.0	0.560	13.96
4.00	0.08912	19.0	0.560	13.96
5.14	0.05007	14.0	0.779	18.80

Table A.5: Scour database for free-flow conditions at D2

Calibration/Training					Validation/Testing				
D	***Q***	***d***	***v***	**D2**	***D***	***Q***	***d***	***v***	**D2**
(cm)	**(m^3/s)**	**(cm)**	**(m/s)**	**(cm)**	**(cm)**	**(m^3/s)**	**(cm)**	**(m/s)**	**(cm)**
2.10	0.01697	8.6	0.524	13.52	2.10	0.01697	9.0	0.443	13.92
2.10	0.01697	8.4	0.396	14.72	2.10	0.02610	10.0	0.343	17.02
2.10	0.02610	10.8	0.396	16.92	2.10	0.04123	12.0	0.674	13.92
2.10	0.02610	11.0	0.280	17.42	2.10	0.05249	12.0	0.714	17.02
2.10	0.04123	10.6	0.717	14.02	2.10	0.06501	14.2	1.129	17.41
2.10	0.04123	11.2	0.757	13.22	5.14	0.02233	7.8	0.594	9.90
2.10	0.05249	14.0	0.714	16.92	5.14	0.06494	19.6	1.111	13.10
2.10	0.05249	18.2	0.754	17.42	5.14	0.07286	15.4	0.970	10.70
2.10	0.06501	13.6	1.102	17.61	5.14	0.06831	16.0	0.874	11.00
2.10	0.06501	17.2	1.111	16.61	3.20	0.07475	13.8	0.990	11.40
5.14	0.02233	7.2	0.560	8.50	3.20	0.06627	14.8	0.939	10.30
5.14	0.02233	8.6	0.505	11.00	3.20	0.05450	14.8	0.727	8.00
5.14	0.06494	18.4	1.111	12.50	3.20	0.03538	13.0	0.896	4.60
5.14	0.06494	18.2	1.120	14.10	3.20	0.03129	8.0	0.626	11.10
5.14	0.07286	16.0	1.000	12.10	3.20	0.02188	7.0	0.505	9.40
5.14	0.07286	12.6	0.852	9.70	3.20	0.01514	6.4	0.542	9.50
5.14	0.06831	15.4	0.779	10.90	4.00	0.01553	6.0	0.485	5.60
5.14	0.06831	15.8	0.998	12.40	4.00	0.02374	9.8	0.700	7.30
3.20	0.07475	15.0	1.057	11.10	4.00	0.03937	10.0	0.804	8.60
3.20	0.07475	17.8	1.000	12.20	4.00	0.06039	16.0	0.767	12.00
3.20	0.06627	16.2	1.029	9.50	4.00	0.08071	22.2	0.828	12.80
3.20	0.06627	19.2	0.863	10.80	4.00	0.08912	18.6	0.852	11.30
3.20	0.05450	13.2	0.929	7.60	4.00	0.08912	18.6	0.852	11.90
3.20	0.05450	13.8	0.714	8.90	5.14	0.05007	16.4	0.767	17.50
3.20	0.03538	10.8	0.779	5.10	2.10	0.01697	9.4	0.505	13.72
3.20	0.03538	12.0	0.727	4.10	2.10	0.02610	8.0	0.343	17.12
3.20	0.03129	7.2	0.626	12.90	2.10	0.04123	10.2	0.794	13.62
3.20	0.03129	8.2	0.754	10.90	2.10	0.05249	15.8	0.714	17.12
3.20	0.02188	6.6	0.524	9.40	2.10	0.06501	13.4	1.102	16.81
3.20	0.02188	10.0	0.657	10.30	5.14	0.02233	9.2	0.524	8.80
3.20	0.01514	4.0	0.542	9.80	5.14	0.06494	17.8	1.120	13.50
3.20	0.01514	5.6	0.594	7.70	5.14	0.07286	16.4	1.038	11.00
4.00	0.01553	5.6	0.485	4.00	5.14	0.06831	18.2	0.929	12.10
4.00	0.01553	6.0	0.443	6.80	3.20	0.07475	15.0	0.970	12.10
4.00	0.02374	8.2	0.828	7.70	3.20	0.06627	17.3	0.863	10.70
4.00	0.02374	6.0	0.840	7.10	3.20	0.05450	18.0	0.594	8.00
4.00	0.03937	10.0	0.792	10.40	3.20	0.03538	12.8	0.727	5.00
4.00	0.03937	12.8	0.657	7.90	3.20	0.03129	10.2	0.700	12.60
4.00	0.06039	16.2	0.443	11.90	3.20	0.02188	8.2	0.657	10.00
4.00	0.06039	17.6	0.767	12.10	3.20	0.01514	6.8	0.542	9.70
4.00	0.08071	18.2	0.885	13.00	4.00	0.01553	5.8	0.714	6.60
4.00	0.08071	17.8	0.767	10.70	4.00	0.02374	7.0	0.828	7.60
4.00	0.08912	17.8	0.907	10.10	4.00	0.03937	11.0	1.357	9.60
4.00	0.08912	20.8	0.828	15.00	4.00	0.06039	13.8	0.828	12.10
4.00	0.08912	17.8	0.907	11.30	4.00	0.08071	18.2	0.885	12.40
4.00	0.08912	20.8	0.828	15.00	4.00	0.08912	19.0	0.560	13.10
5.14	0.05007	13.2	0.792	18.40	4.00	0.08912	19.0	0.560	13.10
5.14	0.05007	15.4	0.816	16.80	5.14	0.05007	14.0	0.779	18.30

Table A.6: Scour database for free-flow conditions at D3

Calibration/Training				
D	***Q***	***d***	***v***	**D3**
(cm)	**(m^3/s)**	**(cm)**	**(m/s)**	**(cm)**
2.10	0.01697	8.6	0.524	13.24
2.10	0.01697	9.0	0.443	13.74
2.10	0.02610	8.0	0.343	16.75
2.10	0.02610	10.8	0.396	17.75
2.10	0.04123	10.2	0.794	13.05
2.10	0.04123	12.0	0.674	13.05
2.10	0.05249	15.8	0.714	16.85
2.10	0.05249	14.0	0.714	17.75
2.10	0.06501	13.4	1.102	16.79
2.10	0.06501	17.2	1.111	15.89
5.14	0.02233	9.2	0.524	7.05
5.14	0.02233	8.6	0.505	8.35
5.14	0.06494	19.6	1.111	10.55
5.14	0.06494	18.4	1.111	10.75
5.14	0.07286	16.0	1.000	7.35
5.14	0.07286	15.4	0.970	8.45
5.14	0.06831	16.0	0.874	8.55
5.14	0.06831	15.4	0.779	10.95
3.20	0.07475	15.0	1.057	8.95
3.20	0.07475	17.8	1.000	10.95
3.20	0.06627	19.2	0.863	10.35
3.20	0.06627	17.3	0.863	8.95
3.20	0.05450	14.8	0.727	8.55
3.20	0.05450	13.8	0.714	6.55
3.20	0.03538	13.0	0.896	4.15
3.20	0.03538	10.8	0.779	2.85
3.20	0.03129	7.2	0.626	10.95
3.20	0.03129	8.0	0.626	9.85
3.20	0.02188	8.2	0.657	9.55
3.20	0.02188	6.6	0.524	7.95
3.20	0.01514	4.0	0.542	7.75
3.20	0.01514	5.6	0.594	8.95
4.00	0.01553	5.6	0.485	3.05
4.00	0.01553	6.0	0.485	4.95
4.00	0.02374	8.2	0.828	5.45
4.00	0.02374	6.0	0.840	4.25
4.00	0.03937	10.0	0.804	6.95
4.00	0.03937	12.8	0.657	7.85
4.00	0.06039	16.2	0.443	8.75
4.00	0.06039	17.6	0.767	10.75
4.00	0.08071	17.8	0.767	8.35
4.00	0.08071	18.2	0.885	12.05
4.00	0.08912	17.8	0.907	9.15
4.00	0.08912	20.8	0.828	10.95
4.00	0.08912	17.8	0.907	9.15
4.00	0.08912	20.8	0.828	10.95
5.14	0.05007	13.2	0.792	15.00
5.14	0.05007	15.4	0.816	16.40

Validation/Testing				
D	***Q***	***d***	***v***	**D3**
(cm)	**(m^3/s)**	**(cm)**	**(m/s)**	**(cm)**
2.10	0.01697	8.4	0.396	13.54
2.10	0.02610	10.0	0.343	16.95
2.10	0.04123	10.6	0.717	13.05
2.10	0.05249	12.0	0.714	16.95
2.10	0.06501	13.6	1.102	16.49
5.14	0.02233	7.8	0.594	7.45
5.14	0.06494	17.8	1.120	10.75
5.14	0.07286	12.6	0.852	7.55
5.14	0.06831	18.2	0.929	9.45
3.20	0.07475	13.8	0.990	10.45
3.20	0.06627	14.8	0.939	9.55
3.20	0.05450	13.2	0.929	6.95
3.20	0.03538	12.0	0.727	3.05
3.20	0.03129	8.2	0.754	10.15
3.20	0.02188	7.0	0.505	8.95
3.20	0.01514	6.4	0.542	8.05
4.00	0.01553	6.0	0.443	4.75
4.00	0.02374	9.8	0.700	4.95
4.00	0.03937	10.0	0.792	7.45
4.00	0.06039	16.0	0.767	9.15
4.00	0.08071	18.2	0.885	8.75
4.00	0.08912	18.6	0.852	9.25
4.00	0.08912	18.6	0.852	9.25
5.14	0.05007	16.4	0.767	14.50
2.10	0.01697	9.4	0.505	12.64
2.10	0.02610	11.0	0.280	17.45
2.10	0.04123	11.2	0.757	13.05
2.10	0.05249	18.2	0.754	17.45
2.10	0.06501	14.2	1.129	16.39
5.14	0.02233	7.2	0.560	7.15
5.14	0.06494	18.2	1.120	10.55
5.14	0.07286	16.4	1.038	8.35
5.14	0.06831	15.8	0.998	9.15
3.20	0.07475	15.0	0.970	10.55
3.20	0.06627	16.2	1.029	9.15
3.20	0.05450	18.0	0.594	6.55
3.20	0.03538	12.8	0.727	3.95
3.20	0.03129	10.2	0.700	10.95
3.20	0.02188	10.0	0.657	8.95
3.20	0.01514	6.8	0.542	8.95
4.00	0.01553	5.8	0.714	4.85
4.00	0.02374	7.0	0.828	5.45
4.00	0.03937	11.0	1.357	7.25
4.00	0.06039	13.8	0.828	9.75
4.00	0.08071	22.2	0.828	11.15
4.00	0.08912	19.0	0.560	10.75
4.00	0.08912	19.0	0.560	10.75
5.14	0.05007	14.0	0.779	16.00

Table A.7: Scour database for free-flow conditions at L1

Calibration/Training					Validation/Testing				
D	***Q***	***d***	***v***	**L1**	***D***	***Q***	***d***	***v***	**L1**
(cm)	**(m^3/s)**	**(cm)**	**(m/s)**	**(cm)**	**(cm)**	**(m^3/s)**	**(cm)**	**(m/s)**	**(cm)**
2.10	0.01697	8.4	0.396	14.88	2.10	0.01697	9.0	0.443	15.18
2.10	0.01697	9.4	0.505	15.58	2.10	0.02610	8.0	0.343	16.46
2.10	0.02610	10.8	0.396	16.76	2.10	0.04123	10.2	0.794	13.56
2.10	0.02610	11.0	0.280	16.36	2.10	0.05249	12.0	0.714	16.36
2.10	0.04123	12.0	0.674	13.76	2.10	0.06501	13.6	1.102	18.67
2.10	0.04123	10.6	0.717	13.46	5.14	0.02233	7.2	0.560	11.27
2.10	0.05249	14.0	0.714	16.76	5.14	0.06494	19.6	1.111	14.37
2.10	0.05249	18.2	0.754	16.36	5.14	0.07286	16.0	1.000	13.37
2.10	0.06501	13.4	1.102	18.47	5.14	0.06831	15.4	0.779	13.57
2.10	0.06501	17.2	1.111	18.97	3.20	0.07475	13.8	0.990	11.97
5.14	0.02233	7.8	0.594	10.97	3.20	0.06627	14.8	0.939	10.67
5.14	0.02233	8.6	0.505	12.07	3.20	0.05450	13.2	0.929	10.27
5.14	0.06494	18.4	1.111	14.57	3.20	0.03538	13.0	0.896	5.77
5.14	0.06494	17.8	1.120	13.37	3.20	0.03129	8.0	0.626	11.97
5.14	0.07286	12.6	0.852	12.57	3.20	0.02188	8.2	0.657	10.67
5.14	0.07286	15.4	0.970	13.57	3.20	0.01514	5.6	0.594	10.37
5.14	0.06831	18.2	0.929	12.97	4.00	0.01553	6.0	0.485	6.57
5.14	0.06831	15.8	0.998	13.97	4.00	0.02374	9.8	0.700	8.37
3.20	0.07475	15.0	1.057	11.17	4.00	0.03937	10.0	0.792	9.47
3.20	0.07475	17.8	1.000	12.67	4.00	0.06039	16.0	0.767	11.37
3.20	0.06627	16.2	1.029	10.47	4.00	0.08071	22.2	0.828	13.47
3.20	0.06627	17.3	0.863	12.17	4.00	0.08912	18.6	0.852	13.37
3.20	0.05450	14.8	0.727	9.87	4.00	0.08912	18.6	0.852	13.37
3.20	0.05450	18.0	0.594	10.47	5.14	0.05007	13.2	0.792	17.80
3.20	0.03538	10.8	0.779	6.57	2.10	0.01697	8.6	0.524	15.28
3.20	0.03538	12.0	0.727	5.37	2.10	0.02610	10.0	0.343	16.36
3.20	0.03129	7.2	0.626	12.57	2.10	0.04123	11.2	0.757	13.66
3.20	0.03129	8.2	0.754	11.38	2.10	0.05249	15.8	0.714	16.46
3.20	0.02188	7.0	0.505	10.57	2.10	0.06501	14.2	1.129	18.77
3.20	0.02188	10.0	0.657	10.87	5.14	0.02233	9.2	0.524	11.17
3.20	0.01514	6.4	0.542	10.47	5.14	0.06494	18.2	1.120	14.27
3.20	0.01514	4.0	0.542	8.97	5.14	0.07286	16.4	1.038	12.67
4.00	0.01553	5.6	0.485	6.37	5.14	0.06831	16.0	0.874	13.97
4.00	0.01553	5.8	0.714	7.17	3.20	0.07475	15.0	0.970	12.27
4.00	0.02374	8.2	0.828	8.87	3.20	0.06627	19.2	0.863	10.97
4.00	0.02374	6.0	0.840	7.97	3.20	0.05450	13.8	0.714	10.27
4.00	0.03937	10.0	0.804	9.47	3.20	0.03538	12.8	0.727	6.07
4.00	0.03937	11.0	1.357	11.67	3.20	0.03129	10.2	0.700	12.37
4.00	0.06039	13.8	0.828	10.97	3.20	0.02188	6.6	0.524	10.67
4.00	0.06039	17.6	0.767	12.57	3.20	0.01514	6.8	0.542	9.27
4.00	0.08071	18.2	0.885	14.57	4.00	0.01553	6.0	0.443	6.67
4.00	0.08071	17.8	0.767	11.97	4.00	0.02374	7.0	0.828	8.47
4.00	0.08912	17.8	0.907	12.77	4.00	0.03937	12.8	0.657	10.57
4.00	0.08912	20.8	0.828	14.37	4.00	0.06039	16.2	0.443	11.97
4.00	0.08912	17.8	0.907	12.77	4.00	0.08071	18.2	0.885	13.97
4.00	0.08912	20.8	0.828	14.37	4.00	0.08912	19.0	0.560	13.87
5.14	0.05007	15.4	0.816	17.80	4.00	0.08912	19.0	0.560	13.87
5.14	0.05007	14.0	0.779	18.40	5.14	0.05007	16.4	0.767	18.10

Table A.8: Scour database for free-flow conditions at L2

Calibration/Training

D (cm)	*Q* (m^3/s)	*d* (cm)	*v* (m/s)	L2 (cm)
2.10	0.01697	8.6	0.524	13.94
2.10	0.01697	9.4	0.505	13.74
2.10	0.02610	8.0	0.343	15.46
2.10	0.02610	11.0	0.280	15.96
2.10	0.04123	10.2	0.794	12.36
2.10	0.04123	11.2	0.757	12.86
2.10	0.05249	15.8	0.714	15.46
2.10	0.05249	18.2	0.754	15.96
2.10	0.06501	13.4	1.102	16.79
2.10	0.06501	14.2	1.129	17.79
5.14	0.01363	6.2	1.633	7.48
5.14	0.01363	6.4	1.635	6.78
5.14	0.03249	12.4	0.370	9.79
5.14	0.03249	10.4	0.242	8.69
5.14	0.04413	13.2	0.657	14.09
5.14	0.04413	12.5	0.560	9.89
5.14	0.02233	7.8	0.594	9.05
5.14	0.02233	8.6	0.505	9.65
5.14	0.06494	19.6	1.111	12.45
5.14	0.06494	18.4	1.111	12.05
5.14	0.07286	16.0	1.000	11.15
5.14	0.07286	15.4	0.970	9.65
5.14	0.06831	16.0	0.874	10.15
5.14	0.06831	15.8	0.998	12.65
3.20	0.07475	15.0	1.057	11.45
3.20	0.07475	15.0	0.970	9.65
3.20	0.06627	19.2	0.863	8.45
3.20	0.06627	17.3	0.863	10.55
3.20	0.05450	14.8	0.727	7.35
3.20	0.05450	13.8	0.714	8.35
3.20	0.03538	13.0	0.896	4.05
3.20	0.03538	12.0	0.727	2.65
3.20	0.03129	7.2	0.626	11.75
3.20	0.03129	8.0	0.626	11.05
3.20	0.02188	8.2	0.657	10.15
3.20	0.02188	6.6	0.524	9.35
3.20	0.01514	6.4	0.542	8.75
3.20	0.01514	4.0	0.542	7.65
4.00	0.01553	5.6	0.485	3.35
4.00	0.01553	5.8	0.714	5.05
4.00	0.02374	8.2	0.828	6.25
4.00	0.02374	7.0	0.828	7.15
4.00	0.03937	10.0	0.804	8.35
4.00	0.03937	12.8	0.657	7.75
4.00	0.06039	13.8	0.828	9.75
4.00	0.06039	17.6	0.767	11.65
4.00	0.08071	18.2	0.885	13.05
4.00	0.08071	22.2	0.828	10.15
4.00	0.08912	17.8	0.907	12.15
4.00	0.08912	20.8	0.828	14.25
4.00	0.08912	17.8	0.907	11.15
4.00	0.08912	20.8	0.828	14.25
5.14	0.05007	13.2	0.792	15.80
5.14	0.05007	14.0	0.779	17.10

Validation/Testing

D (cm)	*Q* (m^3/s)	*d* (cm)	*v* (m/s)	L2 (cm)
2.10	0.01697	9.0	0.443	13.84
2.10	0.02610	10.0	0.343	15.66
2.10	0.04123	12.0	0.674	12.56
2.10	0.05249	12.0	0.714	15.66
2.10	0.06501	13.6	1.102	17.39
5.14	0.01363	6.8	1.709	7.38
5.14	0.03249	12.0	0.313	9.69
5.14	0.04413	12.8	0.626	13.99
5.14	0.02233	7.2	0.560	9.25
5.14	0.06494	17.8	1.120	12.45
5.14	0.07286	12.6	0.852	10.25
5.14	0.06831	15.4	0.779	12.45
3.20	0.07475	13.8	0.990	10.65
3.20	0.06627	14.8	0.939	8.95
3.20	0.05450	13.2	0.929	8.05
3.20	0.03538	10.8	0.779	3.35
3.20	0.03129	8.2	0.754	11.05
3.20	0.02188	7.0	0.505	10.05
3.20	0.01514	5.6	0.594	8.05
4.00	0.01553	6.0	0.485	4.75
4.00	0.02374	9.8	0.700	6.35
4.00	0.03937	10.0	0.792	8.15
4.00	0.06039	16.0	0.767	10.35
4.00	0.08071	17.8	0.767	12.95
4.00	0.08912	18.6	0.852	12.45
4.00	0.08912	18.6	0.852	12.45
5.14	0.05007	15.4	0.816	16.00
2.10	0.01697	8.4	0.396	13.84
2.10	0.02610	10.8	0.396	15.96
2.10	0.04123	10.6	0.717	12.46
2.10	0.05249	14.0	0.714	15.96
2.10	0.06501	17.2	1.111	17.19
5.14	0.01363	7.0	1.686	7.18
5.14	0.03249	11.4	0.396	9.29
5.14	0.04413	13.8	0.792	10.49
5.14	0.02233	9.2	0.524	9.15
5.14	0.06494	18.2	1.120	12.25
5.14	0.07286	16.4	1.038	10.25
5.14	0.06831	18.2	0.929	11.25
3.20	0.07475	17.8	1.000	10.15
3.20	0.06627	16.2	1.029	9.45
3.20	0.05450	18.0	0.594	7.55
3.20	0.03538	12.8	0.727	5.25
3.20	0.03129	10.2	0.700	11.55
3.20	0.02188	10.0	0.657	10.05
3.20	0.01514	6.8	0.542	8.45
4.00	0.01553	6.0	0.443	4.95
4.00	0.02374	6.0	0.840	6.65
4.00	0.03937	11.0	1.357	8.15
4.00	0.06039	16.2	0.443	11.35
4.00	0.08071	18.2	0.885	13.05
4.00	0.08912	19.0	0.560	12.95
4.00	0.08912	19.0	0.560	12.95
5.14	0.05007	16.4	0.767	17.00

Table A.9: Scour database for free-flow conditions at L3

Calibration/Training					Validation/Testing				
D	***Q***	***d***	***v***	**L3**	***D***	***Q***	***d***	***v***	**L3**
(cm)	**(m^3/s)**	**(cm)**	**(m/s)**	**(cm)**	**(cm)**	**(m^3/s)**	**(cm)**	**(m/s)**	**(cm)**
2.10	0.01697	8.6	0.524	13.39	2.10	0.01697	8.4	0.396	13.49
2.10	0.01697	9.0	0.443	13.79	2.10	0.02610	10.0	0.343	16.22
2.10	0.02610	8.0	0.343	15.92	2.10	0.04123	12.0	0.674	12.52
2.10	0.02610	10.8	0.396	16.42	2.10	0.05249	12.0	0.714	16.22
2.10	0.04123	10.6	0.717	12.82	2.10	0.06501	13.6	1.102	16.39
2.10	0.04123	11.2	0.757	12.62	5.14	0.02233	7.8	0.594	8.36
2.10	0.05249	15.8	0.714	15.82	5.14	0.06494	18.4	1.111	10.66
2.10	0.05249	14.0	0.714	16.42	5.14	0.07286	12.6	0.852	7.96
2.10	0.06501	13.4	1.102	15.89	5.14	0.06831	16.0	0.874	10.06
2.10	0.06501	14.2	1.129	17.89	3.20	0.07475	15.0	1.057	9.76
5.14	0.02233	7.2	0.560	6.66	3.20	0.06627	16.2	1.029	9.46
5.14	0.02233	8.6	0.505	8.76	3.20	0.05450	13.2	0.929	8.36
5.14	0.06494	17.8	1.120	10.96	3.20	0.03538	10.8	0.779	3.36
5.14	0.06494	18.2	1.120	9.76	3.20	0.03129	8.0	0.626	10.66
5.14	0.07286	15.4	0.970	7.46	3.20	0.02188	7.0	0.505	9.66
5.14	0.07286	16.4	1.038	8.46	3.20	0.01514	4.0	0.542	7.66
5.14	0.06831	15.4	0.779	11.46	4.00	0.01553	6.0	0.485	3.96
5.14	0.06831	18.2	0.929	9.96	4.00	0.02374	8.2	0.828	4.86
3.20	0.07475	13.8	0.990	9.06	4.00	0.03937	10.0	0.804	6.56
3.20	0.07475	17.8	1.000	10.46	4.00	0.06039	16.0	0.767	9.86
3.20	0.06627	14.8	0.939	11.06	4.00	0.08071	18.2	0.885	9.46
3.20	0.06627	19.2	0.863	8.06	4.00	0.08912	18.6	0.852	10.06
3.20	0.05450	14.8	0.727	8.96	4.00	0.08912	18.6	0.852	10.06
3.20	0.05450	13.8	0.714	6.46	5.14	0.05007	16.4	0.767	13.80
3.20	0.03538	13.0	0.896	2.96	2.10	0.01697	9.4	0.505	13.59
3.20	0.03538	12.8	0.727	3.96	2.10	0.02610	11.0	0.280	16.22
3.20	0.03129	7.2	0.626	9.66	2.10	0.04123	10.2	0.794	12.62
3.20	0.03129	10.2	0.700	11.46	2.10	0.05249	18.2	0.754	16.22
3.20	0.02188	6.6	0.524	10.36	2.10	0.06501	17.2	1.111	16.59
3.20	0.02188	10.0	0.657	9.46	5.14	0.02233	9.2	0.524	8.36
3.20	0.01514	6.4	0.542	6.66	5.14	0.06494	19.6	1.111	10.36
3.20	0.01514	6.8	0.542	8.46	5.14	0.07286	16.0	1.000	8.26
4.00	0.01553	5.6	0.485	2.26	5.14	0.06831	15.8	0.998	10.76
4.00	0.01553	6.0	0.443	4.26	3.20	0.07475	15.0	0.970	9.96
4.00	0.02374	9.8	0.700	5.26	3.20	0.06627	17.3	0.863	10.76
4.00	0.02374	6.0	0.840	4.66	3.20	0.05450	18.0	0.594	6.46
4.00	0.03937	10.0	0.792	6.06	3.20	0.03538	12.0	0.727	3.16
4.00	0.03937	12.8	0.657	7.26	3.20	0.03129	8.2	0.754	10.36
4.00	0.06039	13.8	0.828	8.66	3.20	0.02188	8.2	0.657	10.36
4.00	0.06039	17.6	0.767	11.26	3.20	0.01514	5.6	0.594	7.46
4.00	0.08071	17.8	0.767	9.06	4.00	0.01553	5.8	0.714	4.06
4.00	0.08071	22.2	0.828	9.66	4.00	0.02374	7.0	0.828	4.76
4.00	0.08912	17.8	0.907	9.66	4.00	0.03937	11.0	1.357	6.06
4.00	0.08912	20.8	0.828	10.26	4.00	0.06039	16.2	0.443	10.86
4.00	0.08912	17.8	0.907	9.66	4.00	0.08071	18.2	0.885	9.66
4.00	0.08912	20.8	0.828	10.26	4.00	0.08912	19.0	0.560	10.06
5.14	0.05007	13.2	0.792	14.00	4.00	0.08912	19.0	0.560	10.06
5.14	0.05007	15.4	0.816	13.60	5.14	0.05007	14.0	0.779	13.80

Table A.10: Scour database for free-flow conditions at R1

Calibration/Training					Validation/Testing				
D	***Q***	***d***	***v***	**R1**	***D***	***Q***	***d***	***v***	**R1**
(cm)	**(m^3/s)**	**(cm)**	**(m/s)**	**(cm)**	**(cm)**	**(m^3/s)**	**(cm)**	**(m/s)**	**(cm)**
2.10	0.01697	9.0	0.443	14.58	2.10	0.01697	8.6	0.524	14.78
2.10	0.01697	8.4	0.396	15.38	2.10	0.02610	10.0	0.343	16.48
2.10	0.02610	8.0	0.343	16.38	2.10	0.04123	12.0	0.674	13.58
2.10	0.02610	10.8	0.396	16.68	2.10	0.05249	12.0	0.714	16.48
2.10	0.04123	10.2	0.794	12.98	2.10	0.06501	14.2	1.129	17.74
2.10	0.04123	11.2	0.757	13.68	5.14	0.02233	7.8	0.594	11.18
2.10	0.05249	15.8	0.714	16.38	5.14	0.06494	19.6	1.111	13.88
2.10	0.05249	14.0	0.714	16.68	5.14	0.07286	16.0	1.000	12.98
2.10	0.06501	13.4	1.102	17.54	5.14	0.06831	15.4	0.779	13.88
2.10	0.06501	13.6	1.102	17.74	3.20	0.07475	15.0	1.057	12.38
5.14	0.02233	9.2	0.524	11.08	3.20	0.06627	16.2	1.029	11.08
5.14	0.02233	8.6	0.505	12.18	3.20	0.05450	14.8	0.727	9.78
5.14	0.06494	18.4	1.111	13.68	3.20	0.03538	10.8	0.779	6.48
5.14	0.06494	18.2	1.120	14.28	3.20	0.03129	8.0	0.626	12.08
5.14	0.07286	12.6	0.852	12.28	3.20	0.02188	8.2	0.657	10.78
5.14	0.07286	15.4	0.970	13.08	3.20	0.01514	5.6	0.594	9.88
5.14	0.06831	16.0	0.874	14.28	4.00	0.01553	5.6	0.485	6.38
5.14	0.06831	18.2	0.929	12.78	4.00	0.02374	8.2	0.828	8.38
3.20	0.07475	13.8	0.990	12.98	4.00	0.03937	12.8	0.657	9.58
3.20	0.07475	17.8	1.000	11.88	4.00	0.06039	16.0	0.767	11.48
3.20	0.06627	14.8	0.939	10.88	4.00	0.08071	18.2	0.885	14.28
3.20	0.06627	19.2	0.863	11.28	4.00	0.08912	17.8	0.907	13.88
3.20	0.05450	13.8	0.714	10.38	4.00	0.08912	17.8	0.907	13.88
3.20	0.05450	18.0	0.594	9.38	5.14	0.05007	15.4	0.816	18.00
3.20	0.03538	13.0	0.896	6.18	2.10	0.01697	9.4	0.505	15.08
3.20	0.03538	12.8	0.727	6.88	2.10	0.02610	11.0	0.280	16.48
3.20	0.03129	7.2	0.626	12.78	2.10	0.04123	10.6	0.717	13.58
3.20	0.03129	8.2	0.754	11.88	2.10	0.05249	18.2	0.754	16.48
3.20	0.02188	7.0	0.505	10.88	2.10	0.06501	17.2	1.111	17.54
3.20	0.02188	10.0	0.657	10.18	5.14	0.02233	7.2	0.560	11.28
3.20	0.01514	6.4	0.542	10.58	5.14	0.06494	17.8	1.120	14.08
3.20	0.01514	4.0	0.542	8.58	5.14	0.07286	16.4	1.038	12.78
4.00	0.01553	6.0	0.485	6.08	5.14	0.06831	15.8	0.998	13.08
4.00	0.01553	6.0	0.443	6.88	3.20	0.07475	15.0	0.970	12.28
4.00	0.02374	6.0	0.840	8.48	3.20	0.06627	17.3	0.863	11.28
4.00	0.02374	7.0	0.828	8.08	3.20	0.05450	13.2	0.929	9.48
4.00	0.03937	10.0	0.804	9.28	3.20	0.03538	12.0	0.727	6.38
4.00	0.03937	10.0	0.792	10.08	3.20	0.03129	10.2	0.700	12.48
4.00	0.06039	13.8	0.828	11.08	3.20	0.02188	6.6	0.524	10.68
4.00	0.06039	16.2	0.443	12.48	3.20	0.01514	6.8	0.542	9.38
4.00	0.08071	17.8	0.767	12.18	4.00	0.01553	5.8	0.714	6.18
4.00	0.08071	18.2	0.885	14.48	4.00	0.02374	9.8	0.700	8.08
4.00	0.08912	18.6	0.852	12.68	4.00	0.03937	11.0	1.357	9.48
4.00	0.08912	20.8	0.828	14.88	4.00	0.06039	17.6	0.767	12.48
4.00	0.08912	18.6	0.852	12.68	4.00	0.08071	22.2	0.828	13.08
4.00	0.08912	20.8	0.828	14.88	4.00	0.08912	19.0	0.560	13.48
5.14	0.05007	13.2	0.792	17.80	4.00	0.08912	19.0	0.560	13.48
5.14	0.05007	16.4	0.767	18.80	5.14	0.05007	14.0	0.779	18.10

Table A.11: Scour database for free-flow conditions at R2

Calibration/Training

D (cm)	*Q* (m^3/s)	*d* (cm)	*v* (m/s)	R2 (cm)
2.10	0.01697	9.0	0.443	14.30
2.10	0.01697	8.4	0.396	12.70
2.10	0.02610	10.8	0.396	16.68
2.10	0.02610	11.0	0.280	15.98
2.10	0.04123	10.2	0.794	13.28
2.10	0.04123	11.2	0.757	11.98
2.10	0.05249	14.0	0.714	15.98
2.10	0.05249	18.2	0.754	16.68
2.10	0.06501	13.4	1.102	17.11
2.10	0.06501	17.2	1.111	16.11
5.14	0.01363	6.2	1.633	7.19
5.14	0.01363	7.0	1.686	6.69
5.14	0.03249	12.0	0.313	9.16
5.14	0.03249	10.4	0.242	8.46
5.14	0.04413	13.2	0.657	12.67
5.14	0.04413	12.5	0.560	9.87
5.14	0.02233	7.8	0.594	10.11
5.14	0.02233	8.6	0.505	11.51
5.14	0.06494	19.6	1.111	13.21
5.14	0.06494	18.4	1.111	11.11
5.14	0.07286	15.4	0.970	9.81
5.14	0.07286	16.4	1.038	12.61
5.14	0.06831	16.0	0.874	9.61
5.14	0.06831	15.4	0.779	13.21
3.20	0.07475	13.8	0.990	10.61
3.20	0.07475	15.0	0.970	11.61
3.20	0.06627	19.2	0.863	10.81
3.20	0.06627	17.3	0.863	9.91
3.20	0.05450	14.8	0.727	7.61
3.20	0.05450	13.8	0.714	8.81
3.20	0.03538	13.0	0.896	4.91
3.20	0.03538	12.0	0.727	6.21
3.20	0.03129	8.2	0.754	13.21
3.20	0.03129	10.2	0.700	10.61
3.20	0.02188	8.2	0.657	9.21
3.20	0.02188	6.6	0.524	8.51
3.20	0.01514	4.0	0.542	7.81
3.20	0.01514	5.6	0.594	7.61
4.00	0.01553	6.0	0.485	3.61
4.00	0.01553	6.0	0.443	5.61
4.00	0.02374	6.0	0.840	6.61
4.00	0.02374	7.0	0.828	5.11
4.00	0.03937	10.0	0.792	6.31
4.00	0.03937	11.0	1.357	9.21
4.00	0.06039	16.0	0.767	10.41
4.00	0.06039	16.2	0.443	11.41
4.00	0.08071	18.2	0.885	10.71
4.00	0.08071	22.2	0.828	13.71
4.00	0.08912	17.8	0.907	11.21
4.00	0.08912	18.6	0.852	12.41
4.00	0.08912	17.8	0.907	12.41
4.00	0.08912	18.6	0.852	11.41
5.14	0.05007	13.2	0.792	17.20
5.14	0.05007	16.4	0.767	16.30

Validation/Testing

D (cm)	*Q* (m^3/s)	*d* (cm)	*v* (m/s)	R2 (cm)
2.10	0.01697	8.6	0.524	14.30
2.10	0.02610	10.0	0.343	16.08
2.10	0.04123	12.0	0.674	12.78
2.10	0.05249	12.0	0.714	16.08
2.10	0.06501	13.6	1.102	16.71
5.14	0.01363	6.8	1.709	7.09
5.14	0.03249	11.4	0.396	9.06
5.14	0.04413	12.8	0.626	12.57
5.14	0.02233	7.2	0.560	10.91
5.14	0.06494	17.8	1.120	13.01
5.14	0.07286	12.6	0.852	11.11
5.14	0.06831	18.2	0.929	12.11
3.20	0.07475	15.0	1.057	11.21
3.20	0.06627	14.8	0.939	9.91
3.20	0.05450	13.2	0.929	7.61
3.20	0.03538	10.8	0.779	5.41
3.20	0.03129	8.0	0.626	11.91
3.20	0.02188	7.0	0.505	8.91
3.20	0.01514	6.4	0.542	7.71
4.00	0.01553	5.6	0.485	3.81
4.00	0.02374	8.2	0.828	6.21
4.00	0.03937	10.0	0.804	6.71
4.00	0.06039	13.8	0.828	10.91
4.00	0.06039	13.8	0.828	10.91
4.00	0.08071	17.8	0.767	10.91
4.00	0.08912	19.0	0.560	12.41
4.00	0.08912	19.0	0.560	12.41
5.14	0.05007	15.4	0.816	16.40
2.10	0.01697	9.4	0.505	13.10
2.10	0.02610	8.0	0.343	16.18
2.10	0.04123	10.6	0.717	12.08
2.10	0.05249	15.8	0.714	16.18
2.10	0.06501	14.2	1.129	16.31
5.14	0.01363	6.4	1.635	6.59
5.14	0.03249	12.4	0.370	9.06
5.14	0.04413	13.8	0.792	10.37
5.14	0.02233	9.2	0.524	10.21
5.14	0.06494	18.2	1.120	12.61
5.14	0.07286	16.0	1.000	11.71
5.14	0.06831	15.8	0.998	12.81
3.20	0.07475	17.8	1.000	11.21
3.20	0.06627	16.2	1.029	10.81
3.20	0.05450	18.0	0.594	8.51
3.20	0.03538	12.8	0.727	6.01
3.20	0.03129	7.2	0.626	12.51
3.20	0.02188	10.0	0.657	9.71
3.20	0.01514	6.8	0.542	7.61
4.00	0.01553	5.8	0.714	5.51
4.00	0.02374	9.8	0.700	6.01
4.00	0.03937	12.8	0.657	8.21
4.00	0.06039	17.6	0.767	11.01
4.00	0.06039	17.6	0.767	11.01
4.00	0.08071	18.2	0.885	11.91
4.00	0.08912	20.8	0.828	12.41
4.00	0.08912	20.8	0.828	12.41
5.14	0.05007	14.0	0.779	16.40

Table A.12: Scour database for free-flow conditions at R3

Calibration/Training					Validation/Testing				
D	***Q***	***d***	***v***	**R3**	***D***	***Q***	***d***	***v***	**R3**
(cm)	**(m^3/s)**	**(cm)**	**(m/s)**	**(cm)**	**(cm)**	**(m^3/s)**	**(cm)**	**(m/s)**	**(cm)**
2.10	0.01697	8.4	0.396	12.68	2.10	0.01697	9.0	0.443	12.38
2.10	0.01697	9.4	0.505	11.68	2.10	0.02610	10.0	0.343	15.96
2.10	0.02610	10.8	0.396	16.36	2.10	0.04123	10.6	0.717	13.06
2.10	0.02610	11.0	0.280	15.76	2.10	0.05249	15.8	0.714	15.76
2.10	0.04123	10.2	0.794	12.56	2.10	0.06501	13.6	1.102	16.38
2.10	0.04123	12.0	0.674	13.26	5.14	0.02233	9.2	0.524	8.30
2.10	0.05249	14.0	0.714	16.36	5.14	0.06494	18.4	1.111	8.50
2.10	0.05249	18.2	0.754	15.76	5.14	0.07286	15.4	0.970	8.70
2.10	0.06501	13.4	1.102	16.78	5.14	0.06831	18.2	0.929	9.40
2.10	0.06501	14.2	1.129	16.18	3.20	0.07475	15.0	1.057	9.40
5.14	0.02233	7.2	0.560	8.60	3.20	0.06627	16.2	1.029	8.50
5.14	0.02233	7.8	0.594	7.50	3.20	0.05450	13.2	0.929	5.80
5.14	0.06494	19.6	1.111	8.30	3.20	0.03538	13.0	0.896	3.70
5.14	0.06494	18.2	1.120	9.80	3.20	0.03129	7.2	0.626	9.50
5.14	0.07286	16.0	1.000	7.80	3.20	0.02188	7.0	0.505	9.10
5.14	0.07286	12.6	0.852	9.30	3.20	0.01514	4.0	0.542	7.50
5.14	0.06831	16.0	0.874	8.30	4.00	0.01553	6.0	0.485	3.80
5.14	0.06831	15.4	0.779	11.40	4.00	0.02374	9.8	0.700	5.50
3.20	0.07475	13.8	0.990	9.20	4.00	0.03937	10.0	0.804	6.40
3.20	0.07475	15.0	0.970	10.70	4.00	0.06039	16.0	0.767	9.00
3.20	0.06627	14.8	0.939	8.40	4.00	0.08071	18.2	0.885	9.40
3.20	0.06627	19.2	0.863	10.30	4.00	0.08912	18.6	0.852	11.00
3.20	0.05450	14.8	0.727	4.60	4.00	0.08912	18.6	0.852	11.00
3.20	0.05450	18.0	0.594	8.60	5.14	0.05007	13.2	0.792	13.30
3.20	0.03538	10.8	0.779	3.20	2.10	0.01697	8.6	0.524	11.98
3.20	0.03538	12.0	0.727	6.30	2.10	0.02610	8.0	0.343	15.76
3.20	0.03129	8.0	0.626	8.20	2.10	0.04123	11.2	0.757	12.56
3.20	0.03129	8.2	0.754	10.70	2.10	0.05249	12.0	0.714	15.96
3.20	0.02188	8.2	0.657	9.50	2.10	0.06501	17.2	1.111	16.38
3.20	0.02188	10.0	0.657	8.30	5.14	0.02233	8.6	0.505	8.40
3.20	0.01514	5.6	0.594	6.80	5.14	0.06494	17.8	1.120	9.40
3.20	0.01514	6.8	0.542	7.50	5.14	0.07286	16.4	1.038	7.50
4.00	0.01553	5.6	0.485	2.30	5.14	0.06831	15.8	0.998	9.60
4.00	0.01553	6.0	0.443	4.80	3.20	0.07475	17.8	1.000	10.40
4.00	0.02374	8.2	0.828	5.80	3.20	0.06627	17.3	0.863	9.40
4.00	0.02374	7.0	0.828	5.00	3.20	0.05450	13.8	0.714	7.80
4.00	0.03937	10.0	0.792	5.60	3.20	0.03538	12.8	0.727	4.20
4.00	0.03937	12.8	0.657	7.10	3.20	0.03129	10.2	0.700	10.10
4.00	0.06039	13.8	0.828	9.30	3.20	0.02188	6.6	0.524	9.30
4.00	0.06039	16.2	0.443	8.80	3.20	0.01514	6.4	0.542	7.40
4.00	0.08071	17.8	0.767	9.40	4.00	0.01553	5.8	0.714	4.40
4.00	0.08071	22.2	0.828	11.50	4.00	0.02374	6.0	0.840	5.50
4.00	0.08912	17.8	0.907	9.80	4.00	0.03937	11.0	1.357	6.50
4.00	0.08912	20.8	0.828	11.70	4.00	0.06039	17.6	0.767	9.00
4.00	0.08912	17.8	0.907	9.80	4.00	0.08071	18.2	0.885	11.00
4.00	0.08912	20.8	0.828	11.70	4.00	0.08912	19.0	0.560	11.40
5.14	0.05007	15.4	0.816	13.20	4.00	0.08912	19.0	0.560	11.40
5.14	0.05007	14.0	0.779	14.60	5.14	0.05007	16.4	0.767	13.50

Table A.13: Scour database for pressure-flow conditions at U1

Calibration/Training				
D	***Q***	***d***	***v***	**U1**
(cm)	**(m^3/s)**	**(cm)**	**(m/s)**	**(cm)**
5.14	0.02198	7.4	0.464	10.52
5.14	0.02198	8.2	0.420	9.52
5.14	0.03274	12.6	0.505	17.60
5.14	0.03274	11.6	0.505	17.50
5.14	0.03476	12.0	0.485	15.92
5.14	0.03476	11.8	0.524	15.32
5.14	0.04715	15.4	0.714	18.72
5.14	0.04715	16.0	0.828	17.72
5.14	0.05974	15.6	0.626	18.65
5.14	0.05974	19.6	0.610	18.55
4.00	0.01373	8.4	0.280	16.49
4.00	0.01373	9.4	0.242	16.89
4.00	0.02285	22.4	0.343	18.20
4.00	0.02285	22.8	0.485	18.50
4.00	0.03631	12.4	0.505	16.19
4.00	0.03631	14.0	0.524	17.39
4.00	0.05038	14.6	0.560	17.52
4.00	0.05038	13.4	0.524	17.92
3.20	0.06309	17.0	0.524	18.35
3.20	0.06309	21.6	0.485	18.55
3.20	0.01959	7.4	0.443	17.26
3.20	0.01959	9.4	0.505	16.96
3.20	0.02712	11.0	0.626	17.32
3.20	0.02712	10.0	0.524	16.42
3.20	0.03665	9.6	0.642	17.16
3.20	0.03665	12.8	0.642	16.76
3.20	0.04755	16.8	0.714	15.64
3.20	0.04755	12.0	0.714	14.84
3.20	0.06123	14.8	0.657	14.52
3.20	0.06123	16.6	0.626	14.32
2.10	0.01817	8.8	0.594	13.02
2.10	0.01817	9.8	0.594	13.92
3.20	0.02392	8.0	0.741	15.75
3.20	0.02392	8.0	0.767	15.95
2.10	0.03657	10.0	0.626	16.61
2.10	0.03657	9.6	0.594	16.21
2.10	0.04982	14.0	0.594	9.80
2.10	0.04982	15.8	0.642	10.40
2.10	0.06219	13.6	0.594	16.02
2.10	0.06219	14.2	0.594	16.52
2.10	0.03411	13.0	0.396	12.86
2.10	0.03411	13.2	0.370	13.16
3.20	0.05974	13.0	1.000	18.79
3.20	0.05974	18.0	0.990	18.89

Validation/Testing				
D	***Q***	***d***	***v***	**U1**
(cm)	**(m^3/s)**	**(cm)**	**(m/s)**	**(cm)**
5.14	0.02198	10.0	0.464	9.92
5.14	0.03274	11.8	0.485	17.60
5.14	0.03476	11.8	0.485	15.52
5.14	0.04715	16.4	0.840	18.32
5.14	0.05974	13.4	0.696	18.55
4.00	0.01373	9.0	0.280	16.69
4.00	0.02285	21.8	0.396	18.40
4.00	0.03631	10.8	0.505	16.99
4.00	0.05038	13.2	0.560	17.82
3.20	0.06309	19.4	0.420	18.45
3.20	0.01959	9.6	0.396	17.06
3.20	0.02712	10.8	0.626	17.22
3.20	0.03665	9.8	0.642	17.16
3.20	0.04755	14.0	0.714	15.14
3.20	0.06123	13.0	0.626	14.42
2.10	0.01817	8.3	0.524	13.12
3.20	0.02392	9.4	0.700	15.75
2.10	0.03657	8.8	0.542	16.41
2.10	0.04982	15.2	0.542	9.80
2.10	0.06219	13.4	0.610	16.12
2.10	0.03411	13.0	0.396	12.96
3.20	0.05974	15.0	1.010	18.79
5.14	0.02198	6.8	0.485	10.12
5.14	0.03274	11.8	0.626	17.60
5.14	0.03476	11.4	0.626	15.32
5.14	0.04715	16.6	0.741	18.42
5.14	0.05974	15.4	0.714	18.65
4.00	0.01373	8.6	0.313	16.79
4.00	0.02285	22.2	0.280	18.40
4.00	0.03631	12.4	0.420	16.39
4.00	0.05038	15.0	0.485	17.92
3.20	0.06309	19.8	0.443	18.55
3.20	0.01959	5.4	0.524	17.06
3.20	0.02712	10.2	0.626	16.72
3.20	0.03665	11.4	0.626	16.96
3.20	0.04755	18.2	0.754	15.44
3.20	0.06123	17.0	0.594	14.42
2.10	0.01817	7.4	0.686	13.32
3.20	0.02392	10.0	0.754	15.75
2.10	0.03657	8.2	0.610	16.31
2.10	0.04982	14.0	0.686	10.00
2.10	0.06219	17.2	0.642	16.32
2.10	0.03411	13.4	0.370	12.96
3.20	0.05974	16.0	1.000	18.89

Table A.14: Scour database for pressure-flow conditions at U2

Calibration/Training					Validation/Testing				
D	***Q***	***d***	***v***	**U2**	***D***	***Q***	***d***	***v***	**U2**
(cm)	**(m^3/s)**	**(cm)**	**(m/s)**	**(cm)**	**(cm)**	**(m^3/s)**	**(cm)**	**(m/s)**	**(cm)**
5.14	0.02198	6.8	0.485	12.38	5.14	0.02198	7.4	0.464	13.38
5.14	0.02198	10.0	0.464	13.68	5.14	0.03274	11.8	0.626	18.51
5.14	0.03274	11.8	0.485	18.51	5.14	0.03476	11.8	0.485	15.19
5.14	0.03274	11.6	0.505	18.41	5.14	0.04715	16.0	0.828	18.37
5.14	0.03476	11.4	0.626	15.79	5.14	0.05974	15.6	0.626	18.91
5.14	0.03476	11.8	0.524	15.09	4.00	0.01373	8.4	0.280	15.81
5.14	0.04715	16.6	0.741	18.37	4.00	0.02285	21.8	0.396	18.40
5.14	0.04715	15.4	0.714	18.07	4.00	0.03631	10.8	0.505	17.30
5.14	0.05974	19.6	0.610	19.01	4.00	0.05038	13.2	0.560	17.33
5.14	0.05974	15.4	0.714	18.51	3.20	0.06309	19.4	0.420	18.46
4.00	0.01373	9.0	0.280	16.71	3.20	0.01959	9.4	0.505	14.98
4.00	0.01373	9.4	0.242	15.51	3.20	0.02712	10.8	0.626	15.67
4.00	0.02285	22.8	0.485	18.50	3.20	0.03665	9.8	0.642	17.82
4.00	0.02285	22.4	0.343	18.20	3.20	0.04755	14.0	0.714	14.69
4.00	0.03631	12.4	0.505	17.20	3.20	0.06123	13.0	0.626	14.32
4.00	0.03631	14.0	0.524	17.90	2.10	0.01817	7.4	0.686	11.69
4.00	0.05038	14.6	0.560	18.03	3.20	0.02392	9.4	0.700	14.32
4.00	0.05038	15.0	0.485	17.03	2.10	0.03657	10.0	0.626	16.16
3.20	0.06309	17.0	0.524	18.46	2.10	0.04982	15.2	0.542	9.30
3.20	0.06309	21.6	0.485	18.66	2.10	0.06219	13.4	0.610	16.66
3.20	0.01959	7.4	0.443	14.98	2.10	0.03411	13.2	0.370	10.40
3.20	0.01959	9.6	0.396	16.08	3.20	0.05974	16.0	1.000	16.48
3.20	0.02712	11.0	0.626	16.77	5.14	0.02198	8.2	0.420	12.48
3.20	0.02712	10.0	0.524	15.47	5.14	0.03274	12.6	0.505	18.51
3.20	0.03665	9.6	0.642	18.12	5.14	0.03476	12.0	0.485	15.09
3.20	0.03665	12.8	0.642	17.72	5.14	0.04715	16.4	0.840	18.07
3.20	0.04755	12.0	0.714	14.39	5.14	0.05974	13.4	0.696	18.81
3.20	0.04755	18.2	0.754	15.19	4.00	0.01373	8.6	0.313	15.71
3.20	0.06123	14.8	0.657	13.12	4.00	0.02285	22.2	0.280	18.40
3.20	0.06123	16.6	0.626	14.52	4.00	0.03631	12.4	0.420	17.20
2.10	0.01817	8.3	0.524	11.69	4.00	0.05038	13.4	0.524	17.93
2.10	0.01817	8.8	0.594	13.59	3.20	0.06309	19.8	0.443	18.56
3.20	0.02392	8.0	0.741	14.12	3.20	0.01959	5.4	0.524	15.38
3.20	0.02392	8.0	0.767	14.32	3.20	0.02712	10.2	0.626	15.67
2.10	0.03657	8.2	0.610	16.66	3.20	0.03665	11.4	0.626	18.02
2.10	0.03657	8.8	0.542	15.56	3.20	0.04755	16.8	0.714	14.99
2.10	0.04982	14.0	0.594	9.40	3.20	0.06123	17.0	0.594	13.52
2.10	0.04982	15.8	0.642	9.20	2.10	0.01817	9.8	0.594	12.19
2.10	0.06219	17.2	0.642	17.16	3.20	0.02392	10.0	0.754	14.12
2.10	0.06219	13.6	0.594	16.36	2.10	0.03657	9.6	0.594	15.96
2.10	0.03411	13.4	0.370	10.60	2.10	0.04982	14.0	0.686	9.30
2.10	0.03411	13.0	0.396	10.10	2.10	0.06219	14.2	0.594	16.86
3.20	0.05974	15.0	1.010	15.98	2.10	0.03411	13.0	0.396	10.30
3.20	0.05974	13.0	1.000	16.68	3.20	0.05974	18.0	0.990	16.48

Table A.15: Scour database for pressure-flow conditions at U3

Calibration/Training					Validation/Testing				
D	***Q***	***d***	***v***	**U3**	***D***	***Q***	***d***	***v***	**U3**
(cm)	**(m^3/s)**	**(cm)**	**(m/s)**	**(cm)**	**(cm)**	**(m^3/s)**	**(cm)**	**(m/s)**	**(cm)**
5.14	0.02198	6.8	0.485	11.92	5.14	0.02198	8.2	0.420	11.12
5.14	0.02198	10.0	0.464	9.82	5.14	0.03274	12.6	0.505	16.45
5.14	0.03274	11.8	0.626	17.15	5.14	0.03476	11.8	0.485	13.29
5.14	0.03274	11.8	0.485	16.25	5.14	0.04715	15.4	0.714	15.66
5.14	0.03476	12.0	0.485	13.09	5.14	0.05974	15.4	0.714	18.65
5.14	0.03476	11.4	0.626	14.89	4.00	0.01373	8.6	0.313	16.00
5.14	0.04715	16.6	0.741	16.16	4.00	0.02285	22.2	0.280	17.68
5.14	0.04715	16.0	0.828	14.36	4.00	0.03631	10.8	0.505	16.99
5.14	0.05974	15.6	0.626	18.65	4.00	0.05038	14.6	0.560	16.05
5.14	0.05974	19.6	0.610	18.55	3.20	0.06309	21.6	0.485	17.72
4.00	0.01373	9.0	0.280	16.30	3.20	0.01959	7.4	0.443	14.26
4.00	0.01373	8.4	0.280	14.80	3.20	0.02712	10.8	0.626	14.10
4.00	0.02285	22.4	0.343	18.78	3.20	0.03665	9.6	0.642	17.40
4.00	0.02285	21.8	0.396	17.48	3.20	0.04755	14.0	0.714	14.04
4.00	0.03631	12.4	0.505	16.19	3.20	0.06123	16.6	0.626	13.54
4.00	0.03631	14.0	0.524	17.39	2.10	0.01817	8.8	0.594	11.22
4.00	0.05038	13.2	0.560	15.85	3.20	0.02392	8.0	0.741	12.76
4.00	0.05038	13.4	0.524	18.05	2.10	0.03657	8.2	0.610	13.98
3.20	0.06309	17.0	0.524	18.32	2.10	0.04982	14.0	0.594	7.80
3.20	0.06309	19.4	0.420	17.52	2.10	0.06219	13.4	0.610	15.85
3.20	0.01959	9.6	0.396	14.26	2.10	0.03411	13.2	0.370	9.01
3.20	0.01959	9.4	0.505	14.46	3.20	0.05974	16.0	1.000	17.50
3.20	0.02712	11.0	0.626	15.60	5.14	0.02198	7.4	0.464	10.72
3.20	0.02712	10.2	0.626	14.00	5.14	0.03274	11.6	0.505	16.75
3.20	0.03665	12.8	0.642	18.90	5.14	0.03476	11.8	0.524	14.29
3.20	0.03665	11.4	0.626	17.00	5.14	0.04715	16.4	0.840	14.36
3.20	0.04755	12.0	0.714	13.34	5.14	0.05974	13.4	0.696	18.55
3.20	0.04755	16.8	0.714	14.84	4.00	0.01373	9.4	0.242	15.80
3.20	0.06123	14.8	0.657	13.34	4.00	0.02285	22.8	0.485	17.68
3.20	0.06123	13.0	0.626	13.74	4.00	0.03631	12.4	0.420	16.39
2.10	0.01817	7.4	0.686	12.22	4.00	0.05038	15.0	0.485	16.35
2.10	0.01817	8.3	0.524	11.22	3.20	0.06309	19.8	0.443	17.62
3.20	0.02392	8.0	0.767	12.96	3.20	0.01959	5.4	0.524	14.36
3.20	0.02392	9.4	0.700	12.66	3.20	0.02712	10.0	0.524	14.40
2.10	0.03657	10.0	0.626	13.98	3.20	0.03665	9.8	0.642	17.10
2.10	0.03657	9.6	0.594	12.98	3.20	0.04755	18.2	0.754	14.74
2.10	0.04982	15.8	0.642	8.00	3.20	0.06123	17.0	0.594	13.54
2.10	0.04982	14.0	0.686	7.60	2.10	0.01817	9.8	0.594	11.32
2.10	0.06219	13.6	0.594	15.75	3.20	0.02392	10.0	0.754	12.76
2.10	0.06219	14.2	0.594	17.05	2.10	0.03657	8.8	0.542	13.58
2.10	0.03411	13.4	0.370	9.21	2.10	0.04982	15.2	0.542	8.00
2.10	0.03411	13.0	0.396	8.91	2.10	0.06219	17.2	0.642	16.15
3.20	0.05974	15.0	1.010	17.10	2.10	0.03411	13.0	0.396	9.11
3.20	0.05974	18.0	0.990	17.70	3.20	0.05974	13.0	1.000	17.30

Table A.16: Scour database for pressure-flow conditions at D1

Calibration/Training					Validation/Testing				
D	***Q***	***d***	***v***	**D1**	***D***	***Q***	***d***	***v***	**D1**
(cm)	**(m^3/s)**	**(cm)**	**(m/s)**	**(cm)**	**(cm)**	**(m^3/s)**	**(cm)**	**(m/s)**	**(cm)**
5.14	0.02198	6.8	0.485	15.80	5.14	0.02198	10.0	0.464	14.20
5.14	0.02198	8.2	0.420	11.30	5.14	0.03274	12.6	0.505	18.26
5.14	0.03274	11.8	0.626	18.66	5.14	0.03476	12.0	0.485	15.88
5.14	0.03274	11.8	0.485	18.16	5.14	0.04715	15.4	0.714	19.10
5.14	0.03476	11.4	0.626	15.78	5.14	0.05974	19.6	0.610	19.50
5.14	0.03476	11.8	0.524	16.58	4.00	0.01373	9.0	0.280	15.96
5.14	0.04715	16.0	0.828	19.30	4.00	0.02285	21.8	0.396	18.22
5.14	0.04715	16.4	0.840	19.00	4.00	0.03631	10.8	0.505	18.26
5.14	0.05974	15.4	0.714	19.50	4.00	0.05038	13.4	0.524	17.15
5.14	0.05974	15.6	0.626	19.40	3.20	0.06309	17.0	0.524	18.98
4.00	0.01373	8.6	0.313	16.06	3.20	0.01959	5.4	0.524	17.65
4.00	0.01373	9.4	0.242	15.76	3.20	0.02712	10.8	0.626	17.83
4.00	0.02285	22.4	0.343	19.52	3.20	0.03665	9.8	0.642	18.84
4.00	0.02285	22.2	0.280	18.12	3.20	0.04755	14.0	0.714	15.66
4.00	0.03631	12.4	0.505	17.76	3.20	0.06123	16.6	0.626	14.58
4.00	0.03631	14.0	0.524	19.16	2.10	0.01817	7.4	0.686	13.79
4.00	0.05038	13.2	0.560	17.35	3.20	0.02392	8.0	0.741	16.00
4.00	0.05038	14.6	0.560	17.15	2.10	0.03657	8.2	0.610	16.11
3.20	0.06309	21.6	0.485	18.98	2.10	0.04982	15.2	0.542	10.20
3.20	0.06309	19.4	0.420	18.88	2.10	0.06219	13.4	0.610	17.16
3.20	0.01959	7.4	0.443	17.55	2.10	0.03411	13.2	0.370	13.17
3.20	0.01959	9.6	0.396	17.75	3.20	0.05974	18.0	0.990	18.81
3.20	0.02712	10.0	0.524	17.23	5.14	0.02198	7.4	0.464	12.60
3.20	0.02712	11.0	0.626	17.93	5.14	0.03274	11.6	0.505	18.16
3.20	0.03665	9.6	0.642	18.74	5.14	0.03476	11.8	0.485	15.88
3.20	0.03665	12.8	0.642	18.84	5.14	0.04715	16.6	0.741	19.30
3.20	0.04755	18.2	0.754	15.76	5.14	0.05974	13.4	0.696	19.40
3.20	0.04755	16.8	0.714	15.66	4.00	0.01373	8.4	0.280	15.96
3.20	0.06123	14.8	0.657	14.68	4.00	0.02285	22.8	0.485	18.42
3.20	0.06123	17.0	0.594	14.48	4.00	0.03631	12.4	0.420	18.16
2.10	0.01817	8.3	0.524	14.49	4.00	0.05038	15.0	0.485	17.15
2.10	0.01817	8.8	0.594	13.69	3.20	0.06309	19.8	0.443	18.88
3.20	0.02392	8.0	0.767	16.10	3.20	0.01959	9.4	0.505	17.75
3.20	0.02392	9.4	0.700	15.70	3.20	0.02712	10.2	0.626	17.43
2.10	0.03657	8.8	0.542	16.61	3.20	0.03665	11.4	0.626	18.74
2.10	0.03657	9.6	0.594	15.81	3.20	0.04755	12.0	0.714	15.66
2.10	0.04982	14.0	0.594	10.40	3.20	0.06123	13.0	0.626	14.58
2.10	0.04982	15.8	0.642	9.80	2.10	0.01817	9.8	0.594	13.69
2.10	0.06219	13.6	0.594	16.96	3.20	0.02392	10.0	0.754	15.80
2.10	0.06219	14.2	0.594	17.36	2.10	0.03657	10.0	0.626	16.41
2.10	0.03411	13.4	0.370	13.67	2.10	0.04982	14.0	0.686	9.80
2.10	0.03411	13.0	0.396	13.07	2.10	0.06219	17.2	0.642	17.06
3.20	0.05974	15.0	1.010	18.91	2.10	0.03411	13.0	0.396	13.47
3.20	0.05974	13.0	1.000	18.71	3.20	0.05974	16.0	1.000	18.81

Table A.17: Scour database for pressure-flow conditions at D2

Calibration/Training					Validation/Testing				
D	***Q***	***d***	***v***	**D2**	***D***	***Q***	***d***	***v***	**D2**
(cm)	**(m^3/s)**	**(cm)**	**(m/s)**	**(cm)**	**(cm)**	**(m^3/s)**	**(cm)**	**(m/s)**	**(cm)**
5.14	0.02198	6.8	0.485	17.74	5.14	0.02198	10.0	0.464	16.14
5.14	0.02198	8.2	0.420	12.14	5.14	0.03274	11.8	0.626	18.76
5.14	0.03274	12.6	0.505	18.36	5.14	0.03476	11.8	0.485	15.52
5.14	0.03274	11.8	0.485	18.86	5.14	0.04715	15.4	0.714	19.10
5.14	0.03476	11.4	0.626	15.42	5.14	0.05974	19.6	0.610	19.18
5.14	0.03476	11.8	0.524	15.92	4.00	0.01373	9.0	0.280	18.16
5.14	0.04715	16.0	0.828	19.30	4.00	0.02285	21.8	0.396	18.27
5.14	0.04715	16.4	0.840	19.10	4.00	0.03631	10.8	0.505	17.75
5.14	0.05974	15.4	0.714	19.48	4.00	0.05038	14.6	0.560	17.47
5.14	0.05974	15.6	0.626	19.18	3.20	0.06309	21.6	0.485	18.77
4.00	0.01373	8.4	0.280	18.16	3.20	0.01959	7.4	0.443	17.76
4.00	0.01373	9.4	0.242	18.56	3.20	0.02712	10.8	0.626	17.49
4.00	0.02285	22.4	0.343	18.47	3.20	0.03665	12.8	0.642	18.66
4.00	0.02285	22.8	0.485	17.97	3.20	0.04755	12.0	0.714	15.56
4.00	0.03631	12.4	0.420	17.05	3.20	0.06123	13.0	0.626	14.42
4.00	0.03631	14.0	0.524	18.75	2.10	0.01817	8.3	0.524	13.62
4.00	0.05038	13.4	0.524	17.67	3.20	0.02392	8.0	0.767	15.56
4.00	0.05038	15.0	0.485	17.17	2.10	0.03657	8.2	0.610	14.69
3.20	0.06309	17.0	0.524	18.67	2.10	0.04982	14.0	0.594	10.10
3.20	0.06309	19.4	0.420	18.87	2.10	0.06219	13.6	0.594	17.02
3.20	0.01959	5.4	0.524	17.96	2.10	0.03411	13.4	0.370	10.38
3.20	0.01959	9.6	0.396	17.16	3.20	0.05974	13.0	1.000	18.10
3.20	0.02712	11.0	0.626	18.19	5.14	0.02198	7.4	0.464	12.84
3.20	0.02712	10.2	0.626	17.09	5.14	0.03274	11.6	0.505	18.56
3.20	0.03665	9.6	0.642	18.36	5.14	0.03476	12.0	0.485	15.72
3.20	0.03665	9.8	0.642	18.76	5.14	0.04715	16.6	0.741	19.20
3.20	0.04755	18.2	0.754	15.86	5.14	0.05974	13.4	0.696	19.38
3.20	0.04755	16.8	0.714	15.36	4.00	0.01373	8.6	0.313	18.16
3.20	0.06123	14.8	0.657	14.52	4.00	0.02285	22.2	0.280	18.07
3.20	0.06123	16.6	0.626	14.32	4.00	0.03631	12.4	0.505	17.55
2.10	0.01817	7.4	0.686	13.42	4.00	0.05038	13.2	0.560	17.17
2.10	0.01817	8.8	0.594	14.32	3.20	0.06309	19.8	0.443	18.77
3.20	0.02392	8.0	0.741	16.16	3.20	0.01959	9.4	0.505	17.36
3.20	0.02392	10.0	0.754	15.36	3.20	0.02712	10.0	0.524	17.09
2.10	0.03657	8.8	0.542	14.59	3.20	0.03665	11.4	0.626	18.76
2.10	0.03657	9.6	0.594	14.99	3.20	0.04755	14.0	0.714	15.86
2.10	0.04982	15.8	0.642	10.50	3.20	0.06123	17.0	0.594	14.32
2.10	0.04982	14.0	0.686	9.70	2.10	0.01817	9.8	0.594	13.82
2.10	0.06219	14.2	0.594	16.92	3.20	0.02392	9.4	0.700	15.56
2.10	0.06219	17.2	0.642	17.42	2.10	0.03657	10.0	0.626	14.89
2.10	0.03411	13.2	0.370	10.28	2.10	0.04982	15.2	0.542	9.70
2.10	0.03411	13.0	0.396	10.78	2.10	0.06219	13.4	0.610	17.12
3.20	0.05974	16.0	1.000	18.60	2.10	0.03411	13.0	0.396	10.58
3.20	0.05974	18.0	0.990	17.60	3.20	0.05974	15.0	1.010	17.90

Table A.18: Scour database for pressure-flow conditions at D3

Calibration/Training					Validation/Testing				
D	***Q***	***d***	***v***	**D3**	***D***	***Q***	***d***	***v***	**D3**
(cm)	**(m^3/s)**	**(cm)**	**(m/s)**	**(cm)**	**(cm)**	**(m^3/s)**	**(cm)**	**(m/s)**	**(cm)**
5.14	0.02198	8.2	0.420	12.88	5.14	0.02198	6.8	0.485	13.88
5.14	0.02198	10.0	0.464	14.88	5.14	0.03274	12.6	0.505	18.60
5.14	0.03274	11.8	0.626	19.00	5.14	0.03476	11.8	0.485	14.89
5.14	0.03274	11.6	0.505	18.50	5.14	0.04715	16.6	0.741	17.07
5.14	0.03476	12.0	0.485	14.89	5.14	0.05974	15.4	0.714	19.25
5.14	0.03476	11.8	0.524	16.09	4.00	0.01373	9.0	0.280	18.60
5.14	0.04715	15.4	0.714	16.87	4.00	0.02285	21.8	0.396	16.88
5.14	0.04715	16.0	0.828	17.37	4.00	0.03631	10.8	0.505	17.09
5.14	0.05974	15.6	0.626	19.15	4.00	0.05038	14.6	0.560	16.52
5.14	0.05974	13.4	0.696	19.35	3.20	0.06309	19.4	0.420	18.41
4.00	0.01373	8.6	0.313	18.40	3.20	0.01959	7.4	0.443	17.88
4.00	0.01373	8.4	0.280	19.00	3.20	0.02712	10.8	0.626	17.59
4.00	0.02285	22.2	0.280	16.28	3.20	0.03665	12.8	0.642	18.78
4.00	0.02285	22.8	0.485	17.28	3.20	0.04755	18.2	0.754	15.29
4.00	0.03631	12.4	0.505	15.99	3.20	0.06123	16.6	0.626	14.22
4.00	0.03631	14.0	0.524	17.39	2.10	0.01817	8.8	0.594	13.36
4.00	0.05038	13.4	0.524	16.72	3.20	0.02392	9.4	0.700	15.00
4.00	0.05038	15.0	0.485	16.32	2.10	0.03657	8.2	0.610	14.56
3.20	0.06309	17.0	0.524	18.21	2.10	0.04982	15.8	0.642	10.00
3.20	0.06309	21.6	0.485	18.41	2.10	0.06219	13.6	0.594	16.95
3.20	0.01959	5.4	0.524	17.88	2.10	0.03411	13.0	0.396	9.48
3.20	0.01959	9.4	0.505	17.38	3.20	0.05974	15.0	1.010	15.94
3.20	0.02712	10.0	0.524	17.79	5.14	0.02198	7.4	0.464	13.08
3.20	0.02712	10.2	0.626	17.39	5.14	0.03274	11.8	0.485	18.70
3.20	0.03665	9.6	0.642	18.88	5.14	0.03476	11.4	0.626	15.59
3.20	0.03665	11.4	0.626	18.48	5.14	0.04715	16.4	0.840	17.37
3.20	0.04755	14.0	0.714	15.89	5.14	0.05974	19.6	0.610	19.25
3.20	0.04755	16.8	0.714	15.09	4.00	0.01373	9.4	0.242	18.90
3.20	0.06123	14.8	0.657	13.52	4.00	0.02285	22.4	0.343	17.08
3.20	0.06123	13.0	0.626	14.52	4.00	0.03631	12.4	0.420	17.29
2.10	0.01817	7.4	0.686	13.36	4.00	0.05038	13.2	0.560	16.62
2.10	0.01817	8.3	0.524	14.16	3.20	0.06309	19.8	0.443	18.21
3.20	0.02392	8.0	0.741	15.60	3.20	0.01959	9.6	0.396	17.68
3.20	0.02392	8.0	0.767	15.00	3.20	0.02712	11.0	0.626	17.49
2.10	0.03657	8.8	0.542	15.06	3.20	0.03665	9.8	0.642	18.78
2.10	0.03657	9.6	0.594	13.76	3.20	0.04755	12.0	0.714	15.49
2.10	0.04982	15.2	0.542	10.00	3.20	0.06123	17.0	0.594	14.52
2.10	0.04982	14.0	0.594	9.30	2.10	0.01817	9.8	0.594	13.36
2.10	0.06219	13.4	0.610	16.85	3.20	0.02392	10.0	0.754	15.20
2.10	0.06219	14.2	0.594	17.75	2.10	0.03657	10.0	0.626	14.86
2.10	0.03411	13.2	0.370	9.58	2.10	0.04982	14.0	0.686	9.40
2.10	0.03411	13.0	0.396	9.18	2.10	0.06219	17.2	0.642	17.45
3.20	0.05974	16.0	1.000	17.34	2.10	0.03411	13.4	0.370	9.28
3.20	0.05974	18.0	0.990	15.84	3.20	0.05974	13.0	1.000	15.94

Table A.19: Scour database for pressure-flow conditions at L1

Calibration/Training					Validation/Testing				
D	***Q***	***d***	***v***	**L1**	***D***	***Q***	***d***	***v***	**L1**
(cm)	**(m^3/s)**	**(cm)**	**(m/s)**	**(cm)**	**(cm)**	**(m^3/s)**	**(cm)**	**(m/s)**	**(cm)**
5.14	0.02198	8.2	0.420	10.19	5.14	0.02198	6.8	0.485	14.19
5.14	0.02198	10.0	0.464	14.29	5.14	0.03274	11.8	0.626	17.18
5.14	0.03274	12.6	0.505	17.58	5.14	0.03476	11.8	0.485	15.00
5.14	0.03274	11.8	0.485	16.98	5.14	0.04715	16.0	0.828	18.58
5.14	0.03476	11.4	0.626	14.90	5.14	0.05974	19.6	0.610	19.20
5.14	0.03476	11.8	0.524	15.50	4.00	0.01373	8.6	0.313	16.80
5.14	0.04715	16.6	0.741	18.58	4.00	0.02285	21.8	0.396	18.47
5.14	0.04715	15.4	0.714	19.38	4.00	0.03631	10.8	0.505	17.15
5.14	0.05974	15.4	0.714	19.30	4.00	0.05038	13.2	0.560	17.33
5.14	0.05974	15.6	0.626	19.00	3.20	0.06309	17.0	0.524	18.59
4.00	0.01373	9.0	0.280	16.80	3.20	0.01959	5.4	0.524	17.50
4.00	0.01373	8.4	0.280	16.70	3.20	0.02712	10.8	0.626	16.84
4.00	0.02285	22.4	0.343	19.17	3.20	0.03665	9.6	0.642	16.96
4.00	0.02285	22.8	0.485	18.27	3.20	0.04755	18.2	0.754	15.03
4.00	0.03631	12.4	0.505	16.85	3.20	0.06123	16.6	0.626	14.55
4.00	0.03631	14.0	0.524	18.05	2.10	0.01817	8.8	0.594	13.37
4.00	0.05038	14.6	0.560	17.13	3.20	0.02392	8.0	0.741	15.49
4.00	0.05038	15.0	0.485	17.53	2.10	0.03657	8.2	0.610	16.69
3.20	0.06309	21.6	0.485	18.59	2.10	0.04982	15.2	0.542	9.90
3.20	0.06309	19.4	0.420	18.39	2.10	0.06219	13.6	0.594	16.36
3.20	0.01959	7.4	0.443	17.80	2.10	0.03411	13.2	0.370	13.46
3.20	0.01959	9.6	0.396	17.50	3.20	0.05974	13.0	1.000	18.77
3.20	0.02712	10.0	0.524	16.14	5.14	0.02198	7.4	0.464	13.29
3.20	0.02712	10.2	0.626	17.14	5.14	0.03274	11.6	0.505	17.08
3.20	0.03665	12.8	0.642	17.36	5.14	0.03476	12.0	0.485	15.10
3.20	0.03665	9.8	0.642	16.76	5.14	0.04715	16.4	0.840	19.38
3.20	0.04755	14.0	0.714	14.73	5.14	0.05974	13.4	0.696	19.30
3.20	0.04755	16.8	0.714	15.43	4.00	0.01373	9.4	0.242	16.70
3.20	0.06123	14.8	0.657	14.55	4.00	0.02285	22.2	0.280	18.37
3.20	0.06123	17.0	0.594	14.35	4.00	0.03631	12.4	0.420	16.85
2.10	0.01817	7.4	0.686	13.17	4.00	0.05038	13.4	0.524	17.23
2.10	0.01817	8.3	0.524	13.47	3.20	0.06309	19.8	0.443	18.49
3.20	0.02392	8.0	0.767	15.59	3.20	0.01959	9.4	0.505	17.50
3.20	0.02392	9.4	0.700	15.29	3.20	0.02712	11.0	0.626	17.04
2.10	0.03657	10.0	0.626	16.99	3.20	0.03665	11.4	0.626	17.06
2.10	0.03657	9.6	0.594	16.29	3.20	0.04755	12.0	0.714	14.83
2.10	0.04982	14.0	0.594	10.00	3.20	0.06123	13.0	0.626	14.45
2.10	0.04982	14.0	0.686	9.30	2.10	0.01817	9.8	0.594	13.37
2.10	0.06219	14.2	0.594	16.76	3.20	0.02392	10.0	0.754	15.49
2.10	0.06219	17.2	0.642	16.36	2.10	0.03657	8.8	0.542	16.39
2.10	0.03411	13.4	0.370	13.86	2.10	0.04982	15.8	0.642	9.80
2.10	0.03411	13.0	0.396	13.36	2.10	0.06219	13.4	0.610	16.46
3.20	0.05974	15.0	1.010	18.97	2.10	0.03411	13.0	0.396	13.66
3.20	0.05974	16.0	1.000	18.77	3.20	0.05974	18.0	0.990	18.87

Table A.20: Scour database for pressure-flow conditions at L2

Calibration/Training					Validation/Testing				
D	***Q***	***d***	***v***	**L2**	***D***	***Q***	***d***	***v***	**L2**
(cm)	**(m^3/s)**	**(cm)**	**(m/s)**	**(cm)**	**(cm)**	**(m^3/s)**	**(cm)**	**(m/s)**	**(cm)**
5.14	0.02198	6.8	0.485	14.38	5.14	0.02198	10.0	0.464	14.28
5.14	0.02198	8.2	0.420	10.58	5.14	0.03274	11.8	0.626	17.59
5.14	0.03274	12.6	0.505	18.09	5.14	0.03476	11.8	0.485	15.60
5.14	0.03274	11.8	0.485	17.49	5.14	0.04715	16.6	0.741	18.76
5.14	0.03476	12.0	0.485	15.20	5.14	0.05974	15.4	0.714	18.59
5.14	0.03476	11.8	0.524	16.00	4.00	0.01373	8.6	0.313	17.69
5.14	0.04715	15.4	0.714	19.06	4.00	0.02285	22.4	0.343	18.61
5.14	0.04715	16.0	0.828	18.36	4.00	0.03631	10.8	0.505	16.70
5.14	0.05974	15.6	0.626	18.89	4.00	0.05038	13.4	0.524	17.09
5.14	0.05974	13.4	0.696	18.39	3.20	0.06309	17.0	0.524	18.36
4.00	0.01373	9.0	0.280	17.89	3.20	0.01959	5.4	0.524	16.48
4.00	0.01373	9.4	0.242	17.49	3.20	0.02712	10.8	0.626	15.78
4.00	0.02285	21.8	0.396	18.61	3.20	0.03665	9.6	0.642	18.20
4.00	0.02285	22.2	0.280	18.41	3.20	0.04755	18.2	0.754	14.86
4.00	0.03631	12.4	0.505	16.70	3.20	0.06123	13.0	0.626	14.46
4.00	0.03631	14.0	0.524	17.40	2.10	0.01817	7.4	0.686	13.62
4.00	0.05038	13.2	0.560	16.79	3.20	0.02392	8.0	0.767	15.37
4.00	0.05038	14.6	0.560	17.59	2.10	0.03657	8.8	0.542	15.66
3.20	0.06309	21.6	0.485	18.26	2.10	0.04982	15.8	0.642	9.40
3.20	0.06309	19.4	0.420	18.46	2.10	0.06219	13.6	0.594	15.66
3.20	0.01959	7.4	0.443	16.98	2.10	0.03411	13.0	0.396	10.56
3.20	0.01959	9.4	0.505	16.18	3.20	0.05974	13.0	1.000	17.50
3.20	0.02712	10.0	0.524	15.58	5.14	0.02198	7.4	0.464	13.78
3.20	0.02712	11.0	0.626	16.88	5.14	0.03274	11.6	0.505	17.59
3.20	0.03665	12.8	0.642	18.20	5.14	0.03476	11.4	0.626	15.70
3.20	0.03665	11.4	0.626	17.50	5.14	0.04715	16.4	0.840	18.86
3.20	0.04755	12.0	0.714	15.06	5.14	0.05974	19.6	0.610	18.79
3.20	0.04755	14.0	0.714	14.66	4.00	0.01373	8.4	0.280	17.69
3.20	0.06123	14.8	0.657	14.56	4.00	0.02285	22.8	0.485	18.51
3.20	0.06123	16.6	0.626	14.46	4.00	0.03631	12.4	0.420	16.80
2.10	0.01817	8.3	0.524	13.32	4.00	0.05038	15.0	0.485	17.39
2.10	0.01817	9.8	0.594	14.22	3.20	0.06309	19.8	0.443	18.36
3.20	0.02392	9.4	0.700	15.37	3.20	0.01959	9.6	0.396	16.28
3.20	0.02392	10.0	0.754	15.07	3.20	0.02712	10.2	0.626	16.58
2.10	0.03657	10.0	0.626	14.86	3.20	0.03665	9.8	0.642	17.60
2.10	0.03657	8.2	0.610	16.26	3.20	0.04755	16.8	0.714	14.76
2.10	0.04982	15.2	0.542	9.30	3.20	0.06123	17.0	0.594	14.56
2.10	0.04982	14.0	0.594	9.60	2.10	0.01817	8.8	0.594	13.52
2.10	0.06219	13.4	0.610	15.46	3.20	0.02392	8.0	0.741	15.27
2.10	0.06219	14.2	0.594	15.96	2.10	0.03657	9.6	0.594	15.06
2.10	0.03411	13.2	0.370	10.76	2.10	0.04982	14.0	0.686	9.40
2.10	0.03411	13.0	0.396	10.26	2.10	0.06219	17.2	0.642	15.96
3.20	0.05974	15.0	1.010	16.90	2.10	0.03411	13.4	0.370	10.36
3.20	0.05974	16.0	1.000	18.30	3.20	0.05974	18.0	0.990	16.90

Table A.21: Scour database for pressure-flow conditions at L3

Calibration/Training					Validation/Testing				
D	***Q***	***d***	***v***	**L3**	***D***	***Q***	***d***	***v***	**L3**
(cm)	**(m^3/s)**	**(cm)**	**(m/s)**	**(cm)**	**(cm)**	**(m^3/s)**	**(cm)**	**(m/s)**	**(cm)**
5.14	0.02198	8.2	0.420	10.27	5.14	0.02198	6.8	0.485	12.17
5.14	0.02198	10.0	0.464	13.47	5.14	0.03274	12.6	0.505	17.28
5.14	0.03274	11.8	0.626	18.08	5.14	0.03476	12.0	0.485	15.11
5.14	0.03274	11.6	0.505	17.08	5.14	0.04715	16.6	0.741	16.98
5.14	0.03476	11.4	0.626	15.11	5.14	0.05974	15.4	0.714	19.35
5.14	0.03476	11.8	0.524	15.71	4.00	0.01373	8.6	0.313	16.62
5.14	0.04715	15.4	0.714	17.58	4.00	0.02285	21.8	0.396	15.87
5.14	0.04715	16.0	0.828	16.88	4.00	0.03631	12.4	0.420	14.97
5.14	0.05974	15.6	0.626	19.45	4.00	0.05038	14.6	0.560	15.42
5.14	0.05974	13.4	0.696	19.05	3.20	0.06309	21.6	0.485	17.55
4.00	0.01373	9.0	0.280	16.52	3.20	0.01959	9.6	0.396	16.89
4.00	0.01373	8.4	0.280	17.02	3.20	0.02712	11.0	0.626	16.88
4.00	0.02285	22.4	0.343	16.07	3.20	0.03665	9.6	0.642	18.80
4.00	0.02285	22.8	0.485	15.77	3.20	0.04755	14.0	0.714	14.72
4.00	0.03631	10.8	0.505	14.37	3.20	0.06123	16.6	0.626	14.40
4.00	0.03631	12.4	0.505	15.07	2.10	0.01817	8.8	0.594	12.77
4.00	0.05038	13.2	0.560	14.12	3.20	0.02392	8.0	0.741	14.22
4.00	0.05038	15.0	0.485	15.62	2.10	0.03657	10.0	0.626	14.29
3.20	0.06309	17.0	0.524	17.75	2.10	0.04982	14.0	0.594	9.00
3.20	0.06309	19.8	0.443	17.35	2.10	0.06219	13.6	0.594	16.22
3.20	0.01959	5.4	0.524	17.09	2.10	0.03411	13.2	0.370	9.16
3.20	0.01959	7.4	0.443	16.89	3.20	0.05974	15.0	1.010	15.87
3.20	0.02712	10.0	0.524	16.78	5.14	0.02198	7.4	0.464	12.57
3.20	0.02712	10.8	0.626	17.08	5.14	0.03274	11.8	0.485	17.38
3.20	0.03665	12.8	0.642	18.90	5.14	0.03476	11.8	0.485	15.61
3.20	0.03665	11.4	0.626	18.60	5.14	0.04715	16.4	0.840	17.18
3.20	0.04755	18.2	0.754	14.82	5.14	0.05974	19.6	0.610	19.15
3.20	0.04755	16.8	0.714	14.72	4.00	0.01373	9.4	0.242	16.62
3.20	0.06123	14.8	0.657	13.20	4.00	0.02285	22.2	0.280	15.87
3.20	0.06123	13.0	0.626	14.50	4.00	0.03631	14.0	0.524	14.57
2.10	0.01817	7.4	0.686	12.87	4.00	0.05038	13.4	0.524	15.32
2.10	0.01817	8.3	0.524	12.37	3.20	0.06309	19.4	0.420	17.45
3.20	0.02392	8.0	0.767	14.02	3.20	0.01959	9.4	0.505	16.89
3.20	0.02392	10.0	0.754	14.52	3.20	0.02712	10.2	0.626	16.78
2.10	0.03657	8.2	0.610	14.99	3.20	0.03665	9.8	0.642	18.80
2.10	0.03657	9.6	0.594	13.79	3.20	0.04755	12.0	0.714	14.72
2.10	0.04982	15.8	0.642	9.30	3.20	0.06123	17.0	0.594	14.40
2.10	0.04982	14.0	0.686	9.00	2.10	0.01817	9.8	0.594	12.57
2.10	0.06219	13.4	0.610	15.82	3.20	0.02392	9.4	0.700	14.22
2.10	0.06219	14.2	0.594	16.42	2.10	0.03657	8.8	0.542	14.09
2.10	0.03411	13.4	0.370	9.46	2.10	0.04982	15.2	0.542	9.10
2.10	0.03411	13.0	0.396	9.06	2.10	0.06219	17.2	0.642	16.22
3.20	0.05974	16.0	1.000	16.87	2.10	0.03411	13.0	0.396	9.06
3.20	0.05974	18.0	0.990	15.77	3.20	0.05974	13.0	1.000	15.67

Table A.22: Scour database for pressure-flow conditions at R1

Calibration/Training					Validation/Testing				
D	***Q***	***d***	***v***	**R1**	***D***	***Q***	***d***	***v***	**R1**
(cm)	**(m^3/s)**	**(cm)**	**(m/s)**	**(cm)**	**(cm)**	**(m^3/s)**	**(cm)**	**(m/s)**	**(cm)**
5.14	0.02198	6.8	0.485	15.09	5.14	0.02198	10.0	0.464	13.99
5.14	0.02198	8.2	0.420	11.09	5.14	0.03274	12.6	0.505	17.99
5.14	0.03274	11.8	0.626	18.19	5.14	0.03476	12.0	0.485	15.10
5.14	0.03274	11.8	0.485	16.99	5.14	0.04715	16.6	0.741	18.30
5.14	0.03476	11.4	0.626	15.00	5.14	0.05974	15.4	0.714	17.65
5.14	0.03476	11.8	0.524	15.70	4.00	0.01373	8.4	0.280	16.35
5.14	0.04715	15.4	0.714	18.30	4.00	0.02285	21.8	0.396	18.10
5.14	0.04715	16.0	0.828	17.90	4.00	0.03631	12.4	0.420	17.16
5.14	0.05974	15.6	0.626	17.75	4.00	0.05038	13.2	0.560	17.20
5.14	0.05974	19.6	0.610	17.45	3.20	0.06309	19.4	0.420	18.30
4.00	0.01373	8.6	0.313	16.85	3.20	0.01959	7.4	0.443	18.05
4.00	0.01373	9.0	0.280	16.35	3.20	0.02712	10.0	0.524	16.92
4.00	0.02285	22.2	0.280	18.50	3.20	0.03665	12.8	0.642	16.88
4.00	0.02285	22.8	0.485	18.10	3.20	0.04755	14.0	0.714	15.45
4.00	0.03631	12.4	0.505	16.86	3.20	0.06123	14.8	0.657	14.50
4.00	0.03631	14.0	0.524	18.06	2.10	0.01817	7.4	0.686	13.37
4.00	0.05038	14.6	0.560	17.10	3.20	0.02392	9.4	0.700	15.79
4.00	0.05038	13.4	0.524	17.60	2.10	0.03657	8.2	0.610	16.96
3.20	0.06309	17.0	0.524	18.40	2.10	0.04982	14.0	0.594	10.00
3.20	0.06309	21.6	0.485	18.30	2.10	0.06219	13.6	0.594	16.48
3.20	0.01959	5.4	0.524	18.25	2.10	0.03411	13.0	0.396	13.96
3.20	0.01959	9.6	0.396	17.15	3.20	0.05974	16.0	1.000	18.80
3.20	0.02712	10.8	0.626	17.42	5.14	0.02198	7.4	0.464	13.09
3.20	0.02712	10.2	0.626	16.82	5.14	0.03274	11.6	0.505	17.19
3.20	0.03665	9.8	0.642	17.08	5.14	0.03476	11.8	0.485	15.60
3.20	0.03665	11.4	0.626	16.38	5.14	0.04715	16.4	0.840	17.90
3.20	0.04755	12.0	0.714	15.05	5.14	0.05974	13.4	0.696	17.65
3.20	0.04755	16.8	0.714	16.05	4.00	0.01373	9.4	0.242	16.35
3.20	0.06123	16.6	0.626	14.60	4.00	0.02285	22.4	0.343	18.20
3.20	0.06123	13.0	0.626	14.40	4.00	0.03631	10.8	0.505	17.46
2.10	0.01817	8.3	0.524	13.97	4.00	0.05038	15.0	0.485	17.20
2.10	0.01817	9.8	0.594	12.97	3.20	0.06309	19.8	0.443	18.30
3.20	0.02392	8.0	0.767	15.59	3.20	0.01959	9.4	0.505	17.25
2.10	0.03657	10.0	0.626	17.06	3.20	0.02712	11.0	0.626	17.02
2.10	0.03657	10.0	0.626	17.06	3.20	0.03665	9.6	0.642	16.68
2.10	0.03657	9.6	0.594	16.56	3.20	0.04755	18.2	0.754	15.85
2.10	0.04982	15.2	0.542	10.30	3.20	0.06123	17.0	0.594	14.50
2.10	0.04982	14.0	0.686	9.80	2.10	0.01817	8.8	0.594	13.17
2.10	0.06219	13.4	0.610	16.38	3.20	0.02392	10.0	0.754	15.79
2.10	0.06219	14.2	0.594	16.68	2.10	0.03657	8.8	0.542	16.56
2.10	0.03411	13.2	0.370	13.36	2.10	0.04982	15.8	0.642	10.20
2.10	0.03411	13.0	0.396	14.16	2.10	0.06219	17.2	0.642	16.48
3.20	0.05974	13.0	1.000	19.10	2.10	0.03411	13.4	0.370	13.76
3.20	0.05974	18.0	0.990	18.80	3.20	0.05974	15.0	1.010	18.90

Table A.23: Scour database for pressure-flow conditions at R2

Calibration/Training					Validation/Testing				
D	***Q***	***d***	***v***	**R2**	***D***	***Q***	***d***	***v***	**R2**
(cm)	**(m^3/s)**	**(cm)**	**(m/s)**	**(cm)**	**(cm)**	**(m^3/s)**	**(cm)**	**(m/s)**	**(cm)**
5.14	0.02198	6.8	0.485	15.48	5.14	0.02198	10.0	0.464	14.48
5.14	0.02198	8.2	0.420	11.08	5.14	0.03274	12.6	0.505	18.19
5.14	0.03274	11.8	0.626	18.19	5.14	0.03476	11.4	0.626	15.90
5.14	0.03274	11.8	0.485	18.69	5.14	0.04715	16.0	0.828	18.05
5.14	0.03476	12.0	0.485	15.90	5.14	0.05974	19.6	0.610	19.25
5.14	0.03476	11.8	0.485	15.50	4.00	0.01373	8.4	0.280	18.26
5.14	0.04715	16.6	0.741	17.95	4.00	0.02285	21.8	0.396	19.96
5.14	0.04715	15.4	0.714	18.25	4.00	0.03631	10.8	0.505	18.55
5.14	0.05974	15.4	0.714	19.45	4.00	0.05038	14.6	0.560	17.05
5.14	0.05974	15.6	0.626	19.25	3.20	0.06309	19.4	0.420	18.55
4.00	0.01373	8.6	0.313	18.16	3.20	0.01959	9.6	0.396	18.38
4.00	0.01373	9.0	0.280	18.26	3.20	0.02712	10.8	0.626	16.98
4.00	0.02285	22.2	0.280	20.06	3.20	0.03665	12.8	0.642	17.48
4.00	0.02285	22.8	0.485	18.96	3.20	0.04755	14.0	0.714	14.79
4.00	0.03631	12.4	0.505	18.55	3.20	0.06123	16.6	0.626	13.86
4.00	0.03631	14.0	0.524	17.55	2.10	0.01817	7.4	0.686	13.12
4.00	0.05038	13.4	0.524	17.25	3.20	0.02392	8.0	0.741	13.92
4.00	0.05038	15.0	0.485	18.05	2.10	0.03657	8.2	0.610	15.58
3.20	0.06309	17.0	0.524	18.55	2.10	0.04982	15.8	0.642	9.40
3.20	0.06309	21.6	0.485	18.45	2.10	0.06219	13.6	0.594	16.08
3.20	0.01959	5.4	0.524	18.48	2.10	0.03411	13.0	0.396	10.87
3.20	0.01959	7.4	0.443	18.18	3.20	0.05974	16.0	1.000	17.46
3.20	0.02712	10.0	0.524	17.38	5.14	0.02198	7.4	0.464	13.38
3.20	0.02712	11.0	0.626	16.78	5.14	0.03274	11.6	0.505	18.29
3.20	0.03665	9.8	0.642	18.48	5.14	0.03476	11.8	0.524	15.90
3.20	0.03665	11.4	0.626	17.48	5.14	0.04715	16.4	0.840	18.15
3.20	0.04755	18.2	0.754	14.89	5.14	0.05974	13.4	0.696	19.25
3.20	0.04755	16.8	0.714	14.69	4.00	0.01373	9.4	0.242	18.16
3.20	0.06123	14.8	0.657	13.56	4.00	0.02285	22.4	0.343	19.46
3.20	0.06123	17.0	0.594	14.46	4.00	0.03631	12.4	0.420	17.75
2.10	0.01817	8.3	0.524	13.32	4.00	0.05038	13.2	0.560	17.25
2.10	0.01817	9.8	0.594	12.72	3.20	0.06309	19.8	0.443	18.45
3.20	0.02392	9.4	0.700	13.72	3.20	0.01959	9.4	0.505	18.18
3.20	0.02392	10.0	0.754	14.02	3.20	0.02712	10.2	0.626	16.78
2.10	0.03657	8.8	0.542	14.78	3.20	0.03665	9.6	0.642	17.68
2.10	0.03657	9.6	0.594	16.88	3.20	0.04755	12.0	0.714	14.69
2.10	0.04982	15.2	0.542	9.50	3.20	0.06123	13.0	0.626	14.06
2.10	0.04982	14.0	0.594	9.30	2.10	0.01817	8.8	0.594	12.92
2.10	0.06219	14.2	0.594	15.98	3.20	0.02392	8.0	0.767	13.92
2.10	0.06219	17.2	0.642	16.68	2.10	0.03657	10.0	0.626	14.98
2.10	0.03411	13.2	0.370	10.37	2.10	0.04982	14.0	0.686	9.40
2.10	0.03411	13.4	0.370	11.27	2.10	0.06219	13.4	0.610	16.18
3.20	0.05974	15.0	1.010	17.76	2.10	0.03411	13.0	0.396	10.87
3.20	0.05974	18.0	0.990	16.96	3.20	0.05974	13.0	1.000	17.16

Table A.24: Scour database for pressure-flow conditions at R3

Calibration/Training					Validation/Testing				
D	***Q***	***d***	***v***	**R3**	***D***	***Q***	***d***	***v***	**R3**
(cm)	**(m^3/s)**	**(cm)**	**(m/s)**	**(cm)**	**(cm)**	**(m^3/s)**	**(cm)**	**(m/s)**	**(cm)**
5.14	0.02198	6.8	0.485	13.06	5.14	0.02198	8.2	0.420	10.66
5.14	0.02198	7.4	0.464	10.06	5.14	0.03274	11.8	0.626	18.39
5.14	0.03274	12.6	0.505	18.79	5.14	0.03476	12.0	0.485	15.49
5.14	0.03274	11.8	0.485	17.69	5.14	0.04715	15.4	0.714	15.65
5.14	0.03476	11.8	0.485	14.49	5.14	0.05974	15.4	0.714	18.35
5.14	0.03476	11.4	0.626	15.69	4.00	0.01373	9.0	0.280	18.75
5.14	0.04715	16.6	0.741	16.15	4.00	0.02285	22.4	0.343	17.42
5.14	0.04715	16.0	0.828	15.45	4.00	0.03631	10.8	0.505	15.46
5.14	0.05974	15.6	0.626	18.35	4.00	0.05038	14.6	0.560	16.19
5.14	0.05974	19.6	0.610	18.15	3.20	0.06309	17.0	0.524	18.27
4.00	0.01373	8.6	0.313	19.45	3.20	0.01959	9.6	0.396	16.80
4.00	0.01373	9.4	0.242	18.65	3.20	0.02712	10.8	0.626	16.86
4.00	0.02285	21.8	0.396	16.82	3.20	0.03665	9.6	0.642	17.22
4.00	0.02285	22.2	0.280	17.52	3.20	0.04755	18.2	0.754	14.79
4.00	0.03631	12.4	0.420	15.26	3.20	0.06123	16.6	0.626	12.81
4.00	0.03631	14.0	0.524	15.66	2.10	0.01817	8.3	0.524	12.81
4.00	0.05038	13.2	0.560	16.49	3.20	0.02392	8.0	0.767	14.75
4.00	0.05038	13.4	0.524	16.09	2.10	0.03657	10.0	0.626	14.31
3.20	0.06309	21.6	0.485	18.37	2.10	0.04982	15.2	0.542	9.00
3.20	0.06309	19.8	0.443	17.87	2.10	0.06219	13.4	0.610	15.76
3.20	0.01959	5.4	0.524	18.70	2.10	0.03411	13.2	0.370	9.24
3.20	0.01959	7.4	0.443	16.70	3.20	0.05974	13.0	1.000	16.86
3.20	0.02712	10.0	0.524	16.66	5.14	0.02198	10.0	0.464	12.46
3.20	0.02712	10.2	0.626	16.96	5.14	0.03274	11.6	0.505	18.39
3.20	0.03665	12.8	0.642	16.92	5.14	0.03476	11.8	0.524	15.49
3.20	0.03665	11.4	0.626	18.32	5.14	0.04715	16.4	0.840	15.85
3.20	0.04755	14.0	0.714	14.79	5.14	0.05974	13.4	0.696	18.35
3.20	0.06123	14.8	0.657	12.71	4.00	0.01373	8.4	0.280	18.65
3.20	0.06123	14.8	0.657	12.71	4.00	0.02285	22.8	0.485	17.12
3.20	0.06123	13.0	0.626	13.61	4.00	0.03631	12.4	0.505	15.66
2.10	0.01817	7.4	0.686	13.31	4.00	0.05038	15.0	0.485	16.19
2.10	0.01817	9.8	0.594	12.61	3.20	0.06309	19.4	0.420	18.17
3.20	0.02392	8.0	0.741	15.55	3.20	0.01959	9.4	0.505	16.90
3.20	0.02392	9.4	0.700	14.15	3.20	0.02712	11.0	0.626	16.86
2.10	0.03657	8.2	0.610	14.91	3.20	0.03665	9.8	0.642	17.02
2.10	0.03657	9.6	0.594	14.11	3.20	0.04755	16.8	0.714	14.39
2.10	0.04982	14.0	0.594	9.20	3.20	0.06123	17.0	0.594	13.21
2.10	0.04982	15.8	0.642	8.00	2.10	0.01817	8.8	0.594	13.21
2.10	0.06219	14.2	0.594	16.36	3.20	0.02392	10.0	0.754	15.35
2.10	0.06219	17.2	0.642	15.76	2.10	0.03657	8.8	0.542	14.31
2.10	0.03411	13.0	0.396	9.14	2.10	0.04982	14.0	0.686	8.20
2.10	0.03411	13.4	0.370	9.54	2.10	0.06219	13.6	0.594	15.96
3.20	0.05974	15.0	1.010	16.86	2.10	0.03411	13.0	0.396	9.34
3.20	0.05974	16.0	1.000	16.56	3.20	0.05974	18.0	0.990	16.76